GEORGIA INSTITUTE OF TECHNOLOGY
OFFICE OF CONTRACT ADMINISTRATION
SPONSORED PROJECT INITIATION

Date: FEBRUARY 23, 1977

Project Title: NOISE SUPPRESSION IN JET INLETS

Project No: E-16-609

Project Director: DR. B. T. ZINN

Sponsor: AIR FORCE OFFICE OF SCIENTIFIC RESEARCH

Agreement Period: From 2/1/77 Until ~~1/31/79~~ 31 Jan 80

(PERFORMANCE PERIOD)

Type Agreement: CONTRACT NO. F49620-77-C-0066

Amount:
$78,247 AFOSR
  4,573 GIT(E-16-381)
$82,820 TOTAL   (PARTIALLY FUNDED AT $24,024 THROUGH 9/30/77)

Reports Required: INTERIM SCIENTIFIC REPORTS; FINAL SCIENTIFIC REPORT.

Sponsor Contact Person (s):

Technical Matters

LTC ROBERT C. SMITH
AFOSR/NA
BLDG. 410
BOLLING AFB, DC   20332
(202)693-0016

Contractual Matters
(thru OCA)

JOAN O. MARSHALL
CONTRACTING OFFICER
AFOSR/PMD
BUILDING 410
BOLLING AFB, DC   20332
(202)693-0363

Defense Priority Rating: DOC-9 UNDER DMS REG. 1

Assigned to: AEROSPACE ENGINEERING   (School/Laboratory)

COPIES TO:

Project Director
Division Chief (EES)
School/Laboratory Director
Dean/Director-EES
Accounting Office
Procurement Office
Security Coordinator (OCA) ✓
Reports Coordinator (OCA)

Library, Technical Reports Section
Office of Computing Services
Director, Physical Plant
EES Information Office
Project File (OCA)
Project Code (GTRI)
Other_____

GEORGIA INSTITUTE OF TECHNOLOGY
OFFICE OF CONTRACT ADMINISTRATION

SPONSORED PROJECT TERMINATION

Date: _____ 9/2/80 _____

Project Title: Noise Suppression in Jet Inlets

Project No: E-16-609

Project Director: B. T. Zinn

Sponsor: Air Force Office of Scientific Research

Effective Termination Date: _____ 1/31/80 _____

Clearance of Accounting Charges: 1/31/80 _____

Grant/Contract Closeout Actions Remaining:

- _ Final Invoice and Closing Documents
- _ Final Fiscal Report
- _ Final Report of Inventions
- _ Govt. Property Inventory & Related Certificate
- X Classified Material Certificate
- _ Other _____

Assigned to: __ Aerospace Engineering _____ (School/~~Laboratory~~)

COPIES TO:

Project Director
Division Chief (EES)
School/Laboratory Director
Dean/Director—EES
Accounting Office
Procurement Office
Security Coordinator (OCA)
Reports Coordinator (OCA)

Library, Technical Reports Section
EES Information Office
Project File (OCA)
Project Code (GTRI)
Other C. E. Smith _____

AFOSR Interim Scientific Report

AFOSR-TR-

NOISE SUPPRESSION IN JET INLETS

Prepared for

Air Force Office of Scientific Research
Director of Aerospace Sciences

Bolling AFB, D. C.

by

Ben T. Zinn

William L. Meyer

William A. Bell

School of Aerospace Engineering
Georgia Institute of Technology
Atlanta, Georgia 30332

Approved for public release; distribution unlimited

AFOSR Contract No. F49620-77-C-0066   February 1978

SECURITY CLASSIFICATION OF THIS PAGE (When Data Entered)

REPORT DOCUMENTATION PAGE		READ INSTRUCTIONS BEFORE COMPLETING FORM
1. REPORT NUMBER AFOSR-TR	2. GOVT ACCESSION NO.	3. RECIPIENT'S CATALOG NUMBER
4. TITLE (and Subtitle) Noise Suppression in Jet Inlets		5. TYPE OF REPORT & PERIOD COVERED Interim February 1, 1977-Jan 31,1978
		6. PERFORMING ORG. REPORT NUMBER
7. AUTHOR(s) Ben T. Zinn William L. Meyer William A. Bell		8. CONTRACT OR GRANT NUMBER(s) AFOSR-F49620-77-C-0066
9. PERFORMING ORGANIZATION NAME AND ADDRESS School of Aerospace Engineering Georgia Institute of Technology Atlanta, Georgia 30332		10. PROGRAM ELEMENT, PROJECT, TASK AREA & WORK UNIT NUMBERS 681 300 297-47B1 61102F
11. CONTROLLING OFFICE NAME AND ADDRESS Air Force Office of Scientific Research Director of Aerospace Sciences Bolling AFB, DC		12. REPORT DATE February 1978
		13. NUMBER OF PAGES 67
14. MONITORING AGENCY NAME & ADDRESS(if different from Controlling Office)		15. SECURITY CLASS. (of this report) Unclassified
		15a. DECLASSIFICATION/DOWNGRADING SCHEDULE

16. DISTRIBUTION STATEMENT (of this Report)

Approved for Public Release Redistribution Unlimited.

17. DISTRIBUTION STATEMENT (of the abstract entered in Block 20, if different from Report)

18. SUPPLEMENTARY NOTES

19. KEY WORDS (Continue on reverse side if necessary and identify by block number)

Acoustic Radiation
Duct Acoustics
Jet Propulsion Noise
Aircraft Noise

20. ABSTRACT (Continue on reverse side if necessary and identify by block number)

    This report summarizes the work performed during the first year of a research effort to determine the sound fields associated with jet engine inlet configurations. A solution approach for axisymmetric bodies based upon the integral formulation of the wave equation has been developed. This solution approach circumvents the uniqueness problems which normally occur at certain frequencies when "straight forward" solutions of the integral equation are obtained. A numerical method and a computer program for solving for the acoustic field associated with

DD FORM 1473 EDITION OF 1 NOV 65 IS OBSOLETE
1 JAN 73

general inlet configurations and boundary conditions have also been developed. To evaluate the numerical method, computed and exact results are compared for a sphere and a finite length cylinder. For continuous boundary conditions, the agreement is within ten per cent over a range of nondimensional frequencies from one to ten. For discontinuous boundary conditions, the numerical errors increase by a factor of two. This report presents results for a given inlet configuration and the computed and exact solutions are shown to agree to within ten per cent over the nondimensional frequency range from one to ten.

ABSTRACT

This report summarizes the work performed during the first year of a
research effort to determine the sound fields associated with jet engine
inlet configurations. A solution approach for axisymmetric bodies based
upon the integral formulation of the wave equation has been developed.
This solution approach circumvents the uniqueness problems which normally
occur at certain frequencies when "straight forward" solutions of the in-
tegral equation are obtained. A numerical method and a computer program
for solving for the acoustic field associated with general inlet config-
urations and boundary conditions have also been developed. To evaluate
the numerical method, computed and exact results are compared for a sphere
and a finite length cylinder. For continuous boundary conditions, the
agreement is within ten per cent over a range of nondimensional frequencies
from one to ten. For discontinuous boundary conditions, the numerical errors
increase by a factor of two. This report presents results for a given inlet
configuration and the computed and exact solutions are shown to agree to
within ten per cent over the nondimensional frequency range from one to
ten.

I. INTRODUCTION

This report summarizes the results obtained during the first year of support under AFOSR Contract Number F49620-77-C-0066. This contract was initiated on February 1, 1977.

The research conducted under this contract is directed towards developing analytical techniques for predicting the characteristics of the radiated sound fields from jet engine inlets. Such capabilities are necessary to evaluate the effectiveness of potential sound source modifications and the efficiency of sound suppression techniques for fan and compressor noise attenuation in inlets. During the first year, the conducted research efforts have concentrated on the development of an efficient analytical technique for the prediction of the radiated fields associated with lined inlet configurations. In the second year, experimental investigations will be conducted to provide data for comparison with the theoretical predictions.

During the first year, a solution approach based upon an integral formulation of the wave equation has been developed and used to determine the characteristics of the sound fields of several previously investigated geometries. Efficient numerical techniques have been devised for solving the integral equation, and the necessary computer programs have been written and tested. These programs are now capable of computing the surface and radiated sound fields for arbitrary geometries with lined or unlined surfaces and sound sources of arbitrary spatial dependence. These capabilities are necessary for the investigations of sound fields from jet inlet configurations.

The efforts conducted under this contract has resulted in three publications[1,2,3] which are included in Appendices A-C of this report. These publications provide more detailed descriptions of the research efforts conducted

under this contract. The research performed during the first year is summarized in the following sections.

II. ANALYTICAL TECHNIQUE

The general analytical method used to determine the radiated sound fields from arbitrary geometries is described in Appendix A. This technique is based on the integral form of the solutions to the wave equation. This general formulation has been specialized to axisymmetric configurations, which are applicable to jet engine configurations which are of interest in this study, in Appendix B.

The study of sound radiation involves the determination of the acoustic field over an infinite domain. However, with the integral formulation of the wave equation, the acoustic potential, which is proportional to the acoustic pressure, can be computed at any point in the far field solely from the values of the potential distribution at the surface. Thus, the problem is reduced to solving for the acoustic field at the surface only instead of over an infinite domain.

Several problems are encountered while solving the integral equation governing the surface potential distribution. At certain frequencies the equation fails to yield a unique solution. These frequencies correspond to internal eigenfrequencies (or resonant frequencies) of the geometry under consideration. This nonuniqueness manifests itself when numerically solving the integral equation by causing the coefficient matrix of the system of linear algebraic equations which results from the application of approximate quadrature to the integral equation to become ill-conditioned, causing large numerical errors.

Using a method proposed by Burton and Miller (Ref. 13 of Appendix A), this behavior can be eliminated. This method consists of adding the integral equation for the normal velocity multiplied by a coupling constant. It is then proven that the solution for the acoustic potential field from the combined equation is unique for imaginary values of the coupling constant. This analytical method was therefore incorporated in this study. Although other techniques can be used to avoid the uniqueness problem at certain frequencies (Refs. 4, 6, and 14 of Appendix A), the combined integral equation of Burton and Miller was found to give the best results, and it required minimum computation times.

In order to use the Burton and Miller method two problems had to be resolved. First, a strong singularity exists in the integrand of the combined integral equation developed by Burton and Miller. In the present study, this equation was reformulated to obtain an equation containing only weakly singular terms which could be handled numerically. The second problem is connected with the choice of the coupling constant used by Burton and Miller in combining the integral equations for the potential and normal velocity. It has been found in this study that an optimum value for this parameter for use in numerical computations can be found. Although Burton and Miller showed that the parameter must contain a nonzero imaginary component, they gave no indication of how the results are affected by this parameter. The value which gives the best numerical results is i/k where $i = \sqrt{-1}$ and k is the wave number.

III. NUMERICAL METHOD

A. Integration Procedure

To determine the acoustic field associated with a geometry, the integral
equation describing the surface potential distribution must first be solved.
Using this distribution, the potential at any exterior point can then be
determined to generate the far field sound pattern. For general geometries,
the integral equations cannot be solved exactly, and approximate methods
must be used. These methods result in a system of linear, algebraic equations
with complex coefficients which can be solved by complex Gauss-Jordan reduc-
tion to obtain the acoustic potential distribution at the surface.

For the axisymmetric formulation used in this investigation, the surface
shape is defined by a line in the radial r and axial z directions, and this
line is rotated about the axis. The integral equation can then be separated
into two line integrals; one in the tangential direction and one along the
surface contour in the r - z plane. In the tangential direction, the line
integrals are given by Eqns. (15)-(17) of Appendix B, which, in general,
must be solved numerically. A 96-point Gaussian quadrature formula was used
to evaluate these integrals. The computational error is approximately in-
versely proportional to the number of points used to evaluate the integrals
in the tangential direction. Along the surface contour in the r - z plane,
the integration of Eq. (18) in Appendix B is required. The integral over
the perimeter is first separated into integrals over n subintervals of either
constant or varying lengths. The acoustic potential is assumed constant over
each subinterval and it is taken outside the integral. Finally, a two-point
Gaussian quadrature formula is used to evaluate the components of the func-
tions defined by Eqs. (15)-(17) of Appendix B in the r - z plane over each
subinterval. Increasing the order of the Gaussian quadrature does not sig-

4

nificantly affect the accuracy of the computations. However, the error was found to decrease proportionately as the number subintervals n was increased.

In another solution approach, the potential was assumed to vary linearly over each interval in order to improve the accuracy of the correct potential values. However, the results using this linear interpolation scheme were not as accurate as in the above-mentioned approach. The cause of the inaccuracies in this scheme have not been extensively studied because of time restrictions. However, the errors appear to arise from the implementation procedure used. When linear interpolation was applied to a finite cylinder, problems arose at the corner points. At these points the normal to the surface appearing in the integral equation is undefined. If the potential is assumed constant over each subinterval, subintervals can be taken on either side of this point which in effect avoids the corner points. The method used in applying the linear interpolation about these points strongly influences the computed results. Although several techniques were tried, none proved entirely satisfactory. Also, for general surfaces for which the subintervals may be of unequal length, the difficulty in implementing the linear interpolation technique and its questionable value make this method impractical. Therefore, it will not be used in future studies unless significant improvements can be made.

In another study involving the numerical evaluation of the integral equations, the effect of the coupling constant (α appearing in Eq. (23) of Appendix A) was investigated. In the method of Burton and Miller, the integral equations for the acoustic potential and normal velocity at the surface are combined into one equation. The terms from the potential equation are of order k whereas the terms from the expression for the normal velocity are of

order k^2. Thus, as the frequency is increased, the terms of order k^2 dominate. The results become less accurate because the combined equation in effect becomes the equation for the normal velocity. This equation, like the integral formula for the acoustic potential, yields large errors at certain frequencies when numerically evaluated. By choosing the coupling constant to be i/k, the terms of order k^2 are now reduced to order k. Now, as the frequency is increased, the terms from the expression for the normal velocity do not become dominant, and the uniqueness problem is avoided at all frequencies.

B. Evaluation of Geometric Parameters and Boundary Conditions

The geometric parameters appearing in the integral Helmholtz equation (see Equation (23) of Appendix A) are the distances between points on the surface, the normal vector at each point, and the lengths of the subintervals in the axial plane. The method for computing these parameters is presented in Section III of Appendix C.

There are two types of boundary conditions which must be specified over the surface. The first consists of a forcing function which generates the acoustic field. In a jet engine inlet, most of the acoustic field is produced by disturbances caused by the interaction between the flow field produced by the fan blades and the stator waves. A literature search was conducted to determine the spatial dependence of the sound generated by the stator-blade interaction so that the resulting radiated sound pattern could be computed. Because of the complexity of the resulting expressions[4], there was not sufficient time to use these predictions in the present research effort. However, both the analytical and numerical methods used in computing the radiated sound field in the present study are capable of handling forcing functions

of arbitrary spatial dependence in the r - z plane, such as those encountered in jet engine inlets.

The second type of boundary condition is given by specifying the reaction of the surface to the wave motion. For rigid surfaces, the normal velocity (i.e., the normal derivative of the acoustic potential) is zero and all the sound incident on the surface is reflected. For nonrigid or sound absorbing surfaces, the normal velocity is nonzero since the surface now vibrates in response to the wave motion. The normal velocity at the surface is propor- tional to the pressure oscillations (i.e., the acoustic potential) of the surrounding fluid and the constant of proportionality is called the surface admittance. The integral wave equation involves both the acoustic potential and the normal acoustic velocity which means there is one equation for two unknowns. By using the admittance relationship, the normal velocity can be expressed in terms of the acoustic potential and the admittance. The result- ing equation can then be solved for the potential.

The admittance is a measure of the sound absorption characteristics of the surface. In jet engine inlets the surfaces are often lined with Helm- holtz resonator arrays which absorb sound and reduce the noise radiated to the surroundings. Expressions for the admittances of these sound absorbing devices have been derived[5] and they can be used in the present investigation. In fact, the capability exists to predict the sound field produced from a jet engine inlet for arbitrary sound source and admittance characteristics.

C. Computer Program

A computer program written in Extended FORTRAN IV has been developed for use on a CDC CYBER 70 computer for solving the system of linear alge- braic equations which result from the numerical approximation to the inte- gral wave equation. This program has been thoroughly checked out using

7

simple geometries for which exact solutions can be obtained. The program

employs standard functions common to all FORTRAN compilers so that it can

be used with minimum modifications on other computers. Generality is main-

tained in order to accommodate arbitrary surface geometries and boundary

conditions. In the cases run to date, the computation time for determining

the surface potential is given by the following approximate formula

$$t = 0.05 \ (n)^2$$

where t is the computation time in seconds and n is the number of subinter-

vals used in the numerical evaluation of the integral equation. Approximately

one second per point is required for the far field potential. For the cases

run thus far, the run times have been from 20 to 140 seconds for 20 to 53

subintervals. Efforts toward maximizing the programming and numerical effi-

ciency have resulted in these relatively short run times.

IV. RESULTS AND SUMMARY

A. Simple Geometries

To check the numerical schemes used in this investigation, preliminary

computations using a sphere and a cylinder of finite length were obtained.

The results are presented in Section III of Appendix B. In all cases, 20

subintervals were taken in the r - z plane and a 20-point Gaussian quadrature

was used to evaluate the integrals in the tangential direction. The results

for these simple geometries can be summarized as follows:

(1) The coupling parameter used in the Burton and Miller (α in Eq. (23)

   Appendix A) should be taken as i/k where k is the wave number and

   i is $\sqrt{-1}$.

(2) For the cylinder, the error in the computed results increases with
    increasing frequency. For continuous boundary conditions the error
    is less than 10% at all frequencies.

(3) Discontinuous boundary conditions, where the admittance is specified
    over part of the surface and a forcing function over the remainder,
    decrease accuracy of the results. The computed and exact values agree
    to within 10% for low nondimensional wave numbers (i.e., $ka < 5$ where
    a is the radius of the cylinder). Errors of 40% at the point of dis-
    continuity occur at a nondimensional wave number of 10. The remainder
    of the points agree to within 12% at this frequency.

(4) In the tangential plane, the spatial distribution of the acoustic
    potential varies as $\cos m\theta$ where m is an integer. Increasing m
    does not affect the accuracy of the results significantly.

(5) The computed far field acoustic potentials are at least as accurate
    as the computed surface potentials.

(6) The far field results are accurate at distances greater than the
    length of one subinterval from the surface.

B. Inlet Configuration

The studies of the acoustic fields of the sphere and cylinder served to
evaluate and refine the numerical procedures and programming techniques. The
next configuration investigated was an inlet used in a study by NASA[6]. This
inlet is shown in Fig. 1 and it was chosen because:

(1) unlike most inlets used in research studies, it does not have a bell-
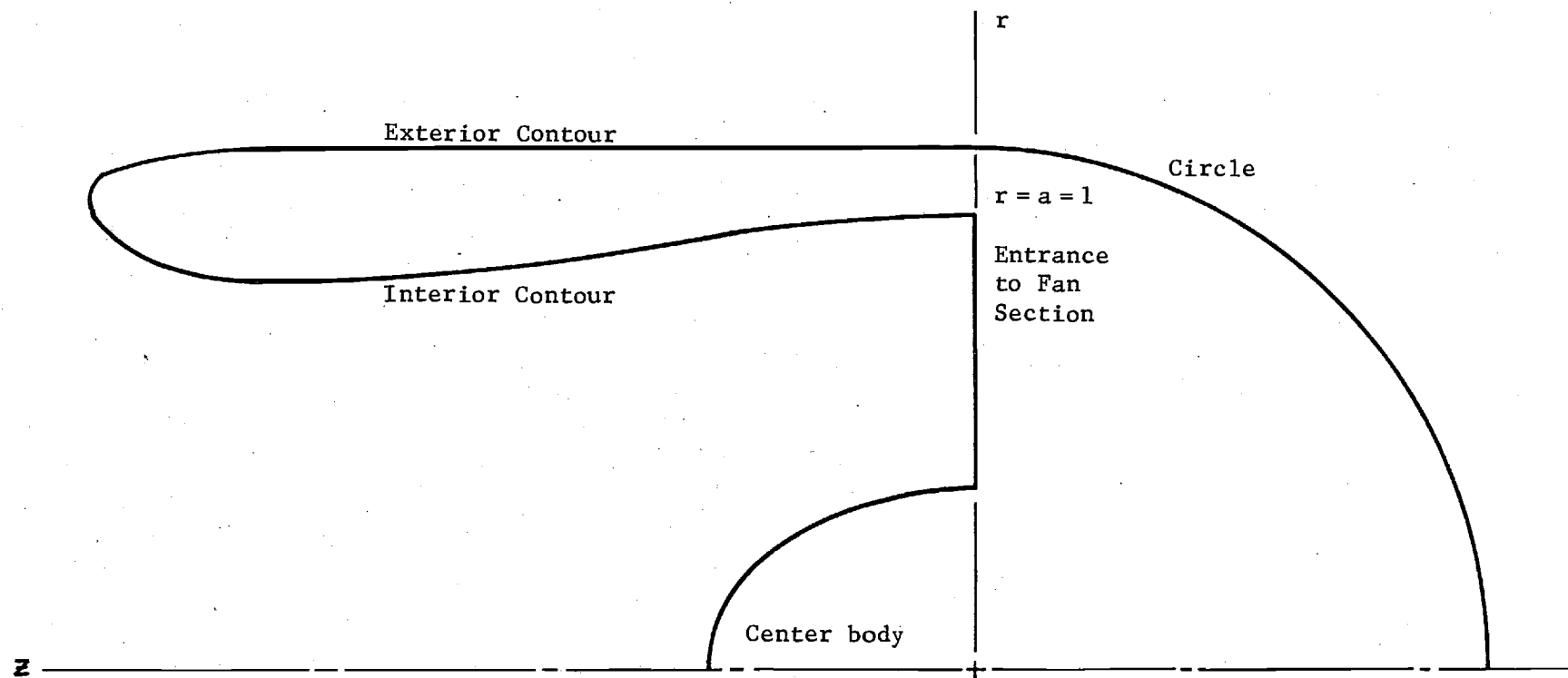   mouth shape but is shaped like a typical inlet used in existing
    aircraft;

Exterior Contour

Circle

$r = a = 1$

Entrance
to Fan
Section

Interior Contour

Center body

r

z

Figure 1. Inlet Geometry

(2) complete details on generating the inlet boundary are given; and

(3) it is being used in a related study being conducted at Georgia
    Tech concerning the prediction of the sound field inside the
    inlet; so the sound field, at least inside the duct, can be com-
    pared with results obtained independently by other numerical
    methods.

The back side of the inlet is presently assumed to be spherical.

To obtain exact results for comparison with the numerical computations, a spherical source was assumed to be placed at $(r,z) = (0,0)$. The acoustic potential and normal velocity for this source can be readily computed at every point. In particular, they can be computed on the surface of the inlet. The value of the normal velocity at each point along the surface of the inlet is then used as the boundary condition in the integral equation. From this boundary condition the value of the potential can then be numerical-ly computed using the techniques described in Chapter III and compared with the exact potential known from the spherical source solution. As seen in Fig. 2, the normal acoustic velocity distribution, which represents a forcing function is highly discontinuous and it provides a severe test of the numeri-cal techniques employed.

The numerical and exact solutions for the surface acoustic potential are compared in Fig. 2 for 32 and 54 subintervals taken along the perimeter of the inlet in the r - z plane. Because of the errors in approximating the lengths of each subinterval, the exact solutions differ slightly as the distance along the perimeter S increases. The centerbody in Fig. 1 extends from $0 \leq S \leq 0.8$, the fan inlet covers $0.8 < S \leq 1.4$, the interior contour extends from $1.4 < S \leq 3.5$, the exterior from $3.5 < S \leq 5.5$, and the circular arc lies within the interval
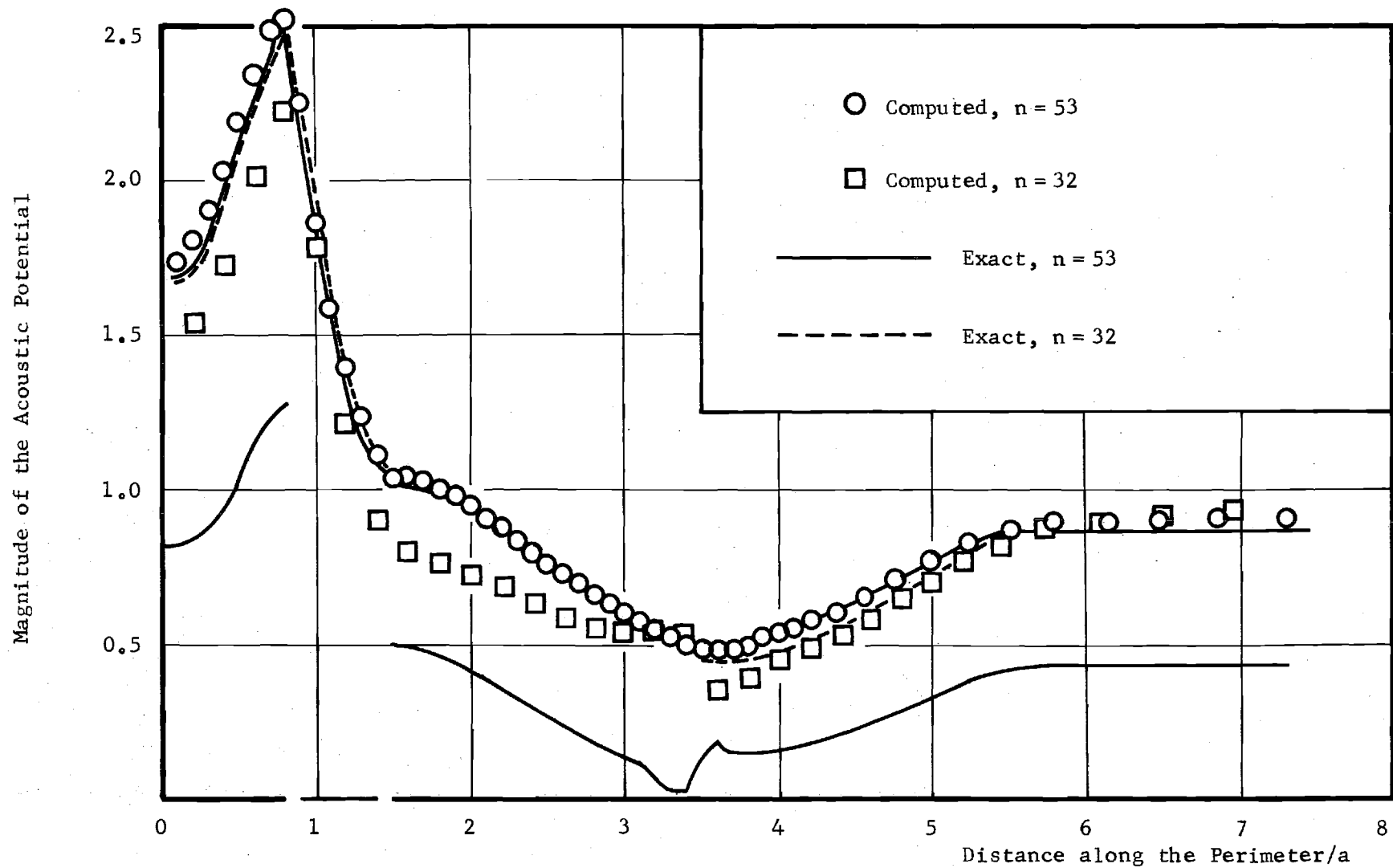
Figure 2. Effect of Increasing the Number of Subintervals in Computing
the Surface Potential for the Inlet Configuration at k a = 1, m = 0.

$5.5 < S \leq 7.45$. Increasing the number of points decreases the error proportionately as indicated by the data in Fig. 2 at a nondimensional frequency to a' of unity, where a is the radius of the inlet at the fan entrance section. The absolute average error in the results decrease from 10.2 per cent for 32 subintervals to 4.16 per cent for 53 subintervals. The computation time increased from 53 seconds to 143 seconds, respectively.

As shown in Fig. 3, the errors increase with increasing frequency. Like the cylinder, the maximum error of the potential for the inlet configuration occurs at the points of discontinuity. The average error increases from 4.16 per cent at $ka = 1$ to 15 per cent at $ka = 10$.

For the data in Figs. 2 and 3, the acoustic potential is assumed constant in the tangential plane. The results for a $\cos(m\theta)$ distribution are presented in Fig. 4 at $ka = 2$. These results show the insensitivity of the accuracy of the computed results to the tangential distribution for $m = 1, 2$.

Based on the results obtained thus far, the numerical and programming techniques are capable of yielding reliable results for arbitrary geometries and boundary conditions. At higher frequencies, $(ka < 5)$ it appears that more points must be taken to increase the accuracy of the computed results.

Next year, experiments will be conducted to measure the acoustic field radiated from an open-ended pipe for comparison with the computed results. A parametric study of the effect of the placement and quality of sound treatment on sound abatement in an inlet configuration will be conducted. Further improvements in the programming and numerical methods will also be investigated.
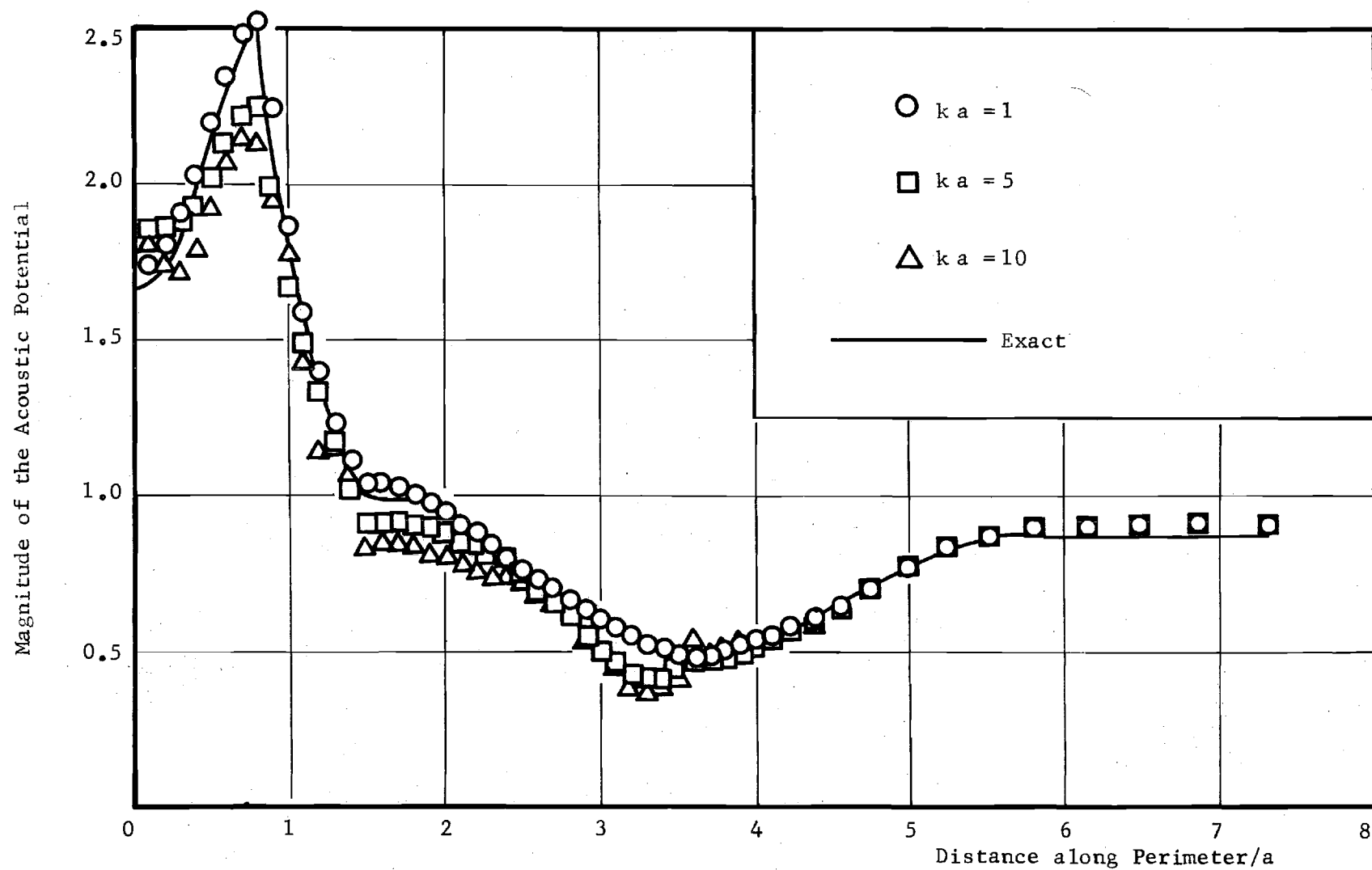
Figure 3. Effect of Increasing Frequency for the Inlet Configuration at m = 0, n = 53 on the Computed Surface Potential.
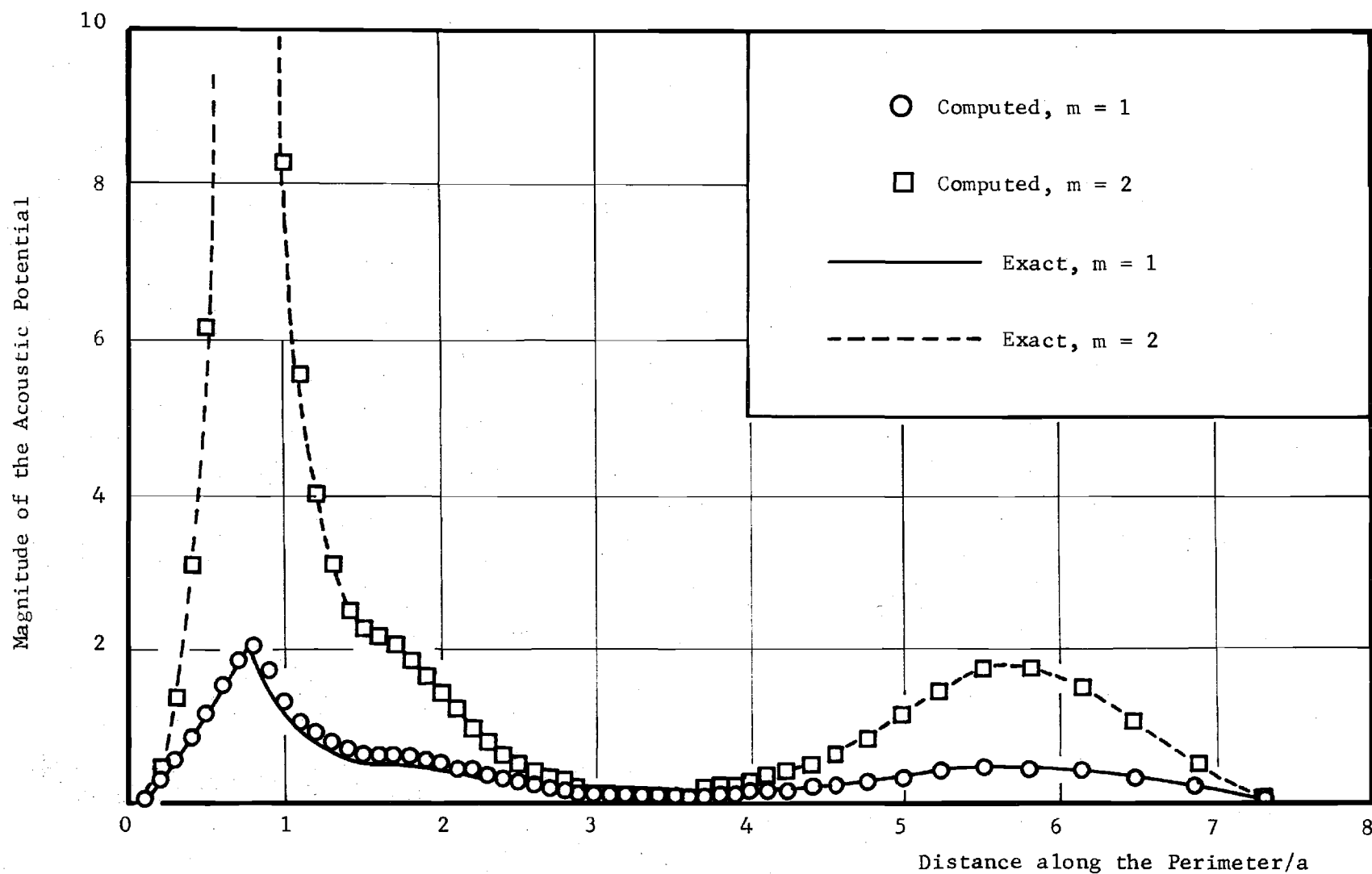
Figure 4. Effect of Mode Number m on the Computed Surface Potential of the Inlet Configuration for $k\,a = 2$ and $n = 53$.

REFERENCES

1. Meyer, W. L., Bell, W. A., and Zinn, B. T., "Boundary Integral Solutions of Three Dimensional Acoustic Radiation Problems," accepted for publication in the Journal of Sound and Vibration.

2. Meyer, W. L., Bell, W. A., and Zinn, B. T., "Prediction of the Sound Field Radiation from Axisymmetric Surfaces," AIAA Paper No. 78-195, presented at the AIAA 16th Aerospace Sciences Meeting, Huntsville, AL., January 1978.

3. Bell, W. A., Meyer, W. L., and Zinn, B. T., "Predicting the Acoustics of Arbitrarily Shaped Bodies Using an Integral Approach," AIAA Journal, Vol. 15, No. 6, June 1977, pp. 813-820.

4. Goldstein, M. E., Aeroacoustics, McGraw-Hill, 1976, Chapter 4.

5. Bell, W. A., Daniel, B. R., and Zinn, B. T., "Acoustic Liner Performance in the Presence of a Mean Flow and Three-Dimensional Wave Motion," AIAA Paper No. 74-61, presented at the AIAA 12th Aerospace Sciences Meeting, Washington, D. C., January 30 - February 1, 1974.

6. Miller, B. A., Dastoli, B. J., and Wesoky, H. L., "Effect of Entry-Lip Design on Aerodynamics and Acoustics of High-Throat-Mach-Number Inlets for the Quiet, Clean, Short-Haul Experimental Engine," NASA TM- X-3222, May 1975.

APPENDIX A

Integral Solutions of Three Dimensional

Acoustic Radiation Problems[*]

W. L. Meyer[**], W. A. Bell[†], B. T. Zinn[††]

School of Aerospace Engineering
Georgia Institute of Technology
Atlanta, Georgia 30332

Abstract

This paper is concerned with the development of a procedure for generating the sound fields radiated by arbitrarily shaped, three dimensional bodies from an integral representation of the solutions of the Helmholtz equation. The method of Burton and Miller is employed to eliminate the nonuniqueness in the external Helmholtz formulae which occurs at the internal eigenfrequencies of the geometry under consideration. Also, a representation of the most singular component in the Burton and Miller formulation is developed resulting in an integral equation which is amenable to numerical solutions. A simple numerical scheme is introduced which reduces the large amounts of computer storage and time normally required for the solution of similar problems. This numerical scheme is then used to obtain solutions for the radiated sound field generated by a vibrating piston set in a sphere. The numerical solutions for the surface and far field sound patterns are compared with exact analytical solutions and deviations of ten percent at most are noted. Since the symmetry of the sphere was not taken advantage of in these computations, the numerical schemes employed are applicable to general three dimensional sound radiation problems.

I. Introduction

The development of a simple analytical form and an efficient numerical method for the prediction of the characteristics of the sound fields radiated by three dimensional bodies is the main concern of this paper. Such prediction techniques have a variety of applications in science and engineering; for example, the determination of the sound fields radiated by aircraft and underwater vehicles. The approach developed in this investigation is by no means limited to acoustic radiation problems as other wave phenomena are governed by similar equations. Thus, the analytical and numerical methods employed here are also directly applicable to other fields of engineering such as electromagnetic antenna theory

and wave scattering problems.

This research was undertaken with the objective of determining the applicability of certain integral equation formulations for the exterior Helmholtz problem in the prediction of the radiated sound fields produced by three dimensional bodies. In principle, integral formulations appear very attractive as they (1) eliminate the need to consider the infinite domains normally associated with radiation problems; (2) reduce the dimensionality of the problem by one (e.g., from a three dimensional partial differential equation to a two dimensional surface integral equation); and (3) can readily handle arbitrary geometries and boundary conditions. All three properties are very advantageous from a computational point of view as the first two significantly reduce the computer storage requirement for solution and the third eliminates the need to extensively modify the computer code when the geometry or the boundary conditions are altered.

Difficulties arise, however, in the use of the Helmholtz formulae as their solution depends upon the numerical evaluation of singular, oscillatory integrands.[1-5] Also, most external boundary integral representations suffer from a nonuniqueness of the solution at frequencies corresponding to the eigenfrequencies of the associated internal problem of the same geometry.[6-8] Keeping these difficulties in mind, the work presented in this paper is specifically concerned with the following problems: (1) the development of an accurate and efficient numerical scheme for handling the oscillatory, singular integrands encountered in the application of the Helmholtz formulae; (2) the determination of the most effective procedure for handling the nonuniqueness of the radiation solution at eigenvalues of the associated internal acoustic problem; and (3) the determination of the accuracy of the resulting solutions.

While there are many papers in the literature (e.g., see Refs. 1-8) dealing with integral solutions of radiation problems, none of these addresses the important problem of determing the applicability and relative efficiency of the various integral formulations and numerical procedures which can be employed to obtain the desired solutions. Instead, most of these investigations are limited to discussions of the potential advantages of the use of certain integral formulations, various possible approaches for the numerical solution of the resulting integral equations, the nonuniqueness of the solutions of the integral equations which govern the radiation problems, and potential means for alleviating this nonuniqueness problem. The few papers (e.g., see Refs. 1-6 and 9) that deal with the numerical solutions of specific problems are either limited to two dimensional problems or three dimensional problems with simple boundary conditions, such as perfectly reflecting surfaces, which greatly simplify the analytical form and the numerical solution procedure. In the present investigation the analytical and numerical schemes are applied to problems involving general boundary conditions.

II. Theoretical Considerations.

In this section an outline of the development of the theory upon which the calculations are based is presented. The basic integral representation of the solution of the Helmholtz equation is rigorously developed in Ref. (10) and will not be repeated here; however, derivations that are directly related to the present investigation are presented in detail.

A. Formulation of the Integral Equation

The standard three dimensional Helmholtz formula for an external (radiation) problem is[7,10]

$$\int\int_{S_q} \left\{ \varphi(Q) \, \frac{\partial G(P,Q)}{\partial n_q} - G(P,Q) \, \frac{\partial \varphi(Q)}{\partial n_q} \right\} dS_q = 4 \, \pi \, \varphi \, (P)$$

(1)

(See Fig.1.) where G(P,Q) is a fundamental solution of the Helmholtz equation; that is:

$$G(P,Q) = \frac{e^{ikr(P,Q)}}{r(P,Q)} \tag{2}$$

and k is the wave number. In Eq. (1) $\frac{\partial}{\partial n_q}$ represents an outward normal derivative with respect to the body (i.e. inward with respect to the exterior region) of the function with respect to the variable Q; i.e.

$$\frac{\partial \varphi(Q)}{\partial n_q} = \vec{\nabla}_q \varphi(Q) \cdot \vec{n}_q \tag{3}$$

where φ is the acoustic potential.

Introducing the modified admittance, Y, defined as

$$Y(Q) = \frac{\partial \varphi(Q)}{\partial n_q} / \varphi(Q) \tag{4}$$

Eq. (1) can be rewritten as

$$\iint_{S_q} \varphi(Q) \left\{ \frac{\partial G(P,Q)}{\partial n_q} - G(P,Q) Y(Q) \right\} dS_q = 4\pi \varphi(P) \tag{5}$$

Thus, using Eq. (1) or Eq. (5), the acoustic potential $\varphi(P)$ at any point outside the surface of the body S can be determined if the acoustic potential on the surface of the body $\varphi(Q)$ and either its normal derivative $\frac{\partial \varphi(Q)}{\partial n_q}$ (the acoustic velocity) or the admittance Y(Q) on the surface of the body are known.

If the point P is allowed to approach the surface of the body, Eq. (5) becomes

$$\iint_{S_q} \left\{ \varphi(Q) \frac{\partial G(P,Q)}{\partial n_q} - G(P,Q) \frac{\partial \varphi(Q)}{\partial n_q} \right\} dS_q = 2\pi \varphi(P) \tag{6}$$

if the surface S is sufficiently smooth. Using Eq. (4), Eq. (6) becomes

$$\int\int_{S_q} \varphi(Q) \left\{ \frac{\partial G(P,Q)}{\partial n_q} - G(P,Q)\, Y(Q) \right\} dS_q = 2\pi\varphi(P) \qquad (7)$$

The integral Eqs. (6) or (7)* can now be solved for the acoustic potential on the surface if either the acoustic velocity or the admittance is known at each point on the body. Also if the acoustic velocity is known over part of the body (i.e. the driving surface) and the admittance over the remainder, Eq. (6) may be applied on the driving surface and Eq. (7) over the rest of the body.

Both G and its first normal derivative with respect to the variable Q, which appear in the kernels of Eqs. (6) and (7), become singular when the point Q approaches the point P on the surface (See Eq. (2).). It can be shown, however, that the integrals are regular in spite of this singularity of the kernels, and no analytical problems arise because of it. However, the singular kernels do present numerical difficulties which will be discussed in Section III.

An analytical problem does arise in the solution of Eqs. (6) and (7) when the wave number k, which appears in the simple source solution G (See Eq.(2).) approaches a resonant frequency (i.e. an eigenvalue) of the related internal problem.[7,11] At these frequencies Eqs. (6) and (7) do not yield a unique solution.

B. The Uniqueness Problem

Since the uniqueness problem occurs only at certain wave numbers corresponding to internal eigenvalues it might be suggested that the problem be simply avoided by considering only wave numbers which are not close to internal

---

* It will be noted here that Eq. (7) yields a homogeneous set of equations if only the admittance is known. Thus to obtain a unique solution the acoustic potential must be known on part of the body.

eigenvalues. This is not feasible, however, because: (1) if the body is truly arbitrary in shape the internal eigenvalues are not known a priori and the corresponding internal problem would also have to be solved in order to determine what wave numbers to avoid; (2) the integral equation is discretized for numerical integration, which results in a system of algebraic equations, so that there is no longer a specific value but a range of values at which the coefficient matrix becomes ill-conditioned which results in large numerical errors;[*] and (3) the interval between successive eigenvalues decreases with increasing wave number and it becomes impossible to stay "sufficiently" far away from the internal eigenvalues at high wave numbers (e.g., k on the order of 10).

It has been suggested[6] that one method to assure the uniqueness of the solution is to obtain an overdetermined system of algebraic equations by combining the system of algebraic equations generated from the standard integral equation (e.g., Eq. (6)) with additional algebraic equations generated from the integral relation

$$\int\int_{S_q} \left\{ \varphi(Q) \frac{\partial G(P,Q)}{\partial n_q} - G(P,Q) \frac{\partial \varphi(Q)}{\partial n_q} \right\} dS_q = 0 \qquad (8)$$

where the point P lies inside the surface S. There are two problems with this approach. The first is determining the number of extra relations required to "pick-out" the proper solution from the set of possible solutions of the non-unique integral equation; and, the second is choosing the placement of the

---

[*] If the admittance is non-zero the internal eigenvalues of the problem are in general complex. However, even if only real wave numbers are considered the nonuniqueness problem still exists if the imaginary part of the complex eigenvalue is sufficiently close to zero.

points which are used to generate the extra relations. As there is no known procedure for choosing either the optimum number of extra relations or the points from which they are generated, this method can not be relied upon to give consistently good results.

Ursell[12] has suggested that the uniqueness problem be avoided by the use of a different fundamental solution (i.e. a different G function; see Eq. (2)). Although the use of a different fundamental solution does not change the resulting integral equations and analytically eliminates the uniqueness problem rather elegantly, the function itself is difficult to construct numerically as it entails the computation of infinite series. Thus the elegance of the method is offset by the large increases in computer time and storage required for its implementation, especially when considering three dimensional problems.

Another method for overcoming the uniqueness problem is based upon the fact that a unique solution can be obtained by solving a modified integral equation consisting of the original integral equation (6) and its differentiated form[7], that is

$$\int\int_{S_q} \left\{ \varphi(Q)\ \frac{\partial^2 G(P,Q)}{\partial n_p \partial n_q} - \frac{\partial G(P,Q)}{\partial n_p}\ \frac{\partial \varphi(Q)}{\partial n_q} \right\}\ dS_q = 2\pi\ \frac{\partial \varphi(P)}{\partial n_p} \tag{9}$$

Equation (9) also describes the behavior of the acoustic potential on the surface of the body, and it has a set of related internal eigenvalues which is mutually exclusive of the set of related internal eigenvalues of Eq. (6). Thus, neither equation ever fails to yield a unique solution at the same k value as the other. Using this fact, the following linear combination of Eqs. (6) and (9)

$$\int\int_{S_q} \left\{ \varphi(Q) \frac{\partial G(P,Q)}{\partial n_q} - G(P,Q) \frac{\partial \varphi(Q)}{\partial n_q} \right\} dS_q$$

$$+ \alpha \int\int_{S_q} \left\{ \varphi(Q) \frac{\partial^2 G(P,Q)}{\partial n_p \partial n_q} - \frac{\partial G(P,Q)}{\partial n_p} \frac{\partial \varphi(Q)}{\partial n_q} \right\} dS_q \qquad (10)$$

$$= 2\pi \left(\varphi(P) + \alpha \frac{\partial \varphi(P)}{\partial n_p} \right)$$

where α is a coupling constant, should yield a unique solution for all values of the wave number k.

Specifically, Burton and Miller[13], have shown that the following relationships exist between the coupling constant α and the wave number k

Im $(\alpha) \neq 0 \rightarrow$ k real or imaginary

Im $(\alpha) = 0 \rightarrow$ k complex \qquad (11)

which assures a unique solution. Unfortunately, the differentiated form of the integral equation (9) contains the following term

$$\int\int_{S_q} \varphi(Q) \frac{\partial^2 G(P,Q)}{\partial n_p \partial n_q} dS_q \qquad (12)$$

which is strongly singular as the point Q approaches the point P. Because of its singular form this term cannot be directly integrated numerically.

Two methods for approaching this problem have been suggested. The first solution is to "regularize" the singular component by an integration of the entire equation[14] (See Eq. (10).). This method requires an excessive amount of computing time as an additional integration must be performed over the surface of the body. The other approach suggests the use of a transformation to interpret the singular integral[15] (See Eq. (12).). In Ref. (15) two alternate

forms of the singular integral are put forth. The first requires further manipulation to be of use as it contains yet another singular integral. The second requires an excessive amount of computer storage space as it necessitates additional information that will allow the computation of the tangential derivative of the acoustic potential on the two dimensional surface of the body. It must also be noted that the acoustic potential is the unknown in most problems so that some differencing procedure is required to generate the solution $\varphi(Q)$.

C. Treatment of the Singular Integral

In this section the first relationship developed in Ref. (15) (See pp. 1283-1284.) is used as a starting point for deriving the desired expressions. It is shown in Ref. (15) that

$$
\iint_{S_q} \varphi(Q) \frac{\partial^2 G(P,Q)}{\partial n_p \partial n_q} dS_q
$$

$$
= \iint_{S_q} \varphi(Q) (n_p \cdot n_q) \nabla_p \cdot \nabla_q G(P,Q) dS_q
$$

$$
+ \iint_{S_q} \varphi(Q) (n_p \times n_q) \cdot (\nabla_p \times \nabla_q G(P,Q)) dS_q
$$

$$
- \iint_{S_q} \varphi(Q) n_q \cdot \nabla_q \times (n_p \times \nabla_p G(P,Q)) dS_q
$$

(13)

The first two integrals on the right hand side are regular; however, the third is not. It is also shown that after some manipulation an alternate form of the third term is

$$
\iint_{S_q} \left[n_q \times \nabla_q \varphi(Q) \right] \cdot \left[n_p \times \nabla_p G(P,Q) \right] dS_q
$$

(14)

This integral is regular so that the singular integral has been shown to be equivalent to the sum of three regular integrals. It should be noted that the first term in this integral, $\left[n_q \times \nabla_q \, \varphi(Q) \right]$, is the tangential derivative of the acoustic potential on the surface of the body alluded to in the previous subsection.

An interesting property of this integral, Eq. (14), is that if the acoustic potential $\varphi(Q)$ is a constant on the surface of the body, the integral is zero as in this case $n_q \times \nabla_q \, \varphi(Q) = 0$. Since the two formulations are equivalent it follows that

$$
- \iint\limits_{S_q} \varphi(Q) \, n_q \cdot \nabla_q \times (n_p \times \nabla_p \, G(P,Q)) \, dS_q
$$

$$
= \iint\limits_{S_q} \left[n_q \times \nabla_q \, \varphi(Q) \right] \cdot \left[n_p \times \nabla_p \, G(P,Q) \right] \, dS_q
$$

(15)

Writing the third integral on the right hand side of Eq. (13) as

$$
- \iint\limits_{S_q} (\varphi(Q) - \varphi(P)) \, n_q \cdot \nabla_q \times (n_p \times \nabla_p \, G(P,Q)) \, dS_q
$$

(16)

$$
- \varphi(P) \iint\limits_{S_q} n_q \cdot \nabla_q \times (n_p \times \nabla_p \, G(P,Q)) \, dS_q
$$

where $\varphi(P)$ is a constant with respect to the variable Q, we see that the last integral is identically zero by setting $\varphi(Q) \equiv 1$ in Eq. (15).

Hence, the first term in Eq. (16) is not only regular but it can also be readily integrated numerically. As point Q approaches point P the entire integral goes to zero. Thus it has been shown that the singular integral which appears in the "unique" formulation of this problem can be expressed in the

following form

$$\iint\limits_{S_q} \varphi(Q) \frac{\partial^2 G(P,Q)}{\partial n_p \partial n_q} \, dS_q$$

$$= \iint\limits_{S_q} \varphi(Q) \, (n_p \cdot n_q) \, \nabla_p \cdot \nabla_q \, G(P,Q) \, dS_q$$

(17)

$$+ \iint\limits_{S_q} \varphi(Q) \, (n_p \times n_q) \cdot (\nabla_p \times \nabla_q \, G(P,Q)) \, dS_q$$

$$- \iint\limits_{S_q} \left[\varphi(Q) - \varphi(P) \right] n_q \cdot \nabla_q \times (n_p \times \nabla_p \, G(P,Q)) \, dS_q$$

which will be used in the numerical computations of this paper.

D. Computational Considerations

Because of the special form of the fundamental solution of the Helmholtz equation, $G(P,Q) = G(Q,P)$, (See Eq. (2).) certain simplifications can be made; specifically

$$\nabla_p \cdot \nabla_q \, G(P,Q) = - \nabla_q^2 \, G(P,Q) = k^2 \, G(P,Q)$$

(18)

$$\nabla_p \times \nabla_q \, G(P,Q) = - \nabla_q \times \nabla_q \, G(P,Q) = 0$$

Using the above relationships Eq. (17) can be rewritten as follows:

$$\iint\limits_{S_q} \varphi(Q) \frac{\partial^2 G(P,Q)}{\partial n_p \partial n_q} \, dS_q$$

$$= - \iint\limits_{S_q} \varphi(Q) \, (n_p \cdot n_q)(ik)^2 \, G(P,Q) \, dS_q$$

(19)

$$- \iint\limits_{S_q} \left[\varphi(Q) - \varphi(P) \right] n_q \cdot \nabla_q \times (n_p \times \nabla_p \, G(P,Q)) \, dS_q$$

To reduce Eq. (19) to a form more amenable to numerical computation it is convenient to let $\varphi(Q) = 1$ so that

$$\iint\limits_{S_q} \frac{\partial^2 G(P,Q)}{\partial n_p \partial n_q} \, dS_q$$

$$= -\iint\limits_{S_q} (n_p \cdot n_q)(ik)^2 \, G(P,Q) \, dS_q \tag{20}$$

Using Eq. (20) the left hand side of Eq. (19) can be rewritten as

$$\iint\limits_{S_q} \varphi(Q) \, \frac{\partial^2 G(P,Q)}{\partial n_p \partial n_q} \, dS_q$$

$$= \iint\limits_{S_q} \left[\varphi(Q) - \varphi(P) \right] \frac{\partial^2 G(P,Q)}{\partial n_p \partial n_q} \, dS_q \tag{21}$$

$$- \varphi(P) \iint\limits_{S_q} (n_p \cdot n_q)(ik)^2 \, G(P,Q) \, dS_q$$

If Eq. (2) is employed and the indicated differentiations are performed the right hand side, Eq. (21) can be rewritten in the following form

$$\iint\limits_{S_q} \left[\varphi(Q) - \varphi(P) \right] \frac{e^{ikr(P,Q)}}{r(P,Q)} \left\{ \left[(ik)^2 - \frac{3\,i\,k}{r(P,Q)} + \frac{3}{[r(P,Q)]^2} \right] \right.$$

$$\left. \frac{\partial r(P,Q)}{\partial n_p} \frac{\partial r(P,Q)}{\partial n_q} - \frac{n_p \cdot n_q}{r(P,Q)} \left[ik - \frac{1}{r(P,Q)} \right] \right\} dS_q$$

$$- \varphi(P) \iint\limits_{S_q} \frac{e^{ikr(P,Q)}}{r(P,Q)} (ik)^2 (n_p \cdot n_q) \, dS_q \tag{22}$$

where $\dfrac{\partial r(P,Q)}{\partial n_p} = \vec{\nabla}_p \, r(P,Q) \cdot \vec{n}_p$. Using the results developed in this section

the formulation of Burton and Miller[13] (See Eq. (10).) reduces to

$$\int\int_{S_q} \varphi(Q) \; \frac{e^{ikr(P,Q)}}{r(P,Q)} \; (ik - \frac{1}{r(P,Q)}) \; \frac{\partial r(P,Q)}{\partial n_q} \; dS_q$$

$$- \alpha \, \varphi(P) \int\int_{S_q} \frac{e^{ikr(P,Q)}}{r(P,Q)} \; (ik)^2 \; (n_p \cdot n_q) \; dS_q$$

$$+ \alpha \int\int_{S_q} \left[\varphi(Q) - \varphi(P) \right] \frac{e^{ikr(P,Q)}}{r(P,Q)} \left\{ \left[(ik)^2 - \frac{3ik}{r(P,Q)} + \frac{3}{[r(P,Q)]^2} \right] \right.$$

$$\frac{\partial r(P,Q)}{\partial n_p} \frac{\partial r(P,Q)}{\partial n_q} - \frac{n_p \cdot n_q}{r(P,Q)} (ik - \frac{1}{r(P,Q)}) \left. \right\} dS_q$$

$$- \int\int_{S_q} \frac{\partial \varphi(Q)}{\partial n_q} \; \frac{e^{ikr(P,Q)}}{r(P,Q)} \; dS_q$$

$$- \alpha \int\int_{S_q} \frac{\partial \varphi(Q)}{\partial n_q} \; \frac{e^{ikr(P,Q)}}{r(P,Q)} \; (ik - \frac{1}{r(P,Q)}) \; \frac{\partial r(P,Q)}{\partial n_p} \; dS_q$$

$$= 2 \, \pi (\varphi(P) + \alpha \, \frac{\partial \varphi(P)}{\partial n_p}) \tag{23}$$

The above equation, although it may appear more complicated, is actually considerably simpler from a numerical point of view than solving Eq. (10) with Eqs. (13) and (14). In summary, the above formulation of the sound radiation problem provides unique solutions at all wave numbers k and contains no singular integrals.

III. Numerical Considerations.

To determine the radiated sound field generated by an arbitrarily shaped three dimensional body, Eq. (23) must first be solved for the distribution of the acoustic potential on the surface of the body, $\varphi(Q)$. Then this data needs

to be substituted into Eq. (1) to determine the radiated sound field. Inspection

of Eq. (23) indicates that all of the integrands appearing in this equation are

both oscillatory and singular due to the factor $\dfrac{e^{ikr(P,Q)}}{r(P,Q)}$ which appears in

each. Therefore care must be exercised in the numerical representation of these

kernels.

When considering the numerical evaluation of an integral on an arbitrary

two dimensional surface, such elegant computational methods as Gaussian quad-

rature[16,17] (which has been found by the authors of this paper to yield accurate

results in two dimensional sound radiation problems[18]) cannot be used in the

numerical representation of the kernels. The only simple approach available to

obtain a more accurate representation of the kernels is to evaluate them at

more points on the surface of the body. Unfortunately, this is usually accom-

panied by an attendant increase in the size of the coefficient matrix which

must be solved to obtain the acoustic potential. The computer time required

to solve this matrix goes up roughly as the square of the number of unknowns

for most methods of solution (e.g., Gauss-Jordan reduction).

Two considerations enter into the determination of the size of the coeffi-

cient matrix: (1) the heuristic determination of the number of points required

on the surface of the body to represent the acoustic potential to the desired

accuracy; and (2) the computer time and storage space available to solve the

coefficient matrix resulting from the discretization of the integral equation.

The storage space available is usually much smaller than the number of

points required for the accurate evaluation of the singular, oscillatory kernels.

In view of the above considerations the following scheme is used to obtain

a numerical solution. First, the surface of the body is divided into a number

of area elements which corresponds to the number of points where the acoustic

potential is to be calculated on the surface. It has been determined that

better results are obtained in general if the area elements are "regular" (i.e,

not too elongated in any direction), although the exact shape is unimportant, and they should be of roughly equal area. A point is then chosen in the "center" of each area element (usually the centroid of the plane figure projected to the body surface). These points will be denoted as calculational points (i.e. P points) as this is where the acoustic potential will be calculated. Next, each of the original area elements is subdivided into a number of smaller area elements, the sum of which corresponds to the number of points where the singular, oscillatory kernels must be evaluated on the surface of the body to assure their accurate representation. A point is thus chosen on the surface of the body in the "center" of each of the smaller area elements as before. These points will be denoted as computational points (i.e. Q points) since the kernel functions are computed there.

The calculational points may or may not be a subset of the computational points on the surface of the body. If they are a subset some computer space may be saved; however, the computational point must be avoided when it corresponds to a calculational point (i.e. when the point Q corresponds to the point P) since the kernels are then singular. Thus each term in the coefficient matrix is now the sum of a number of terms generated by a number of evaluations of each kernel function.

Since the integrals are all regular a better approximation may be obtained by placing computational points closer to the calculational point when one is close to the singularity of the kernel function. Thus the computational area elements may be further subdivided to obtain a more accurate representation of the integral about the point P.

An illustration of how the above procedure is accomplished is presented below using Eq. (23) which is rewritten in the following more compact form

$$\int\limits_{S_q} \int \varphi(Q)\, A(P,Q)\, dS_q + \varphi(P) \int\limits_{S_q} \int B(P,Q)\, dS_q$$

$$+ \int\limits_{S_q} \int \left[\varphi(Q) - \varphi(P)\right] C(P,Q)\, dS_q - 2\pi\varphi(P) \tag{24}$$

$$= 2\pi\alpha\, \frac{\partial\varphi(P)}{\partial n_p} + \int\limits_{S_q} \int D(P,Q)\, dS_q$$

where the proper form of the integrands can be readily obtained. Next, Eq. (24) is discretized as follows:

$$\sum_{\substack{Q=1 \\ Q\neq P}}^{n} \varphi(Q)\, A(P,Q)\, \Delta S_Q + \varphi(P) \sum_{\substack{Q=1 \\ Q\neq P}}^{n} B(P,Q)\, \Delta S_Q$$

$$+ \sum_{\substack{Q=1 \\ Q\neq P}}^{n} \left[\varphi(Q) - \varphi(P)\right] C(P,Q)\, \Delta S_Q$$

$$+ \varphi(P) \sum_{q=1}^{m} \left[A(P,q) + B(P,q)\right] \Delta S_q - 2\pi\varphi(P) \tag{25}$$

$$= \sum_{\substack{Q=1 \\ Q\neq P}}^{n} D(P,Q)\, \Delta S_Q + \sum_{q=1}^{m} D(P,q)\, \Delta S_q + 2\pi\alpha\, \frac{\partial\varphi(P)}{\partial n_p}$$

$$P = 1,2,\ldots,N$$

where N is the number of calculational points; n is the number of computational points (not including the subdivided element about P), and m is the number of computational points in the subdivided element. In the above representation the normal component of the acoustic velocity, $\frac{\partial\varphi(Q)}{\partial n_q}$, on the body is assumed known and is therefore included in the integrand $D(P,Q)$. Additional input data required to obtain a solution include: (1) the coordinates of each computational point;

(2) the area associated with each computational point and (3) the outward normal vector at each computational point. The information required at the calculational points is included in the above.

If the resulting matrix of coefficients is large, there are many iterative schemes which can be employed in its solution[19]; however, if the matrix is small Gaussian elimination with back substitution may be used. Once the acoustic potential is determined on the surface, Eq. (1) may be used to generate the acoustic potential at any point in the field surrounding the body. In this computation the point Q never coincides with point P and the integrands are never singular; however, they are still oscillatory and care must still be taken to get an accurate representation of the integrals.

Due to the availability of analytical solutions for comparison purposes, the developed numerical procedure has been applied to predict the sound radiated by a sphere. However, it should be reiterated that no advantage was taken of the sphere's relatively simple geometry (i.e. its symmetry) in the numerical computations. Once the needed input data was generated it was treated like any other arbitrarily shaped three dimensional body. The sphere was subdivided into 80 triangles by first taking an icosahedron (a three dimensional figure whose surface consists of 20 equilateral triangles) inscribed in a unit sphere and dividing each triangle into four others (See Ref. (1), pp. 1630-1631.). This was accomplished by finding the midpoint of each side of each triangle and projecting it to the surface of the sphere as shown in Fig. 2. The centroid of each triangle was then found and also projected to the surface of the sphere. These 80 points correspond to the previously described calculational points.

To obtain the computational points this method was simply repeated three more times yielding 5120 points. Around each calculational point the three surrounding triangles were then divided once more, and at the calculational point

itself the triangle was divided twice more as shown in Fig. 3. The spherical

area was then computed for each computational triangle (i.e. the sum of the

areas of all the computational triangles is 4 π, the surface area of the unit

sphere). This yielded all the geometrical input data required, as; for a unit

sphere the coordinates of the computational points and the elements of the

outward normals are the same in rectangular coordinates.

IV. Results and Discussion.

In the calculations performed in this study the surface of the radiating

sphere was divided into two parts. On one part (the driving surface) the normal

acoustic velocity, $\frac{\partial \varphi}{\partial n}$, was specified while on the other part (the admittance

surface) the modified admittance function Y, defined by Eq. (4), was specified

indicating either sound absorption or amplification by this part of the surface

(See Fig. 4.). The sphere was chosen for this study as exact analytical solutions

can be obtained for comparison with the numerical solutions obtained by solving

the integral equations.

Using the well known separation of variables technique it can be shown that

the acoustic potential for the sphere can be represented as follows

$$\varphi(r,\theta,\xi)= h_m(\zeta) \left\{ (1-\eta^2)^{\frac{1}{2}n} \frac{d^n}{d\eta^n} P_m(\eta) \right\} \begin{Bmatrix} \cos n \xi \\ \sin n \xi \end{Bmatrix} \tag{26}$$

either on or in the field surrounding the surface of the sphere. In the above

expression $\eta = \cos \theta$, $\zeta = kr$, h_m is a spherical Hankel function of order m,

and P_m is a Legendre polynomial of degree m. It should be noted that when

n = 0 all ξ dependence drops out so that the problem becomes axi-symmetric.

It can also be shown[20] that the acoustic potential for a piston vibrating

in an otherwise hard (i.e. Y = 0) sphere is given by

$$\varphi(r,\theta,\xi) = (\frac{\partial \varphi}{\partial n} /2 k) \sum_{m=0}^{\infty} \left[P_{m-1}(\eta_0) - P_{m+1}(\eta_0) \right] \left\{ \frac{h_m(\zeta)}{\frac{d}{d\zeta} h_m(\zeta_0)} \right\} P_m(\eta)$$

$$\tag{27}$$

both on the surface of the sphere and in the field surrounding it. In Eq. (27), θ_o denotes the edge of the piston set in the sphere, a is the radius of the sphere, $\zeta_o = ka$, $\eta_o = \cos \theta_o$, $P_{-1}(\eta_o) = 1$ (when m = 0), and the remaining quantities are the same as those appearing in Eq. (26). The solution is always axi-symmetric as there is no ξ dependence. Also, both solutions (i.e. Eqs. (26) and (27)) represent radiated sound fields as they satisfy the necessary radiation conditions when $r \rightarrow \infty$.

In all the calculations performed in this study the acoustic velocity is specified on a quarter of the sphere's surface as shown in Fig. 4. Also, the sphere is of unit radius (i.e. a = 1) and the coupling constant α, required in applying the method of Burton and Miller, has been taken as the pure imaginary number i as k is a real number (See Eq. (11).).

The radiative fields computed in this study are summarized in Table I where the assigned values of m and n describe a specific solution (See Eq. (26).). For each investigated case Table I contains the exact solutions on the surface and far fields, the input boundary conditions derived from the known exact solution, and the average percent error obtained by comparing the exact and computed solutions.

To check the numerical approach and computer code Case # 1 was investigated initially (See Table I.). Under these conditions the analytical solution for the surface potential, $\varphi = h_o(kr)$, is a constant as is the input data (i.e. $\frac{\partial \varphi}{\partial n}$ and Y). A comparison between the numerical and exact solutions for the amplitude $|\varphi|$ of the acoustic potential[*] on the surface of the sphere and in the far field is presented in Fig. (5) where excellent agreement between the two solutions is noted. The computation of the surface solution required three minutes of computing

---

[*] The amplitude was chosen for comparison as both the real and imaginary parts

of the acoustic potential show similar trends and errors.

time on the Georgia Tech CDC Cyber 70 model 74 computer. This time is indicative

of all the cases considered in this study. The far field distribution of the

acoustic potential was calculated using both the exact surface distribution

and the calculated surface distribution. The far field calculation using the

exact surface distribution was done as a check on the computer code and the

results agreed with the exact solution (obtained from Eq. (26)) to seven sig-

nificant figures in both the real and imaginary parts. To calculate both distri-

butions simultaneously, under two minutes of computing time was required which

is also indicative of all the cases run.

The second investigated solution (See Case # 2, Table I.) was the same

solution as Case # 1 but with a wave number $k = \pi$ which coincides with the first

internal eigenvalue of the sphere. This case was run to check the validity of

the theory. Again the solution for the surface potential and the input data are

constants both on and off the surface of the sphere. A comparison between the

computed and exact solutions on the sphere surface and in the far field are pre-

sented in Fig. (6). Examination of this figure indicates that in this case the

agreement is not as good as in Case # 1, although the average error was still

under ten percent. The far field distribution of the acoustic potential was cal-

culated as before. Employing the exact surface distribution the results compared

with the exact far field solution to four significant figures in both the real

and imaginary parts. In examining Fig. 6 it is interesting to note that there

was no increase in the error from the surface distribution to the far field. It

was found that there was no significant increase in error from the surface to

the far field distribution in any of the cases run.

The exact solution for Case # 3 (obtained from Eq. (26) with the data in

Table I) is $\varphi = h_1$ (kr) cos θ. In contrast to the previous cases this solution

is θ dependent. A comparision between the exact and numerical solutions on the

surface of the sphere is presented in Fig. 7, and a far field comparison is pre-

sented in Fig. 8. Examination of the data shows that in this case the error was actually reduced in going from the surface to the far field. Furthermore in the far field, the calculated surface distribution gives better results than does the exact surface distribution.

The next case investigated (Case # 4) was run at the second internal eigenvalue of the sphere, k = 4.49340946. The results for the acoustic potential on the surface of the sphere are presented in Fig. 9. As can be seen the results deteriorate somewhat at an internal eigenvalue of the problem. It is interesting to note that the error increases with θ and it reaches its maximum value at $\theta = 180^{\circ}$, the center of the admittance surface. The results for the far field are presented in Fig. 10. All of the cases considered so far were axisymmetric, that is, there was no ξ dependence; a property that was also retained by the developed numerical solutions.

This next case (Case # 5) is truly three dimensional as there is a ξ dependence in the solutions. Referring to Eq. (26) and Table I the exact solution on the surface of the sphere is found to be $\varphi = h_1(kr) \sin \theta \sin \xi$. The average percent error was not calculated in this case due to the zeros which appear in the exact solution, but the errors remained small (i.e. under ten percent). The far field distribution of the acoustic potential was calculated and no increase in error was detected.

In the next three cases a hard sphere (i.e. Y = 0 on the admittance surface) with a unit driver (i.e. $\frac{\partial \varphi}{\partial n} = 1$ on the driving surface) was considered. The exact solutions for these cases can be obtained from Eq. (27). In these studies the wave number k was varied to determine the value of k at which the accuracy of the solution deteriorates for a fixed number of 80 calculational points that was used in these numerical studies.

The solution for Case # 6 where k = 2, are presented in Fig. 11 for both the surface distribution of $|\varphi|$ and the far field solution. In this case the far field is considered to be at kr = 100.

In this next case (Case # 7) the wave number is increased to k = 5. As can be seen from Fig. 12, the error is still under ten percent on both the surface of the sphere and in the far field (i.e. kr = 100). When the wave number is increased to k = 10 (Case # 8) the error becomes rather large. The average error in the calculation of the surface potential is sixty percent. So it can be seen that there are not enough calculated points to accurately represent the potential function, φ. The far field is calculated at kr = 100 and the error drops a bit but it still remains high at twelve percent.

V. Summary.

In summary, a solution approach has been developed in this paper which may be used to yield a unique solution for the distribution of the acoustic potential on the surface of an arbitrary three dimensional body at all values of the wave number. Also, a numerical scheme was developed to solve the equation accurately and efficiently. Computer programs were run to verify the applicability of the developed solution method and to find its limit of accuracy for a fixed number of points. The procedure was found to be both accurate and versatile as the computer code required no major modifications to handle the various boundary conditions imposed on the surface of the body.

References

1. Chen, L. H. and Schweikert, D. G., Oct. 1963, <u>Journal of the Acoustical Society of America</u>, Vol. 35, No. 10, pp. 1626-1632, "Sound Radiation From an Arbitrary Body".

2. Banaugh, R. P. and Goldsmith, W., Oct. 1963, <u>Journal of the Acoustical Society of America</u>, Vol. 35, No. 10, pp. 1590-1601, "Diffraction of Steady Acoustic Waves by Surfaces of Arbitrary Shape".

3. Chertock, G., July 1964, <u>Journal of the Acoustical Society of America</u>, Vol. 36, No. 7, pp. 1305-1313, "Sound from Vibrating Surfaces".

4. Greenspan, D. and Werner, P., 1966, <u>Archives of Rational Mechanics and Analysis</u>, Vol. 23, Pt. 4, pp. 288-316, "A Numerical Method for the Exterior Dirichlet Problem for the Reduced Wave Equation".

5. Copley, L. G., Apr. 1967, <u>Journal of the Acoustical Society of America</u>, Vol. 4, No. 4, pp. 807-816, "Integral Equation Method for Radiation from Vibrating Bodies".

6. Schenck, H. A., Jan. 1968, <u>Journal of the Acoustical Society of America</u>, Vol. 44, No. 1, pp. 41-58, "Improved Integral Formulation for Radiation Problems".

7. Burton, A. J., Jan. 1973, NPL Report NAC 30, National Physical Laboratory, Teddington Middlesex, "The Solution of Helmholtz' Equation in Exterior Domains using Integral Equations".

8. Jones, D. S., 1974, <u>Quarterly Journal of Mechanics and Applied Mathematics</u>, Vol. 27, Pt. 1, pp. 129-142, "Integral Equations for the Exterior Acoustic Problem".

9. George, R. C. Tai and Richard P. Shaw, Sept. 1974, <u>Journal of the Acoustical Society of America</u>, Vol. 56, No. 3, pp. 796-804, "Helmholtz- Equation Eigenvalues and Eigenmodes for Arbitrary Domains".

10. Baker, B. B. and Copson, E. T., 1950, <u>The Mathematical Theory of Huygens'</u> <u>Principle</u>, Ch. I, Oxford at the Clarendon Press.

11. Jones, D. S., July 1974, <u>Proceedings of the IEEE</u>, Vol. 121, No. 7, pp. 573-582, "Numerical Methods for Antenna Problems".

12. Ursell, F., 1973, <u>Proceedings of the Cambridge Philosophical Society</u>, Vol. 74, pp. 117-125, "On the Exterior Problems of Acoustics".

13. Burton, A. J. and Miller, G. F., 1971, <u>Proceedings of the Royal Society</u> <u>of London</u>, A323, pp. 201-210, "The Application of Integral Equation Methods to the Numerical Solution of Some Exterior Boundary Value Problems".

14. Panich, O. I., 1965, <u>USP. MAT. NAUK.</u>, 20, Pt. 1, pp. 221-226, "On the Question of the Solubility of the Exterior Boundary Problem for the Wave Equation and Maxwell's Equation," (Russian).

15. Stallybrass, M. P., May 1967, <u>Journal of Mathematics and Mechanics</u>, Vol. 16, No. 11, pp. 1247-1286, "On a Pointwise Variational Principle for the Approximate Solution of Linear Boundary Value Problems".

16. Abramowitz, M. and Stegun, I. A., Eds., May 1968, <u>Handbook of Mathematical</u> <u>Functions</u>, Ch. 25, Dover Publications, Inc., New York (5th Printing)

17. Scheid, F., 1968, <u>Theory and Problems of Numerical Analysis</u>, Ch. 15, McGraw-Hill Book Co., New York.

18. Bell, W. A., Meyer, W. L. and Zinn, B. T., July 20-23, 1976, 3rd AIAA Aero-Acoustics Conference, Palo Alto, Calif., AIAA Paper No. 76-494, "Predicting the Acoustical Properties of Arbitrarily Shaped Bodies by Use of an Integral Approach".

19. Isaacson, E. and Keller, H. B., 1966, <u>Analysis of Numerical Methods</u>, Ch. 2, John Wiley & Sons, Inc., New York.

20. Morse, P. M. and Ingard, K. U., 1968, <u>Theoretical Acoustics</u>, p. 343, McGraw-Hill, Inc., New York.

Case #	m	n	k	kr Far Field	Exact Solutions		Input Conditions		Average Error %
					Surface $\varphi =$	Far Field $\varphi =$	Driving Surface $\dfrac{\partial \varphi}{\partial n} =$	Admittance Surface $Y =$	
1	0	0	1	50	$0.841 - 0.540i$	$-0.00524 - 0.0193i$	$-0.301 + 1.38i$	$-1.0 + i$	< 1
2	0	0	π	50	$\dfrac{i}{\pi} = 0.318\,i$	$-0.00524 - 0.0193i$	$-1.0 + \dfrac{i}{\pi}$	$-1.0 + \pi\,i$	< 9
3	1	0	2	100	$(0.435 - 0.351i)$ $\cos\theta$	$(-0.00867 + 0.00498)$ $\cos\theta$	$(0.0385 + 1.12i)$ $\cos\theta$	$-1.2 + 1.6\,i$	< 3
4	1	0	4.49	100	$(0.228i)\cos\theta$	$(-0.00867 + 0.00498)$ $\cos\theta$	$(-0.976 - 0.239i)$ $\cos\theta$	$-1.05 + 4.28i$	< 14
5	1	1	2	100	$(0.435 - 0.351i)$ $\sin\theta\sin\xi$	$(-0.00867 + 0.00498)$ $\sin\theta\sin\xi$	$(0.0385 + 1.12i)$ $\sin\theta\sin\xi$	$-1.2 + 1.6\,i$	not calculated

Parameters m and n refer to
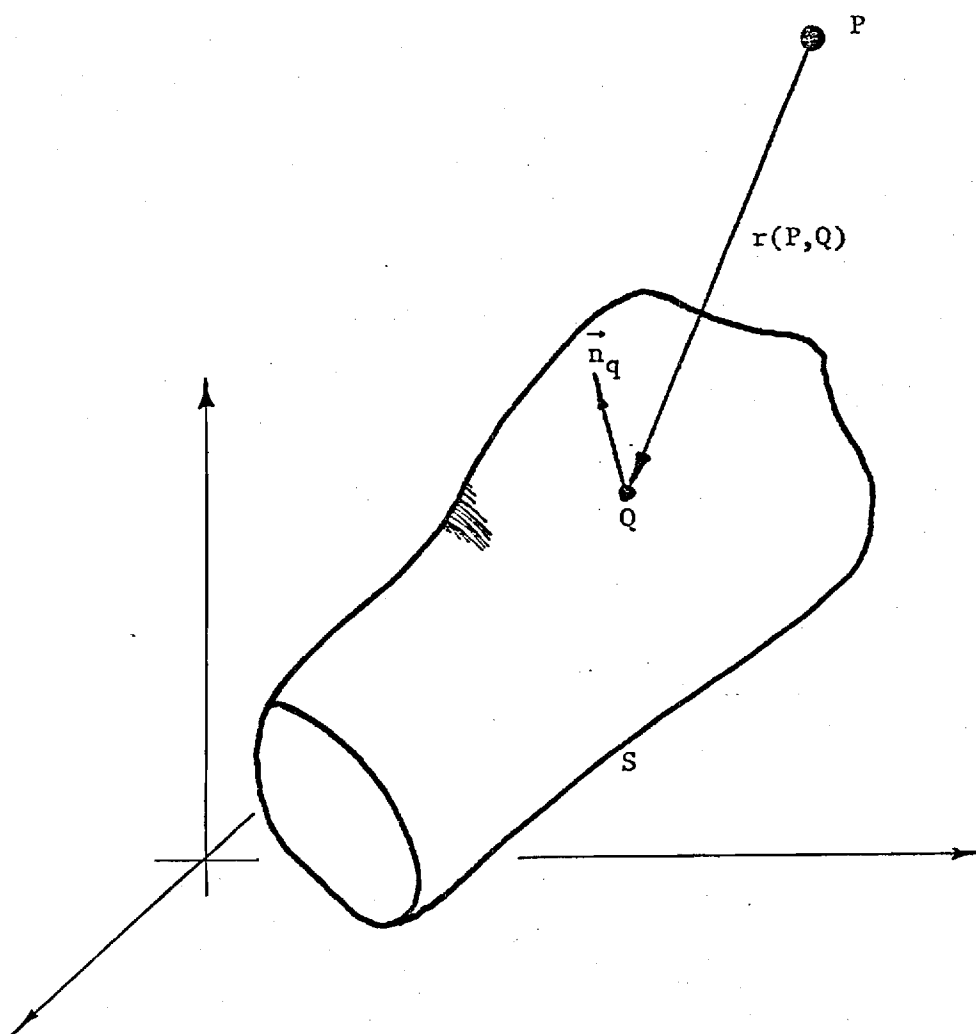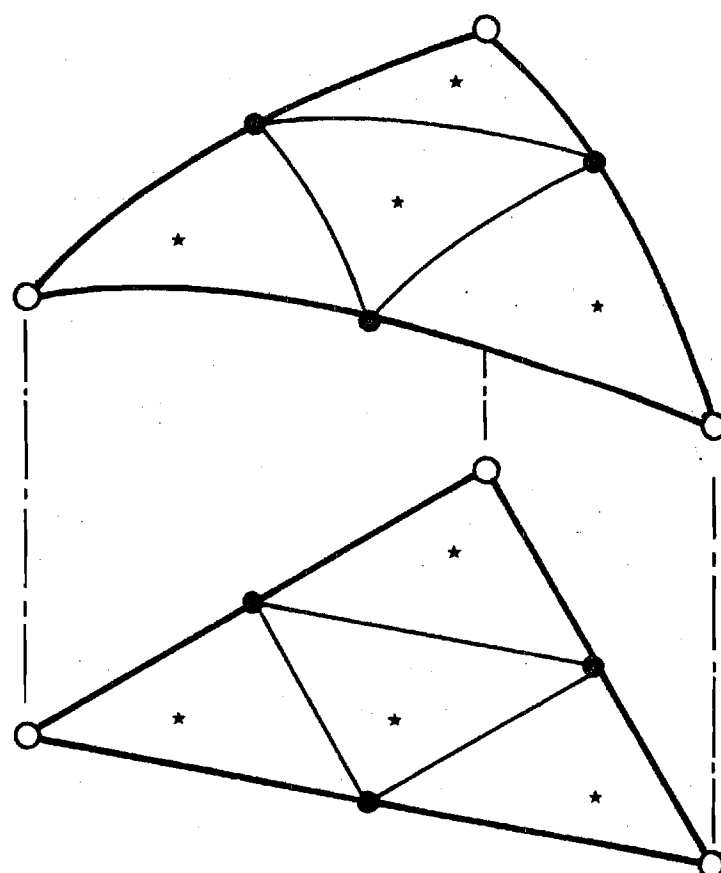Eq. (26)

Table I.

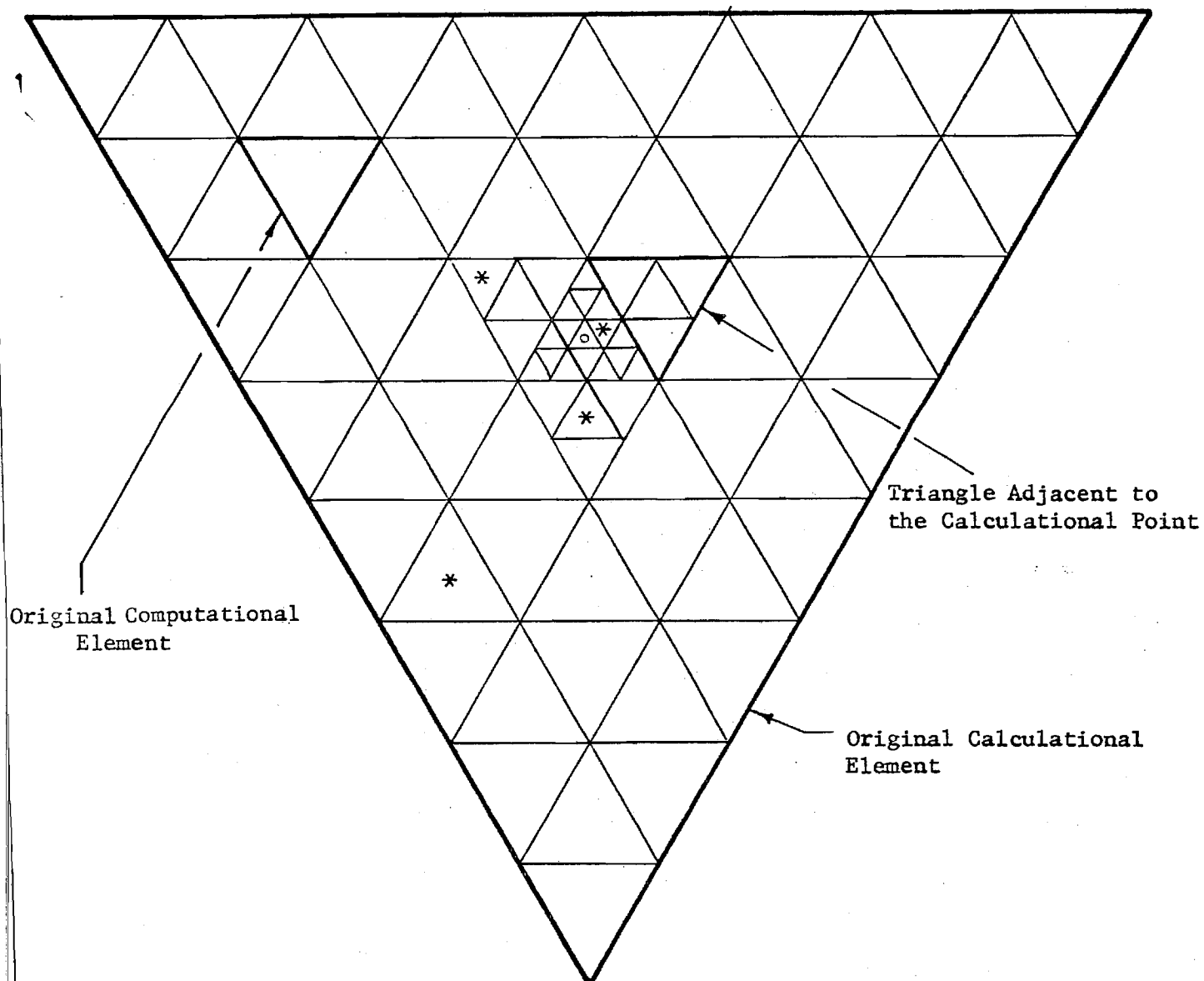Figure 1. General Description of the Acoustic Radiation Problem.

O   Already on Sphere

⬤   Midpoint of Sides Projected to
      the Surface of the Sphere

★   Centroids of the Plane Triangles
      Projected to the Surface of the Sphere

Figure 2. Method of Dividing the Surface of the Sphere.

Figure 3. Division of the Surface of the Sphere Around a
Calculational Point.
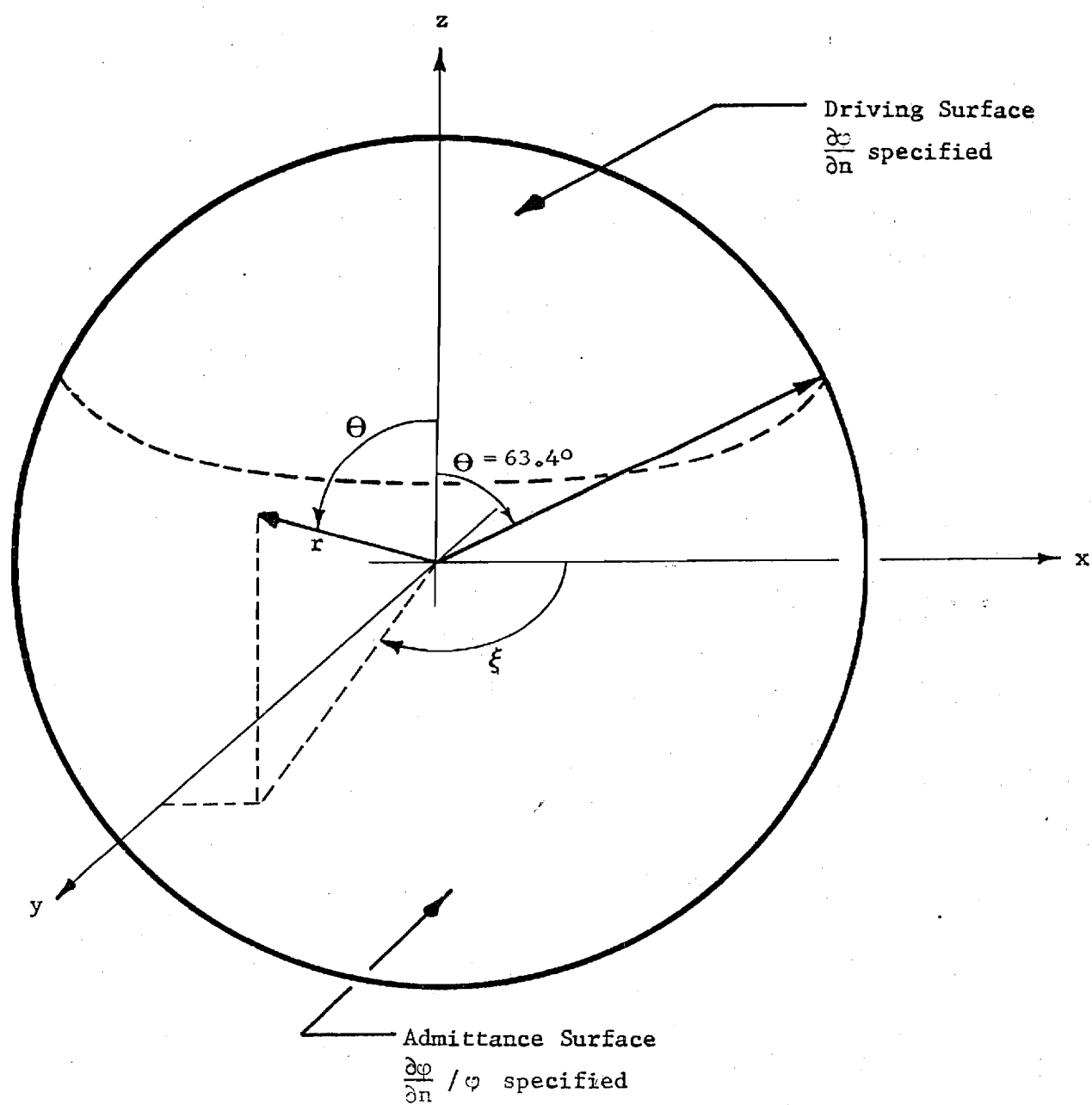
Figure 4. Specifications of Boundary Conditions on the Surface
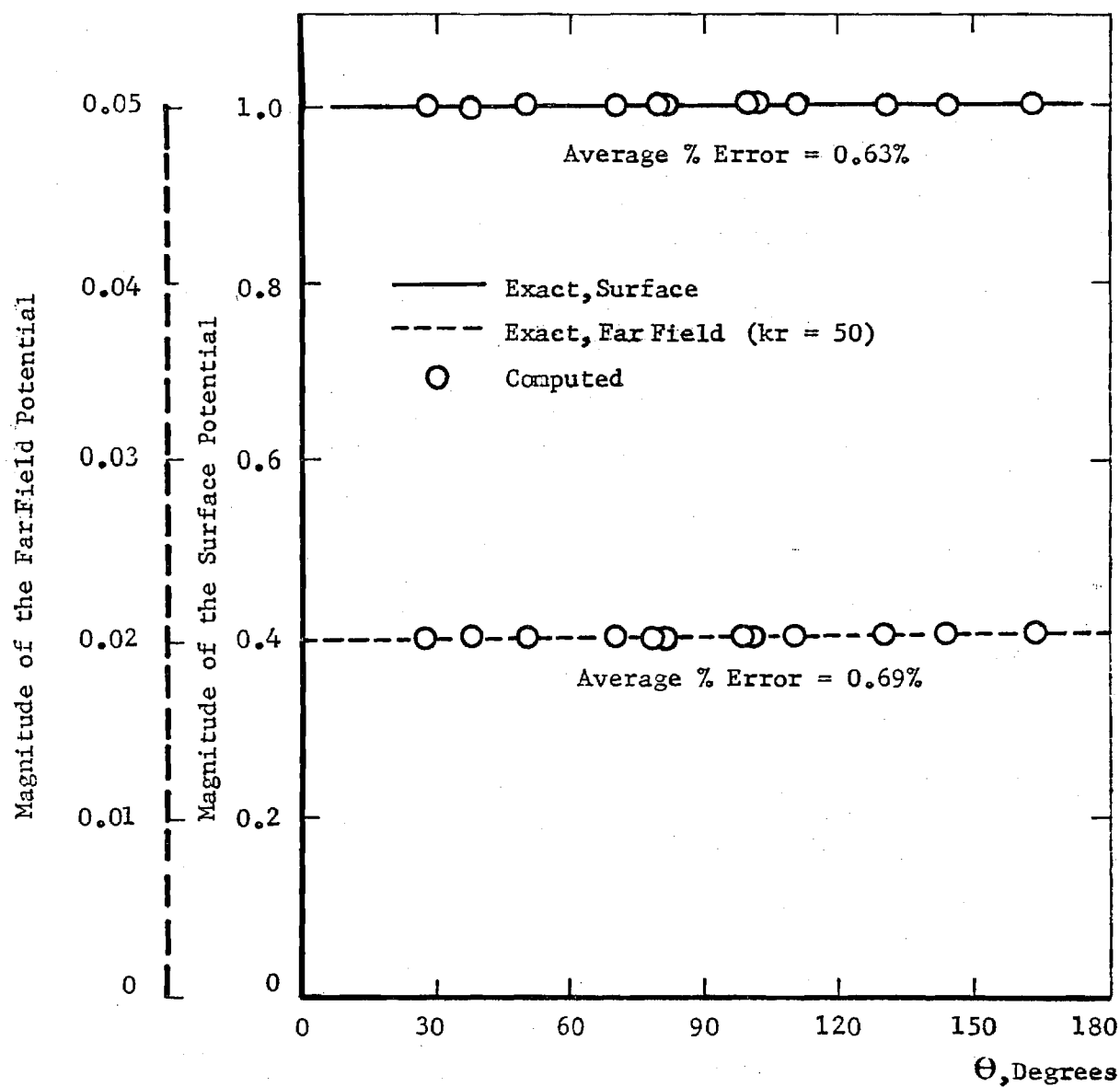of the Sphere.

Magnitude of the Far Field Potential

Magnitude of the Surface Potential

Average % Error = 0.63%

Exact, Surface
Exact, Far Field (kr = 50)
Computed

Average % Error = 0.69%

0.05 — 1.0

0.04 — 0.8

0.03 — 0.6

0.02 — 0.4

0.01 — 0.2

0 — 0

0   30   60   90   120   150   180

Θ, Degrees

Figure 5. Exact and Calculated Values of $|\varphi|$ for $\varphi = h_o(r)$
on the Surface and in the Far Field of the Sphere.

Magnitude of the Far Field Potential

Magnitude of the Surface Potential

0.04 — 0.4

0.03 — 0.3

Exact, Surface
Exact, Far Field (kr=50)
Computed

Average % Error = 8.7%

0.02 — 0.2

Average % Error = 8.7%

0.01 — 0.1

0

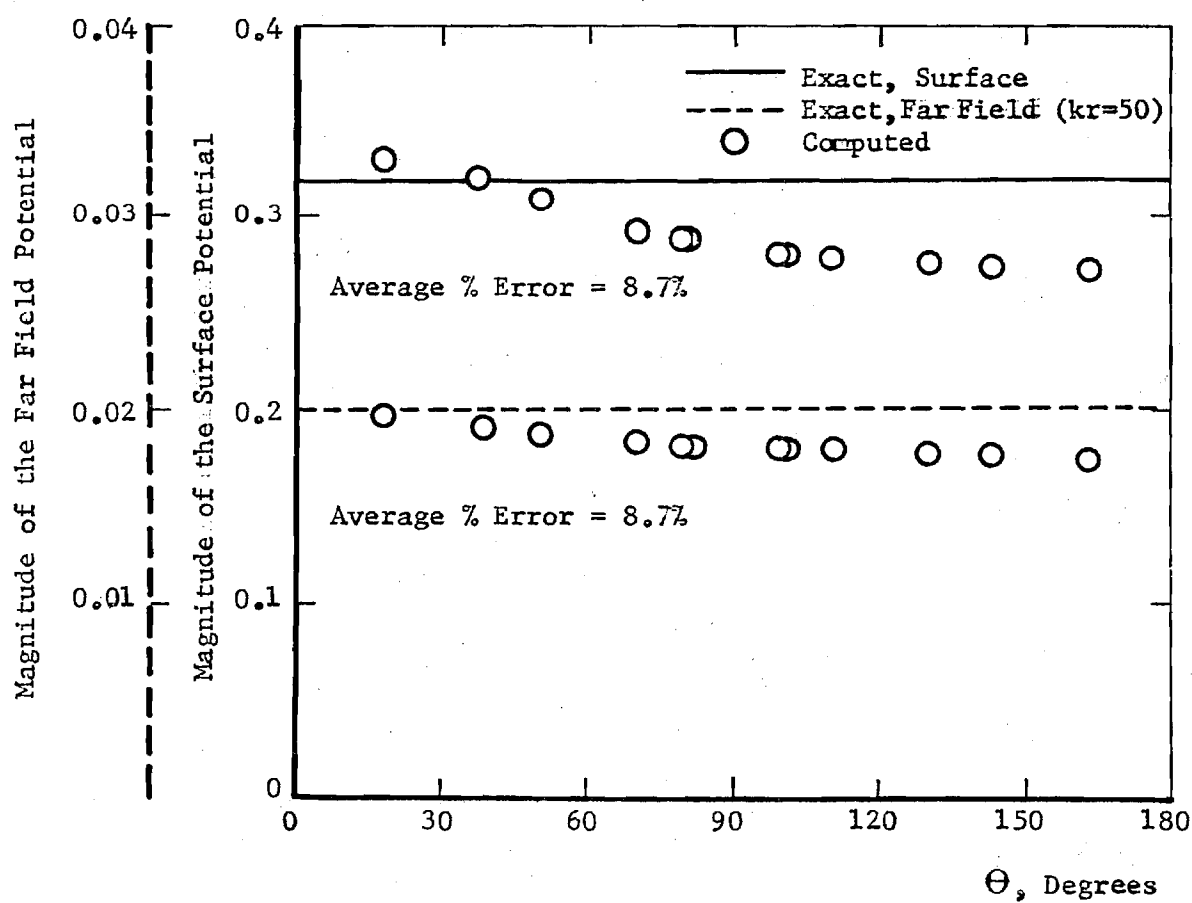0   30   60   90   120   150   180

Θ, Degrees

Figure 6. Exact and Calculated Values of $|\varphi|$ for $\varphi = h_o(\pi r)$ on the Surface and in the Far Field of the Sphere.
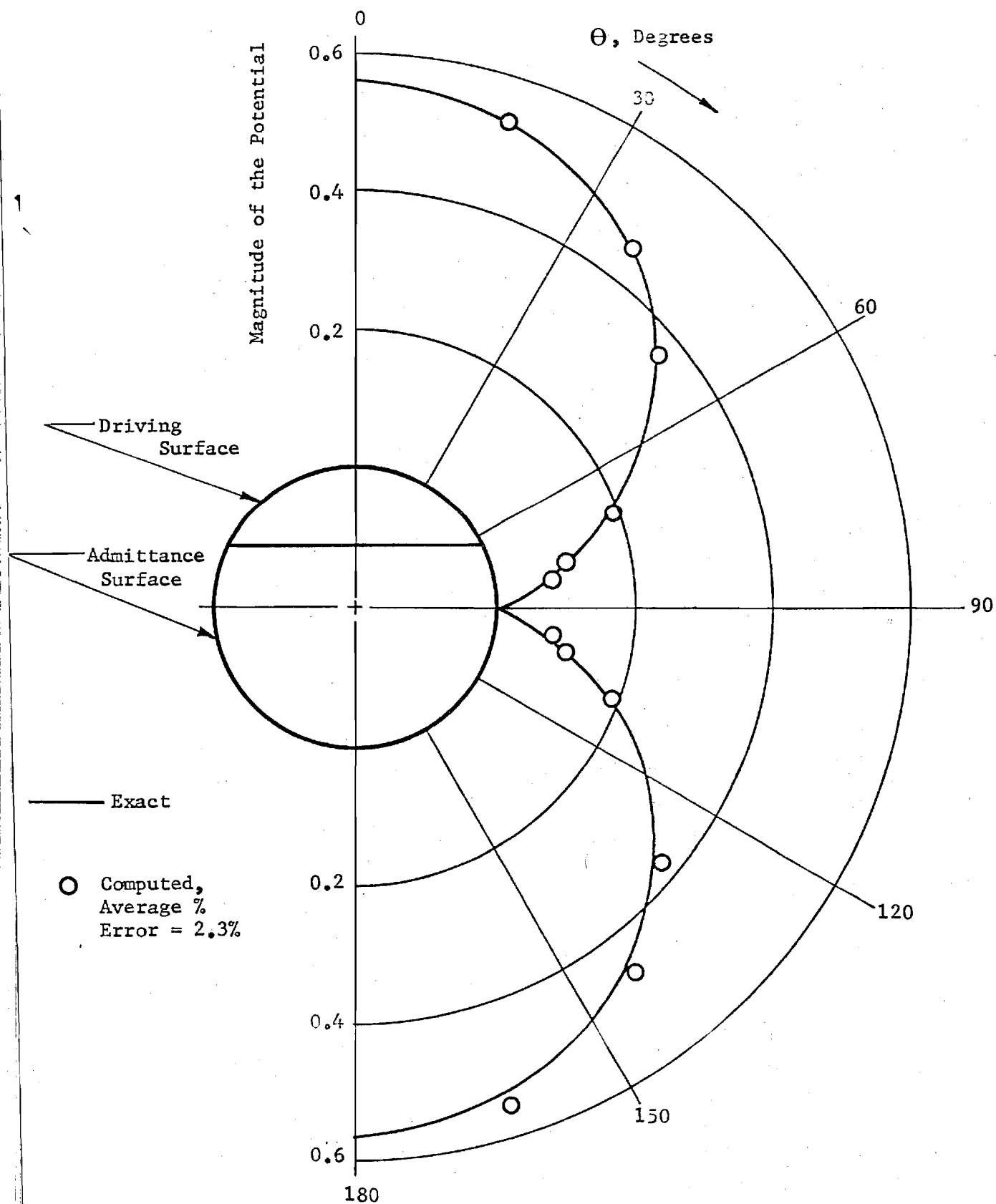
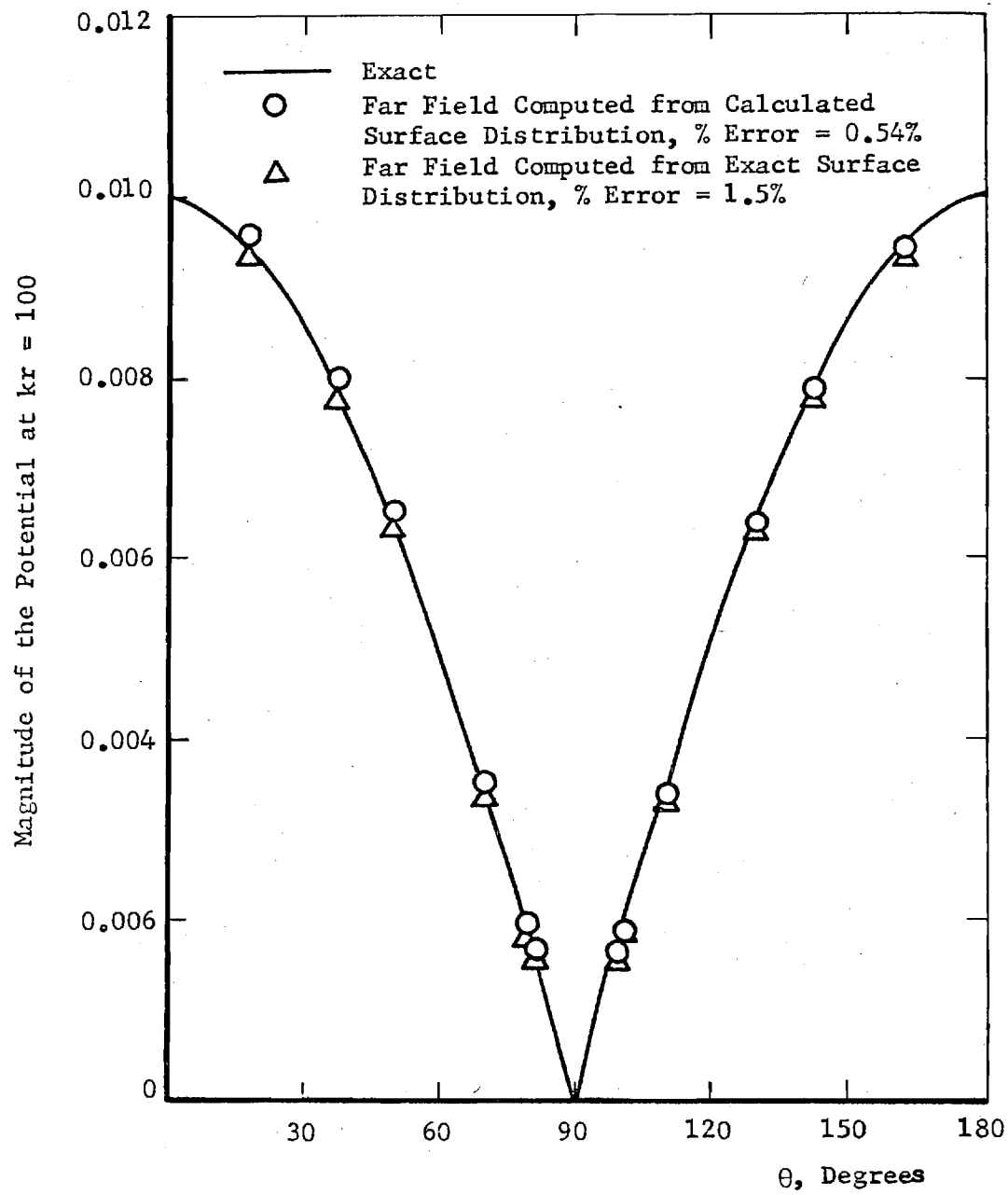Figure 7. Exact and Calculated Values of $|\varphi|$ for $\varphi = h_1(2r)\cos\Theta$ on the Surface of the Sphere.

Figure 8. Exact and Calculated Values of $|\varphi|$ using the Exact and Calculated Surface Distribution of φ for $\varphi = h_1(2r) \cos \Theta$ in the Far Field of the Sphere.
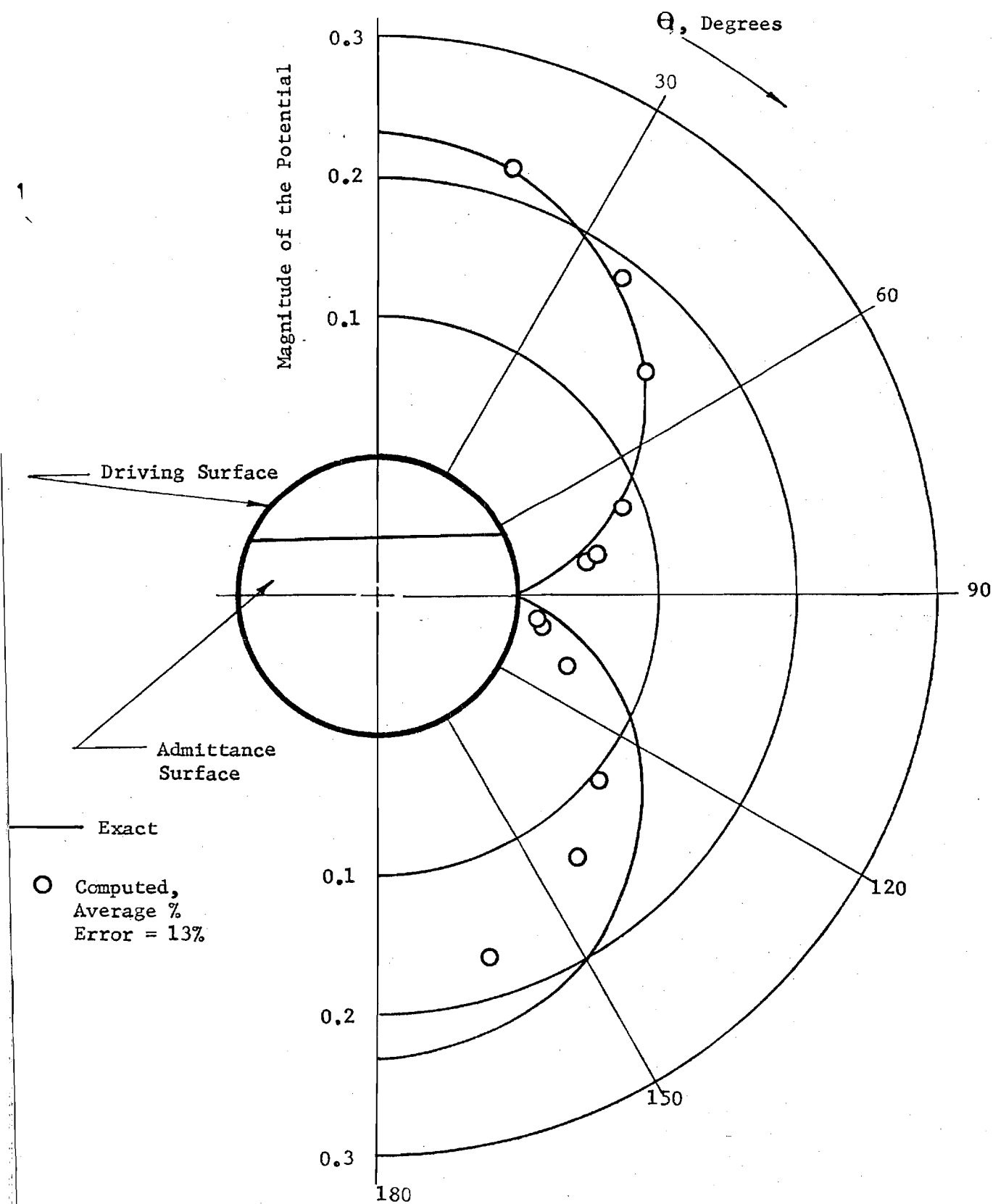
Figure 9. Exact and Calculated Values of $|\varphi|$ for $\varphi = h_1(4.49r) \cos \vartheta$ on the Surface of the Sphere.
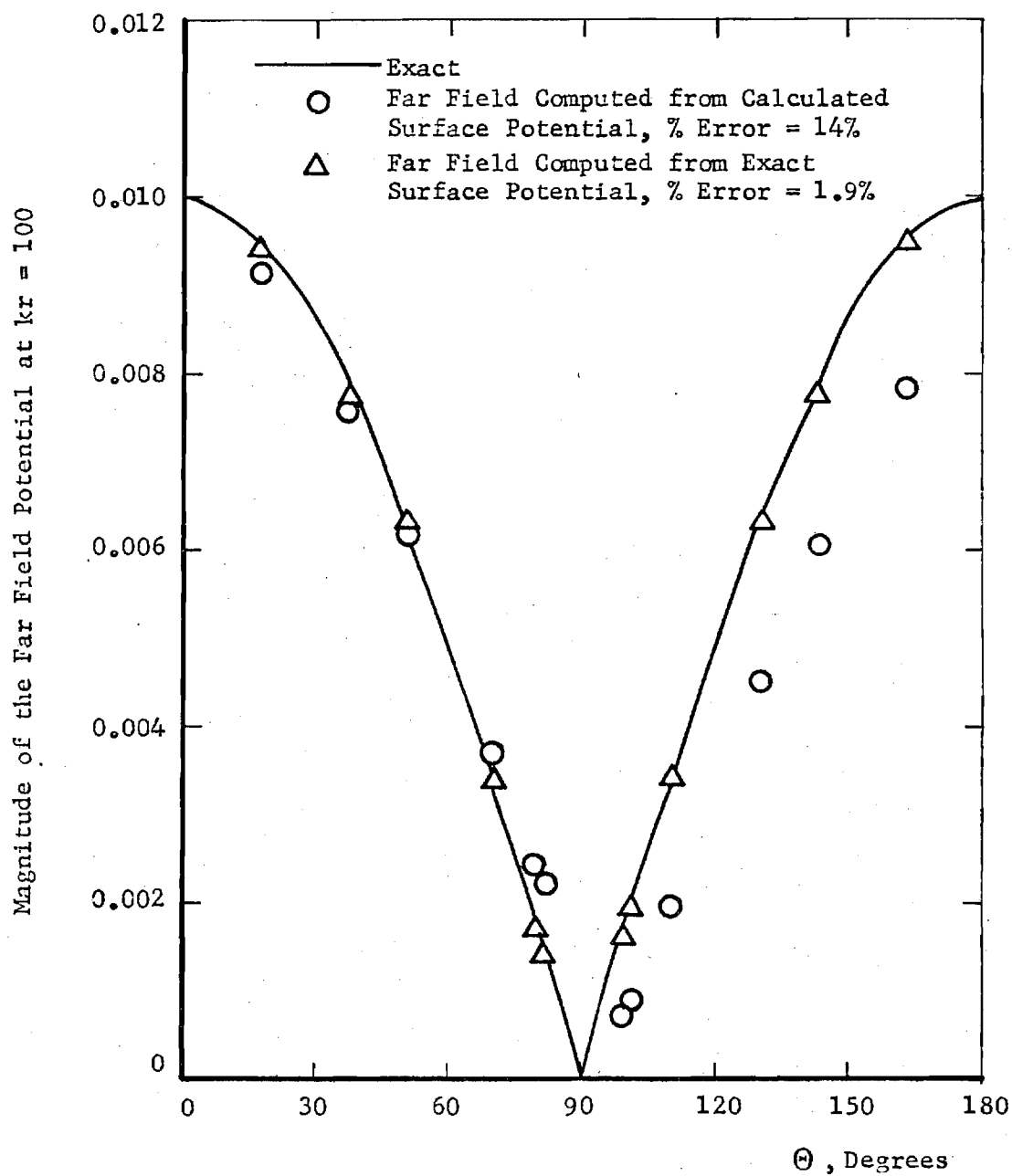
Figure 10. Exact and Calculated Values of $|\varphi|$ using the Exact and Calculated Surface Distribution of φ for $\varphi = h_1(4.49r) \cos \Theta$ in the Far Field of the Sphere.

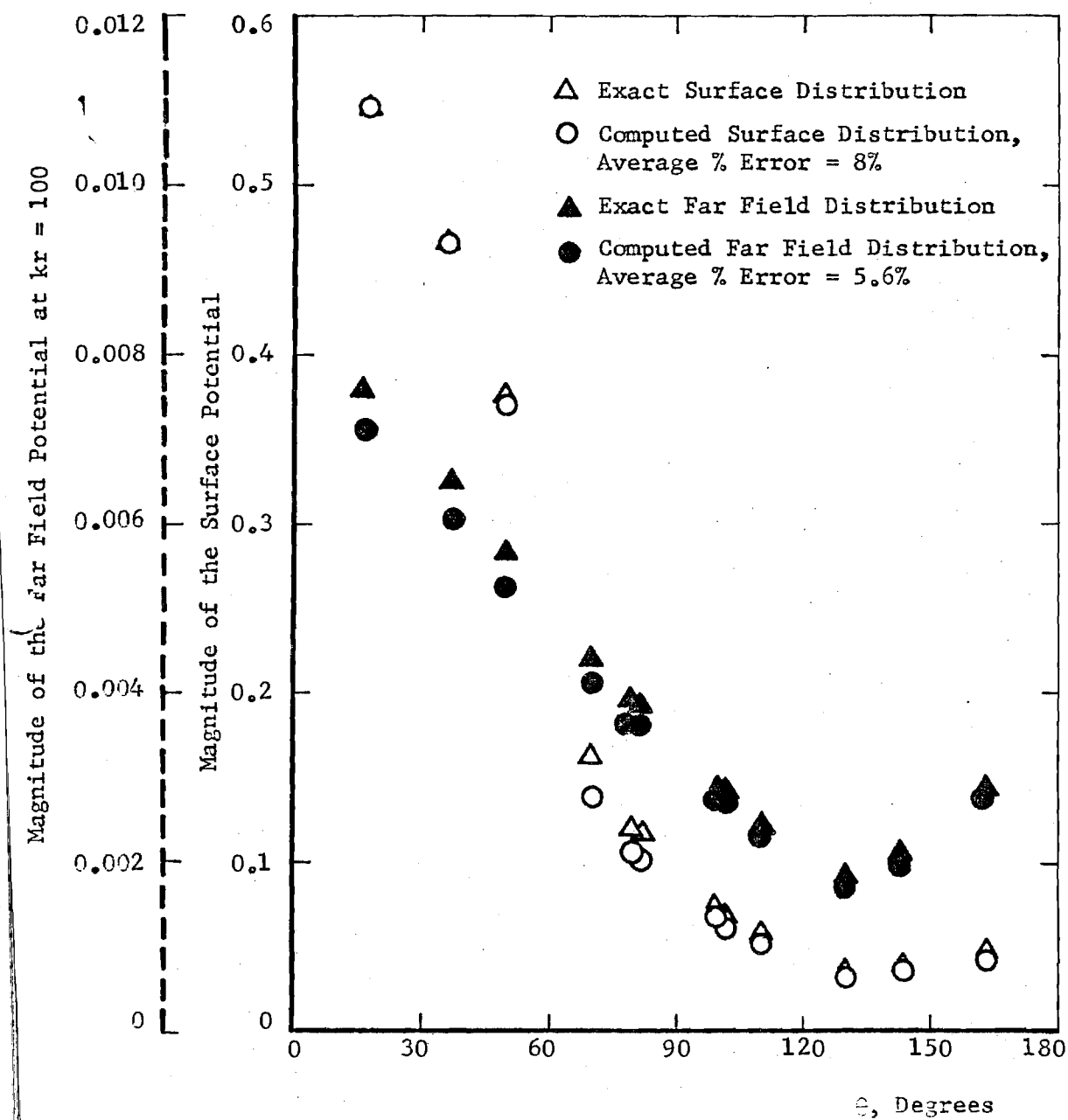Figure 11. Exact and Calculated Values of $|\varphi|$ for a Hard Sphere with a Unit Driver (k = 2) on the Surface and in the Far Field.
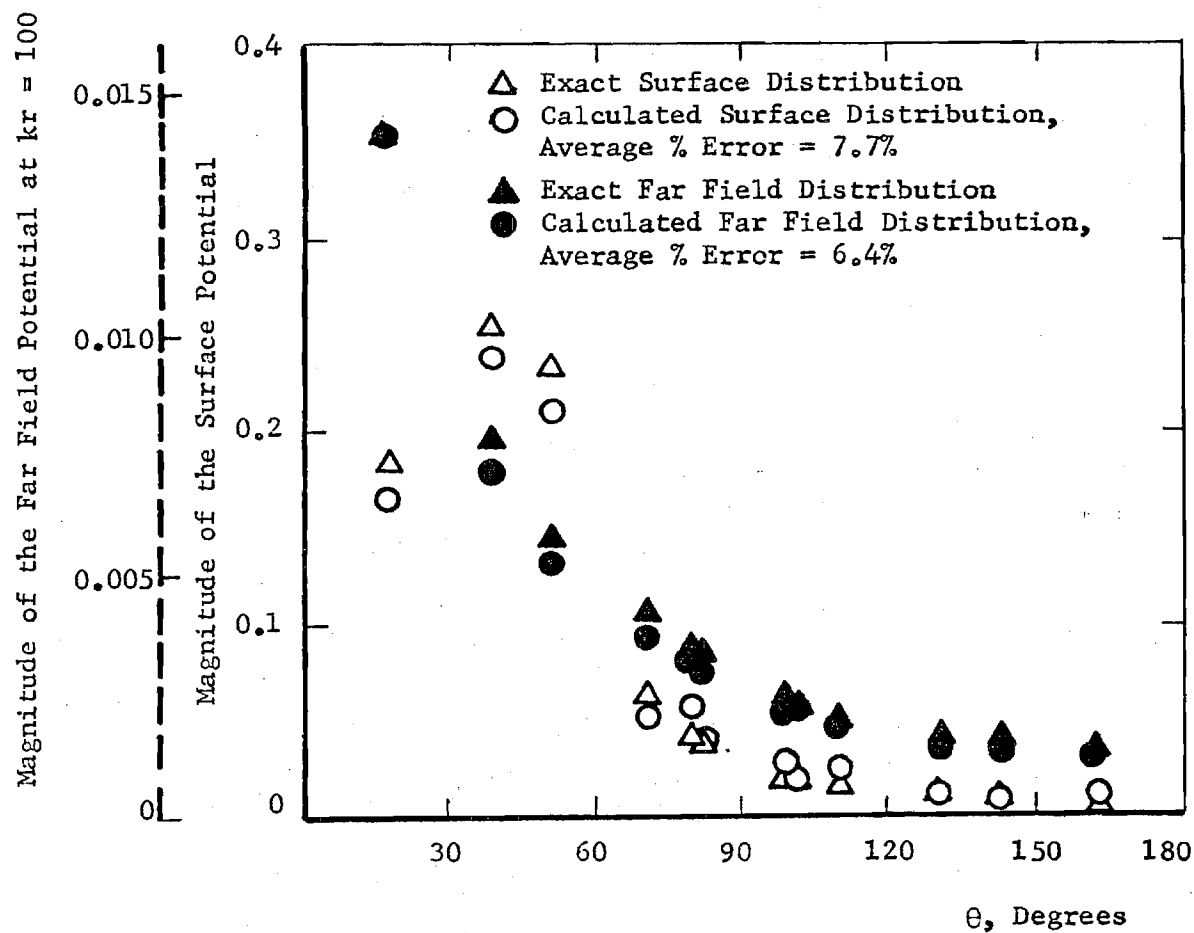
Figure 12. Exact and Calculated Values of $|\varphi|$ for a Hard Sphere with a Unit Driver (k = 5) on the Surface and in the Far Field.

APPENDIX B

PREDICTION OF THE SOUND FIELD RADIATED FROM AXISYMMETRIC SURFACES

W. L. Meyer,[*] W. A. Bell,[**] and B. T. Zinn[***]

School of Aerospace Engineering
Georgia Institute of Technology
Atlanta, Georgia 30332

Abstract

A general analytical method for determining the radiated sound fields from axisymmetric surfaces of arbitrary cross section with general boundary conditions is developed. The method is based on an integral representation of the external solutions of the Helmholtz equation valid at all wave numbers. The axisymmetric formulation of the problem reduces its solution to the numerical evaluation of line integrals by Gaussian quadrature. The applicability of the solution approach for both a sphere and finite cylinder is demonstrated by comparing the numerical results with exact analytical solutions for both discontinuous and continuous boundary conditions.

I. Introduction

To reduce the noise radiated to the community from turbofan inlets, the effects of sound suppression material in the inlet and the spatial distribution of the sound source on the radiated sound levels and patterns must be determined. Analytical techniques for predicting these effects must be capable of dealing with general axisymmetric geometries and complicated boundary conditions which are encountered in multiply-lined inlets. To determine the radiated sound field, an additional requirement is that the methods be applicable to infinite domains. The objective of this paper is to develop a general analytical method for determining the radiated sound fields from axisymmetric surfaces of arbitrary cross section and with general boundary conditions.

The method used in this investigation is based on an integral form of the solutions of the Helmholtz equation.[1-6] With this formulation the acoustic potential anywhere external to the surface can be found once the potential distribution on the surface is known. Thus, to determine the radiated sound field the problem reduces to the determination of the distribution of the acoustic potential on the two-dimensional surface of the geometry under consideration instead of solving the Helmholtz equation in the surrounding infinite three dimensional domain.

It has been previously shown[1-5] that when applied to exterior sound radiation problems the solution technique fails to produce unique solutions at frequencies corresponding to interior eigenvalues of the geometries under consideration. Unless special precautions are taken, straight-forward numerical solutions of the developed integral equation at frequencies close to the eigenvalues of the internal problem produce large errors. A technique proposed by Burton and Miller[4] for avoiding this uniqueness problem and the associated numerical errors is used

 * Assistant Research Engineer, Member AIAA
 ** Research Engineer, Member AIAA
*** Regents' Professor, Associate Fellow, AIAA

in this investigation. This technique involves a reformulation of the "classical" integral equation and the solutions obtained are valid at all frequencies.

The resulting integral equation for the surface acoustic potential is solved numerically and, for axisymmetric geometries, the equation reduces to the evaluation of a line integral. Thus, the axisymmetric case can be reduced to an equivalent one-dimensional problem. This equation is discretized and the resulting system of algebraic equations is solved using complex Gauss-Jordan elimination. Since the coefficient matrix involves the free space Green's function, which becomes singular as two points on the surface approach one another, numerical techniques are presented which can deal with these singularities and yield accurate results. Gaussian integration is used to increase the accuracy of the solution without significant penalties in computer storage and time requirements. The applicability of the integral formulation and the accuracy of the numerical techniques are demonstrated by computing the surface and far field distributions of the acoustic potential on both a sphere and a finite cylinder. The numerical results are compared with known exact solutions generated by the separation of variables technique. Surfaces with spatially varying forcing functions and admittances are considered, for different tangential modes, to evaluate the capability of the integral approach to handle boundary conditions of a general nature. With the sphere, agreement between computed and exact results is to three significant figures. For the cylinder agreement is to two significant figures. The effect on the accuracy of discontinuous boundary conditions involving nonzero admittances over the surface and of the corners encountered in the cylindrical configuration are also presented.

II. Theory

In this section the general three dimensional integral representation of the solutions of the Helmholtz equation is developed for application to radiation problems. This particular formulation yields unique solutions at all frequencies and does not have strong singularities which are difficult to handle numerically. The general integral equation is then specialized for axisymmetric geometries. A more detailed development is given in Ref. 5.

General Theory

Beginning with the three dimensional Helmholtz equation which governs the spatial dependence of the acoustic field for sinusoidal oscillations

$$\nabla^2 \varphi + k^2 \varphi = 0 \tag{1}$$

where φ is the acoustic potential and k is the wave number. The standard integral representation of the exterior solutions is found to be[1,6]

$$\int\int_{S_q} \left(\varphi(Q) \frac{\partial G(P,Q)}{\partial n_q} - G(P,Q) \frac{\partial \varphi(Q)}{\partial n_q} \right) dS_q = 4\pi \, \varphi(P) \tag{2}$$

The term $\frac{\partial}{\partial n_q}$ represents an outward normal derivative with respect to the body as shown in Fig. 1; that is

$$\frac{\partial \varphi(Q)}{\partial n_q} = \vec{\nabla}_q \, \varphi(Q) \cdot \vec{n}_q \tag{3}$$

Also, $G(P,Q)$ is a fundamental three dimensional solution of the Helmholtz equation and is taken to be the free space Green's Function for a point source[6] defined as

$$G(P,Q) = \frac{e^{ikr(P,Q)}}{r(P,Q)} \tag{4}$$

From Eq. (3), if the acoustic potential and the normal acoustic velocity $\frac{\partial \varphi(Q)}{\partial n_q}$ are known at each point on the surface of the body then the acoustic potential may be calculated anywhere in the exterior domain.

To solve for the surface potential, the point P is moved to the surface of the body. Equation (2) then becomes

$$\int\int_{S_q} \left(\varphi(Q) \frac{\partial G(P,Q)}{\partial n_q} - G(P,Q) \frac{\partial \varphi(Q)}{\partial n_q} \right) dS_q = 2\pi \, \varphi(P) \tag{5}$$

if the surface of the body is sufficiently smooth. Introducing a modified admittance function defined as

$$Y(Q) \equiv \frac{\partial \varphi(Q)}{\partial n_q} \Big/ \varphi(Q) \tag{6}$$

Eq. (5) can be written as

$$\int\int_{S_q} \varphi(Q) \frac{\partial G(P,Q)}{\partial n_q} dS_q - \int\int_{S_{q_1}} \varphi(Q) G(P,Q) Y(Q) dS_{q_1}$$

$$= 2\pi \varphi(P) + \int\int_{S_{q_2}} \frac{\partial \varphi(Q)}{\partial n_q} G(P,Q) \, dS_{q_2} \tag{7}$$

where $\int_q = \int_{q_1} + \int_{q_2}$.

If either the acoustic velocity or the admittance is known at each point on the surface of the body then the acoustic potential may be calculated at each point using Eq. (7).

Unfortunately this equation does not yield unique solutions when the wave number k is an internal eigenvalue of the body under consideration. Since these eigenvalues are not known a priori for general bodies the formulation cannot be relied upon to give consistently good results. There are many papers in the literature[2,3,4] dealing with this problem. The relative merits and shortcomings of the methods employed are discussed in detail in

The soundest approach from an analytical point of view is given by Burton and Miller[4] who have suggested the use of the differential forms of Eq. (5) which governs the spatial dependence of the acoustic velocity.

$$2\pi \frac{\partial \varphi(P)}{\partial n_p} = \int\int_{S_q} \left[\varphi(Q) \frac{\partial^2 G(P,Q)}{\partial n_p \partial n_q} - \frac{\partial G(P,Q)}{\partial n_p} \frac{\partial \varphi(Q)}{\partial n_q} \right] dS_q$$

This equation can also be solved for $\varphi(Q)$ once the normal velocity or admittance is specified at the surface. However, this equation has its own set of associated eigenvalues at which unique solutions cannot be obtained. Burton and Miller suggest taking a linear combination of the two equations to obtain

$$\int\int_{S_q} \left(\varphi(Q) \frac{\partial G(P,Q)}{\partial n_q} - G(P,Q) \frac{\partial \varphi(Q)}{\partial n_q} \right) dS_q$$

$$+ \alpha \int\int_{S_q} \left(\varphi(Q) \frac{\partial^2 G(P,Q)}{\partial n_p \partial n_q} - \frac{\partial G(P,Q)}{\partial n_p} \frac{\partial \varphi(Q)}{\partial n_q} \right) dS_q$$

$$= 2\pi \left(\varphi(P) + \alpha \frac{\partial \varphi(P)}{\partial n_p} \right) \tag{8}$$

Since the two sets of associated internal eigenvalues are mutually exclusive the linear combination of equations should yield unique solutions if the complex coupling constant α is properly chosen. It is shown that α must meet the following restrictions to guarantee that Eq. (8) yield unique solutions

$$\text{Im } (\alpha) \neq 0 \qquad k \text{ real or imaginary}$$
$$\text{Im } (\alpha) = 0 \qquad k \text{ complex} \tag{9}$$

A problem arises in the numerical solution of Eq. (8) as the third term on the right hand side is strongly singular in its present form as the point Q approaches the point P on the surface of the body. Meyer, Bell and Zinn[5] have shown that this difficulty can be overcome by the proper interpretation of this singular term. Employing a vector transformation[7] and taking the Cauchy Principle Value Eq. (8) is shown to be equivalent to

$$\int\int_{S_q} \left(\varphi(Q) \frac{\partial G(P,Q)}{\partial n_q} - G(P,Q) \frac{\partial \varphi(Q)}{\partial n_q} \right) dS_q$$

$$+ \alpha \int\int_{S_q} (\varphi(Q) - \varphi(P)) \frac{\partial^2 G(P,Q)}{\partial n_p \partial n_q} dS_q \tag{10}$$

$$- \alpha \, \varphi(P) \int\int_{S_q} (n_p \cdot n_q)(ik)^2 G(P,Q) \, dS_q$$

$$- \alpha \int\int_{S_q} \frac{\partial G(P,Q)}{\partial n_p} \frac{\partial \varphi(Q)}{\partial n_q} dS_q = 2\pi \left(\varphi(P) + \alpha \frac{\partial \varphi(P)}{\partial n_p} \right)$$

All of the terms in Eq. (10) are now regular and therefore are directly integrable; however, all the integrands are oscillatory and singular so that care must be taken in their numerical approximation.

Axisymmetric Formulation

When dealing with a body of revolution as shown in Fig. 2 an axisymmetric formulation of the problem is advantageous.[8] This being the case an element of area becomes

$$dS_q = \tau\, dS\, d\theta$$

where S is the distance along the perimeter of the surface in the τ-z plane.

Assuming an acoustic velocity distribution of the form

$$\frac{\partial \varphi}{\partial n} = v(S) \cos m\,\theta \qquad (12)$$

and defining a potential function

$$\phi(S) \equiv \frac{\varphi}{\cos m\,\theta} \qquad (13)$$

Eq. (10) becomes

$$\int\int_{S_q} \phi(S_Q)\, \frac{\partial G(P,Q)}{\partial n_q}\, \cos m\,\theta_q\, dS_q$$

$$- \alpha\, \phi(S_p) \int\int_{S_q} G(P,Q)(i\kappa)^2 (n_p \cdot n_q)\, dS_q$$

$$+ \alpha \int\int_{S_q} \left[\phi(S_q) \cos m\,\theta_q - \phi(S_p) \right] \frac{\partial^2 G(P,Q)}{\partial n_p \partial n_q}\, dS_q$$

$$\qquad (14)$$

$$- \int\int_{S_q} v(S_q)\, G(P,Q) \cos m\,\theta_q\, dS_q$$

$$- \alpha \int\int_{S} v(S_q)\, \frac{\partial G(P,Q)}{\partial n_p}\, \cos m\,\theta_q\, dS_q$$

$$= 2\pi \left[\phi(S_p) + \alpha\, v(S_p) \right]$$

In the above equation θ_p has been assumed to be zero so that $\cos m\,\theta_p = 1$.

Now, three sets of functions are defined:

Influence Functions

$$I_1(S_p,S_q) = 2 \int_o^{\pi} G(P,Q) \cos m\,\theta_q\, d\theta_q$$

$$\qquad (15)$$

$$I_2(S_p,S_q) = 2\alpha \int_o^{\pi} \frac{\partial G(P,Q)}{\partial n_p} \cos m\,\theta_q\, d\theta_q$$

Kernel Functions

$$K_1(S_p,S_q) = 2 \int_o^{\pi} \frac{\partial G(P,Q)}{\partial n_q} \cos m\,\theta_q\, d\theta_q$$

$$\qquad (16)$$

$$K_2(S_p,S_q) = 2\alpha \int_o^{\pi} \frac{\partial^2 G(P,Q)}{\partial n_p \partial n_q} \cos m\,\theta_q\, d\theta_q$$

Forcing Functions

$$F_1(S_p,S_q) = 2\alpha \int_o^{\pi} G(P,Q)(ik)^2 (n_p \cdot n_q)\, d\theta_q$$

$$\qquad (17)$$

$$F_2(S_p,S_q) = 2\alpha \int_o^{\pi} \frac{\partial^2 G(P,Q)}{\partial n_p \partial n_q}\, d\theta_q$$

Substituting Eqs. (15)-(17) into Eq. (14) gives

$$\int_o^{\ell} \phi(S_q) \left\{ K_1(S_p,S_q) + K_2(S_p,S_q) \right\} dS_q$$

$$- \phi(S_p) \int_o^{\ell} \left\{ F_1(S_p,S_q) + F_2(S_p,S_q) \right\} dS_q$$

$$\qquad (18)$$

$$- \int_o^{\ell} v(S_q) \left\{ I_1(S_p,S_q) + I_2(S_p,S_q) \right\} dS_q$$

$$= 2\pi \left[\phi(S_p) + \alpha\, v(S_p) \right]$$

where ℓ is the length of the generating line of the surface of revolution. The S-θ coordinate directions have now been effectively uncoupled so that the problem has been reduced to the evaluation of line integrals in the coordinate directions on the surface of the body. This formulation does not restrict the form or type of boundary conditions on the body; it merely assumes that the boundary conditions can be represented by a sum (expanded in a set) of tangential modes.

III. Results

Numerical results have been obtained for a sphere and cylinder using the numerical technique described in Ref. 9. Basically, this method consists of first specifying the τ-z coordinates and the normal vector at each point on the surface. From these quantities the distances r and the normal derivatives $\frac{\partial}{\partial n_q}$ can be obtained. The integral in Eq. (18) is then separated into n integrals taken over subintervals of length ℓ/n. The acoustic potential is assumed constant over each subinterval and the integrations are performed numerically using a four-point Gauss-Legendre quadrature in the τ-z plane. A twenty-point Gauss-Legendre quadrature formula is used in the circumferential direction.

Exact results were obtained using separation of variables.[6] To eliminate the need for evaluating the resulting infinite series, the normal velocity and admittance distributions were selected so that only one term in the series remains.

3

To investigate the effect of the coupling constant α in Eq. (18), the surface potential distributions were obtained for α = 0, i, and i/k for twenty points on the sphere. The exact solution assumed for this case is

$$\varphi(P) = \frac{e^{ikr(P)}}{r(P)} \qquad (19)$$

where r is the distance from the origin to a point P on the surface. As shown in Fig. 3, with α = 0 the computed magnitudes of the acoustic potential are in error by 12 per cent at wave numbers close to the internal eigenfrequencies of π, 2π and 3π. These results are those that would be obtained from Eq. (5). The relatively large errors are expected from the analysis of Burton[1] and from previous investigations using Eq. (5).[2,5] Burton proves that setting the imaginary part of α nonzero guarantees unique solutions when Eq. (18) is used. Although the maximum error is reduced for α = i to less than 4 per cent when the nondimensional frequency k is less than seven, significant errors are still evident at the higher frequencies as shown in Fig. 3.

In this study consistently good results are obtained only when α = i/k. In Fig. 3, the computed and exact results with α = i/k agree to three significant figures. The reason for this behavior is currently under investigation; however, for all the cases presented hereafter this value of α is chosen and the exact surface distribution is given by Eq. (19) when m = 0.

A problem of more practical importance is the finite axisymmetric duct since this surface approximates an engine configuration. The surface potential distributions are presented in Fig. 4 for a zero admittance everywhere on the surface. The velocity distribution is specified over the entire surface and the potential given by Eq. (19) has a magnitude independent of frequency and a phase linearly proportional to the frequency. In Fig. 4 the magnitude and phase are plotted against the distance along the perimeter S. The largest errors in the magnitude of the potential of about 10 percent occur on the ends of the cylinder and at the corners. The results at the ends can be improved without increasing the number of points by area weighting rather than by taking equidistant points along the perimeter. The errors at the corners are caused by the discontinuous normal derivative in going from the cylinder to the end. The errors in the phase are less than four per cent in all cases. The errors in magnitude increase with increasing frequency, but even when k = 10 the numerical results are within 10 per cent of the exact solutions.

In most practical problems the boundary conditions are discontinuous with the acoustic velocity or potential specified over part of the surface and the admittance over the rest. To determine the effect of the discontinuities on the numerical results, a cylinder with the velocity specified on the ends and the admittance specified in the center was investigated and the results are presented in Fig. 5. Although the errors of the numerical results for this case are increased compared with the errors shown in Fig. 4, the errors are within 10 per cent for values of k less than 5. However, when k = 10 errors of up to 40 per cent in the magnitude of the potential are encountered close to the discontinuity in the boundary condition. This result suggests

that more points need to be taken at higher frequencies with discontinuous boundary conditions present.

At higher tangential modes, the variation in the circumferential direction behaves as cos m θ where m = 0,1,2..... To check the numerical integration scheme in the circumferential direction, the surface acoustic potential was computed for m = 1 and m = 2. The results are presented in Fig. 6 for k = 2 with the velocity specified and the admittance zero everywhere on the surface. The computed and exact results are in agreement to within two per cent for both m = 1 and m = 2.

It has been shown[5] that once the surface potential has been accurately computed, the far field can be determined to at least the accuracy of the surface potential. This result is confirmed by the data presented in Fig. 7 for a cylinder with the velocity specified everywhere on the surface at k = 2. The results at 20 radii from the surface are in agreement with exact results to within one per cent even though the surface errors at some points is above two per cent. Data in Fig. 8 show that accurate results are obtained at distances greater than one integration stepsize from the surface. At closer distances errors from the numerical evaluation of the singularity in the Green's function defined by Eq. (4) leads to large errors.

IV. Summary and Conclusions

An integral solution of the Helmholtz equation is developed for use in acoustic radiation problems. Unlike previous formulations which give poor results at frequencies corresponding to eigenfrequencies of the surface under consideration, the formulation used in this study is valid at all frequencies. The surface potentials computed numerically for a sphere and cylinder using 20 points along the perimeter are accurate to within ten per cent for nondimensional frequencies ka of from one to ten where k is the wave number and a is the radius of the sphere or cylinder. For discontinuous boundary conditions, the numerical and exact values are in agreement to within 10 per cent for ka < 5. At higher frequencies the results are as much as 40 per cent in error at the point of discontinuity which suggests taking more points in evaluating the integral Helmholtz equation to increase the accuracy when discontinuous boundary conditions are specified. At distances greater than the numerical integration stepsize, the far field results are at least as accurate as the corresponding surface potential solutions.

References

1. Burton, A. J., "The Solution of Helmholtz' Equation in Exterior Domains using Integral Equations," NPL Report NAC 30, National Physical Laboratory, Teddington, Middlesex, Jan. 1973.

2. Schenck, H. A., "Improved Integral Formulation for Radiation Problems," Journal of the Acoustical Society of America," Vol. 44, No. 1, Jan. 1968, pp. 41-58.

3. Ursell, F., "On the Exterior Problems of Acoustics," Proceedings of the Cambridge Philosophical Society, Vol. 74, 1973, pp. 117-125.

4. Burton, A. J. and Miller, G. F., "The Application of Integral Equation Methods to the Numerical Solutions of Some Exterior Boundary Value

Problems," Proceedings of the Royal Society of London, A323, 1971, pp. 201-210.

5. W. L. Meyer, W. A. Bell and B. T. Zinn, "Integral Solutions of Three Dimensional Acoustic Radiation Problems," to be published in the Journal of Sound and Vibration.

6. Morse, P. M. and Ingard, K. U., Theoretical Acoustics, McGraw-Hill, New York, 1969, Chapter 7.

7. Stallybrass, M. P., "On a Pointwise Variational Principle for the Approximate Solution of Linear Boundary Value Problems," Journal of Mathematics and Mechanics, Vol. 16, No. 11, May 1967, pp. 1247-1286.

8. Andreasen, M. G., "Scattering from Bodies of Revolution," IEEE Transactions on Antennae and Propagation, March 1965, pp. 303-310.

9. Bell, W. A., Meyer, W. L., and Zinn, B. T., "Predicting the Acoustics of Arbitrarily Shaped Bodies Using an Integral Approach," AIAA Journal, Vol. 15, No. 6, June 1977, pp. 813-820.
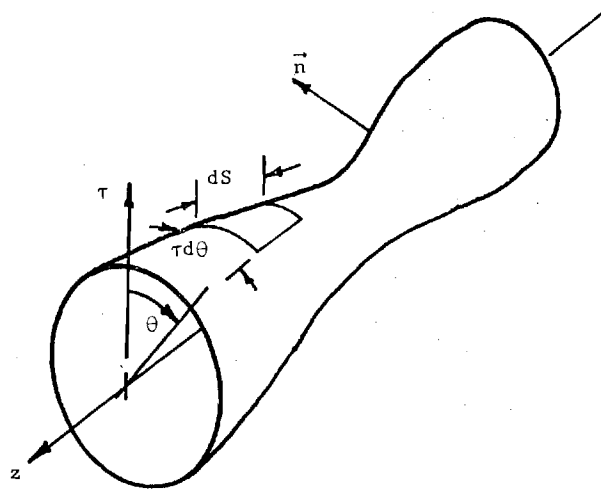
Figure 2. Cylindrical Surface Geometry.
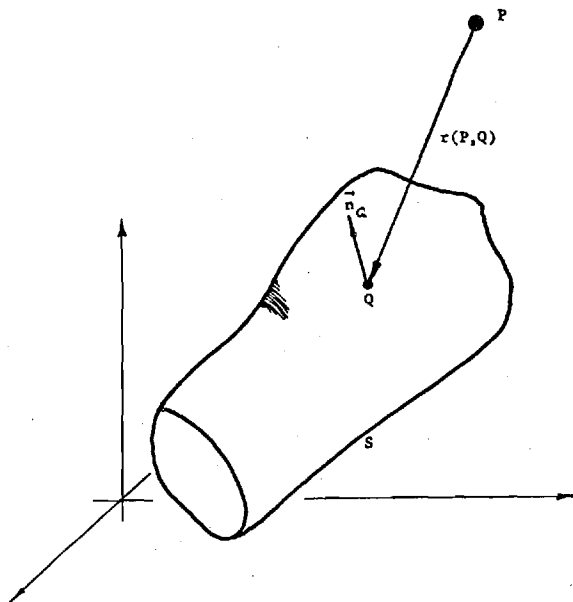
Figure 1. General Description of the Acoustic Radiation Problem
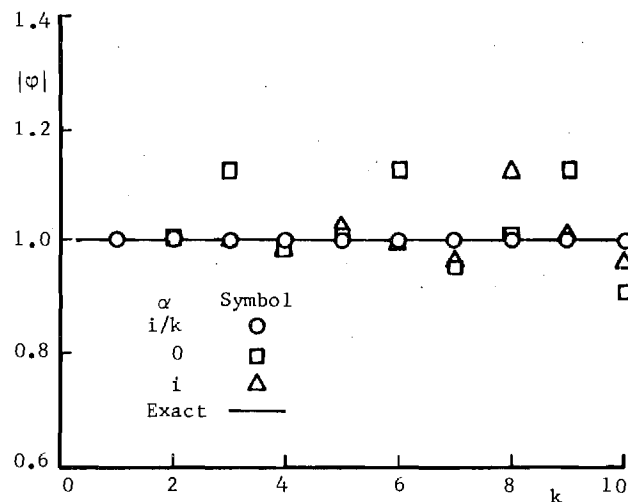
Figure 3. Effect of Coupling Constant α on Computed Surface Potential for a Sphere of Unit Radius with 20 Points.
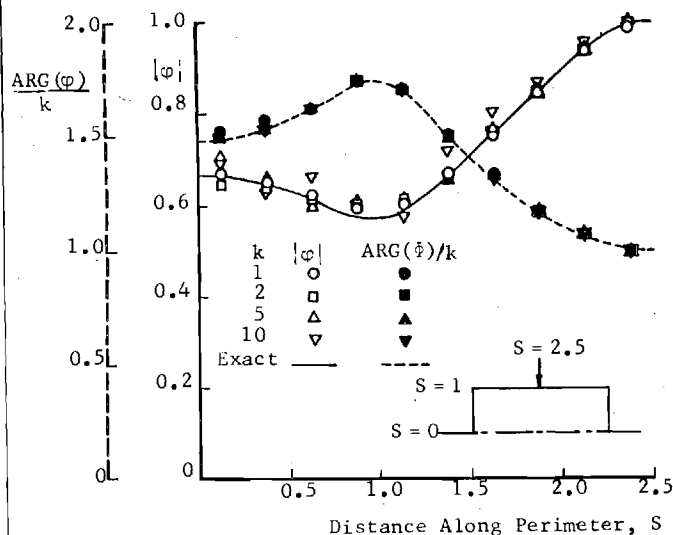
Figure 4. Dependence of the Computed Surface Potential for a Finite Cylinder with a Zero Admittance and Nonzero Normal Velocity Everywhere on the Surface with 20 Points.
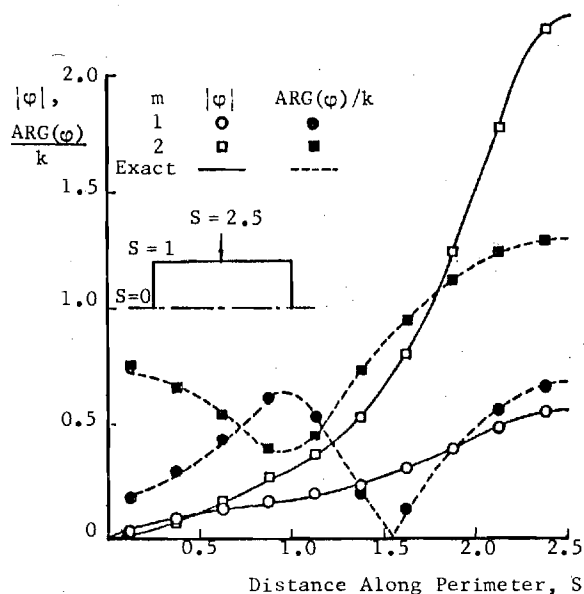
Figure 6. Computed Surface Potential for a Cylinder at the First and Second Tangential Modes for k = 2 and 20 Points.
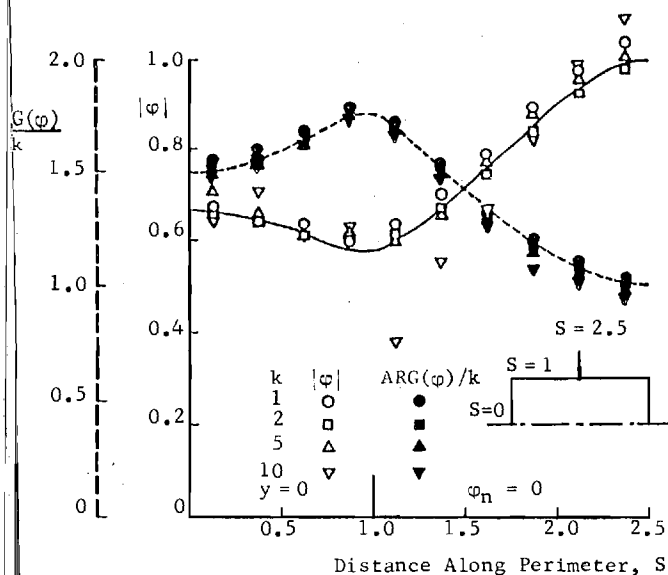
Figure 5. Effect of Discontinuous Boundary Conditions on the Computed Surface Potential for a Cylinder-20 Points.
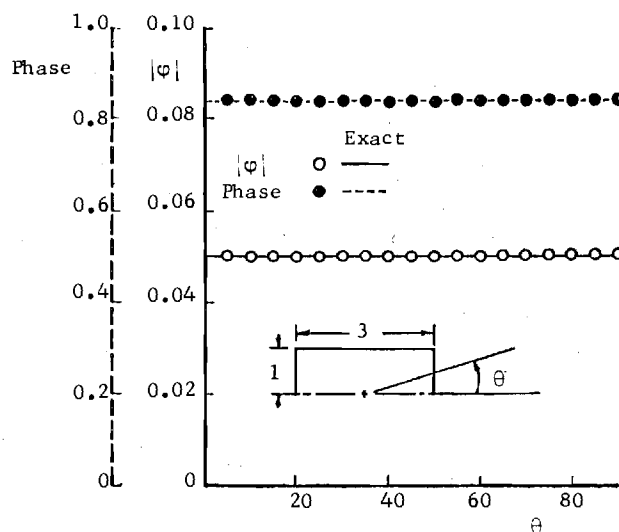
Figure 7. Computed Far Field Potential Distribution for a Cylinder at k = 2, m = 0, and 20 Radii from the Center of the Cylinder.
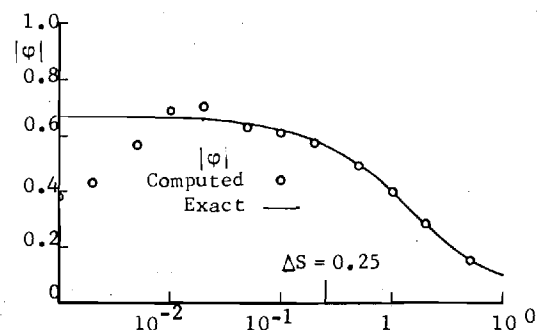
Figure 8. Dependence of the Far Field Solution of a Cylinder upon the Distance from the Surface for k = 2 and m = 0.

6

APPENDIX C

Predicting the Acoustics of Arbitrarily Shaped Bodies Using an Integral Approach

William A. Bell,* William L. Meyer,† and Ben T. Zinn‡

Georgia Institute of Technology, Atlanta, Ga.

An integral solution of the Helmoltz equation is developed for predicting the acoustic properties of arbitrarily shaped bodies. With the integral formulation, the acoustic potentials at the surface are solved independently of the internal acoustic field which, effectively, reduces the dimensionality of the problem by one. Considerable reductions in computation time and storage requirements are thus achieved. Efficient numerical techniques for solving the resulting algebraic equations are presented. Numerical results obtained for the two-dimensional problems of a circle and a rectangle agree to within one percent with available exact solutions. The modes of a star-shaped configuration and a duct with a right-angle bend are also determined to demonstrate the applicability of this method to complicated geometries and general boundary conditions. The acoustic properties of a sphere are investigated using an axisymmetric formulation. With the axisymmetric formulation the numerical and exact results agree to three significant figures.

I. Introduction

THE prediction of the acoustics of arbitrarily shaped bodies has a variety of applications in aerospace engineering. Among them are the determination of the internal and radiated sound fields from airbreathing propulsion systems and the investigation of the stability limits of rocket combustors. These studies are concerned with obtaining solutions to the Helmholtz equation, which is derived from the wave equation when a sinusoidal time dependence is assumed and which describes the spatial dependence of the oscillations. This equation is included in most standard texts on differential equations of mathematical physics (Ref. 1, Ch. 11) and has been extensively studied in both differential and integral form. The differential form is currently the most widely used.

In differential form, solutions of the Helmholtz equation can be obtained by separation of variables.[1,2] This method involves series expansions of the solutions in terms of eigenfunctions of the system. Although this technique has been successfully applied to several practical problems in duct wave propagation,[3-9] it has the following limitations: 1) the series expansions often involve special functions which are difficult to compute; 2) at high frequencies and at the boundaries the series are slowly convergent—therefore, a large number of terms in the series must be retained to ensure accurate results, which often requires excessive computation time; 3) this method can only be used with special coordinate systems and boundary conditions for which the separation of variables can be applied. At present only eleven suitable coordinate systems are known (Ref. 1, p. 513ff).

For arbitrarily shaped bodies, the differential form of the Helmholtz equation can be solved by writing the equation in terms of finite differences (Ref. 1, p. 703ff). Unlike separation of variables, this technique is not limited to ducts with simple geometries. A typical application of finite differences is given by Wynne and Plumblee[10] who solved for the transverse eigenvalues and eigenfunctions of an annular duct with lined walls. This technique involves the simultaneous solution of the acoustic potential value at every point within the duct. Once the potential values are known,

the acoustic pressure and velocity can then be determined. To obtain sufficient accuracy, fine grid sizes must be used which necessitates large computer storage requirements. This drawback was noted by Baumeister,[11] Baumeister and Rice,[12] and Alfredson[13] who used this technique in studies of duct wave propagation. Because of the storage requirements this technique has mainly been applied to two-dimensional problems. For three-dimensional problems numerical methods capable of handling large matrices must be used which require considerable computer time and computational effort.[14] This technique is also impractical in radiation problems which involve infinite domains.

To avoid the limitations of the differential formulation, the integral approach is employed in this study. The integral approach has been successfully applied to a wide range of acoustic problems. In determining the sound radiation field from vibrating surfaces, integral techniques have been widely used.[15-18] For example, Chen and Schweikert[15-16] employed this method to determine the radiation sound patterns for three-dimensional shapes with mixed boundary conditions. To check the accuracy of the results, they computed the radiated field produced by a piston vibrating on a sphere. For this problem an exact solution exists[3] and compares favorably with the numerical results. The integral formulation is also used to solve the problem of scattering by arbitrary shapes.[15-21] Banaugh and Goldsmith, for example, used this technique to investigate the effect of surface shape[19] on scattered sound fields. By applying this method to a circular cylinder, for which exact solutions are available,[3-4] and comparing the exact and numerical solutions, Banaugh and Goldsmith demonstrated the accuracy of the integral solution scheme. Although this method is capable of handling mixed boundary conditions, only surfaces with rigid boundaries were considered in Ref. 19. The effect of mixed boundary conditions was included in studies by Liu and Martenson[22] and Quinn[23] of the internal acoustic pattern of lined ducts with arbitrary shapes. Comparison of the theoretical predictions with experimental data showed generally good agreement. Unpublished work by Zinn and Gaylord[24] demonstrated the applicability of the integral formulation for the determination of the natural frequencies and modes for two-dimensional shapes. In this study the accuracy of the technique was determined by comparing the natural frequencies and mode shapes with available exact solutions for a two-dimensional cylinder with rigid walls. The agreement is to within four decimal places which is two-orders-of-magnitude more accurate than previous results

obtained by solving the differential Helmholtz equations using finite differences.[10] In another study by Tai and Shaw,[25] the integral method was applied to a right triangle. The resulting eigenfrequencies compared with exact solutions to within 5% and the maximum deviation between the numerically computed and exact potential fields was less than 1%.

To demonstrate the accuracy and the versatility of the integral solution technique, results are obtained for several acoustic problems involving a variety of geometries. To obtain a solution, the integral equation is first discretized to form a system of algebraic equations which are then solved for the acoustic potential at discrete points on the boundary. From these values the rest of the sound field is obtained. Methods for increasing the numerical accuracy by use of Gaussian quadrature and other numerical integration methods are presented and discussed. The first problem considered is the numerical evaluation of the resonant frequencies and natural modes of two-dimensional circular, rectangular, and star configurations. Exact and numerical values are compared for the circle and rectangle. The next problem considered is a two-dimensional duct with a right-angle bend with a sound source at one end and sound absorption treatment at various locations along the duct. The results are compared with finite difference solutions. These studies demonstrate the applicability of the integral formulation to complicated geometries and general boundary conditions. The next problem considered is the two-dimensional radiation problem of a piston set in a right circular cylinder. Again, the exact and numerical acoustic fields are computed and compared. Finally, a three-dimensional problem of determining the acoustic properties of a sphere is considered. The internal field is obtained using an axisymmetric formulation.

II. Governing Equations

The integral formulations of the wave equation for internal and radiation acoustic problems are developed in this section for two and three dimensions. The boundary conditions generally encountered in practical problems are then discussed. For clarity, only a brief account of the derivation of the basic equations will be given in this section. For a more detailed and rigorous development, Refs. 26 through 29 can be consulted.

Assume a frictionless, homogeneous gas, and let ρ_0 and p_0 be the density and pressure of the fluid at rest. Representing the acoustic pressure and particle velocity at a time t by p and u, Euler's equation for the conservation of momentum gives

$$\rho_0 \frac{\partial u}{\partial t} + \nabla p = 0 \tag{1}$$

The continuity equation yields the relationship

$$\frac{\partial p}{\partial t} + \rho_0 c_0^2 \nabla \cdot u = 0 \tag{2}$$

where c_0 is the speed of sound. By defining an acoustic potential function Ψ such that

$$u = \nabla \Psi \tag{3}$$

Equation (1) provides the relation

$$p = -\rho_0 \frac{\partial \Psi}{\partial t} \tag{4}$$

and Eq. (2) results in the classical wave equation

$$\nabla^2 \Psi - \frac{1}{c_0^2} \frac{\partial^2 \Psi}{\partial t^2} = 0 \tag{5}$$

The wave equation can also be written in terms of p and u, but it is more convenient to work with an acoustic potential function, from which both the acoustic pressure and particle velocity can readily be obtained.

Equation (5) is the wave equation for a general time dependence and can be written in integral form and solved by using retarded potentials.[21,28] However, for most practical problems a sinusoidal time dependence can be assumed which simplifies the problem considerably. Assume

$$\Psi(r,t) = \phi(r) e^{i\omega t} \tag{6}$$

Substituting Eq. (6) into Eq. (5) gives the Helmholtz equation

$$\nabla^2 \phi + k^2 \phi = 0 \qquad (k = \omega/c_0) \tag{7}$$

which can be solved by simpler methods not involving the use of retarded potentials.

Integral Formulation

To obtain an integral formulation of the Helmholtz equation, consider the problem shown in Fig. 1. Applying Green's theorem to the Helmholtz equation[1,28,29] gives the following integral relation

$$\int_\Gamma [\phi(Q) \frac{\partial G(P,Q)}{\partial n_Q} - G(P,Q) \frac{\partial \phi(Q)}{\partial n_Q}] dS_Q = 0 \tag{8}$$

where ϕ is the acoustic potential function and G is the Green's function defined by Eqs. (14-16), which also satisfies the Helmholtz equation. The Green's function is regular inside the surface except when $P = Q$. At this point G is singular. To remove this singularity from the integral given by Eq. (8), point P is surrounded by a small sphere or circle σ of radius ϵ. The integral will now include a term over σ which, on taking the limit as $\epsilon \to 0$, gives

$$\phi(P) = C \int_\Gamma [G(P,Q) \frac{\partial \phi(Q)}{\partial n_Q} - \phi(Q) \frac{\partial G(P,Q)}{\partial n_Q}] dS_Q \tag{9}$$

where C is $i/4$ for two dimensions and $1/4\pi$ for axisymmetric and three-dimensional shapes.

From Eq. (9) the value of the acoustic potential function at any point P within the surface can be determined from the boundary values of the potential and its normal derivative. Thus, the entire wave pattern within the surface can be constructed. For arbitrarily shaped surfaces for which numerical techniques must be used to obtain a solution, Eq. (9) requires much less computer storage than the differential
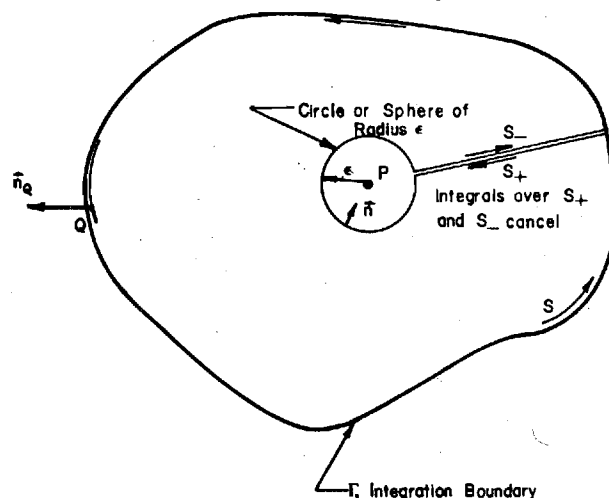

Fig. 1   Integration surface for an interior point.

formulation given by Eq. (7). Using Eq. (9) the value of the potential at each interior point can be obtained independently, whereas the method of finite differences used to solve Eq. (7) requires the simultaneous solution of ϕ for every interior point. The integral formulation avoids the large matrices involved with finite differences.

If the values of both ϕ and $\partial\phi/\partial n$ are known at every point on the boundary then the wave pattern can readily be determined from Eq. (9). However, for most practical acoustic problems either $\partial\phi/\partial n$ or an admittance condition relating ϕ and $\partial\phi/\partial n$ are given. Therefore, the values of the acoustic potential at the boundary must first be determined. The necessary relation is obtained by letting the point τ approach the boundary at some point T to obtain the following relation[26]

$$\phi(T) = 2C\int_\Gamma [G(T,Q)\frac{\partial\phi(Q)}{\partial n_Q} - \phi(Q)\frac{\partial G(T,Q)}{\partial n_Q}]dS_Q \quad (10)$$

Eq. (10) is applicable to a smooth boundary, but has been extended to include cusps and corners.[19,24] To obtain the interior wave pattern, Eq. (10) is first solved for the boundary values of ϕ. These values are then substituted into Eq. (9) to determine the acoustic potential at the interior points. Both Eqs. (9) and (10) involve singular integrands as T approaches Q although for smooth surfaces the integrals themselves are regular.

For exterior problems, analogous expressions to Eqs. (9) and (10) are obtained by taking the point P outside the surface Γ.[4] The integration in Eq. (8) is then carried out over the boundary, around a circle or sphere of radius ϵ with point P as a center, and then around a circle or sphere of radius R, which is arbitrarily large. In this manner the integration includes the entire external domain. However, by applying Sommerfeld's radiation condition, it can be shown that the integral about the infinite sphere or circle approaches zero as R approaches infinity.[4] Thus, the corresponding equations for the external domain become

$$\phi(P) = -C\int_\Gamma [G(P,Q)\frac{\partial\phi(Q)}{\partial n_Q} - \phi(P)\frac{\partial G(P,Q)}{\partial n_Q}]dS_Q \quad (11)$$

and

$$\phi(T) = -2C\int_\Gamma [G(T,Q)\frac{\partial\phi(Q)}{\partial n_Q} - \phi(Q)\frac{\partial G(T,Q)}{\partial n_Q}]dS_Q \quad (12)$$

It is important to note that Eqs. (11) and (12) involve integrations about the boundary of the body only. Thus, the radiated field at any distance from the body can be obtained once the surface acoustic potential is known. With finite differences, the values of the potential at every point in a very large domain would have to be computed in order to obtain the radiated field. Also, an artificial boundary condition at a large distance from the surface must be assumed. These factors make the application of finite differences to problems of this type rather inefficient whereas the integral formulation can readily be adopted to such situations.

Eqs. (9) through (12) are applicable to two-dimensional, axisymmetric, and three-dimensional acoustic problems. In the two-dimensional and axisymmetric cases, these equations involve line integrals; and in the three-dimensional case, the integrals are taken over a surface. Note that the dimensionality of the problem is reduced by one—a valuable simplification.

The Green's functions satisfy the following inhomogeneous forms of the Helmholtz reduction with homogeneous boundary conditions[1]

$$\nabla^2 G + k^2 G = \delta(P-Q) \quad (13)$$

where δ is the Dirac delta function. The Green's functions are[1,17,18]

$$G(P,Q) = H_0^{(1)}(kr) \quad \text{for two dimensions,} \quad (14)$$

$$G(P,Q) = 2\int_0^\pi \frac{e^{ikr}}{r}\cos m\theta d\theta \quad \text{for axisymmetric bodies} \quad (15)$$

and

$$G(P,Q) = e^{-ikr}/r \quad \text{for three dimensions} \quad (16)$$

where r is the distance between points P and Q, and $H_0^{(1)}(kr)$ is the zeroth order Hankel function of the first kind.

Boundary Conditions

The two most common boundary conditions in practical acoustic problems are the Neumann and Robin conditions. The Neumann condition of interest in the present study is

$$\partial\phi/\partial n = A \quad (17)$$

where A is the velocity amplitude of a given sound source. In the absence of a sound source $A = 0$; this condition means that the particle velocity is zero at the boundary which implies a perfectly reflecting, or rigid surface. For surfaces which absorb sound, such as lined duct walls, an admittance condition is usually specified, which leads to the Robin condition. Defined as the radio of the normal component of the particle velocity to the pressure perturbation, the admittance y can be written as

$$y = \rho_0 c_0 (u_n/p) \quad (18)$$

Substituting for u_n and p from Eqs. (3) and (4) gives

$$(\partial\phi/\partial n) + iky\phi = 0 \quad (19)$$

Eq. (19) is the Robin condition.[29] For sound-absorbing materials or devices, the admittance can be either analytically determined[30-32] or measured using the impedance tube or a related technique.[33-34] The effects of a given material on the internal acoustic properties of a particular geometry can be
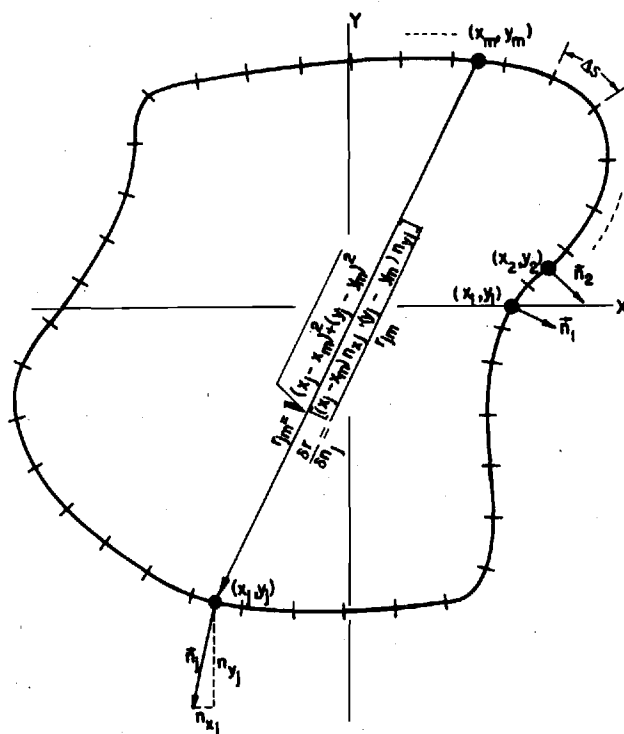
Fig. 2   Geometric considerations for the general problem.

determined by substituting the admittance of the material into Eq. (19) and solving Eqs. (9) and (10) or (11) and (12) for the acoustic potential. Thus, the analytical techniques used in this investigation is applicable to a vast number of duct acoustic problems. Since the admittance of a combustion process can also be measured,[35] this analysis can also be applied to related linear combustion instability problems, provided that the equations are applied to regions where the Helmholtz equation holds and mean flow effects can be neglected. By replacing the combustion process by an admittance condition, studies of combustion instability have been conducted in liquid and solid propellant combustors.[36-37] This research allows the extension of these analyses to more general shapes.

Substituting Eq. (19) into Eq. (10) gives for the internal field

$$\phi(T) + 2C\int_\Gamma \phi(Q)[\frac{\partial G(T,Q)}{\partial n_Q} + iky(Q)G(T,Q)]dS_Q$$

$$= -2C\int_\Gamma A(Q)G(T,Q)dS_Q \tag{20}$$

A similar expression is obtained from Eq. (12) for the exterior problem. For surfaces with spatially varying admittances, the admittance is a function of Q. For most cases considered in this study, y is assumed constant although nonuniform admittance distributions can be easily handled.

III. Solution Technique

In the last section, the integral equations were developed which describe the interior and exterior acoustic fields or a surface with arbitrary shape and mixed boundary conditions. The numerical solution technique for solving these equations to obtain the internal or radiated acoustic patterns is presented in this section and can be divided into four parts. The first is the discretization of the integral equations into a corresponding system of linear, and algebraic equations in ϕ suitable for solution on a computer. The second part is the specification of the geometry and boundary conditions. The third is the computation of the coefficients of the system of equations and the final part is the methods used to solve for the surface potential from the algebraic equations.

Discretization of the Integral Equations

In two dimensions and for axisymmetric problems, Eq. (20) involves a one-dimensional improper integral about the boundary line. For this type of problem several numerical integration techniques[38-39] are available. The simplest is the trapezoidal rule which has been shown to yield excellent results in two-dimensional studies with this type of integral.[19,24,25] Using this numerical integration scheme, Eq. (20) becomes

$$\phi_m + 2C\sum_{j=1}^{N} \phi_j\left[\frac{\partial G(r_{jm})}{\partial n_j} + iky_jG(r_{jm})\right]\Delta S_j$$

$$= -2C\sum_{j=1}^{N} A_jG(r_{jm})\Delta S_j \tag{21}$$

where one equation for ϕ is obtained for each value of m and n is varied from 1 to N. Eq. (21) was initially used in this investigation to generate the N equations for ϕ and accurate results were obtained when the admittance y was zero everywhere on the boundary[40] which is the case considered in previous studies.[19,24,25] However, when a nonzero admittance is assumed, this technique gives inaccurate results because of the contribution from the Green's function when the point j approaches m. Because of the singular nature of the Green's function at the point m, care must be taken when numerically integrating this function over the subinterval m. To increase the accuracy in evaluating the integrand, Eq. (20) is broken up into N integrals given by Eq. (22).

$$\phi_m\left\{1 + 2C\int_{S_{m-\frac{1}{2}}}^{S_{m+\frac{1}{2}}}\left[\frac{\partial G(r_{\frac{1}{2}})}{\partial n_{\frac{1}{2}}} + iky_mG(r_{\frac{1}{2}})\right]dS_j\right\}$$

$$+ 2C\sum_{\substack{j=1\\j\neq m}}^{N} \phi_j\int_{S_{j-\frac{1}{2}}}^{S_{j+\frac{1}{2}}}\left[\frac{\partial G(r_{jm})}{\partial n_j} + iky_jG(r_{jm})\right]dS_j$$

$$= -2C\sum_{j=1}^{N} A_j\int_{S_{j-\frac{1}{2}}}^{S_{j+\frac{1}{2}}} G(r_{jm})dS_j \tag{22}$$

In both Eqs. (21) and (22) the values of ϕ are assumed to be constant over each of the N subintervals. The difference is the method by which the terms involving the Green's function are evaluated. In Eq. (21) an average value is computed over each of the subintervals based on r_{jm}. With Eq. (22) these terms are integrated numerically from $r_{j-\frac{1}{2},m}$ to $r_{j+\frac{1}{2},m}$ using Gaussian quadrature[39-40] to obtain more accurate values. This type of formulation has been used before with trapezoidal instead of Gaussian quadrature formulas.[18] In the present study for two-dimensional and axisymmetric problems, a reduction in error of two orders of magnitude in the numerical results for a nonzero admittance was achieved using Eq. (22) instead of Eq. (21).[40]

Surface Geometry and Boundary Conditions

The first step in solving Eq. (22) is the determination of the coefficients of ϕ_j and ϕ_m. These coefficients depend upon the surface geometry through the terms $\partial/\partial n_j$, r_{jm}, and ΔS_j. By specifying the admittance y and/or the sound velocity amplitude A over every subinterval j, the effect of the boundary conditions are included in the evaluation of the coefficients.

To solve for the terms involving the surface geometry, the first expression inside the integrals of Eq. (22) is written as

$$\frac{\partial G(r)}{\partial n} = \frac{\partial G(r)}{\partial r}\frac{\partial r}{\partial n}$$

Th expressions for $\partial G/\partial r$ are obtained by differentiating Eqs. (14) through (16). Substituting this expression into Eq. (22)

Table 1   Eigenfrequencies and natural modes of a circle for various admittance values

MODE		ADMITTANCE VALUE		
		$y = 0$	$y = 0.3$	$y = 0.3i$
(+ −)	COMPUTED	1.84122	1.8324+0.4423i	1.4441-0.0071i
	EXACT	1.84118	1.8322+0.4432i	1.4384
(+ − / − +)	COMPUTED	3.05423	3.0791+0.53971i	2.5369-0.01511i
	EXACT	3.05424	3.0786+0.5442i	2.5427
(+)	COMPUTED	3.83175	Not Computed	Not Computed
	EXACT	3.83171	3.8188+0.3095i	3.5510
(+ − / − +)	COMPUTED	4.20135	4.2538 0.6199i	3.5816 - 0.0231i
	EXACT	4.20119	4.2532 0.6351i	3.5615
(+ − / − +)	COMPUTED	5.31783	Not Computed	Not Computed
	EXACT	5.31755	5.3953 0.71011i	4.5767

Table 2   Resonant frequencies and natural modes of a rectangle for different admittance values at the ends

MODE		ADMITTANCE VALUE		
		$y = 0$	$y = 0.3$	$y = 0.3i$
(+ −)	COMPUTED	3.1432	3.150 + 0.6199i	2.558+0.0021i
	EXACT	3.1416	3.142 + 0.6190i	2.559
(− + −)	COMPUTED	6.2877	6.302+0.6156i	5.886 +0.0021i
	EXACT	6.2832	6.283 +0.6190i	5.884
(+ −)	COMPUTED	7.0312	7.146 +0.5881i	6.333 - 0.007i
	EXACT	7.0248	Not Computed	6.283
(+ − +)	COMPUTED	8.893	8.934 +0.6101i	8.303-0.011i
	EXACT	8.886	Not Computed	8.299
(+ −)	COMPUTED	9.4329	9.456 +0.6106i	8.847 +0.007i
	EXACT	9.4248	9.425 +0.6190i	8.842i

gives a relation which involves $\partial r/\partial n_j$, r_{jm} and dS. The expressions for $\partial r/\partial n_j$, r_{jm} and dS can be written in parametric form for bodies with simple shapes, and this type of representation has been used in previous studies using simple geometries.[19-20,24,41,42] By taking advantage of symmetry, considerable savings in computer storage and computation times were achieved. In fact, Greenspan and Werner[42] showed that for a circle, Eq. (22) can be reduced to a single equation instead of a system of equations which could readily be solved to obtain the acoustic field. In the study by Tai and Shaw,[25] the method of images (Ref. 1, Ch. 11) was used to greatly reduce the numer of points necessary to compute eigenfrequencies and eigenmodes of a family of triangles. Although these studies demonstrate valuable simplifications which can be made in applying the integral formulation to a particular problem, the techniques used are not applicable to more general problems involving complicated geometries and nonuniform boundary conditions.

In the present study for two dimensions, the expressions for the geometric variables are written in parametric form only for the circle. In the rest of the configurations considered, a general formulation is used. The fact that a parametric representation cannot be used in general cases is not a serious drawback—in fact, it somewhat simplifies the formulation. Consider the general two-dimensional problem depicted in Fig. 2. By specifying the x and y coordinates at the midpoint of each of the subintervals, the distance r_{jm} is readily computed from the expression

$$r_{jm} = \sqrt{(x_j - x_m)^2 + (y_j - y_m)^2} \tag{23}$$

The expression for $\partial r/\partial n_j$ can then be obtained since it represents the dot product of the gradient of r and the normal at j. Thus,

$$\frac{\partial r}{\partial n_j} = \frac{(x_j - x_m)n_{xj} + (y_j - y_m)n_{yj}}{r_{jm}} \tag{24}$$

where n_{xj} is the component of the normal vector j in the x direction (or the cosine of the angle between the normal vector and the x-axis) and n_{yj} is the corresponding y component (the sine of the angle between the normal vector and the y-axis). Analogous expressions for r_{jm} and $\partial r/\partial n_j$ can be obtained for axisymmetric[17-18] and three-dimensional problems. For two-dimensional and axisymmetric problems, the line segment length ΔS_j is simply

$$\Delta S_j = \sqrt{(x_{j+1/2} - x_{j-1/2})^2 + (y_{j+1/2} - y_{j-1/2})^2}$$

or, for N equally spaced subintervals, $S_j = L/N$ where L is the length of the perimeter of the surface. For three-dimensional bodies, ΔS_j is the area of each of the subsurfaces taken over the boundary.
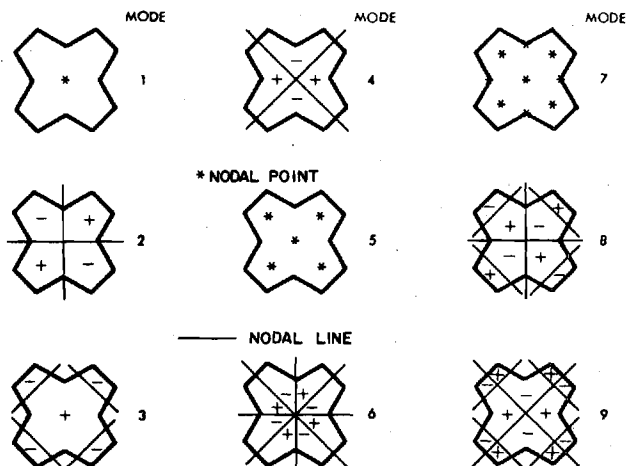
Computation of the Coefficients of the Discretized Integral Equation

Once the geometry has been specified, the coefficient of ϕ in Eq. (22) can be determined by evaluating the Green's functions $G(r_{jm})$ and $\partial G(r_{jm})/\partial r_{jm}$. There are two problems in determining these functions: the first is a rapid, accurate method for computing them over a wide range of the argument kr_{jm}; and the second is the singularity associated with each function as r_{jm} approaches zero.

For the two-dimensional problems to compute the Hankel functions two routines have been used in this study. The first consists of a series expansion using standard formulas for the Hankel function with complex arguments.[39,43] A sufficient number of terms is taken to satisfy a specified degree of accuracy. To minimize time, a different series expansion which was developed by Hitchcock[44] is used for determining these functions in the studies of the rectangle, star, and duct with a right-angle bend. With his formulation, accuracies of 10^{-10} or greater are achieved using nine terms or less in the series expansion. Reductions of up to 50% in computer times can be achieved with this formulation.

For the axisymmetric problem, the integral in Eq. (15) is carried out using a 20-point Gauss-Legendre quadrature formula. For three-dimensional problems, evaluation of the Green's function given by Eq. (16) is straightforward.

The major problem in accurately computing the coefficients in Eq. (22) is the singularity associated with the Green's functions as r_{jm} approaches zero; that is, as the point j approaches m in Fig. 2. The two-dimensional and axisymmetric Green's functions have logarithmic singularities. In this study, the inaccuracies involved are minimized by subdividing the intervals as indicated by Eq. (22).

Determination of the Acoustic Potential

Once the coefficients of the surface potential at each discrete point on the surface are determined, the equations are solved for ϕ using a complex Gauss-Jordan reduction scheme. The interior or exterior points can then be found using the discretized form of Eq. (9).

To determine the eigenfrequencies of a particular geometry, the technique described in Ref. 40 is used. Essentially, this technique consists of: 1) determining the frequency k for which the determinant of the coefficients in the homogeneous form of Eq. (22) is zero, 2) normalizing the equation at the eigenfrequency to obtain the surface distribution of the mode, and 3) using Eq. (9) in discretized form to find the interior sound field.

V. Results

Using the numerical techniques described in the last section, solutions have been obtained for a variety of two-dimensional and axisymmetric problems to demonstrate its broad range of

Fig. 3   Nodal points and lines for the first nine modes of the star.

Table 3   Surface potentials for a circle of unit radius, second mode, $Y = 0$

Angle	Numerical	Exact
12	.9130	.9135
24	.6681	.6691
36	.3077	.3090
48	−.1059	−.1045
60	−.5012	−.5000
72	−.8099	−.8090
84	−.9785	−.9781
96	−.9779	−.9781
108	−.8082	−.8090
120	−.4988	−.5000
132	−.1013	−.1045
144	.3104	.3090
156	.6702	.6691
168	.9141	.9135
180	1.0000	1.0000

Table 4 Surface potential for a rectangle, height to width ratio = 0.5, first mode, rigid walls

	Y	Numerical	Exact
1/2	1/14	1.0061	1.0063
1/2	2/14	1.0060	1.0063
1/2	3/14	1.0055	1.0063
13/28	1/4	1.0000	1.0000
11/28	1/4	.9501	.9499
9/28	1/4	.8524	.8521
7/28	1/4	.7119	.7116
5/28	1/4	.5356	.5354
3/28	1/4	.3325	.3324
1/28	1/4	.1127	.1127

applications. The two-dimensional form of the integral equation has been used to compute the resonant frequencies and natural modes of a circle, rectangle, and star configuration. In addition, the problem of a duct with a right angle bend is considered, and results using Eq. (22) are compared with finite difference solutions. The two-dimensional problem of sound radiation from a right circular cylinder is then considered and the numerical and exact solutions are compared. Finally the acoustic properties of a sphere are computed using the axisymmetric formualtion.

For a circle and rectangle, comparisons between exact and numerical solutions are presented in Tables 1 and 2. In these tables the numerical and exact eigenfrequencies are tabulated for three admittance values, $y=0$, $y=0.3$, $y=0.3i$, with thirty points taken on the boundary. The best agreement between the computed and exact results occurs at the zero admittance condition. For the circle, the real part of the eigenfrequencies compare to five significant figures and the imaginary parts are accurate to 0.001 for the first five modes. When a nonzero admittance condition is introduced, the accuracy is reduced to three significant figures in the real part and to 0.01 in the imaginary part of the eigenfrequencies.

As with the circle, the agreement between the exact and numerical values for the rectangle is good for a rigid boundary but deteriorates when a nonzero admittance is introduced. From Table 2 the agreement is to almost four significant figures in the real part of the eigenfrequency and to within 0.01 in the imaginary part for a rigid wall. The Gaussian integration techniques developed in Sec. III improve
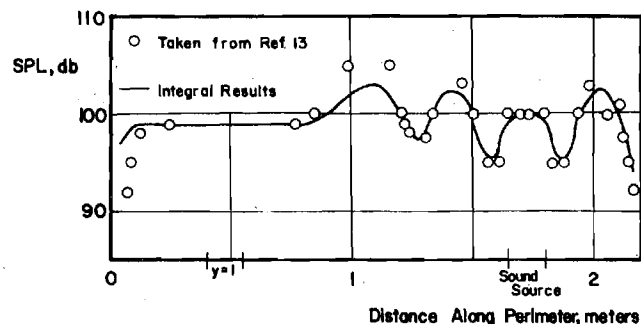
Fig. 5 Comparison of numerical results for a duct with a right-angle bend using the integral and finite difference approaches, Case 1.
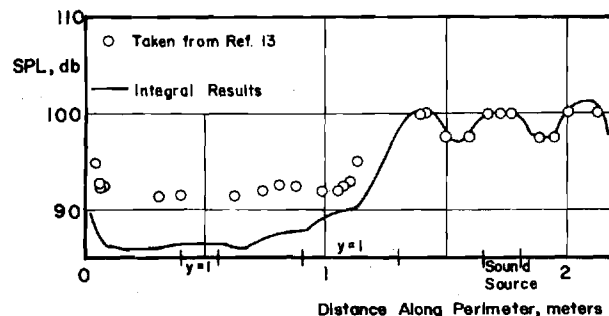
Fig. 6 Comparison of numerical results for a duct with a right-angle bend using the integral and finite difference approaches, Case 2.

the accuracy of the computed eigenfrequencies for a nonzero admittance condition by an order of magnitude.

For the circle the accuracy of the computed natural mode shapes is shown in Table 3. The agreement between the exact and computed eigenmodes for a rigid boundary is to within 0.01% for interior points sufficiently far removed from the boundary. For a nonzero admittance at the surface, the accuracy is to within 2%. These results are obtained using the interior analog of Eq. (21) which explains the deterioration in accuracy of the interior points as the boundary is approached. Equation (22) is used in the studies of the rectangle, star, and duct problems and more accurate results are obtained close to the boundary. For the rectangle, the boundary values of the acoustic potential are presented in Table 4. The agreement between the exact and numerical results is within one-half of a percent. Computation times range from ten sec per eigenfrequency for the circle to 45 sec for the rectangle on UNIVAC 1108 computer. Using the discretized form of Eq. (9), interior points require approximately two sec per point to compute.

In studying the star-shaped boundary, which is of interest in solid-rocket combustion instability problems, the applicability of the integral solution technique to a complicated geometry for which separation of variables does not apply can be assessed. The first nine eigenfrequencies and natural modes for the star are presented in Fig. 3 for a rigid wall with 48 points taken on the surface. The most unique feature of the acoustic field for the star is the appearance of nodal points at some of the resonant modes. In the circle and rectangle nodal lines only are present, and they follow one of the separable coordinates of the boundary. With the star both nodal lines and points can occur which is in qualitative agreement with experimental observations for unstable solid propellant combustors. Computation times are from 60 to 75 sec per mode. The modes of a typical solid propellant configuration during a burn have also been computed and are given in Ref. 45.

The last internal two-dimensional problem investigated is that of a duct with a right-angle bend shown in Fig. 4. The
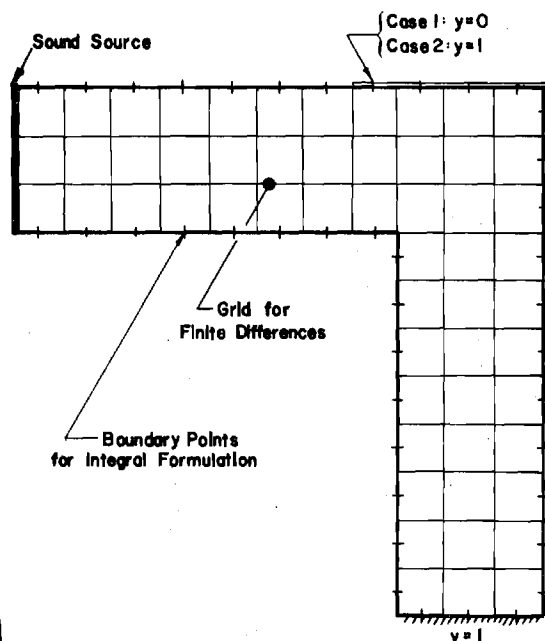
4 Locations of the discrete points, nonzero admittance undaries, and the sound source for the duct with a right-angle bend
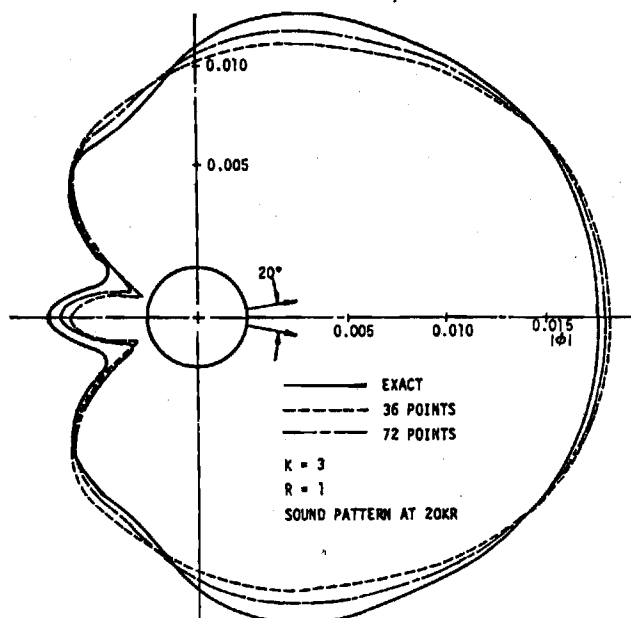
Fig. 7   Sound pattern produced by a 20° vibrating piston set in a circular cylinder.

nonuniform surface admittance, 2) to include a sound source in the integral formulation, and 3) compare the results obtained by the integral technique with the finite difference solutions of Ref. 13.

The results obtained using this configuration are presented in Figs. 5 and 6 and are compared with the solutions obtained uisng the finite difference method. Although the results using the integral approach are in qualitative agreement with the finite difference solution, quantitative agreement is lacking. The same number of boundary points are taken in both cases. Doubling the number of subintervals using Eq. (22) does not improve the agreement between the two sets of data. However, it does show that the results of the integral formulation are self-consistent. An experimental setup is

currently being developed to check these results and should clarify the discrepancy between these two methods.

For two-dimensional radiation problems, excellent results are obtained as shown in Fig. 7. Here the radiated field from a piston set in a right circular cylinder is computed and compared with exact results from Ref. 3. The mean square error is less than 2% while the computation time required is 15 sec to obtain both the surface and far field patterns.

To check the accuracy of the axisymmetric formulation, the first two resonant frequencies and natural mode shapes of a sphere were computed and are presented in Table 5. As with the two-dimensional problems, agreement between the exact and numerical calculations is excellent. Computation times are approximately two minutes per mode; however, no attempt was made to take advantage of the symmetry of the problem which can reduce the computation time by at least a factor of two.

Conclusions and Recommendations

The results for the circle and rectangle show that the integral technique is very accurate in determining resonant frequencies and natural mode shapes. Its application to the star configuration demonstrates its usefulness in studying the acoustics of complicated shapes. For the duct with a right-angle bend, the integral approach is shown to be applicable to nonuniform boundary conditions involving sound sources. The formulation also gives accurate results for two-dimensional radiation problems shown in the study of the right circular cylinder.

With the axisymmetric formulation accurate results are obtained for the internal eigenmodes of a sphere. Extensions to more complicated boundaries can readily be made.

Acknowledgment

Table 5   Resonant frequencies and surface potentials for a sphere of unit radius, first and second modes, axisymmetric formulation

Computed	Resonant frequencies	Exact
2.084-0.0041		2.082
3.346-0.007i		3.342

Angle	Normalized surface potential Computed	Exact
(First mode)		
5	1.00000	1.00000
15	.96960	.96962
25	.90975	.90977
35	.82232	.82228
45	.70992	.70981
55	.57593	.57577
65	.42439	.42423
75	.25992	.25981
85	.08753	.08749
(Second mode)		
5	1.0000	1.0000
15	.9098	.9099
25	.7403	.7405
35	.5121	.5124
45	.2275	.2529
55	−.0072	−.0066
65	−.2346	−.2348
75	−.4051	−.4041
85	−.4953	−.4942

[a] Numerical results obtained using Eq. (21) instead of Eq. (22).

References

[1] Morse, P. M. and Feshback, H., *Methods of Theoretical Physics, Parts I and II*, McGraw-Hill, New York, 1953.

[2] Weinberger, H. F., *A First Course in Partial Differential Equations*, Blaisdell, Waltham, Mass., 1965.

[3] Morse, P. M. and Ingard, K. U., Ch. 9, *Theoretical Acoustics*, McGraw-Hill, New York, 1969.

[4] Skudrzyk, E., *The Foundations of Acoustics*, Springer-Verlag, Vienna, Austria, 1971, Ch. 22 and 23.

[5] Mitchell, C. E., Espander, W. R., and Baer, M. R., "Determination of Decay Coefficients for Combustors with Acoustic Absorbers," NASA CR 120836, Jan. 1972.

[6] Oberg, C. L., "Improved Design Techniques for Acoustic Liners," Rocketdyne, Canoga Park, Calif., Report No. RR-68-5, May 1968.

[7] Oberg, C. L., Wong, T. L., and Schmeltzer, R. A., "Analysis of the Acoustic Behavior of the Baffled Combustion Chambers," NASA CR 72625, Jan. 1970.

[8] Doak, P. E., "Excitation, Transmission and Radiation of Sound from Source Distributions in Hard-Walled Ducts of Finite Length (I): The Effects of Duct Cross-Section Geometry and Source Distribution Space-Time Pattern, (II): The Effect of Duct Length," *Journal of Sound and Vibration*, Vol. 31, Jan. 1973, pp. 1-72, and Feb. 1973, pp. 137-174.

[9] Lansing, D. L. and Zorumski, W. E., "Effects of Wall Admittance Changes on Duct Transmission and Radiation of Sound," *Journal of Sound and Vibration*, Vol. 27, Jan. 1973, pp. 85-100.

[10] Wynne, G. A. and Plumblee, H. E., "Calculation of Eigenvalues of the Finite Difference Equations Describing Sound Propagation in a Duct Carrying Shear Flow," *presented at the 79th Meeting of the Acoustical Society of America*, Atlantic City, N.J., April 21, 1970.

[11] Baumeister, K. J., "Application of Finite Difference Techniques to Noise Propagation in Jet Engines," NASA TMX-68621, Nov. 1973.

[12] Baumeister, K. J. and Rice, E. J., "A Difference Theory for Noise Propagation in an Acoustically Lined Duct with Mean Flow," *AIAA Progress in Astronautics and Aeronautics: Aeroacoustics: Jet*

and Combustion Noise, Vol. 37, Editor: Henry T. Nagamatsu; Associate Editors: Jack V. O'Keefe and Ira R. Schwartz, MIT Press, Cambridge, Mass., 1975, pp. 435-453.

[13]Alfredson, R. J., "A Note on the Use of the Finite Difference Method for Predicting Steady State Sound Fields," *Acustica*, Vol. 28, May 1973, 296-301.

[14]Cantin, G., "Three-Dimensional Finite Element Studies, Part One: Service Routines," Naval Postgraduate School, Monterey, Calif., NPS-59C 172121A, Dec. 1972.

[15]Chen, L. H. and Schweikert, D. G., "Sound Radiation from an Arbitrary Body," *Journal of the Acoustical Society of America*, Vol. 35, Oct. 1963, pp. 1626-1632.

[16]Chen, L. H., "A Matrix Method of Analysis of Structure-Fluid Interaction Problems," ASME Paper 61-WA-220, Aug. 1961.

[17]Chertock, G., "Sound from Vibrating Surfaces," *Journal of the Acoustical Society of America*, Vol. 36, July 1964, pp. 1305-1313.

[18]Copley, L. G., "Integral Equation Method for Radiation from Vibrating Bodies," *Journal of the Acoustical Society of America*, Vol. 42, April 1967, pp. 807-816.

[19]Banaugh, R. P. and Goldsmith, W., "Diffraction of Steady Acoustic Waves by Surfaces of Arbitrary Shape," *Journal of the Acoustical Society of America*, Vol. 35, Oct. 1963, pp. 1590-1601.

[20]Mitzner, K. M., "Numerical Solution for Transient Scattering from a Hard Surface of Arbitrary Shape-Retarded Potential Technique," *Journal of the Acoustical Society of America*, Vol. 42, Feb. 1967, pp. 391-397.

[21]Shaw, R. P., "Scattering of Plane Acoustic Pulses by an Infinite Plane with a General First-Order Boundary Condition," *Journal of Applied Mechanics*, Sept. 1967, pp. 770-772.

[22]Quinn, D. W., "An Integral Equation Method for Duct Acoustics with Varying Cross Sections and Axially Varying Impedance," *AIAA Journal*, Vol. 15, Feb. 1977, pp. 278-281.

[23]Liu, H. K. and Martenson, A. J., "Optimum Lining Configurations," *Basic Aerodynamic Noise Research*, NASA SP-207, July 1969, pp. 425-434.

[24]Zinn, B. T. and Gaylord, C. G., Unpublished Notes and "An Analytical Investigation of Acoustic Modes of Two and Three Dimensional Solid Rocket Motors," a Thesis Proposal by C. G. Gaylord, School of A. E., Georgia Tech., Atlanta, Ga.

[25]Tai, G. C. and Shaw, R. P., "Eigenvalues and Eigenmodes for the Homogeneous Helmholtz Equation for Arbitrary Domains," Report No. 90, Dept. of E. S., State University of N.Y. at Buffalo, Aug. 1973.

[26]Kellogg, O. D., Ch. VI, *Foundations of Potential Theory*, Dover Publications, New York, 1953.

[27]Webster, A. G., Ch. VIII, *The Dynamics of Particles*, Dover Publications, New York, 1959.

[28]Baker, B. B. and Copson, E. T., Ch. 1, *The Mathematical Theory of Huygens' Principle*, Oxford at the Clarendon Press, 1950.

[29]Burton, A. J., "The Solution of Helmholtz's Equation in Exterior Domains Using Integral Equations," NPL Report NAC 30, National Physical Laboratory, Teddington, Middlesex, Jan. 1973.

[30]Strutt, J. W. (Lord Rayleigh), Ch. 16, *The Theory of Sound*, Vol. II, Dover Publications, New York, 1945.

[31]Ingard, K. U., "On the Theory and Design of Acoustic Resonators," *Journal of the Acoustical Society of America*, Vol. 25, Nov. 1953, pp. 1037-1061.

[32]Crocco, L. and Sirignano, W. A., "Behavior of Supercritical Nozzles under Three-Dimensional Oscillatory Conditions," AGARDograph 117, Butterworth Publications, London, 1967.

[33]Scott, R. A., "An Apparatus for Accurate Measurement of the Acoustic Impedance of Sound Absorbing Materials," *Proceedings of the Physical Society*, Vol. 58, 1946, p. 253.

[34]Zinn, B. T., Bell, W. A., and Daniel, B. R., "Experimental Determination of Three-Dimensional Liquid Nozzle Admittances," *AIAA Journal*, Vol. 11, March 1973, pp. 267-272.

[35]*T-Burner Manual*, Chemical Propulsion Information Agency, CPIA Publication No. 191, Nov. 1969.

[36]Crocco, L. and Cheng, S. I., "Theory of Combustion Instability in Liquid Propellant Rocket Motors," AGARDograph 8, Butterworth Publications, London, 1956.

[37]Culick, F. E. C., "Review of Calculations for Unsteady Burning of a Solid Propellant," *AIAA Journal*, Vol. 6, Dec. 1968, pp. 2241-2255.

[38]Conte, S. D., Chs. 2 and 5, *Elementary Numerical Analysis*, McGraw-Hill, St. Louis, 1965.

[39]Abramowitz, M. and Stegun, I. A., *Handbook of Mathematical Functions*, NBS AMS No. 55, May 1968.

[40]Bell, W. A., "Resonant Frequencies and Natural Modes of Arbitrarily Shaped Ducts," Final Report, NSF Research Initiation Grant GK-42159, Georgia Tech., Atlanta, Ga., April 1, 1976.

[41]Jones, D. S., "Integral Equations for the Exterior Acoustic Problem," *Quarterly Journal of Mechanics & Applied Mathematics*, Vol. 27, Jan. 1974, pp. 129-142.

[42]Greenspan, D. and Werner, P., "A Numerical Method for the Exterior Dirichlet Problem for the Reduced Wave Equation," *Archive for Rational Mechanics and Analysis*, Vol. 23, No. 4, 1966, pp. 288-316.

[43]Gradshteyn, I. S. and Ryzhik, I. M., *Table of Integrals, Series, and Products*, Sixth Printing, Academic Press, New York, 1972, 951.

[44]Hitchcock, A. J. M., "Polynomial Approximations to Bessel Functions of Order Zero and One and to Related Functions," *Math Tables & Other Aids to Computations*, Vol. 11, 1957, pp. 86-88.

[45]Bell, W. A., Meyer, W. L., and Zinn, B. T., "Prediction of the Acoustics of Solid Propellant Rocket Combustors by Integral Techniques," *Proceedings of the 12th JANNAF Meeting*, CPIA Publications No. 273, Vol. II, 1975, pp. 19-33.

AFOSR Annual Technical Report

AFOSR-TR-

NOISE SUPPRESSION IN JET INLETS

Prepared for

Air Force Office of Scientific Research
Director of Aerospace Sciences

Bolling AFB, D. C.

by

Ben T. Zinn

William L. Meyer

William A. Bell

School of Aerospace Engineering
Georgia Institute of Technology
Atlanta, Georgia 30332

Approved for public release; distribution unlimited

AFOSR Contract No. F49620-77-C-0066   February 1979

Conditions of Reproduction

Reproduction, translation, publication, use and disposal in whole
or in part by or for the United States Government is permitted.

REPORT DOCUMENTATION PAGE		READ INSTRUCTIONS BEFORE COMPLETING FORM
1. REPORT NUMBER AFOSR-TR	2. GOVT ACCESSION NO.	3. RECIPIENT'S CATALOG NUMBER
4. TITLE (and Subtitle) Noise Suppression in Jet Inlets		5. TYPE OF REPORT & PERIOD COVERED Interim February 1, 1978–Jan. 31, 1979
		6. PERFORMING ORG. REPORT NUMBER
7. AUTHOR(s) Ben T. Zinn William L. Meyer William A. Bell		8. CONTRACT OR GRANT NUMBER(s) AFOSR-F49620-77-C-0066
9. PERFORMING ORGANIZATION NAME AND ADDRESS School of Aerospace Engineering Georgia Institute of Technology Atlanta, Georgia 30332		10. PROGRAM ELEMENT, PROJECT, TASK AREA & WORK UNIT NUMBERS 681-300 297-47B1 61102F
11. CONTROLLING OFFICE NAME AND ADDRESS Air Force Office of Scientific Research Director of Aerospace Sciences Bolling AFB, DC		12. REPORT DATE February 1979
		13. NUMBER OF PAGES
14. MONITORING AGENCY NAME & ADDRESS(If different from Controlling Office)		15. SECURITY CLASS. (of this report) Unclassified
		15a. DECLASSIFICATION/DOWNGRADING SCHEDULE

16. DISTRIBUTION STATEMENT (of this Report)

Approved forPublic Release Redistribution Unlimited.

17. DISTRIBUTION STATEMENT (of the abstract entered in Block 20, if different from Report)

18. SUPPLEMENTARY NOTES

19. KEY WORDS (Continue on reverse side if necessary and identify by block number)

Acoustic Radiation
Duct Acoustics
Jet Propulsion Noise
Aircraft Noise

20. ABSTRACT (Continue on reverse side if necessary and identify by block number)

      This report summarizes the work performed during the second year of an AFOSR sponsored research program that was primarily concerned with the development of an analytical technique for determining the radiated sound field from axisymmetric jet engine inlet configurations. The analytical technique employed is based upon an integral representation of the external (radiation) solutions of the Helmholtz equation which describe the sound fields external to a given body under either no

DD FORM 1473 EDITION OF 1 NOV 65 IS OBSOLETE
1 JAN 73

flow or constant velocity flow situations. The integral representation developed during the course of this research program is different from earlier works in the sense that it not only yields the correct (unique) solution for all radiation problems at all frequencies, but that the resulting integral equations contain no strong (i.e., non-integrable) singularities and therefore can be solved by straight forward numerical techniques. As part of this research effort two extremely flexible computer programs were developed for the solution of these axisymmetric integral equations. These programs can be used for any closed axisymmetric body with any combination of boundary conditions on its surface, without any modification of the computer codes, to provide accurate solutions for the acoustic properties (i.e., the acoustic pressure, normal velocity, and admittance) both on the body itself and anywhere in the field surrounding the body. Also, as part of this research effort, experiments are now being conducted with various axisymmetric configurations to provide the data that will be used to check the validity of the theoretical predictions. Some preliminary experimental data are presented in this report.

Abstract

This report summarizes the work performed during the second year of an AFOSR sponsored research program that was primarily concerned with the development of an analytical technique for determining the radiated sound field from axisymmetric jet engine inlet configurations. The analytical technique employed is based upon an integral representation of the external (radiation) solutions of the Helmholtz equation which describe the sound fields external to a given body under either no flow or constant velocity flow situations. The integral representation developed during the course of this research program is different from earlier works in the sense that it not only yields the correct (unique) solution for all radiation problems at all frequencies, but that the resulting integral equations contain no strong (i.e., non-integrable) singularities and therefore can be solved by straight forward numerical techniques. As part of this research effort two extremely flexible computer programs were developed for the solution of these axisymmetric integral equations. These programs can be used for any closed axisymmetric body with any combination of boundary conditions on its surface, without any modification of the computer codes, to provide accurate solutions for the acoustic properties (i.e., the acoustic pressure, normal velocity, and admittance) both on the body itself and anywhere in the field surrounding the body. Also, as part of this research effort, experiments are now being conducted with various axisymmetric configurations to provide the data that will be used to check the validity of the theoretical predictions. Some preliminary experimental data are presented in this report.

i

I. Introduction

This report summarizes the results obtained during the second year of support under AFOSR contract number F49620-77-C-0066. This contract was initiated on February 1, 1977 and the results obtained during the first year of support are contained in AFOSR Interim Scientific Report AFOSR-TR-78-0696.

The main objective of the research program conducted under this contract was to develop an analytical technique for predicting the sound field radiated from axisymmetric jet engine inlet configurations and to check the validity of these predictions with relevant experimental data. The development of this analytical solution technique was motivated by the need for a theoretical approach that could be used to predict the effects of sound source modifications and of sound suppression devices (such as acoustically lined surfaces and splitters) upon the sound field radiated from the inlet without having to resort to costly, full scale experimental testing. The experimental investigations are necessary not only for comparison with the results of the analytical technique (which has shown extremely good agreement with known exact solutions)[1,2,3]* but also to assist in the determination of the correct analytical form for describing the boundary conditions necessary to accurately model sound suppression materials in the computer programs.

---

*   These references were included as appendices of the aforementioned Interim Scientific Report, AFOSR-TR-78-0696.

During the first year of this contract the integral equations and computer programs required for investigating the sound fields radiated from certain simple geometries were developed. Specifically, two different formulations of the problem were developed; that is, the full three dimensional formulation and the axisymmetric formulation. Employing both these formulations the sound radiation from both a sphere and a finite length cylinder were investigated. In these studies the effects of different boundary conditions on the accuracy of the integral solution technique was investigated by comparing the predictions of this approach for the sound fields radiated by simple sources with available exact solutions obtained using the Seperation of Variables Technique (which is only applicable to simple geometries such as those investigated). This work is described in detail in three publications[1,2,3] (See footnote on the previous page.) and it was presented at three conferences[A,B,C]*. In summary the first year of study has shown that the integral solution technique developed under this contract is both accurate and efficient from a numerical point of view.

During the second year of this contract two general computer programs were developed for the determination of the acoustic fields both on and around general axisymmetric bodies with general boundary conditions. It will be noted here that although the geometry of the bodies under consideration are constrained to be axisymmetric the allowable acoustic modes are not; that is, any cylindrically symmetric acoustic mode which may be present can be solved for using these computer programs. These programs were written in Extended Fortran IV and they are presented

---

*   Letters refer to the various conference presentations conducted in connection with this program. These presentations are listed in Appendix F.

in Appendix A. They have been fully checked out on the Georgia Tech CDC Cyber 70/74 computer and have been used to theoretically predict the radiated sound fields that are associated with both lined and unlined straight ducts and an actual jet engine inlet configuration[4] shown in Fig. 1.

The details and results of these investigations are described in References 5 and 6 which are reproduced in Appendices B and C respectively. The latter of the two papers has also been accepted for presentation at the AIAA 5th Aeroacoustics Conference in March 1979 in Seattle, Washington. Probably the most significant results of this investigation is the result that the optimum theoretical admittance values found for reducing the sound radiated from a straight duct do not necessarily have the same effect in a dimensionally similar (i.e., the same length to diameter ratio) inlet. That is, the geometrical details of an axisymmetric body need to be taken into consideration when calculating optimum admittance values for acoustic liners. Another result of this investigation is that the admittance at the entrance plane of a straight duct or an inlet is not constant in the radial direction. The assumption of a constant admittance value at the entrance plane of a duct is common to many current theoretical analyses of the duct radiation problem and thus can be a large source of error in these analyses.

Since the use of a constant admittance value at the entrance plane of a duct is so common a series of computer runs were performed to determine just how accurate this assumption is. The runs were done for a straight duct configuration and various admittance values were calculated and compared with certain "classical values". The details of this analysis and the results are presented in Appendix E. In Appendix E a draft copy of a

3
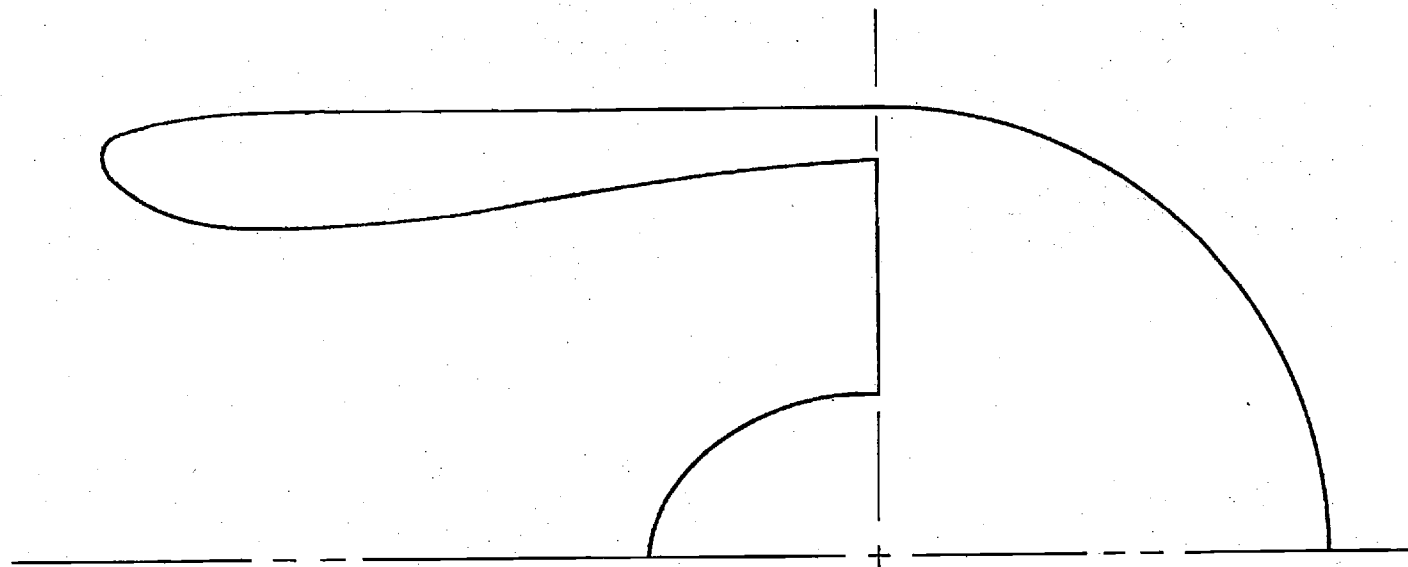
Figure 1. Axisymmetric Inlet Geometry.

4

technical note, to be submitted for publication in the AIAA Journal, is reproduced.

Part of the efforts expended under this contract during the second year of study were devoted to the development of experimental data that could be used to check the validity of the accompanying analytical studies. These efforts consisted of the design and development of appropriate experimental setups and the conduct of the required experiments, which are currently in progress. The experimental data acquired under this program is being compared with corresponding theoretical predictions. Some preliminary results of these comparisons are now available and they are presented in Section IV of this report. The work conducted during the second year of this contract which is not presented in the papers contained in Appendices B and C is summarized in the following sections.

II. Analytical Effort

The analytical efforts during the second year of this AFOSR contract consisted of the development of the general computer programs for handling axisymmetric geometires and their use to perform certain parametric studies of interest. The details and results of these studies are presented in Appendices B, C, and E, and the computer programs themselves are presented in Appendix A. The programs were developed so that they could not only be used for parametric analytical studies but also so that they could easily accept experimental data for any configuation without any major changes in the computer code. Another part of the analytical effort was concerned with the determination of the admittance of the liner which was used in the experimental phase of this program and with the redesign of the liner for future testing (See Appendix D.).

The initial testing under this program was conducted with an available acoustic liner which was developed in a related combustion instability program. This liner was tuned for maximum damping at a frequency, ~ 740 Hertz, which is above the first tangential (i.e., 1T) mode, ~ 695 Hz, of the duct under investigation. Since we are mainly interested in runing experiments below the 1T cut-off frequency to facilitate both the data reduction and the comparison of experimental and analytical values all of the preliminary testing was done in the frequency range 300-650 Hz which is below the 1T cut-off frequency. Thus, the liner was not expected to exert much attenuation. Since most of the planned future testing will also be conducted over a frequency range below the 1T mode of the duct, the available liner will be retuned to be more effective below the 1T cut-off frequency. The retuning of the liner is discussed in detail in Appendix D.

6

III. Experimental Investigations

The main objective of the experimental phase of this program was to obtain experimental data that could be readily compared with the predictions of the analytical models developed under this program. Specifically, the sound fields radiated from lined and unlined axisymmetric duct configurations were to be measured and compared with corresponding theoretical predictions. Since these studies were concerned with the measurements of the radiated sound fields, all of the required experiments were conducted in an anechoic chamber whose properties are described in Fig. 2. A typical experimental setup utilized in the course of this study is shown in Fig. 3; it consists of a lined axisymmetric duct with a sound source at one end and an open termination at the other end. The test body (i.e., the inlet) is placed on one side of the anechoic chamber and an array of microphones is used to measure the radiated sound field. The latter consisted of 5 Brüel and Kjaer condenser-type microphones. The sound source was a University driver and it was placed at the throat of a nozzle that was connected to the axisymmetric body tested as shown in Fig. 4. The available liner used for the preliminary testing was not specifically designed for maximum effectiveness in the frequency range where most of the testing was done. It was tuned for maximum damping at a frequency higher than the 1T mode of the duct under study. It consisted of 180 Helmholtz resonators (20 radial rows by 9 axial rows) which were closed off during the hard walled testing (See Appendix D for the admittance calculation). A diagram of the driver-nozzle-liner set-up and of one of the Helmholtz resonators appears in Fig. 4.
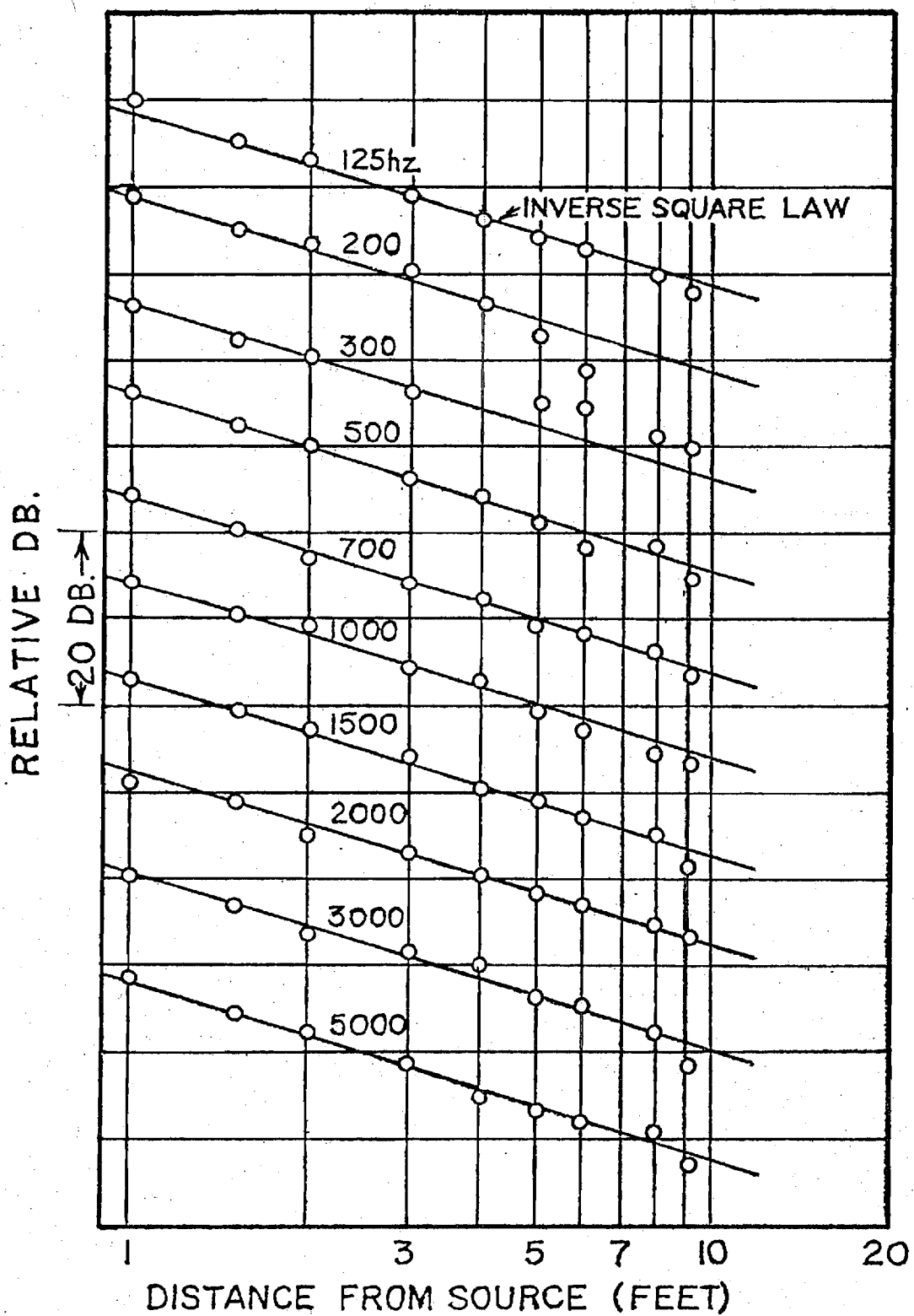
Figure 2. Anechoic Chamber Characteristics.

Chart labels:
- RELATIVE DB. (vertical axis)
- 20 DB. (scale marker)
- 125hz.
- 200
- 300
- 500
- 700
- 1000
- 1500
- 2000
- 3000
- 5000
- INVERSE SQUARE LAW
- DISTANCE FROM SOURCE (FEET)
- 1   3   5   7   10   20

8

ANECHOIC CHAMBER

PLAN VIEW
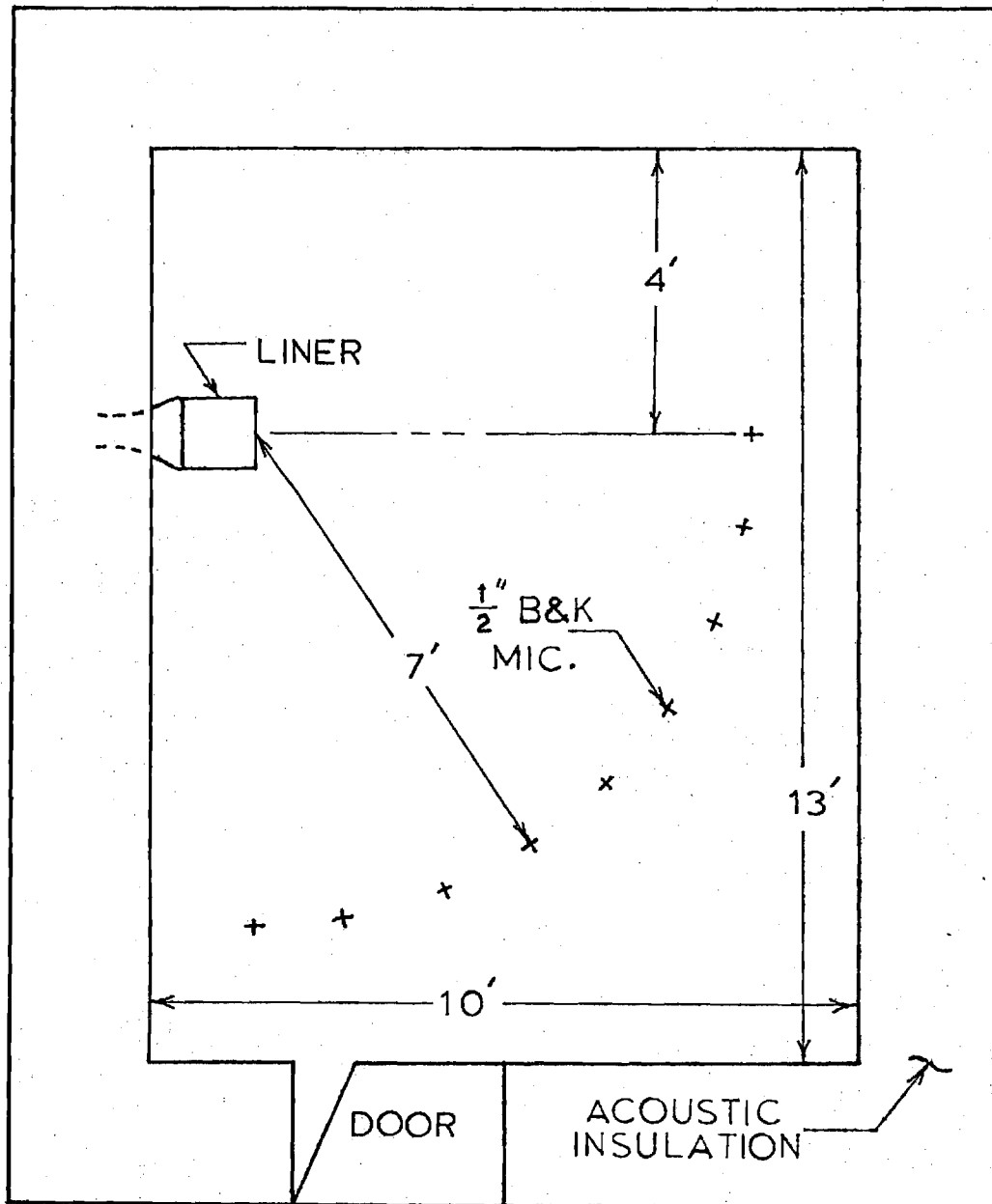
Figure 3. Experimental Set-up for Radiation Studies.

$\frac{1}{4}''$ B&K MIC.

LINER

VER

NOZZLE

$11\frac{3}{8}''$

$16\frac{7}{16}''$

$11\frac{15}{16}''$

PLASTIC PLATE

$1''$

$\frac{1}{2}''$

$\frac{7}{8}''$

$\frac{1}{4}''$

HELMHOLTZ RESONATOR
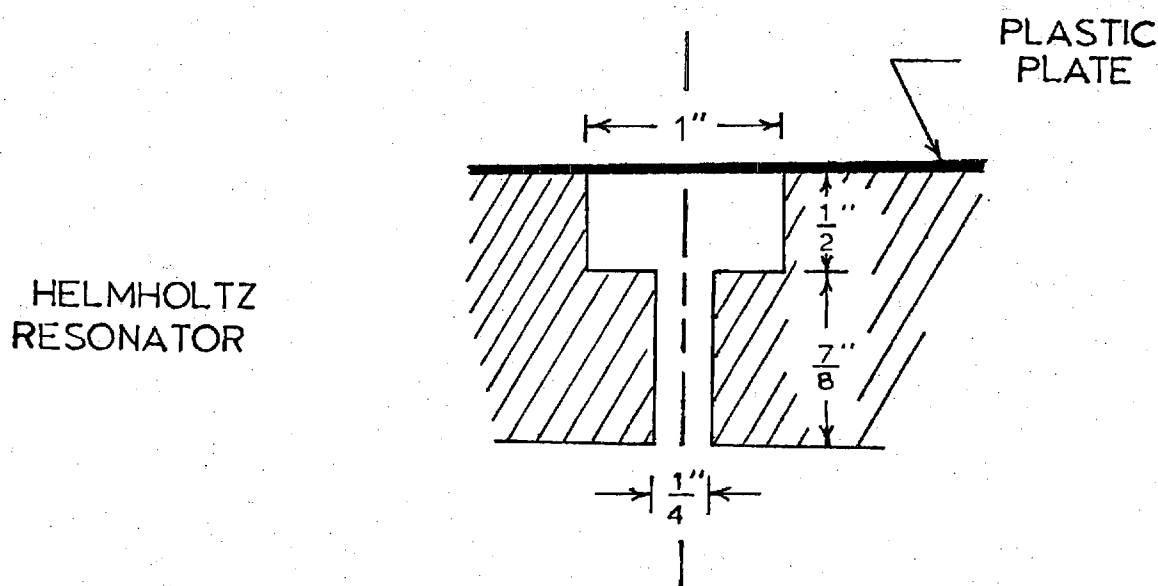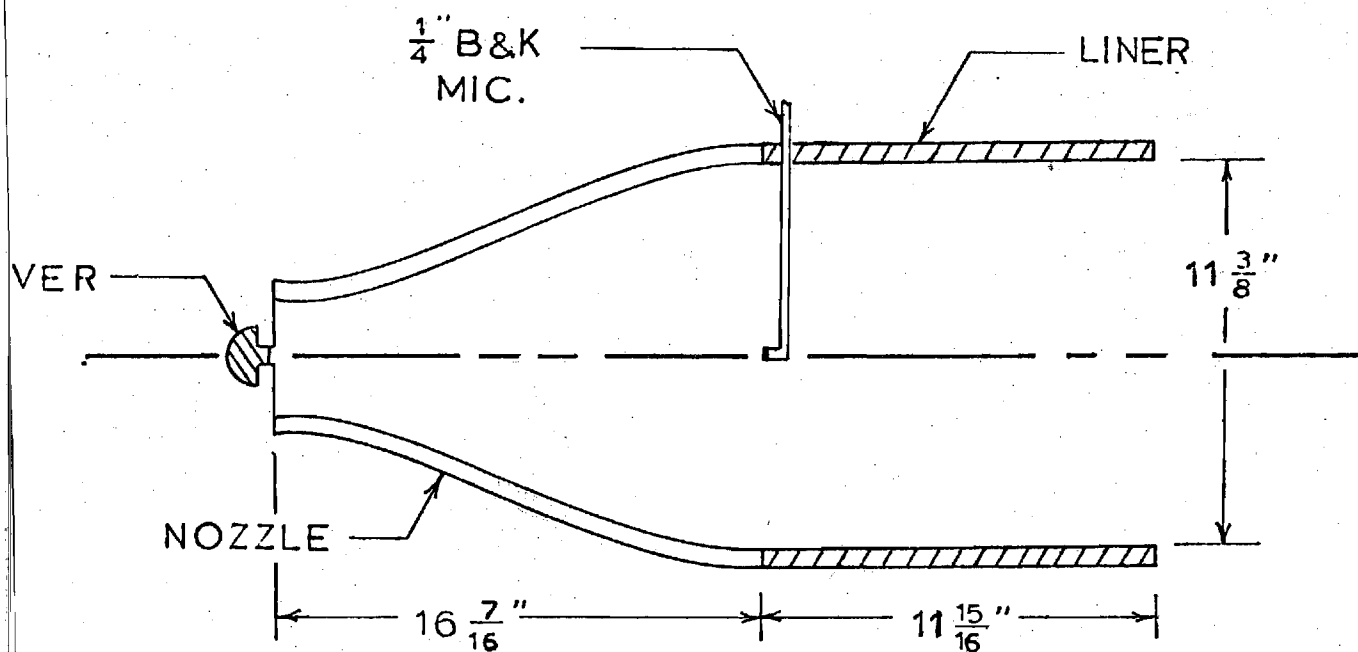
Figure 4. Testing Configuration.

This experimental set-up was found to work very well in that the acoustic waves generated by the driver remained essentially plane up to the nozzle-liner interface. This was determined by traversing a 1/4" B&K microphone radially across the nozzle-liner interface. This being the case only a single measurement of the acoustic pressure, which is needed for input to the analytical computations, was taken at this plane for each test condition.

IV. Preliminary Experimental Results and Comparisons

Some preliminary experiments have been conducted with the straight duct configuration shown in Figs. 3 ad 4. Both lined and unlined configurations were tested; however, not much difference was noted as all the tests were conducted at frequencies below the first tangential (i.e. 1T) mode of the duct and therefore in a region where the liner is only marginally effective as discussed in the previous sections (Also see Appendix D.). Tests were conducted in the frequency range 300 to 650 Hertz with 50 Hz increments. The microphones in the field were placed on a circular arc with a radius of seven feet centered at the entrance plane of the duct (See Figure 3.). The microphones were placed at increments of $11\frac{1}{4}^{\circ}$ from the centerline of the duct to 90°.

Comparisons between the experimental results and the theoretical results were made. Since an experimentally measured value of the sound pressure level at the nozzle-duct interface was used as input for the computer programs, the accuracy of the calculated far field can only be expected to be as good as this measurement. Other sources of error are the "imperfections" of the anechoic chamber at various frequencies as shown in Fig. 2, instrumentation errors, and the lack of perfect correspondence between the experimental and analytical configurations. In this connection it should be pointed out that the theoretical model employs a spherical termination at the rear end of the straight duct as shown in Fig. 5. This was done to improve the efficiency of the computer programs as it has been shown through theoretical studies that the shape of the termination of the

12
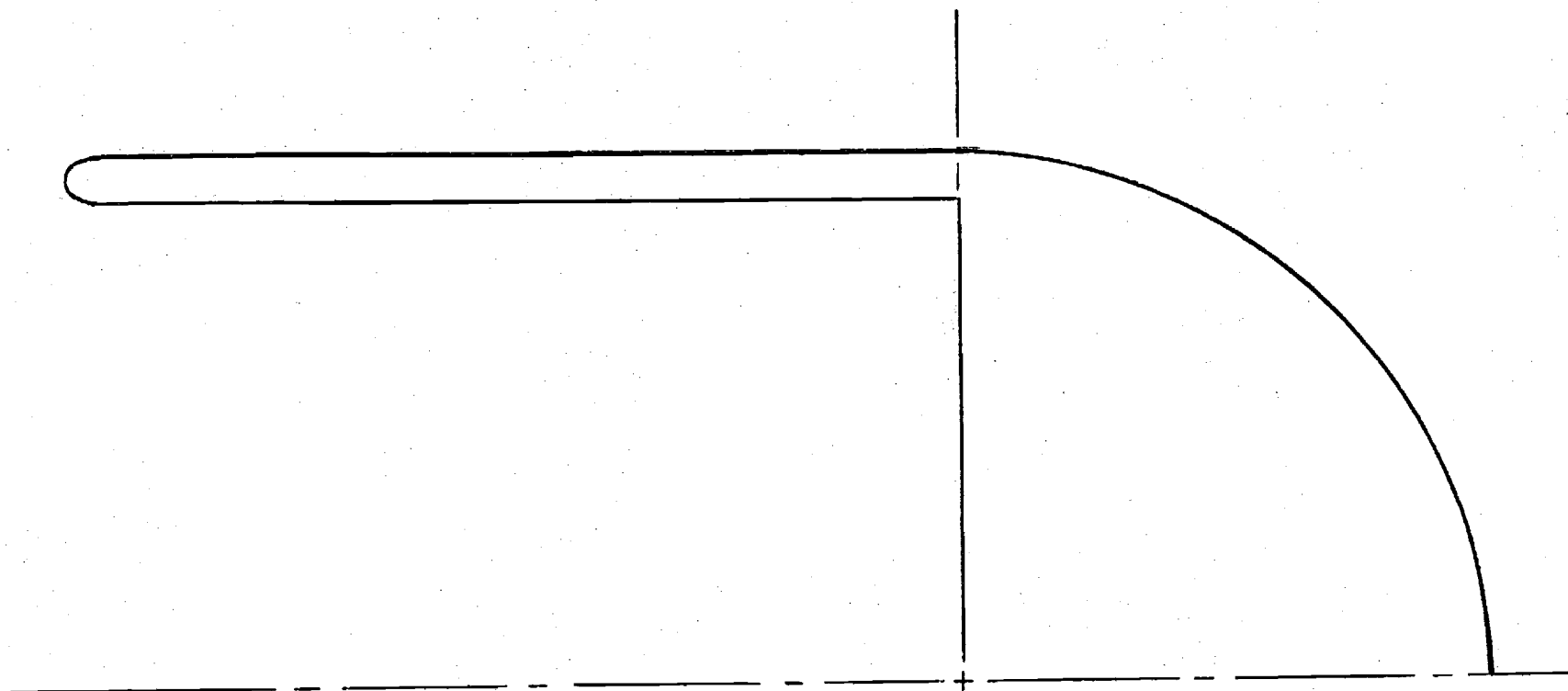
Figure 5. Straight Duct Geometry.

13

duct exerts little influence upon the acoustic field in the forward half plane of the duct.

Comparisons between the measured and calculated results shows good qualitative agreement for both the hard walled (i.e., See Fig. 6.) and the lined (i.e., See Fig. 7.) duct configurations. Good agreement is observed between the hard walled and lined wall cases in that the errors follow the same patterns (i.e., Compare Figs. 6 and 7.) which suggest that most of the observed errors are due to the "non-anechoicness" of the anechoic chamber. The measured data will be further analyzed in the future and they will be published together with additional data collected during the next year of study under this contract.
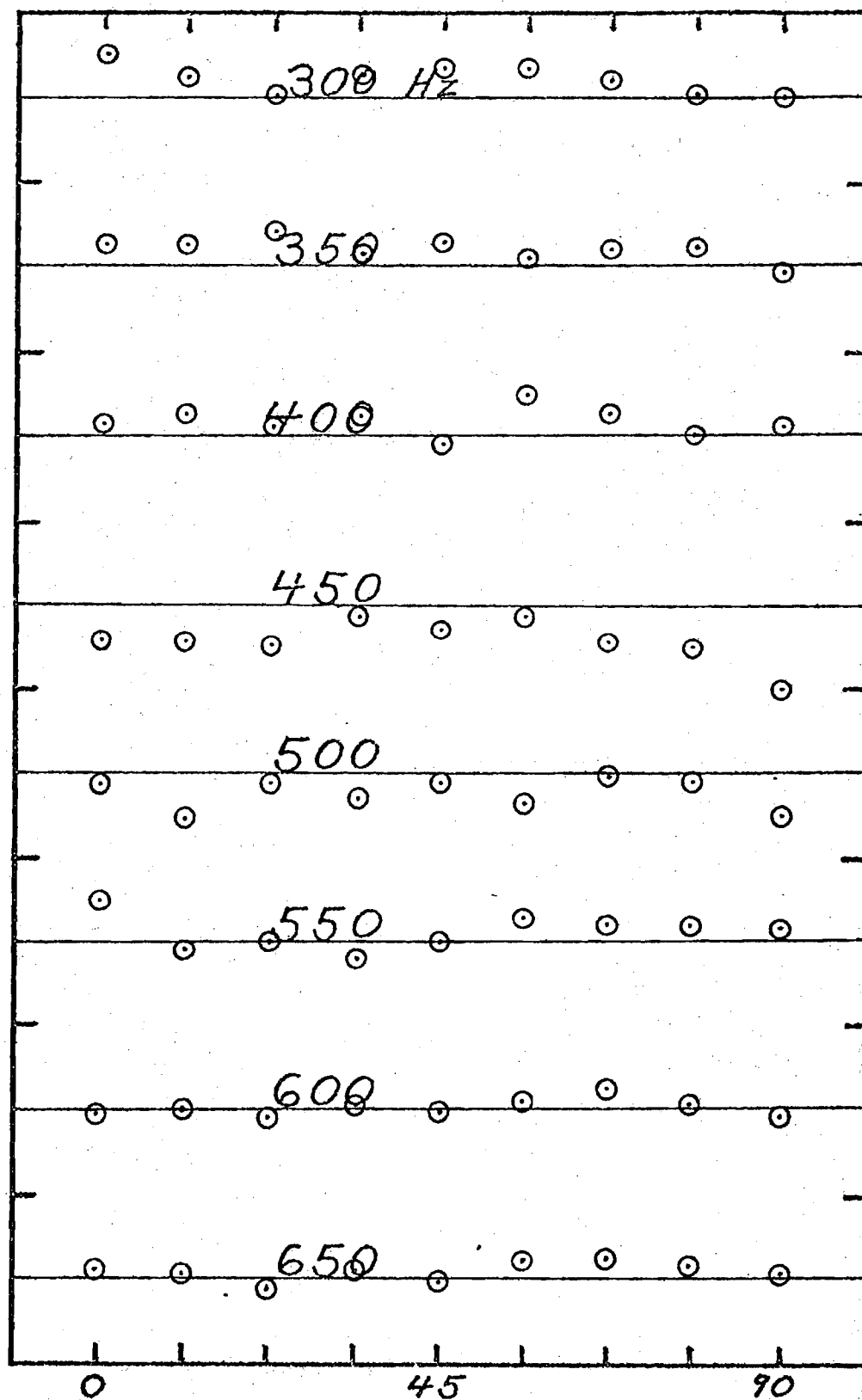
Figure 6. Results for the Hard Walled Straight Duct.

15
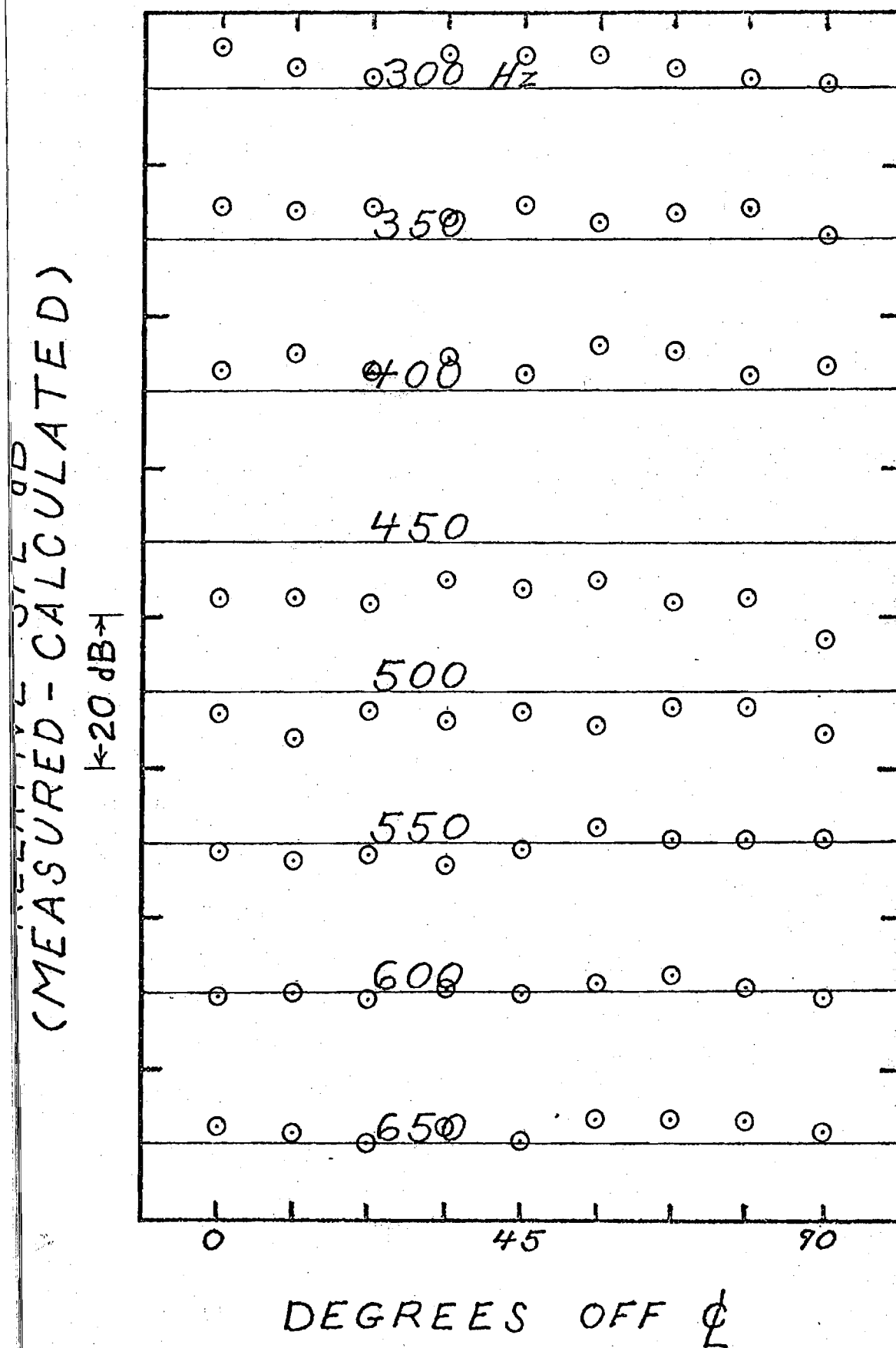
Figure 7. Results for the Lined Straight Duct.

16

References

1. Bell, W. A., Meyer, W. L., and Zinn, B. T., "Predicting the Acoustics of Arbitrarily Shaped Bodies Using an Integral Approach," <u>AIAA Journal</u>, Vol. 15, No. 6, June 1977, pp. 813-820.

2. Meyer, W. L., Bell, W. A., and Zinn, B. T., "Prediction of the Sound Field Radiated from Axisymmetric Surfaces," AIAA Paper No. 78-195, presented at the AIAA 16th Aerospace Sciences Meeting, Huntsville, Alabama, January 16-18, 1978.

3. Meyer, W. L., Bell, W. A., Stallybrass, M. P., and Zinn, B. T., "Boundary Integral Solutions of Three Dimensional Acoustic Radiation Problems," <u>Journal of Sound and Vibration</u>, Vol. 59, No. 2, February 1978, pp. 245-262.

4. Miller, B. A., Dastoli, B. J., and Wesoky, H. L., "Effect of Entry-Lip Design on Aerodynamics and Acoustics of High-Throat-Mach-Number Inlets for the Quiet, Clean, Short-Haul Experimental Engine," NASA TM X-3222, May 1975.

5. Meyer, W. L., Bell, W. A., Stallybrass, M. P., and Zinn, B. T., "Prediction of the Sound Field Radiated from Axisymmetric Surfaces," <u>Journal of the Acoustical Society of America</u>, March 1979.

6. Meyer, W. L., Bell, W. A., and Zinn, B. T., "Sound Radiation from Finite Length Axisymmetric Ducts and Engine Inlets," AIAA Paper No. 79-0675, presented at the 5th AIAA Aeroacoustics Conference, Seattle, Washington, March 12-14, 1979.

Appendix A

Computer Programs Developed for this Project

The computer programs described in this appendix were developed during the second year of this AFOSR research project. They are very general in that they can be used to find the acoustic properties (i.e., the acoustic potential, normal acoustic velocity, and the admittance) both on the surface and surrounding any finite (closed) axisymmetric body. Also, the boundary conditions can be specified at each point on the surface of the body; the only restriction is that the admittance may not be specified everywhere on the body as then the solution of the governing integal equation is non-unique.

The first computer program developed for this project calculates the surface distributions of the acoustic quantities for a general axisymmetric configuration. Required inputs for this program are the geometric description of the body, the boundary conditions, and the problem specification data (i.e., the mode number of the acoustic wave being solved for and the wave number). The geometric input data required includes the $\rho - z$ coordinates of the points in the center of each integration interval, P, the two integration points on either side of the center point, Q, the normal to the body at the center point, NORMAL, and the length of each integration interval in the $\rho - z$ plane, LENGTH. Since the body is assumed to be axisymmetric the program takes care of choosing the integration points in the θ direction through the use of a 96 point Gaussian integration formula.

The boundary conditions are specified in two vectors. The first vector, ICHECK, specifies what type of boundary condition is known at each point in the ρ-z plane.

$$
\text{ICHECK} \quad = \quad \left.\begin{matrix} -1 \\ 0 \\ 1 \end{matrix}\right\} \quad \longrightarrow \quad \left\{\begin{matrix} \varphi & \text{known} \\ \partial\varphi/\partial n & \text{known} \\ y & \text{known} \end{matrix}\right. \qquad (A\text{-}1)
$$

The second vector, CINDATA, contains the actual complex value of the boundary condition at each point. Finally the problem specification data consists of specifying the wave number k and the mode number m (i.e. m = 0 is the axisymmetric mode.)

This program prints out all the input data and all the acoustic quantities on the surface of the body. It also creates an output file which is read by the next program to calculate the acoustic qualtities in the field surrounding the body.

```
      PROGRAM EXPCYL ( INPUT,  OUTPUT,  TAPE10,  TAPE11,
              .               TAPE5 = INPUT,  TAPE6 = OUTPUT)
C
C
C***********************************************************************
C*                                                                    *
C*                                                                    *
C*       THIS PROGRAM CALCULATES EITHER THE ACOUSTIC POTENTIAL OR THE  *
C*       ACOUSTIC VELOCITY OR THE EFFECTIVE ADMITTANCE ON THE SURFACE  *
C*       OF ANY AXISYMMETRIC BODY USEING THE METHOD OF BURTON & MILLER *
C*       WITH MY INTERPRETATION OF THE MOST SINGULAR COMPONENT.        *
C*                                                                    *
C***********************************************************************
C*                                                                    *
C*       WILLIAM A. BELL'S OPTIMAL VALUE OF ALPHA (= I/K)  IS EMPLOYED. *
C*                                                                    *
C***********************************************************************
C*                                                                    *
C*       A CYLINDRICAL FORMULATION OF THE PROBLEM IS EMPLOYED.         *
C*                                                                    *
C*                                                                    *
C***********************************************************************
C
C
      REAL K, LENGTH, NORMAL
      COMPLEX ALPHA, CEQN, CEXACT, CPHI, CVEL, CY, IK, IKSQ, TWOPIA,
              .       CINDATA
C
      COMMON /I/ M, NP, NPP1
      COMMON /R/ K, PI, TWOPI
      COMMON /C/ ALPHA, IK, IKSQ, TWOPIA
      COMMON /ID/ ICHECK ( 102)
      COMMON /RD/ LENGTH ( 102), NORMAL ( 102, 2), P ( 102, 2),
              .        Q ( 102, 2, 2)
      COMMON /CD/ CEQN ( 102, 103), CEXACT ( 102), CPHI ( 102), CVEL ( 102),
              .        CY ( 102), CINDATA ( 102)
      COMMON /NGAUSS/ NGAUST
      COMMON /GAUSS/ GAUSNT ( 48, 2)
C
      CALL INPUT
C
C     INTEGER CONSTANTS
C
      NPP1 = NP + 1
C
C     REAL CONSTANTS
C
      TWOPI = 2.0 * PI
C
C     COMPLEX CONSTANTS
C
      IK = (0.0, 1.0) * K
      IKSQ = IK * IK
      ALPHA = (0.0, 1.0) / K
      TWOPIA = ALPHA * TWOPI
C
      CALL EQN
C
      CALL GAUSS
C
      CALL OUTPUT
C
      STOP "NORMAL"
C
      END
```

20

```fortran
      BLOCK DATA
C
      REAL K
C
      COMMON /I/ M, NP, NPP1
      COMMON /R/ K, PI, TWOPI
      COMMON /NGAUSS/ NGAUST
      COMMON /GAUSS/ GAUSNT (48, 2)
C
      DATA NP / 102 /
C
      DATA PI / 3.1415926535898 /
C
      DATA NGAUST / 48 /
C
      DATA ((GAUSNT(I, J), J = 1, 2), I = 1, 12)
     .     / 0.01627674484960, 0.03255061449236,
     .       0.04881298513605, 0.03251611871387,
     .       0.08129749546443, 0.03244716371406,
     .       0.11369585011067, 0.03234382256858,
     .       0.14597371465490, 0.03220620479403,
     .       0.17809688236762, 0.03203445623199,
     .       0.21003131046057, 0.03182875889441,
     .       0.24174315616384, 0.03158933077073,
     .       0.27319881259105, 0.03131642559686,
     .       0.30436494435450, 0.03101033258631,
     .       0.33520852289263, 0.03067137612367,
     .       0.36569686147231, 0.03029991542083 /
      DATA ((GAUSNT(I, J), J = 1, 2), I = 13, 24)
     .     / 0.39579764982891, 0.02989634413633,
     .       0.42547898840730, 0.02946108995817,
     .       0.45470942216774, 0.02899461415056,
     .       0.48345797392060, 0.02849741106509,
     .       0.51169417715467, 0.02797000761685,
     .       0.53938810832436, 0.02741296272603,
     .       0.56651041856140, 0.02682686672559,
     .       0.59303236477757, 0.02621234073567,
     .       0.61892584012547, 0.02557003600535,
     .       0.64416340378497, 0.02490063322248,
     .       0.66871831004392, 0.02420484179236,
     .       0.69256453664217, 0.02348339908593 /
      DATA ((GAUSNT(I, J), J = 1, 2), I = 25, 36)
     .     / 0.71567681234897, 0.02273706965833,
     .       0.73803064374440, 0.02196664443874,
     .       0.75960234117665, 0.02117293989219,
     .       0.78036904386743, 0.02035679715433,
     .       0.80030874413914, 0.01951908114015,
     .       0.81940031073793, 0.01866067962741,
     .       0.83763351122819, 0.01778250231605,
     .       0.85495903343460, 0.01688547986425,
     .       0.87138850590930, 0.01597056290256,
     .       0.88689451740242, 0.01503872102699,
     .       0.90146063531585, 0.01409094177231,
     .       0.91507142312090, 0.01312822956696 /
      DATA ((GAUSNT(I, J), J = 1, 2), I = 37, 48)
     .     / 0.92771245672231, 0.01215160467109,
     .       0.93937033975276, 0.01116210209984,
     .       0.95003271778444, 0.01016077053501,
     .       0.95968829144874, 0.00914867123078,
     .       0.96832682846326, 0.00812687692570,
     .       0.97593917458514, 0.00709647079115,
     .       0.98251726356301, 0.00605854550424,
     .       0.98805412632962, 0.00501420274293,
     .       0.99254390032376, 0.00396455433844,
     .       0.99598184298721, 0.00291073181793,
     .       0.99836437586318, 0.00185396078895,
     .       0.99968950388323, 0.00079679206555 /
C
      END
```

```
      SUBROUTINE INPUT
C
      REAL K, LENGTH, NORMAL
      COMPLEX CEQN, CEXACT, CPHI, CVEL, CY, CINDATA
C
      COMMON /I/ M, NP, NPP1
      COMMON /R/ K, PI, TWOPI
      COMMON /ID/ ICHECK (102)
      COMMON /RD/ LENGTH (102), NORMAL (102, 2), P (102, 2),
     .          Q (102, 2, 2)
      COMMON /CD/ CEQN (102, 103), CEXACT (102), CPHI (102), CVEL (102),
     .          CY (102), CINDATA (102)
C
      READ (5, 100) ((P(I, J), J = 1, 2), I = 1, NP)
C
      READ (5, 100) (((Q(I, J, KK), KK = 1, 2), J = 1, 2), I = 1, NP)
C
      READ (5, 100) ((NORMAL(I, J), J = 1, 2), I = 1, NP)
C
      READ (5, 100) (LENGTH(I), I = 1, NP)
C
 100  FORMAT (8G10.0)
C
      PRINT 101
C
 101  FORMAT ( "1GEOMETRIC INPUT DATA: " ///
     .         " ", 25X, "-Q(RHO, Z)" /
     .         " ", 4X, "N", 21X, "P(RHO, Z)", 38X, "NORMAL(RHO, Z)",
     .                  27X, "LENGTH" /
     .         " ", 25X, "+Q(RHO, Z)" // " ")
C
      WRITE (6, 102) (Q(I, 1, 1), Q(I, 1, 2), I, P(I, 1), P(I, 2),
     .                NORMAL(I, 1), NORMAL(I, 2), LENGTH(I), Q(I, 2, 1),
     .                Q(I, 2, 2), I = 1, NP)
C
 102  FORMAT (" ", 15X, "(", F13.10, ",", F13.10, ")" /
     .        " ", 2X, I3, 10X, "(", F13.10, ",", F13.10, ")", 21X,
     .                  "(", F13.10, ",", F13.10, ")", 17X,
     .                  F13.10 /
     .        " ", 15X, "(", F13.10, ",", F13.10, ")" / " ")
C
      READ (5, 104) (ICHECK(I), I = 1, NP)
C
 104  FORMAT (16I5)
C
      READ (11, 1100) M, K
C
 1100 FORMAT (I20, G20.0)
C
      READ (11, 100) (CINDATA(I), I = 1, NP)
C
      RETURN
      END
```

```
      SUBROUTINE EQN
C
      REAL K, LENGTH, NORMAL, NP1, NP2, NRHOP, NRHOQ, NZP, NZQ
      COMPLEX ALPHA, CEQN, CEXACT, CPHI, CVEL, CY, IK, IKSQ,
     .         TWOPIA, CINDATA
C
      COMMON /I/ M, NP, NPP1
      COMMON /R/ K, PI, TWOPI
      COMMON /C/ ALPHA, IK, IKSQ, TWOPIA
      COMMON /ID/ ICHECK (102)
      COMMON /RD/ LENGTH (102), NORMAL (102, 2), P (102, 2),
     .         Q (102, 2, 2)
      COMMON /CD/ CEQN (102, 103), CEXACT (102), CPHI (102), CVEL (102),
     .         CY (102), CINDATA (102)
C
C     INITALIZE MATRIX
C
      DO 1 I = 1, NP
      DO 2 J = 1, NPP1
      CEQN(I, J) = (0.0, 0.0)
    2 CONTINUE
      P1 = P(I, 1)
      P2 = P(I, 2)
      NP1 = NORMAL(I, 1)
      NP2 = NORMAL(I, 2)
C
      IF (ICHECK(I)) 3, 4, 5
    3 CONTINUE
      CEXACT(I) = CINDATA(I)
      CVEL(I) = (0.0, 0.0)
      CY(I) = (0.0, 0.0)
      CEQN(I, NPP1) = TWOPI * CEXACT(I)
      CEQN(I, I) = -TWOPIA
      GO TO 6
    4 CONTINUE
      CEXACT(I) = (0.0, 0.0)
      CVEL(I) = CINDATA(I)
      CY(I) = (0.0, 0.0)
      CEQN(I, NPP1) = TWOPIA * CVEL(I)
      CEQN(I, I) = -TWOPI
      GO TO 6
    5 CONTINUE
      CEXACT(I) = (0.0, 0.0)
      CVEL(I) = (0.0, 0.0)
      CY(I) = CINDATA(I)
      CEQN(I, I) = -TWOPI * (1.0 + ALPHA * CY(I))
    6 CONTINUE
    1 CONTINUE
C
C     XI INTEGRATION
C
      DO 7 J = 1, NP
      NRHOQ = NORMAL(J, 1)
      NZQ = NORMAL(J, 2)
      GAUSZ = LENGTH(J) * PI
      DO 8 I = 1, NP
      RHOP = P(I, 1)
      ZP = P(I, 2)
      NRHOP = NORMAL(I, 1)
      NZP = NORMAL(I, 2)
      DO 9 L = 1, 2
      RHOQ = Q(J, L, 1)
      ZQ = Q(J, L, 2)
C
      CALL CALC (RHOP, ZP, NRHOP, NZP, RHOQ, ZQ, NRHOQ, NZQ, GAUSZ,
     .         I, J)
C
    9 CONTINUE
    8 CONTINUE
    7 CONTINUE
C
      RETURN
      END
```

```fortran
      SUBROUTINE CALC (RHOP, ZP, NRHOP, NZP, RHOQ, ZQ, NRHOQ, NZQ,
     .                 GAUSZ, I, J)
C
      REAL K, NDOTN, NRHOP, NRHOQ, NRHOQP, NZP, NZQ, NZQP
      COMPLEX ALPHA, CEQN, CEXACT, CPHI, CVEL, CY, F1, F2, G, GP,
     .        GPP, IK, IKSQ, I1, I2, K1, K2, TWOPIA, CINDATA
C
      COMMON /I/ M, NP, NPP1
      COMMON /R/ K, PI, TWOPI
      COMMON /C/ ALPHA, IK, IKSQ, TWOPIA
      COMMON /ID/ ICHECK (102)
      COMMON /CD/ CEQN (102, 103), CEXACT (102), CPHI (102), CVEL (102),
     .            CY (102), CINDATA (102)
      COMMON /NGAUSS/ NGAUST
      COMMON /GAUSS/ GAUSNT (48, 2)
C
      ZD = ZQ - ZP
      ZSQ = ZD * ZD
      RHOSQ = (RHOQ - RHOP)**2
      RHOQP2 = 2.0 * RHOQ * RHOP
      NRHOQP = NRHOQ * NRHOP
      NZQP = NZQ * NZP
C
C     THETA INTEGRATION
C
      DO 1 IT = 1, NGAUST
      THETA = PI * GAUSNT( IT, 1)
      IF (I .EQ. J) THETA = PI * (1.0 - GAUSNT( IT, 1))
      GAUSZT = GAUSZ * GAUSNT( IT, 2)
C
      COST = COS (THETA)
      COSMT = COS (M * THETA)
C
      R = SQRT (RHOSQ + ZSQ + RHOQP2 * (1.0 - COST))
      DRDNQ = (NRHOQ * (RHOQ - RHOP * COST) + NZQ * ZD) / R
      DRDNP = (NRHOP * (RHOP - RHOQ * COST) - NZP * ZD) / R
      NDOTN = NRHOQP * COST + NZQP
C
      G = RHOQ * CEXP (IK * R) / R
      GP = G * (IK - (1.0 / R))
      GPP = G * (IKSQ - (3.0 * IK / R) + (3.0 / (R * R)))
C
      I1 = G * COSMT
      I2 = ALPHA * GP * DRDNP * COSMT
      F1 = ALPHA * G * IKSQ * NDOTN
      F2 = ALPHA * (GPP * DRDNP * DRDNQ - (GP * NDOTN / R))
      K1 = GP * DRDNQ * COSMT
      K2 = F2 * COSMT
C
      IF (ICHECK(I) .NE. -1) GO TO 3
C
      CEQN(I, NPP1) = CEQN(I, NPP1) + GAUSZT * CEXACT(I) * (F1 + F2)
C
      GO TO 4
    3 CONTINUE
C
      CEQN(I, I) = CEQN(I, I) - GAUSZT * (F1 + F2)
C
    4 CONTINUE
      IF (ICHECK(J)) 11, 12, 13
   11 CONTINUE
C
      CEQN(I, J) = CEQN(I, J) - GAUSZT * (I1 + I2)
      CEQN(I, NPP1) = CEQN(I, NPP1) - GAUSZT * (K1 + K2)
     .                                        * CEXACT(J)
C
      GO TO 14
   12 CONTINUE
C
      CEQN(I, J) = CEQN(I, J) + GAUSZT * (K1 + K2)
      CEQN(I, NPP1) = CEQN(I, NPP1) + GAUSZT * (I1 + I2)
     .                                        * CVEL(J)
C
      GO TO 14
   13 CONTINUE
C
      CEQN(I, J) = CEQN(I, J) + GAUSZT * ((K1 + K2) -
     .                         CY(J) * (I1 + I2))
C
   14 CONTINUE
    1 CONTINUE
C
      RETURN
```

24

```
      SUBROUTINE GAUSS
C
      IMPLICIT COMPLEX (C)
C
      COMMON /I/ MM, NP, NPP1
      COMMON /CD/ CEQN (102, 103), CEXACT (102), CPHI (102), CVEL (102),
     .          CY (102), CINDATA (102)
C
C     UPPER TRIANGULARIZE MATRIX
C
      DO 1 J = 1, NP
      JP1 = J + 1
      CSAVE = CEQN (J, J)
      CEQN(J, J) = (1.0, 0.0)
      DO 2 L = JP1, NPP1
      CEQN(J, L) = CEQN(J, L) / CSAVE
    2 CONTINUE
      IF (J .EQ. NP) GO TO 3
      DO 4 M = JP1, NP
      CSAVE = CEQN(M, J)
      DO 5 I = JP1, NPP1
      CEQN(M, I) = CEQN(M, I) - CEQN(J, I) * CSAVE
    5 CONTINUE
    4 CONTINUE
    1 CONTINUE
C
C     BACK SUBSTITUTION
C
    3 CONTINUE
      CSUM = (0.0, 0.0)
      DO 6 I = 1, NP
      NPMI = NP - I
      NPP1MI = NPMI + 1
      CPHI(NPP1MI) = CEQN(NPP1MI, NPP1) - CSUM
      IF (I .EQ. NP) GO TO 7
      CSUM = (0.0, 0.0)
      DO 8 J = 1, I
      NPP1MJ = NPP1 - J
      CSUM = CPHI(NPP1MJ) * CEQN(NPMI, NPP1MJ) + CSUM
    8 CONTINUE
    6 CONTINUE
    7 CONTINUE
C
      RETURN
      END
```

```
      SUBROUTINE OUTPUT
C
      REAL IEXACT, IPHI, K, LENGTH, MADMIT, MEXACT, MPHI, MVELP, MYP,
     .      NORMAL
      COMPLEX ADMIT, ALPHA, CEQN, CEXACT, CPHI, CVEL, CY, IK, IKSQ,
     .        TWOPIA, VELP, CINDATA
C
      COMMON /I/ M, NP, NPP1
      COMMON /R/ K, PI, TWOPI
      COMMON /C/ ALPHA, IK, IKSQ, TWOPIA
      COMMON /ID/ ICHECK (102)
      COMMON /RD/ LENGTH (102), NORMAL (102, 2), P (102, 2),
     .        Q (102, 2, 2)
      COMMON /CD/ CEQN (102, 103), CEXACT (102), CPHI (102), CVEL (102),
     .        CY (102), CINDATA (102)
      COMMON /NGAUSS/ NGAUST
C
      DIMENSION ADMIT (102), VELP (102), IEXACT (102), IPHI (102),
     .        MADMIT (102), MEXACT (102), MPHI (102), MVELP (102),
     .        MYP (102), PADMIT (102), PEXACT (102), PPHI (102),
     .        PPVELP (102), PVELM (102), PVELP (102), PYP (102),
     .        REXACT (102), RPHI (102)
C
      EQUIVALENCE (CEQN, ADMIT),            (CEQN(1, 2), VELP(1)),
     .        (CEQN(1, 3), IEXACT(1)),     (CEQN(1, 4), IPHI(1)),
     .        (CEQN(1, 5), MADMIT(1)),     (CEQN(1, 6), MEXACT(1)),
     .        (CEQN(1, 7), MPHI(1)),       (CEQN(1, 8), MVELP(1)),
     .        (CEQN(1, 9), MYP(1)),        (CEQN(1, 10), PADMIT(1)),
     .        (CEQN(1, 11), PEXACT(1)),    (CEQN(1, 12), PPHI(1)),
     .        (CEQN(1, 13), PPVELP(1)),    (CEQN(1, 14), PVELM(1)),
     .        (CEQN(1, 15), PVELP(1)),     (CEQN(1, 16), PYP(1)),
     .        (CEQN(1, 17), REXACT(1)),    (CEQN(1, 18), RPHI(1))
C
      PRINT 100
C
  100 FORMAT ("1", 61X, "*********" / " ", 61X, "*        *" /
     .        " ", 61X, "* INPUT *" / " ", 61X, "*        *" /
     .        " ", 61X, "*********" //// " N", 15X,
     .        "EFFECTIVE ADMITTANCE", 20X, "ACOUSTIC VELOCITY", 22X,
     .        "ACOUSTIC POTENTIAL" // " ")
C
      DO 1 I = 1, NP
      REXACT(I) = REAL (CEXACT(I))
      IEXACT(I) = AIMAG (CEXACT(I))
      MEXACT(I) = CABS (CEXACT(I))
      PEXACT(I) = 0.0
      IF (MEXACT(I) .NE. 0.0) PEXACT(I) = ATAN2 (IEXACT(I), REXACT(I))
      MVELP(I) = CABS (CVEL(I))
      PVELP(I) = 0.0
      IF (MVELP(I) .NE. 0.0) PVELP(I) = ATAN2 (AIMAG (CVEL(I)),
     .                  REAL (CVEL(I)))
      MYP(I) = CABS (CY(I))
      PYP(I) = 0.0
      IF (MYP(I) .NE. 0.0) PYP(I) = ATAN2 (AIMAG (CY(I)), REAL (CY(I)))
      IF (ICHECK(I)) 3, 4, 5
    3 CONTINUE
C
      WRITE (6, 101) I, CEXACT(I)
C
  101 FORMAT (" ", I3, 88X, "(", F13.10, ",", F13.10, ")")
C
      GO TO 22
    4 CONTINUE
C
      WRITE (6, 102) I, CVEL(I)
C
  102 FORMAT (" ", I3, 49X, "(", F13.10, ",", F13.10, ")")
C
      GO TO 22
    5 CONTINUE
C
      WRITE (6, 103) I, CY(I)
C
  103 FORMAT (" ", I3, 9X, "(", F13.10, ",", F13.10, ")")
C
   22 CONTINUE
    1 CONTINUE
      NGAUSZ = 2
      NGAUST = 2 * NGAUST
```

26

```fortran
      WRITE (6, 104) K, M, ALPHA, NGAUSZ, NGAUST
C
  104 FORMAT ("1INPUT FOR THIS CASE IS:" ///
     .          " ", 25X, "K =", F10.6, 5X, "M =", I5, 6X, "ALPHA = (",
     .          F5.1, ",", F10.6, ")" //
     .          " ", 14X, "NUMBER OF INTEGRATION POINTS IN THE XI DIRECT",
     .          "ION =", I5, //
     .          " ", 14X, "NUMBER OF GAUSSIAN POINTS IN THE THETA DIRECT",
     .          "ION =", I5, " (GAUSS - LEGENDRE)")
C
      PRINT 105
C
  105 FORMAT ("1THE CALCULATED SURFACE DISTRIBUTIONS OF THE ACOUSTIC P",
     .          "OTENTIAL, THE ACOUSTIC VELOCITY, AND THE EFFECTIVE ADMI",
     .          "TTANCE ARE:" ////
     .          "  N", 11X, "P(RHO, Z)", 14X, "PHI/COS(M*THETA)", 20X,
     .          "VEL/COS(M*THETA)", 18X, "EFFECTIVE ADMITTNACE" // " ")
C
      DO 6 I = 1, NP
      IF (ICHECK(I)) 7, 8, 9
    7 CONTINUE
      VELP(I) = CPHI(I)
      PVELM(I) = CABS (VELP(I))
      PPVELP(I) = 0.0
      IF (PVELM(I) .NE. 0.0) PPVELP(I) = ATAN2 (AIMAG (VELP(I)),
     .                    REAL (VELP(I)))
      CPHI(I) = CEXACT(I)
      RPHI(I) = REAL (CPHI(I))
      IPHI(I) = AIMAG (CPHI(I))
      MPHI(I) = CABS (CPHI(I))
      PPHI(I) = 0.0
      IF (MPHI(I) .NE. 0.0) PPHI(I) = ATAN2 (IPHI(I), RPHI(I))
      ADMIT(I) = VELP(I) / CPHI(I)
      IF (MPHI(I) .EQ. 0.0) ADMIT(I) = (0.0, 0.0)
      MADMIT(I) = CABS (ADMIT(I))
      PADMIT(I) = 0.0
      IF (MADMIT(I) .NE. 0.0) PADMIT(I) = ATAN2 (AIMAG (ADMIT(I)),
     .                    REAL (ADMIT(I)))
C
      WRITE (6, 106) I, P(I, 1), P(I, 2), VELP(I), ADMIT(I)
C
  106 FORMAT (" ", I3, 7X, "(", F5.3, ",", F6.3, ")", 44X, 2G13.5, 10X,
     .          2G13.5)
C
      GO TO 10
    8 CONTINUE
      RPHI(I) = REAL (CPHI(I))
      IPHI(I) = AIMAG (CPHI(I))
      MPHI(I) = CABS (CPHI(I))
      PPHI(I) = 0.0
      IF (MPHI(I) .NE. 0.0) PPHI(I) = ATAN2 (IPHI(I), RPHI(I))
      VELP(I) = CVEL(I)
      PVELM(I) = CABS (VELP(I))
      PPVELP(I) = 0.0
      IF (PVELM(I) .NE. 0.0) PPVELP(I) = ATAN2 (AIMAG (VELP(I)),
     .                    REAL (VELP(I)))
      ADMIT(I) = VELP(I) / CPHI(I)
      MADMIT(I) = CABS (ADMIT(I))
      PADMIT(I) = 0.0
      IF (MADMIT(I) .NE. 0.0) PADMIT(I) = ATAN2 (AIMAG (ADMIT(I)),
     .                    REAL (ADMIT(I)))
C
      WRITE (6, 107) I, P(I, 1), P(I, 2), CPHI(I), ADMIT(I)
C
  107 FORMAT (" ", I3, 7X, "(", F5.3, ",", F6.3, ")", 8X, 2G13.5, 46X,
     .          2G13.5)
```

```
        GO TO 10
 9      CONTINUE
        RPHI(I) = REAL (CPHI(I))
        IPHI(I) = AIMAG (CPHI(I))
        MPHI(I) = CABS (CPHI(I))
        PPHI(I) = 0.0
        IF (MPHI(I) .NE. 0.0) PPHI(I) = ATAN2 (IPHI(I), RPHI(I))
        VELP(I) = CPHI(I) * CY(I)
        PVELM(I) = CABS (VELP(I))
        PPVELP(I) = 0.0
        IF (PVELM(I) .NE. 0.0) PPVELP(I) = ATAN2 (AIMAG (VELP(I)),
       .                          REAL (VELP(I)))
        ADMIT(I) = CY(I)
        MADMIT(I) = CABS (ADMIT(I))
        PADMIT(I) = 0.0
        IF (MADMIT(I) .NE. 0.0) PADMIT(I) = ATAN2 (AIMAG (ADMIT(I)),
       .                          REAL (ADMIT(I)))
C
        WRITE (6, 108) I, P(I, 1), P(I, 2), CPHI(I), VELP(I)
C
 108    FORMAT (" ", I3, 7X, "(", F5.3, ",", F6.3, ")", 8X, 2G13.5, 10X,
       .        2G13.5)
C
 10     CONTINUE
 6      CONTINUE
C
        PRINT 113
C
 113    FORMAT ("1THE MODULUS OF THE ACOUSTIC POTENTIAL, THE ACOUSTIC VE",
       .        "LOCITY, AND THE EFFECTIVE ADMITTANCE ARE:" ////
       .        "  N", 11X, "P(RHO, Z)", 14X, "PHI/COS(M*THETA)", 20X,
       .        "VEL/COS(M*THETA)", 18X, "EFFECTIVE ADMITTANCE" /
       .        " ", 36X, "EXACT          CALC", 20X, "EXACT          CALC",
       .        20X, "EXACT          CALC" // " ")
C
        DO 16 I = 1, NP
        IF (ICHECK(I)) 17, 18, 19
 17     CONTINUE
C
        WRITE (6, 114) I, P(I, 1), P(I, 2), MEXACT(I), MVELP(I), PVELM(I),
       .               MYP(I), MADMIT(I)
C
 114    FORMAT (" ", I3, 7X, "(", F5.3, ",", F6.3, ")", 8X, G13.5, 23X,
       .        2G13.5, 10X, 2G13.5)
C
        GO TO 20
 18     CONTINUE
C
        WRITE (6, 115) I, P(I, 1), P(I, 2), MEXACT(I), MPHI(I), MVELP(I),
       .               MYP(I), MADMIT(I)
C
 115    FORMAT (" ", I3, 7X, "(", F5.3, ",", F6.3, ")", 8X, 2G13.5, 10X,
       .        G13.5, 23X, 2G13.5)
C
        GO TO 20
 19     CONTINUE
C
        WRITE (6, 116) I, P(I, 1), P(I, 2), MEXACT(I), MPHI(I), MVELP(I),
       .               PVELM(I), MYP(I)
C
 116    FORMAT (" ", I3, 7X, "(", F5.3, ",", F6.3, ")", 8X, 2G13.5, 10X,
       .        2G13.5, 10X, G13.5)
C
 20     CONTINUE
 16     CONTINUE
```

```
C
      PRINT 120
C
 120  FORMAT ("1THE PHASE OF THE ACOUSTIC POTENTIAL, THE ACOUSTIC VELO",
     .        "CITY, AND THE EFFECTIVE ADMITTANCE ARE:" ////
     .        "  N", 11X, "P(RHO, Z)", 21X, "PHI", 33X, "VEL", 24X,
     .        "EFFECTIVE ADMITTANCE" /
     .        "  ", 36X, "EXACT          CALC", 20X, "EXACT          CALC",
     .        20X, "EXACT          CALC" // " ")
C
      DO 11 I = 1, NP
      IF (ICHECK(I)) 12, 13, 14
 12   CONTINUE
C
      WRITE (6, 114) I, P(I, 1), P(I, 2), PEXACT(I), PVELP(I),
     .        PPVELP(I), PYP(I), PADMIT(I)
C
      GO TO 15
 13   CONTINUE
C
      WRITE (6, 115) I, P(I, 1), P(I, 2), PEXACT(I), PPHI(I), PVELP(I),
     .        PYP(I), PADMIT(I)
C
      GO TO 15
 14   CONTINUE
C
      WRITE (6, 116) I, P(I, 1), P(I, 2), PEXACT(I), PPHI(I), PVELP(I),
     .        PPVELP(I), PYP(I)
C
 15   CONTINUE
 11   CONTINUE
C
C     WRITE THE SURFACE DISTRIBUTIONS TO THE OUTPUT FILE.
C
      WRITE (10, 121) (CPHI(I), VELP(I), I = 1, NP)
C
 121  FORMAT (4G20.10)
C
      RETURN
      END
```

The following computer program reads the previous programs output file containing the values of the acoustic quantities on the surface of the body and calculates the values of the acoustic quantities at any given point in the field surrounding the body. The required inputs are the points where the acoustic quantities are known on the surface of the body Q, the normals to the body at these points NQ, the length of each integration interval LENGTH, the points in the field where the acoustic quantities are required P, and some arbitrary normal at these points NP as the normal acoustic velocity is calculated. The problem specification data is also required again; that is, k the wave number and m the mode number.

The program prints out all the geometric input data and the acoustic potential and normal acoustic velocity at the field points. It also calculates and prints out the SPL(dB) at each field point.

```
      PROGRAM EXPFF ( INPUT, OUTPUT, TAPE10, TAPE11,
                      TAPE5 = INPUT, TAPE6 = OUTPUT)
C
C
C*****************************************************************
C*                                                              *
C*                                                              *
C*      THIS PROGRAM CALCULATES THE ACOUSTIC POTENTIAL AND THE  *
C*      ACOUSTIC VELOCITY IN THE FIELD SURROUNDING ANY AXISYMMETRIC *
C*      BODY EMPLOYING THE SURFACE DISTRIBUTIONS OF THE ACOUSTIC *
C*      POTENTIAL AND THE NORMAL ACOUSTIC VELOCITY.             *
C*                                                              *
C*****************************************************************
C*                                                              *
C*      A CYLINDRICAL FORMULATION OF THE PROBLEM IS EMPLOYED.   *
C*                                                              *
C*                                                              *
C*****************************************************************
C
C
      REAL K, LENGTH
      COMPLEX CPHIP, CPHIQ, CVELP, CVELQ, IK, IKSQ
C
      COMMON /I/ M, NP, NQ
      COMMON /R/ FOURPI, K, PI, TWOPI
      COMMON /C/ IK, IKSQ
      COMMON /RD/ LENGTH (102), P (9, 2), PNORMAL (9, 2),
     .            Q (102, 2), QNORMAL (102, 2)
      COMMON /CD/ CPHIP (9), CPHIQ (102), CVELP (9), CVELQ (102)
      COMMON /NGAUSS/ NGAUSS
      COMMON /GAUSS/ GAUSST (48, 2)
C
      CALL INPUT
C
C     REAL CONSTANTS
C
      TWOPI = 2.0 * PI
      FOURPI = 4.0 * PI
C
C     COMPLEX CONSTANTS
C
      IK = (0.0, 1.0) * K
      IKSQ = IK * IK
C
      CALL CALC
C
      CALL OUTPUT
C
      STOP "NORMAL"
C
      END
```

31

```fortran
      BLOCK DATA
C
      REAL K
C
      COMMON /I/ M, NP, NQ
      COMMON /R/ FOURPI, K, PI, TWOPI
      COMMON /NGAUSS/ NGAUSS
      COMMON /GAUSS/ GAUSST (48, 2)
C
C     THE NUMBER OF POINTS IN THE FIELD WHERE THE ACOUSTIC POTENTIAL
C     AND THE ACOUSTIC VELOCITY ARE TO BE CALCULATED.
C
      DATA NP / 9 /
C
C     THE NUMBER OF POINTS ON THE SURFACE OF THE BODY WHERE THE
C     ACOUSTIC POTENTIAL AND THE NORMAL ACOUSTIC VELOCITY ARE KNOWN.
C
      DATA NQ / 102 /
C
      DATA PI / 3.1415926535898 /
C
      DATA NGAUSS / 48 /
C
      DATA ((GAUSST(I, J), J = 1, 2), I = 1, 12)
     .    / 0.01627674484960, 0.03255061449236,
     .      0.04881298513605, 0.03251611871387,
     .      0.08129749546443, 0.03244716371406,
     .      0.11369585011067, 0.03234382256858,
     .      0.14597371465490, 0.03220620479403,
     .      0.17809688236762, 0.03203445623199,
     .      0.21003131046057, 0.03182875889441,
     .      0.24174315616384, 0.03158933077073,
     .      0.27319881259105, 0.03131642559686,
     .      0.30436494435450, 0.03101033258631,
     .      0.33520852289263, 0.03067137612367,
     .      0.36569686147231, 0.03029991542083 /
      DATA ((GAUSST(I, J), J = 1, 2), I = 13, 24)
     .    / 0.39579764982891, 0.02989634413633,
     .      0.42547898840730, 0.02946108995817,
     .      0.45470942216774, 0.02899461415056,
     .      0.48345797392060, 0.02849741106509,
     .      0.51169417715467, 0.02797000761685,
     .      0.53938810832436, 0.02741296272603,
     .      0.56651041856140, 0.02682686672559,
     .      0.59303236477757, 0.02621234073567,
     .      0.61892584012547, 0.02557003600535,
     .      0.64416340378497, 0.02490063322248,
     .      0.66871831004392, 0.02420484179236,
     .      0.69256453664217, 0.02348339908593 /
      DATA ((GAUSST(I, J), J = 1, 2), I = 25, 36)
     .    / 0.71567681234897, 0.02273706965833,
     .      0.73803064374440, 0.02196664443874,
     .      0.75960234117665, 0.02117293989219,
     .      0.78036904386743, 0.02035679715433,
     .      0.80030874413914, 0.01951908114015,
     .      0.81940031073793, 0.01866067962741,
     .      0.83762351122819, 0.01778250231605,
     .      0.85495903343460, 0.01688547986425,
     .      0.87138850590930, 0.01597056290256,
     .      0.88689451740242, 0.01503872102699,
     .      0.90146063531585, 0.01409094177231,
     .      0.91507142312090, 0.01312822956696 /
      DATA ((GAUSST(I, J), J = 1, 2), I = 37, 48)
     .    / 0.92771245672231, 0.01215160467109,
     .      0.93937033975276, 0.01116210209984,
     .      0.95003271778444, 0.01016077053501,
     .      0.95968829144874, 0.00914867123078,
     .      0.96832682846326, 0.00812687692570,
     .      0.97593917458514, 0.00709647079115,
     .      0.98251726356301, 0.00605854550424,
     .      0.98805412632962, 0.00501420274293,
     .      0.99254390032376, 0.00396455433844,
     .      0.99598184298721, 0.00291073181793,
     .      0.99836437586318, 0.00185396078895,
     .      0.99968950388323, 0.00079679206555 /
C
      END
```

```
      SUBROUTINE INPUT
C
      REAL K, LENGTH
      COMPLEX CPHIP, CPHIQ, CVELP, CVELQ
C
      COMMON /I/ M, NP, NQ
      COMMON /R/ FOURPI, K, PI, TWOPI
      COMMON /RD/ LENGTH (102), P (9, 2), PNORMAL (9, 2),
     .            Q (102, 2), QNORMAL (102, 2)
      COMMON /CD/ CPHIP (9), CPHIQ (102), CVELP (9), CVELQ (102)
C
      READ (5, 100) ((P(I, J), J = 1, 2), I = 1, NP)
C
      READ (5, 100) ((PNORMAL (I, J), J = 1, 2), I = 1, NP)
C
      READ (5, 100) ((Q(I, J), J = 1, 2), I = 1, NQ)
C
      READ (5, 100) ((QNORMAL (I, J), J = 1, 2), I = 1, NQ)
C
      READ (5, 100) (LENGTH(I), I = 1, NQ)
C
  100 FORMAT (8G10.0)
C
      PRINT 101
C
  101 FORMAT ("1GEOMETRIC INPUT DATA:" ///
     .         " ", 4X, "N", 21X, "Q(RHO, Z)", 38X, "NORMAL(RHO, Z)",
     .         29X, "LENGTH" // " ")
C
      WRITE (6, 102) (I, Q(I, 1), Q(I, 2), QNORMAL(I, 1), QNORMAL(I, 2),
     .                LENGTH(I), I = 1, NQ)
C
  102 FORMAT (" ", 2X, I3, 10X, "(", F13.10, ",", F13.10, ")", 21X,
     .              "(", F13.10, ",", F13.10, ")", 17X,
     .              F13.10)
C
      PRINT 103
C
  103 FORMAT ("1FIELD POINT INPUT DATA:" ///
     .         " ", 4X, "N", 21X, "P(RHO, Z)", 38X, "NORMAL(RHO, Z)" //
     .         " ")
C
      WRITE (6, 104) (I, P(I, 1), P(I, 2), PNORMAL(I, 1), PNORMAL(I, 2),
     .                I = 1, NP)
C
  104 FORMAT (" ", 2X, I3, 9X, "(", F14.10, ",", F14.10, ")", 20X,
     .              "(", F13.10, ",", F13.10, ")")
C
      READ (10, 105) (CPHIQ(I), CVELQ(I), I = 1, NQ)
C
  105 FORMAT (4G20.10)
C
      PRINT 106
C
  106 FORMAT ("1", 61X, "********" / " ", 61X, "*      *" /
     .         " ", 61X, "* BODY *" / " ", 61X, "*      *" /
     .         " ", 61X, "********" //// " N ", 21X, "Q(RHO, Z)", 25X,
     .         "ACOUSTIC POTENTIAL", 21X, "ACOUSTIC VELOCITY" // " ")
C
      WRITE (6, 107) (I, Q(I, 1), Q(I, 2), CPHIQ(I), CVELQ(I),
     .                I = 1, NQ)
C
  107 FORMAT (" ", I3, 9X, "(", F13.10, ",", F13.10, ")",
     .              9X, "(", F14.10, ",", F14.10, ")",
     .              8X, "(", F14.10, ",", F14.10, ")")
C
      READ (11, 1100) M, K
C
 1100 FORMAT (I20, G20.0)
C
      RETURN
      END
```

```fortran
      SUBROUTINE CALC
C
      REAL K, LENGTH, NDOTN, NRHOQP, NZPZD, NZQZD, NZQP
      COMPLEX CPHIP, CPHIQ, CVELP, CVELQ, G, GP, GPP, IK, IKSQ, I1, I2,
     .        I3, I4
C
      COMMON /I/ M, NP, NQ
      COMMON /R/ FOURPI, K, PI, TWOPI
      COMMON /C/ IK, IKSQ
      COMMON /RD/ LENGTH (102), P (9, 2), PNORMAL (9, 2),
     .        Q (102, 2), QNORMAL (102, 2)
      COMMON /CD/ CPHIP (9), CPHIQ (102), CVELP (9), CVELQ (102)
      COMMON /NGAUSS/ NGAUSS
      COMMON /GAUSS/ GAUSST (48, 2)
C
      DO 1 I = 1, NP
      CPHIP(I) = (0.0, 0.0)
      CVELP(I) = (0.0, 0.0)
C
C     XI INTEGRATION
C
      DO 2 J = 1, NQ
      GAUSZ = TWOPI * LENGTH(J)
      ZD = Q(J, 2) - P(I, 2)
      NZQZD = QNORMAL(J, 2) * ZD
      NZPZD = PNORMAL(I, 2) * ZD
      ZSQ = ZD * ZD
      RHOSQ = (Q(J, 1) - P(I, 1))**2
      RHOQP2 = 2.0 * Q(J, 1) * P(I, 1)
      NRHOQP = QNORMAL(J, 1) * PNORMAL(I, 1)
      NZQP = QNORMAL(J, 2) * PNORMAL(I, 2)
      RHOZSQ = RHOSQ + ZSQ
C
C     THETA INTEGRATION
C
      DO 3 IT = 1, NGAUSS
      THETA = PI * GAUSST(IT, 1)
      GAUSZT = GAUSZ * GAUSST(IT, 2)
C
      COST = COS (THETA)
      COSMT = COS (M * THETA)
C
      R = SQRT (RHOZSQ + RHOQP2 * (1.0 - COST))
      DRDNP = (PNORMAL(I, 1) * (P(I, 1) - Q(J, 1) * COST) - NZPZD) / R
      DRDNQ = (QNORMAL(J, 1) * (Q(J, 1) - P(I, 1) * COST) + NZQZD) / R
      NDOTN = NRHOQP * COST + NZQP
C
      G = Q(J, 1) * GAUSZT * COSMT * CEXP (IK * R) / R
      GP = G * (IK - (1.0 / R))
      GPP = G * (IKSQ - (3.0 * IK / R) + (3.0 / (R * R)))
C
      I1 = GP * DRDNQ
      I2 = -G
      I3 = GPP * DRDNQ * DRDNP - (GP * NDOTN / R)
      I4 = -GP * DRDNP
C
      CPHIP(I) = CPHIP(I) + I1 * CPHIQ(J) + I2 * CVELQ(J)
      CVELP(I) = CVELP(I) + I3 * CPHIQ(J) + I4 * CVELQ(J)
C
    3 CONTINUE
    2 CONTINUE
C
      CPHIP(I) = CPHIP(I) / FOURPI
      CVELP(I) = CVELP(I) / FOURPI
C
    1 CONTINUE
C
      RETURN
      END
```

34

```
      SUBROUTINE OUTPUT
C
      REAL IPHI, IPHIP, IVEL, IVELP, K, LENGTH, MPHI, MPHIP, MVEL,
     .     MVELP
      COMPLEX CPHIP, CPHIQ, CVELP, CVELQ, Y
C
      COMMON /I/ M, NP, NQ
      COMMON /R/ FOURPI, K, PI, TWOPI
      COMMON /RD/ LENGTH (102), P (9, 2), PNORMAL (9, 2),
     .            Q (102, 2), QNORMAL (102, 2)
      COMMON /CD/ CPHIP (9), CPHIQ (102), CVELP (9), CVELQ (102)
      COMMON /NGAUSS/ NGAUSS
C
      DIMENSION IPHI (9), IPHIP (9), MPHI (9), MPHIP (9),
     .          PPHI (9), PPHIP (9), RPHI (9), RPHIP (9),
     .          IVEL (9), IVELP (9), MVEL (9), MVELP (9),
     .          PVEL (9), PVELP (9), RVEL (9), RVELP (9)
C
C     INITIALIZE EXACT SOLUTION.
C
      DO 2 I = 1, NP
      RPHI(I) = 0.0
      IPHI(I) = 0.0
      MPHI(I) = 0.0
      PPHI(I) = 0.0
      RVEL(I) = 0.0
      IVEL(I) = 0.0
      MVEL(I) = 0.0
      PVEL(I) = 0.0
    2 CONTINUE
      NGAUSS = 2 * NGAUSS
C
      WRITE (6, 100) K, M, NGAUSS
C
  100 FORMAT ("1INPUT FOR THIS CASE IS:" ///
     .        " ", 60X, "K =", F10.6 // " ", 60X, "M =", I5 //
     .        " ", 13X, "NUMBER OF GAUSSIAN POINTS IN THE THETA DIRECT",
     .        "ION =", I5, " (GAUSS - LEGENDRE)")
C
      DO 5 I = 1, NP
      RPHIP(I) = REAL (CPHIP(I))
      RVELP(I) = REAL (CVELP(I))
      IPHIP(I) = AIMAG (CPHIP(I))
      IVELP(I) = AIMAG (CVELP(I))
      MPHIP(I) = CABS (CPHIP(I))
      MVELP(I) = CABS (CVELP(I))
      PPHIP(I) = 0.0
      PVELP(I) = 0.0
      IF (MPHIP(I) .NE. 0.0) PPHIP(I) = ATAN2 (IPHIP(I), RPHIP(I))
      IF (MVELP(I) .NE. 0.0) PVELP(I) = ATAN2 (IVELP(I), RVELP(I))
    5 CONTINUE
C
      PRINT 103
C
  103 FORMAT ("1", 58X, "**************" / " ", 58X, "*            *" /
     .        " ", 58X, "* CALCULATED *" / " ", 58X, "*            *" /
     .        " ", 58X, "**************" //// " N", 21X, "P(RHO, Z)",
     .        25X, "ACOUSTIC POTENTIAL",
     .        21X, "ACOUSTIC VELOCITY" // " ")
C
      WRITE (6, 102) (I, P(I, 1), P(I, 2), CPHIP(I), CVELP(I),
     .                I = 1, NP)
C
  102 FORMAT (" ", I3, 8X, "(", F14.10, ",", F14.10, ")",
     .              8X, "(", F14.10, ",", F14.10, ")",
     .              8X, "(", F14.10, ",", F14.10, ")")
C
```

35

```
      PRINT 109
C
  109 FORMAT ("1THE MODULUS OF THE ACOUSTIC POTENTIAL AND THE ACOUSTIC",
     .        " VELOCITY ARE:" ////  "  N", 11X, "P(RHO, Z)", 14X,
     .        "PHI/COS(M*THETA)", 20X, "VEL/COS(M*THETA)", 8X,
     .        "SPL (DB)", 16X, "Y" /
     .        " ", 36X, "EXACT       CALC", 20X, "EXACT       CALC" //
     .        " ")
C
      DO 7 I = 1, NP
      SPL = 20.0 * ALOG10 (K * MPHIP(I)) + 146.6
      Y = CVELP(I) / CPHIP(I)
C
      WRITE (6, 110) I, P(I, 1), P(I, 2), MPHI(I), MPHIP(I), MVEL(I),
     .        MVELP(I), SPL, Y
C
  110 FORMAT (" ", I3, 6X, "(", F6.3, ",", F7.3, ")", 7X, 2G13.5, 10X,
     .        2G13.5, 2X, F7.2, 5X, 2G13.5)
C
  7   CONTINUE
C
      PRINT 112
C
  112 FORMAT ("1THE PHASE OF THE ACOUSTIC POTENTIAL AND THE ACOUSTIC V",
     .        "ELOCITY ARE:" ////  "  N", 11X, "P(RHO, Z)", 21X,
     .        "PHI", 33X, "VEL" /
     .        " ", 36X, "EXACT       CALC", 20X, "EXACT       CALC" //
     .        " ")
C
      WRITE (6, 113) (I, P(I, 1), P(I, 2), PPHI(I), PPHIP(I), PVEL(I),
     .        PVELP(I), I = 1, NP)
C
  113 FORMAT (" ", I3, 6X, "(", F6.3, ",", F7.3, ")", 7X, 2G13.5, 10X,
     .        2G13.5)
C
      RETURN
      END
```

Appendix B

Paper accepted for publication in the Journal of the Acoustical Society of America

"Prediction of the Sound Field Radiated From Axisymmetric Surfaces"

PREDICTION OF THE SOUND FIELD RADIATED FROM
AXISYMMETRIC SURFACES

W. L. Meyer[*], W. A. Bell[*], M. P. Stallybrass[**] and B. T. Zinn[*]

*School of Aerospace Engineering
**School of Mathematics
Georgia Institute of Technology
Atlanta, Georgia 30332

Abstract

A general analytical method for determining the radiated sound fields

from axisymmetric surfaces of arbitrary cross section with general boundary

conditions is developed. The method is based on an integral representation

for the external solutions of the Helmholtz equation. An integral equation

is developed governing the surface potential distribution which gives unique

solutions at all wave numbers. The axisymmetric formulation of the problem

reduces its solution to the numerical evaluation of line integrals by

Gaussian quadrature. The applicability of the solution approach for both a

sphere and finite cylinder is demonstrated by comparing the numerical results

with exact analytical solutions for both discontinuous and continuous boundary

conditions. The method is then applied to a jet engine inlet configuration

and the computed results are in good agreement with exact values.

I. Introduction

To reduce the noise radiated to the community from turbofan inlets, the

effects of sound suppression material in the inlet and the spatial distri-

bution of the sound source on the radiated sound levels and patterns must be

determined. Analytical techniques for predicting these effects must be cap-

able of dealing with general axisymmetric geometries and complicated boundary

conditions which are encountered in multiply-lined inlets. For instance, in

a typical inlet the compressor-fan combination represents a noise source

with a nonuniform spatial excitation pattern. Thus, the analytical method should be capable of taking into account sound sources of general spatial distribution. Also, inlets may contain multiple acoustic liners to reduce the radiated sound power and admittance boundary conditions are commonly used to account for the absorption characteristics of the liner. Therefore, the analytical method must be capable of dealing with spatially varying surface admittances. Finally, the method should be capable of predicting the characteristics of the radiated sound field in an infinite domain. Keeping these requirements in mind, the work presented in this paper describes the results of an investigation which has been concerned with the analytical determination of radiated sound fields from axisymmetric surfaces of arbitrary cross section and with general boundary conditions.

The method used in this investigation is based on an integral form of the solutions of the Helmholtz equation.[1-6] With this formulation the acoustic potential anywhere external to the surface can be found once the distribution on the surface is known. Thus, to determine the radiated sound field the problem reduces to the determination of the distribution of the acoustic potential on the two dimensional surface of the geometry under consideration instead of solving the Helmholtz equation in the surrounding infinite three dimensional domain.

It has been previously shown [1-5] that when applied to exterior sound radiation problems the classical techniques fail to produce unique solutions at frequencies corresponding to certain interior eigenvalues of the geometries under consideration. Unless special precautions are taken, straight-forward numerical solution of the integral equation produces large errors at frequencies close to these eigenvalues. For the general geometries of interest in this study, these eigenfrequencies are not known a priori. Therefore,

the frequencies about which large numerical errors can occur cannot be easily avoided. A critical review of available analytical techniques for avoiding these errors is provided by Burton in Ref. 1. In a search for an appropriate technique for use in the present study of inlets, the authors programmed each of these methods for a sphere and obtained numerical results for the surface and radiated sound field. This study showed that the method of Burton and Miller[4] was the most straightforward to implement. However, an interpretation of a strongly singular integral, given in the analysis in Ref. 5 by Meyer, et.al. was necessary for the equations to be amenable to numerical solution. Basically the method proposed by Burton and Miller involves a reformulation of the integral equation for the acoustic potential and the solutions obtained are valid at all frequencies. It also yields the most consistently accurate results for a given number of points at which the acoustic potential is numerically evaluated on the surface. Therefore, the method based on the analysis in Ref. 5 has been chosen for this investigation.

The resulting integral equation for the surface acoustic potential is solved numerically and, for axisymmetric geometries, the equation reduces to the evaluation of line integrals. Thus, the axisymmetric case can be reduced to an equivalent one-dimensional problem. Having discretized the integral equation, the resulting system of algebraic equations is solved using complex Gauss-Jordan elimination. Since the coefficient matrix involves the free space Green's function, which becomes singular as two points on the surface approach one another, numerical techniques are presented which can deal with these singularities and yield accurate results. Gaussian integration is used to increase the accuracy of the solution without significant penalties in computer storage and time requirements. The applicability of the integral formulation and the accuracy of the numerical techniques are demonstrated by

computing the surface and far field distributions of the acoustic potential
on both a sphere and a finite cylinder. The numerical results are compared
with known exact solutions generated by the separation of variables technique.
Surfaces with spatially varying forcing functions and admittances are
considered, for different tangential modes, to evaluate the capability of the
integral approach to handle boundary conditions of a general nature. With
the sphere, agreement between computed and exact results is to three signifi-
cant figures. For the cylinder agreement is to two significant figures. The
effect on the accuracy of discontinuous boundary conditions involving nonzero
admittances over the surface and of the corners encountered in the cylindrical
configuration are also presented. Finally, the numerical results for an
inlet configuration are compared with exact solutions and agreement is to
within ten per cent.

II. Theoretical Considerations

In this section the general three dimensional integral representation of
the solutions of the Helmholtz equation is developed for application to radi-
ation problems. This particular formulation yields unique solutions at all
frequencies and does not have strong singularities which are difficult to
handle numerically. The general integral equation is then specialized for
axisymmetric geometries. A more detailed development is presented in Ref. 5.

General Formulation

Beginning with the three dimensional Helmholtz equation which governs
the spatial dependence of the acoustic field for harmonic oscillations

$$\nabla^2 \varphi + k^2 \varphi = 0 \qquad (1)$$

where φ is the acoustic potential and k is the wave number; the standard integral representation of the exterior potential is found to be[1,6]

$$\iint_S (\varphi(Q) \frac{\partial G(P,Q)}{\partial n_q} - G(P,Q) \frac{\partial \varphi(Q)}{\partial n_q}) dS_q = 4\pi\varphi(P) \tag{2}$$

where the term $\frac{\partial}{\partial n_q}$ represents an outward normal derivative with respect to the body S as shown in Fig. 1; that is,

$$\frac{\partial \varphi(Q)}{\partial n_q} = \vec{\nabla}_q \varphi(Q) \cdot \vec{n}_q \tag{3}$$

Also, G(P,Q) is a fundamental three dimensional solution of the Helmholtz equation and is taken to be the free space Green's Function for a point source[6] defined as

$$G(P,Q) = \frac{e^{ikr(P,Q)}}{r(P,Q)} \tag{4}$$

From Eq. (2), if the acoustic potential and the normal acoustic velocity $\frac{\partial \varphi(Q)}{\partial n_q}$ are known at each point on the surface of the body then the acoustic potential may be calculated anywhere in the exterior domain.

To solve for the surface potential, the point P is moved to the surface of the body, and Eq. (2) then becomes

$$\iint_S (\varphi(Q) \frac{\partial G(P,Q)}{\partial n_q} - G(P,Q) \frac{\partial \varphi(Q)}{\partial n_q}) dS_q = 2\pi\varphi(P) \tag{5}$$

For the inhomogeneous Robin boundary condition employed in this study, a relation between $\partial\varphi(Q)/\partial n_q$ and $\varphi(Q)$ exists which is given by

$$\frac{\partial \varphi(Q)}{\partial n_q} - Y(Q)\varphi(Q) = A(Q), \tag{6}$$

so that Eq. (5) can be written in terms of the potential only; that is,

$$\iint_S \varphi(Q) \frac{\partial G(P,Q)}{\partial n_q} dS_q - \iint_S \varphi(Q)G(P,Q)Y(Q)dS_q \tag{7}$$

$$= 2\pi\varphi(P) + \int\int_S A(Q)\ G(P,Q)\ dS_q$$

If the acoustic velocity $A(Q)$ and the admittance $Y(Q)$ are specified at each point on the surface of the body, then the acoustic potential may be calculated at each point using Eq.(7).

As mentioned earlier this equation does not yield unique solutions when the wave number k is an internal eigenvalue associated with the problem under consideration. Since these eigenvalues are not known a priori for general bodies, the formulation cannot be relied upon to give consistently good results. There are a number of papers in the literature [2,3,4] dealing with this problem, and the relative merits and shortcomings of the methods employed are discussed in detail in Ref. 1.

An attractive approach from an analytical point of view is provided by Burton and Miller[4] who have suggested the use of the following identity to derive an alternative integral equation for the acoustic potential at the surface.

$$2\pi\ \frac{\partial\varphi(P)}{\partial n_p} = \int\int_S \left[\varphi(Q)\ \frac{\partial^2 G(P,Q)}{\partial n_p \partial n_q} - \frac{\partial G(P,Q)}{\partial n_p}\ \frac{\partial\varphi(Q)}{\partial n_q}\right]dS_q \tag{8}$$

This equation can now be solved for $\varphi(P)$ by using Eq. (6) to relate the normal acoustic velocity and the potential at the surface. However this integral equation has its own set of associated eigenvalues at which unique solutions cannot be obtained. To circumvent the problem associated with the solution of the integral equations derived from Eqs.(5) and (8), Burton and Miller suggested the solution of the following linear combination of these equations:

$$\int\int_S \left(\varphi(Q)\ \frac{\partial G(P,Q)}{\partial n_q} - G(P,Q)\ \frac{\partial\varphi(Q)}{\partial n_q}\right)\ dS_q$$

$$+ \alpha \int\int_S (\varphi(Q) \frac{\partial^2 G(P,Q)}{\partial n_p \partial n_q} - \frac{\partial G(P,Q)}{\partial n_p} \frac{\partial \varphi(Q)}{\partial n_q}) \, dS_q$$

$$= 2\pi (\varphi(P) + \alpha \frac{\partial \varphi(P)}{\partial n_p}) \tag{9}$$

where $\partial \varphi / \partial n$ and φ are related by Eq. (6). Equation (9) will yield unique solutions if the complex coupling constant is properly chosen. It is shown that α must meet the following restrictions to guarantee that Eq. (9) yields unique solutions:[*]

$$\text{Im } (\alpha) \neq 0 \qquad k \text{ real or imaginary}$$

$$\text{Im } (\alpha) = 0 \qquad k \text{ complex} \tag{10}$$

A problem arises in the numerical solution of Eq. (9) as the third term on the left hand side is strongly singular in its present form as the point Q approaches the point P on the surface of the body. The authors of this paper have shown that this difficulty can be overcome by a proper interpretation of this singular term.[5] Employing a vector transformation[8] and taking the Cauchy Principle Value, Eq. (9) is shown to be equivalent to

$$\int\int_S \left[\varphi(Q) \frac{\partial G(P,Q)}{\partial n_q} - G(P,Q) \frac{\partial \varphi(Q)}{\partial n_q} \right] dS_q$$

$$+ \alpha \int\int_S [\varphi(Q) - \varphi(P)] \frac{\partial^2 G(P,Q)}{\partial n_p \partial n_q} \, dS_q$$

$$\tag{11}$$

$$- \alpha \varphi(P) \int\int_S (n_p \cdot n_q)(ik)^2 G(P,Q) \, dS_q$$

---

[*] It has been pointed out to us by a reviewer that an equation of the same general form as Eq. (9) has been given by Chertock[7]. However, for an arbitrary, smooth surface, Chertock did not interpret this integral equation correctly. Specifically, the limit indicated in the final term of (A17), Ref. (7), does not exist as may be verified for the simple case of a sphere.

$$- \alpha \int\int_S \frac{\partial G(P,Q)}{\partial n_p} \frac{\partial \varphi(Q)}{\partial n_q} \, dS_q = 2\pi \left[\varphi(P) + \alpha \frac{\partial \varphi(P)}{\partial n_p} \right]$$

All of the terms in Eq. (11) are now well defined; however, all the integrands are oscillatory and singular so that care must be taken in their numerical approximation.

Axisymmetric Formulation

When dealing with a body of revolution as shown in Fig. 2 an axisymmetric formulation of the problem is advantageous.[9] This being the case an element of area dS_q becomes $\rho \, ds \, d\theta$ where s is the distance along the perimeter of the surface in the ρ-z plane. Assuming an acoustic velocity distribution of the form

$$\frac{\partial \varphi}{\partial n} = v(s) \cos m \, \theta \tag{12}$$

and describing the s dependence of the potential function by

$$\Phi(s) \equiv \frac{\varphi}{\cos m \, \theta} \tag{13}$$

and letting $\theta_p = 0$ (so that $\cos \theta_p = 1$) Eq. (11) becomes:

$$\int\int_S \Phi(s_q) \frac{\partial G(P,Q)}{\partial n_q} \cos m \, \theta_q \, dS_q$$

$$- \alpha \, \Phi(s_p) \int\int_S G(P,Q) (ik)^2 (n_p \cdot n_q) \, dS_q$$

$$+ \alpha \int\int_S \left[\Phi(s_q) \cos m \, \theta_q - \Phi(s_p) \right] \frac{\partial^2 G(P,Q)}{\partial n_p \partial n_q} \, dS_q$$

$$\tag{14}$$

$$- \int\int_S v(s_q) \, G(P,Q) \cos m \, \theta_q \, dS_q$$

$$- \alpha \int_S \int v(s_q) \; \frac{\partial G(P,Q)}{\partial n_p} \; \cos m \; \theta_q \; dS_q$$

$$= 2 \pi \left[\bar{\Phi}(s_p) + \alpha \; v(s_p) \right]$$

Now, three sets of functions are defined:

Influence Functions

$$I_1 \; (r_{pq}) = 2 \int_0^{\pi} G(P,Q) \cos m \; \theta_q \; d\theta_q \tag{15}$$

$$I_2 \; (r_{pq}) = 2\alpha \int_0^{\pi} \frac{\partial G(P,Q)}{\partial n_p} \; \cos m \; \theta_q \; d\theta_q$$

Kernel Functions

$$K_1 \; (r_{pq}) = 2 \int_0^{\pi} \frac{\partial G(P,Q)}{\partial n_q} \; \cos m \; \theta_q \; d\theta_q \tag{16}$$

$$K_2 \; (r_{pq}) = 2\alpha \int_0^{\pi} \frac{\partial^2 G(P,Q)}{\partial n_p \partial n_q} \; \cos m \; \theta_q \; d\theta_q, \quad \theta_q \neq \theta_p$$

Forcing Functions

$$F_1 \; (r_{pq}) = 2\alpha \int_0^{\pi} G(P,Q)(ik)^2 (n_p \cdot n_q) \; d\theta_q \tag{17}$$

$$F_2 \; (r_{pq}) = 2\alpha \int_0^{\pi} \frac{\partial^2 G(P,Q)}{\partial n_p \partial n_q} \; d\theta_q \;, \quad \theta_q \neq \theta_p$$

where r_{pq} is the distance between points P and Q and n_p and n_q are the outward normals to the surface at points P and Q, respectively. In evaluating K_2 and F_2, the point at which $\theta_p = \theta_q$ is excluded from the integration. Substituting Eqs. (15)-(17) into Eq. (14) gives

$$\int_0^{\ell} \Phi(s_q) \left\{ K_1 (r_{pq}) + K_2(r_{pq}) \right\} ds_q$$

$$- \Phi(s_p) \int_0^\ell \left\{ F_1(r_{pq}) + F_2(r_{pq}) \right\} ds_q$$

$$- \int_0^\ell v(s_q) \left\{ I_1(r_{pq}) + I_2(r_{pq}) \right\} ds_q \tag{18}$$

$$= 2\pi \left[\Phi(s_p) + \alpha v(s_p) \right]$$

where ℓ is the length of the generating line of the surface of revolution. The s-θ coordinate directions have now been essentially uncoupled so that the problem has been reduced to the evaluation of the line integrals in the coordinate directions on the surface of the body. This formulation does not restrict the form or type of boundary conditions on the body; it merely assumes that the boundary conditions can be represented by a sum (expanded in a set) of tangential modes.

III. Results

The acoustic fields for a sphere, cylinder, and inlet configuration have been computed by numerical solution of Eq. (18) using the techniques described in Ref. 10. Basically, this method consists of first specifying the ρ-z coordinates and the normal vector at each point on the surface. From these quantities the distances and the normal derivatives can be obtained. The integral in Eq. (18) is then separated into n integrals taken over subintervals of length ℓ/n. The acoustic potential is assumed constant over each subinterval and the integrations are performed numerically using Gauss-Legendre quadrature in the ρ-z plane. Over the subinterval containing the point P, the integrand in Eq. (18) becomes infinite since r_{pq} approaches zero. Thus, only an even number of points is used in the quadrature algorithim, since an odd number would necessitate inclusion of the point where $r_{pq} = 0$.

A Gauss-Legendre quadrature formula is used in the circumferential direction

to evaluate Eqs. (15) - (17). All calculations were performed on the Georgia

Tech CDC Cyber 70/74 with sixteen significant figures.

In all geometries investigated, exact solutions were obtained for m = 0

by assuming a monopole source located at point (ρ ,z) = (0,0) inside the sur-

face. The normal velocities and/or admittance values are then computed at

each point on the surface using Eq. (6) and taken as the boundary conditions

in Eq. (18). The surface potential Φ (s$_p$) is then computed from Eq. (18) and

the far field potential is obtained by numerically solving Eq. (2) with Eq. (6).

The computed surface and far field potentials are then compared with the known

potential distribution of the monopole source

$$\varphi(P) = \frac{-e^{ika}}{a} \tag{19}$$

where a is the distance from the source to the observation point. For m = 1

a dipole source was used to generate exact solutions, and for m = 2 a quadra-

pole source was used.

To investigate the effect of the coupling constant α in Eqs. (15) - (17),

the surface potential distributions for a sphere of unit radius with a uni-

formly vibrating surface (i.e. m = 0) were computed for α =0,i, and i/k. Twenty

subintervals were taken in the ρ -z plane, a four-point Gauss-Legendre quadra-

ture formula was used over each subinterval and a twenty-point Gauss-Legendre

formula was used in the θ direction. The magnitude of the potential should be

unity at all points on the surface. The results presented in Fig. 3 show the

computed magnitudes of the surface acoustic potential to be in error by 12

per cent for α = 0 at nondimensional wave numbers ka close to π , 2 π , and 3π.

These results are those that would be obtained from Eq. (7). The relatively

large errors are expected from the analysis of Burton and Miller[4] and from previous

investigations using Eq. (7).[2,5] Burton proves that setting the imaginary

part of α nonzero guarantees unique solutions to Eq. (18), For $\alpha = i$ the maximum error is reduced to less than four per cent except when k is close to 8.0. However, when $\alpha = i$, and for sufficiently high values of ka, Eq. (9) is dominated by terms arising from Eq. (8). As a result, the solution equations become ill-conditioned when ka is sufficiently high and close to one of the eigenfrequencies associated with the integral equation based on Eq. (8). In Table I computed values close to these eigenfrequencies and the eigenfrequencies of Eq. (7) are compared with exact results for $\alpha = 0$, i, and i/k. In all cases, the value of i/k gives the most accurate results. In Table II, the effect of introducing an admittance condition is presented for $\alpha = i/k$. The admittance Y(Q) and forcing function A(Q) in Eq. (6) are chosen so that the relations

$$\frac{\partial \varphi}{\partial n_q} - Y(Q)\varphi = A(Q) \quad ; \quad \varphi = \frac{-e^{ikr}}{r} \tag{20}$$

are satisfied on the surface and the exact solutions can be readily computed. The loss in accuracy when an admittance condition is used is minimal and restricted to the third significant figure. However, for discontinuous boundary conditions, where the forcing function is specified over one part of the surface (i.e., the admittance is zero there) and the admittance is specified over the remaining surface, errors of over ten per cent in the real and imaginary parts of the computed surface potential result. For comparison, the case of a constant forcing function and admittance over the sphere for $\alpha = 0$ is also presented and in all cases yields results of less accuracy than those obtained with $\alpha = i/k$.

In this study consistently good results were obtained with $\alpha = i/k$. In Fig. 3 the computed and exact values for $\alpha = i/k$ agree to three significant figures over the range of nondimensional wave numbers from one to ten. In

fact, for this value of α, the accuracy is significantly better at all wave numbers investigated. While Burton and Miller[4] provide no recommendations for choosing one value of α over any other value with an imaginary component, the choice $\alpha = i/k$ used in the present study can be explained as follows. The terms in Eqs. (15) - (17) which involve α are of order k^2 whereas the remaining terms are of order k. Therefore, at higher wave numbers the terms of order k^2 dominate. By choosing α to vary inversely with the wave number, all terms in Eqs. (15) - (17) remain of the same order with respect to wave number.*

A problem of more practical importance is the finite axisymmetric duct since this surface approximates an engine configuration. The surface potential distributions are presented in Fig. 4 at different nondimensional wave numbers for m = 0. The normal acoustic velocity distribution A(Q) is chosen so that the solution for the acoustic potential satisfies Eq. (19). The parameter α is taken to be i/k. Twenty subintervals are taken in the ρ -z plane and a twenty-point Gauss-Legendre quadrature is used in the θ direction. In Fig. 4 the variations of the magnitude and phase with distance along the perimeter s are presented. The largest errors in the computed magnitude of the potential of about ten per cent occur on the ends of the cylinder and at the corners. The results at the ends can be improved without increasing the number of points by area weighting rather than taking equidistant points along the perimeter. The errors in the phase are less than four per cent in all cases. The errors in the magnitude of the computed surface potential increase with increasing nondimensional wave number;

---

* It is interesting to note that in the report by Chertock[7] he suggests the use of 1/k on the grounds that it has the correct physical dimensions (i.e. length) that will maintain the dimensional homogeneity of Eq. (18).

but, even when ka = 10, the numerical results are within ten per cent of the exact solutions. For $\alpha = 0$ or i the errors are significantly larger above ka = 2.

In most inlet problems the boundary conditions are discontinuous with the acoustic velocity or potential (which is directly proportional to the acoustic pressure) specified over part of the surface and the admittance (representing liners) over the rest. To determine the effect of the discontinuities and the use of an admittance function on the numerical results for m = 0, a cylinder was investigated. The velocity was specified on the ends and the admittance was specified in the center so that the solution for Φ was given by Eq. (19) and Eq. (6) is satisfied. Again, twenty points are used in the ρ-z and θ directions. The results are shown in Fig. 5. Although the errors in the numerical results for this case are higher than those observed in Fig. 4, the errors still remain within 10 per cent for values of ka less than 5. However, when ka = 10 errors of up to 40 per cent in the magnitude of the potential are encountered close to the discontinuity in the boundary condition. This error can be reduced by increasing the number of subintervals in the ρ-z plane. Doubling the number of subintervals halves the error. When both the normal acoustic velocity and the admittance are continuous on the surface, the errors are of the same order of magnitude as those of Fig. 4. For tangential modes, the variation in the circumferential direction behaves as cos m θ where m = 0,1,2..... To check the numerical integration scheme in the circumferential direction, the surface acoustic potential was computed for m = 1 and m = 2 for the cylinder shown in Fig. 4. The results are presented in Fig. 6 for ka = 2 with the normal acoustic velocity specified everywhere on the surface. The computed and exact results (i.e. from a dipole and qudrapole) are in agreement to within two per cent for both m = 1

and $m = 2$.

It has been shown[5] that once the surface potential has been accurately computed, the far field can be determined to at least the same accuracy as the surface potential. This result is confirmed by the data presented in Fig. 7 for the cylinder of Fig. 4 with the velocity specified everywhere on the surface with $ka = 2$ and $m = 0$. The results at 20 radii from the surface are in agreement with exact results obtained from Eq. (19) to within one per cent even though the surface errors at some points are above two per cent. Data in Fig. 8 show that accurate results are obtained at distances greater than one integration stepsize from the surface. At closer distances errors from the numerical evaluation of the singularity in the Green's function defined by Eq. (4) leads to large errors.

The studies of the acoustic fields of the sphere and cylinder served to check out and refine the numerical procedures and programming techniques. The next configuration investigated was an inlet used in a study by NASA.[11] This inlet is shown in Fig. 9 and was chosen because:

(1) unlike most inlets used in research studies, it does not have a bell-mouth shape but is shaped like a typical inlet used in existing aircraft; and

(2) complete details on generating the inlet boundary are given in Ref. 11. For this inlet, all cases were investigated with $\alpha = i/k$.

As seen in Fig. 10, the normal velocity distribution, which represents a forcing function, is highly discontinuous and provides a severe test of the numerical techniques employed. The numerical and exact solutions for the surface acoustic potential are compared in Fig. 10 for 32 and 54 subintervals taken along the perimeter of the inlet in the ρ-z plane. Because of the errors in approximating the lengths of each subinterval, the exact solutions differ

slightly as the distance along the perimeter s increases. The centerbody
in Fig. 9 extends from $0 \leq s \leq 0.8$, the fan inlet covers $0.8 \leq s \leq 1.4$,
the interior contour extends from $1.4 \leq s \leq 3.5$, the exterior from 3.5
$\leq s \leq 5.5$, and the circular arc lies within the interval $5.5 \leq s \leq 7.45$.
Increasing the number of points decreases the error proportionately as
indicated by the data in Fig. 10 at a nondimensional wave number ka of
unity where a is the radius of the inlet at the fan entrance section.
The absolute average error in the results decreases from 10.2 per cent
for 32 subintervals to 4.16 per cent for 53 subintervals. The computation
time increased from 53 seconds to 143 seconds, respectively.

As shown in Fig. 11, the errors increase with increasing frequency.
Like the cylinder, the maximum error in the acousitc potential for the
inlet configuration occurs at the points of discontinuity. The average
error increases from 4.16 per cent at ka = 1 to 15 per cent at ka = 10.

For the data in Figs. 10 and 11, the acoustic potential is assumed
constant in the tangential plane. The results for a $\cos(m\theta)$ distribution
are presented in Fig. 12 at ka = 2. These results show the insensitivity
of the accuracy of the computed results to the tangential distribution
for m = 1,2. The exact soltuions were again generated by assuming dipole
and quadrapole sources located at $(\rho, z) = (0,0)$.

Based on the above results our numerical and programming techniques are
capable of yielding reliable results for arbitrary geometries and boundary
conditions. At higher frequencies, (ka > 5) it appears that more points
must be taken to increase the accuracy of the computed results.

IV. Summary and Conclusions

An integral solution of the Helmholtz equation is developed for use in acoustic radiation problems. Unlike the classical formulation which can lead to integral equations that do not have unique solutions at frequencies corresponding to certain internal eigenfrequencies of the region enclosed by the surface under consideration, the formulation used in this study is valid at all frequencies. Also, unlike most current methods and formulations it is straight forward to implement regardless of how complicated the surface or the boundary conditions may be. The surface potentials computed numerically for a sphere and cylinder using 20 subintervals along the perimeter and for an inlet configuration with 53 subintervals are accurate to within ten per cent for nondimensional wave numbers ka of from one to ten where k is the wave number and a is the characteristic length. For discontinuous boundary conditions, the numerical and exact values are in agreement to within 10 per cent for ka < 5. At higher frequencies the results are as much as 40 per cent in error at points of discontinuity which suggests taking more points in evaluating the integral equation to increase the accuracy when discontinuous boundary conditions are specified. Increasing the number of subintervals decreases the error proportionately. At distances greater than the numerical integration stepsize, the far field results are at least as accurate as the corresponding surface potential solutions.

Acknowledgement

References

1. Burton, A. J., "The Solution of Helmholtz' Equation in Exterior Domains using Integral Equations," NPL Report NAC 30, National Physical Laboratory,

Teddington, Middlesex, Jan. 1973.

2.   Schenck, H. A., "Improved Integral Formulation for Radiation Problems,"
     Journal of the Acoustical Society of America. Vol. 44, No. 1, Jan.
     1968, pp. 41-58.

3.   Ursell, F., "On the Exterior Problems of Acoustics," Proceedings of
     the *Cambridge Philosophical Society*, Vol. 74, 1973, pp. 117-125.

4.   Burton, A. J. and Miller, G. F., "The Application of Integral Equation
     Methods to the Numerical Solutions of Some Exterior Boundary Value
     Problems," *Proceedings of the Royal Society of London*, A. 323, June,
     1971, pp. 201-210.

5.   W. L. Meyer, W. A. Bell, M. P. Stallybrass and B. T. Zinn, "Boundary
     Integral Solutions of Three Dimensional Acoustic Radiation Problems,"
     Journal of Sound and Vibration, Vol. 59, No. 2, July, 1978, pp. 245-262.

6.   Morse, P. M. and Ingard, K. U., *Theoretical Acoustics*, McGraw-Hill,
     New York, 1969, Chapter 7.

7.   Chertock, "Intergral Equation Methods in Sound Radiation and Scattering
     from Arbitrary Surfaces," David W. Taylor, Naval Ship Research and
     Development Center Report 3538, June, 1971.

8.   Stallybrass, M. P., "On a Pointwise Variational Principle for the Approxi-
     mate Solution of Linear Boundary Value Problems," *Journal of Mathematics
     and Mechanics*, Vol. 16, No. 11, May 1967, pp. 1247-1286.

9.   Chertock, G., "Sound Radiation from Vibrating Surfaces," *Journal of the
     Acoustical Society of America*, Vol. 36, No. 7, July 1964, pp. 1305-1313.

10. Bell, W. A., Meyer, W. L., and Zinn, B. T., "Predicting the Acoustics
     of Arbitrarily Shaped Bodies Using an Integral Approach," *AIAA Journal*,
     Vol. 15, No. 6, June 1977, pp. 813-820.

11. Miller, B. A., Dastoli, B. J., and Worosky, H. L., "Effect of Entry-Lip Design on Aerodynamics and Acoustics of High-Throat-Mach-Number Inlets for the Quick, Clean, Short-Haul Experimental Engine," NASA TM X-3222, 1975.

Table I

Effect of the coupling parameter α on the computed values of the surface potential for a sphere. On the surface $A(Q) = (1-ik)e^{ik}$, $Y(Q) = 0$, $\varphi_{exact}^{(Q)} = -e^{ik} =$ constant, $m = 0$. All values of ka correspond to internal eigenfrequencies. Twenty subintervals were taken in the $\rho-z$ plane.

α \\ ka		0	i/k	i	EXACT
π	φ_r	2.0	1.000	0.998	1
	φ_i	-6.3	0.001	-0.012	0
4.493409	φ_r	0.190	0.217	0.308	0.217
	φ_i	0.979	0.976	0.955	0.976
2π	φ_r	-2.0	-1.000	-0.996	-1
	φ_i	12.6	0.000	0.031	0
7.725252	φ_r	-0.081	-0.128	-0.400	-0.128
	φ_i	-0.994	-0.992	-0.872	-0.992
3π	φ_r	2.0	1.000	0.995	1
	φ_i	-19.0	0.000	-0.050	0

Table II

Effect of specifying an admittance on the computed surface potential for a sphere. In all cases $m = 0$, twenty subintervals are taken in the $\rho - z$ plane, and $\varphi_{exact} = -e^{ik}$ everywhere on the surface. For Case I, $A(Q) = e^{ik}$ and $Y(Q) = ik$ everywhere on the surface. For case III, $A(Q) = e^{ik}(1-ik)$ and $Y(Q) = 0$ over 1/5 of the surface and $A(Q) = 0$, $Y = -(1-ik)$ over the remainder. Case II is considered in Table I.

ka		CASE I $\alpha = i/k$	CASE I $\alpha = 0$	CASE II $\alpha = i/k$	CASE III $\alpha = i/k$	EXACT VALUES
1	φ_r	-0.539	-0.537	-0.538	-0.52	-0.540
	φ_i	-0.845	0.849	-0.843	-0.87	-0.842
2	φ_r	0.418	0.422	0.417	0.43	0.416
	φ_i	-0.911	-0.937	-0.909	-0.92	-0.909
3	φ_r	0.993	0.916	0.990	1.00	0.990
	φ_i	-0.142	-0.496	-0.140	-0.16	-0.141
5	φ_r	-0.285	-0.288	-0.284	-0.25	-0.284
	φ_i	0.961	1.145	0.959	1.00	0.959
10	φ_r	0.841	-0.3	0.839	0.90	0.839
	φ_i	0.546	0.9	0.544	0.49	0.544
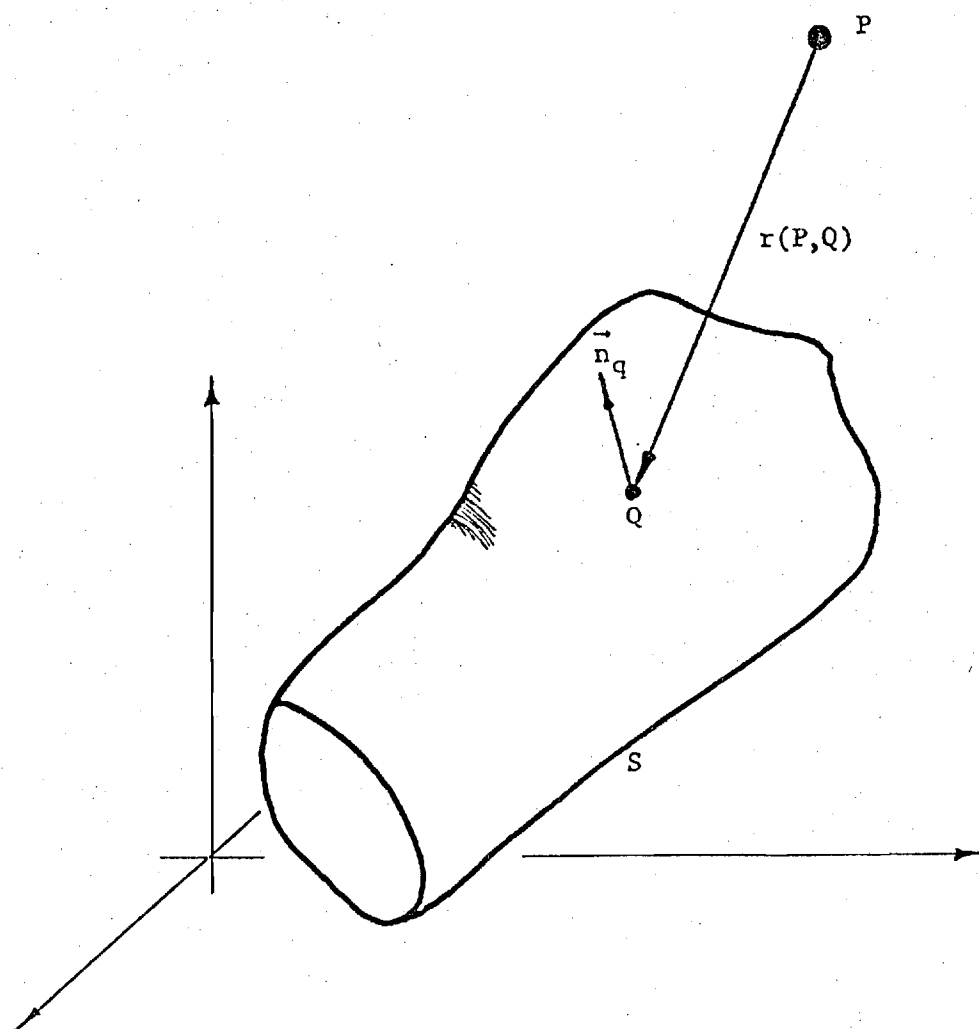
Figure 1. Geometrical Properties of the General
Acoustic Radiation Problem.

Figure 2. Cylindrical Surface Geometry

|φ|

1.4

1.2

1.0

0.8

0.6

0   2   4   6   8   10
k

α
1/k   ◯
0   □
i   △
EXACT —
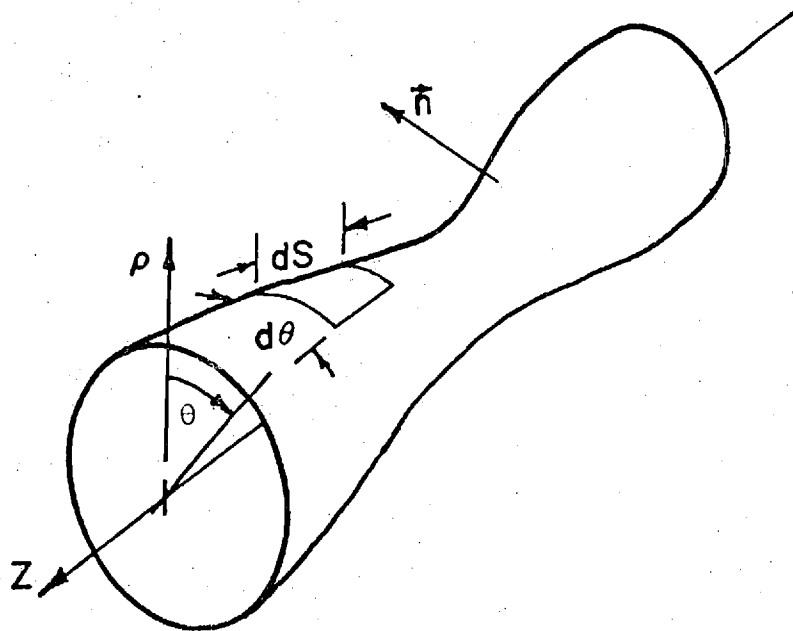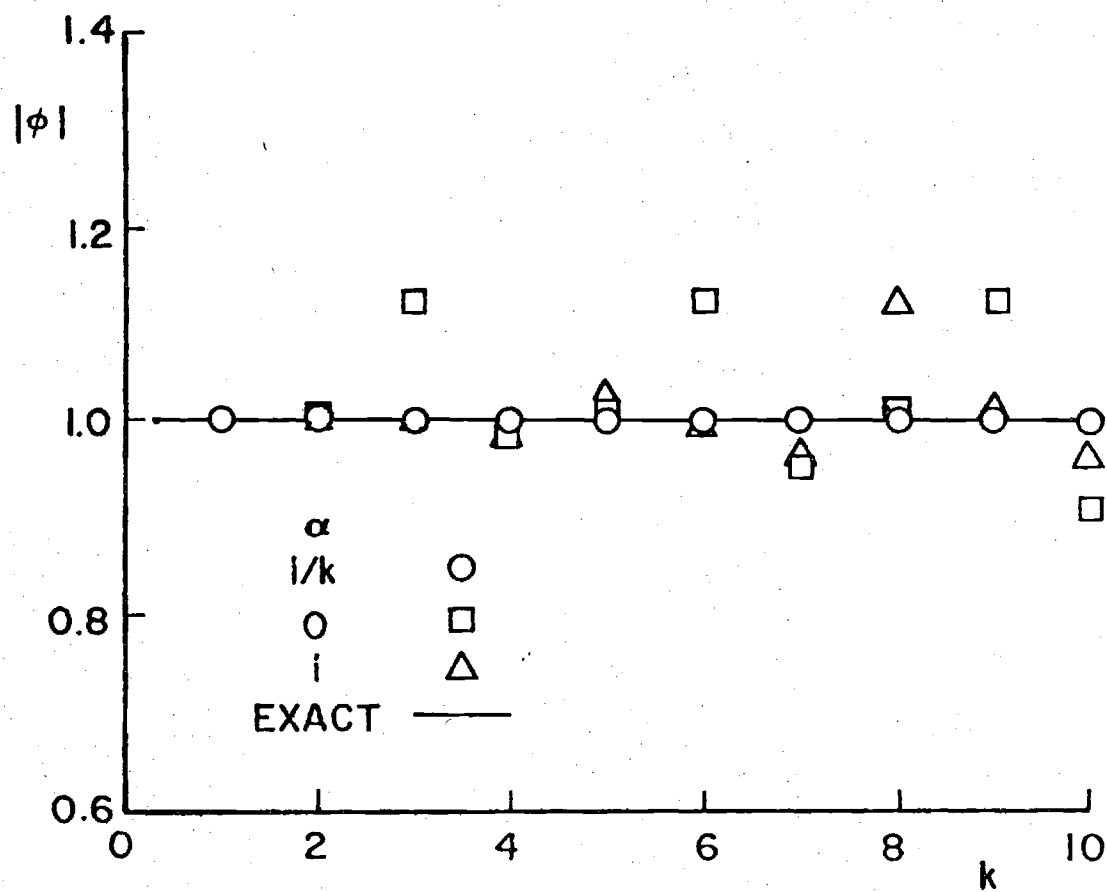
Figure 3. Effect of the Coupling Constant on the Computed
Surface Potential for a Sphere of Unit Radius with
20 Subintervals.
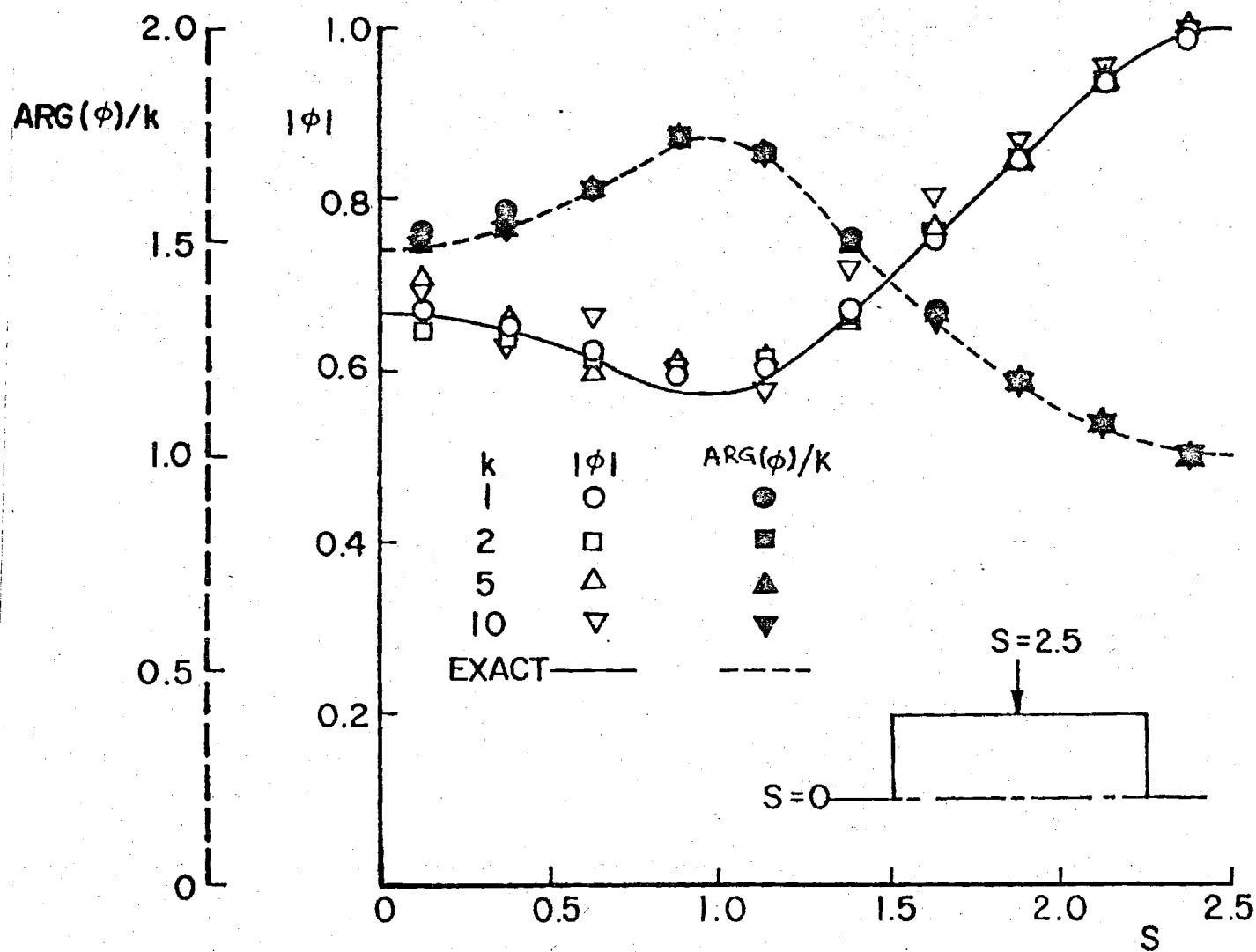
Figure 4. Dependence of the Computed Surface Potential
for a Finite Cylinder with a Zero Admittance
and Nonzero Normal Velocity Everywhere on the
Surface for 20 Subintervals, $\alpha = i/k$.
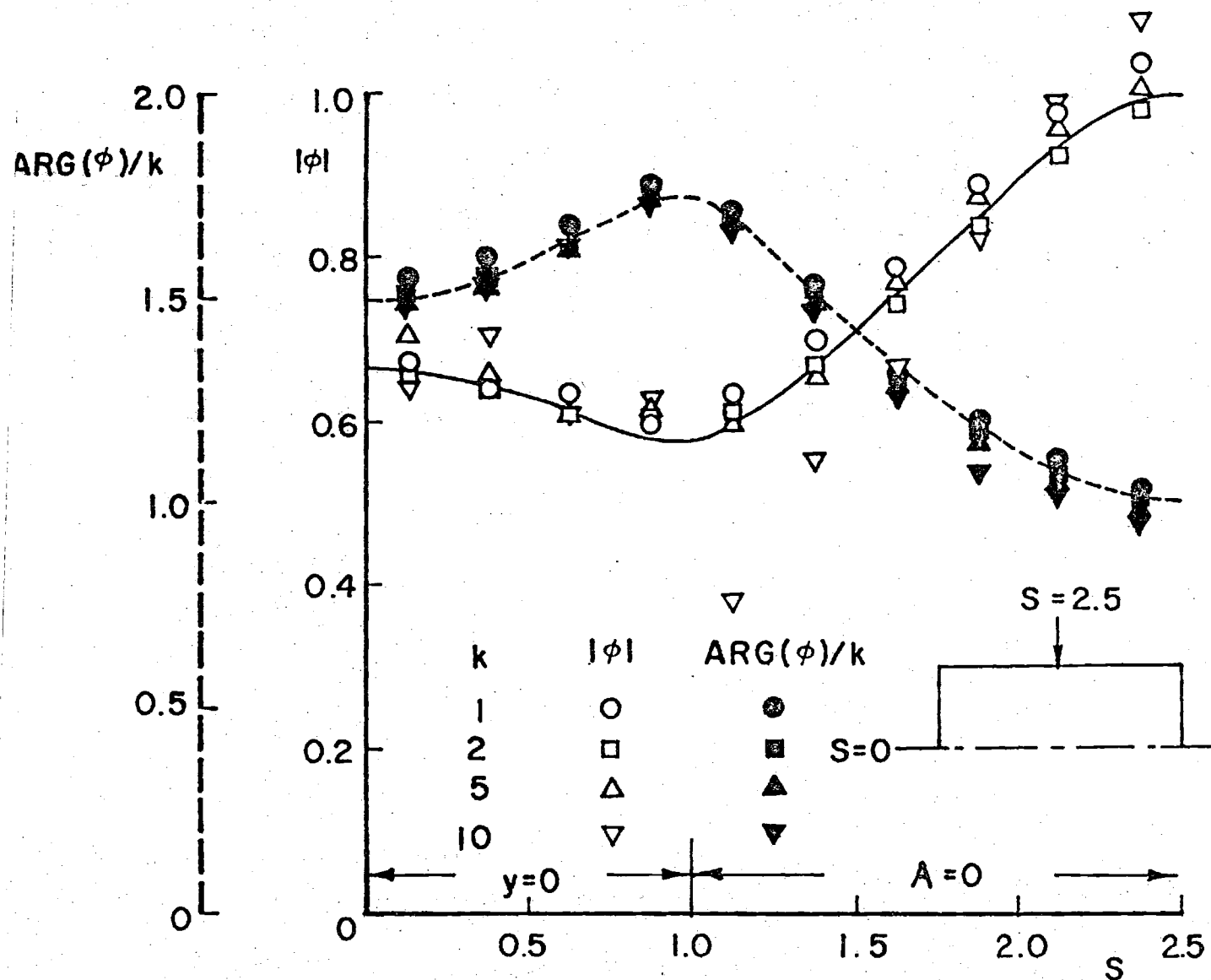
Figure 5. Effect of Discontinuous Boundary Conditions on the Accuracy of the Computed Surface Potential for a Cylinder, $\alpha = i/k$.
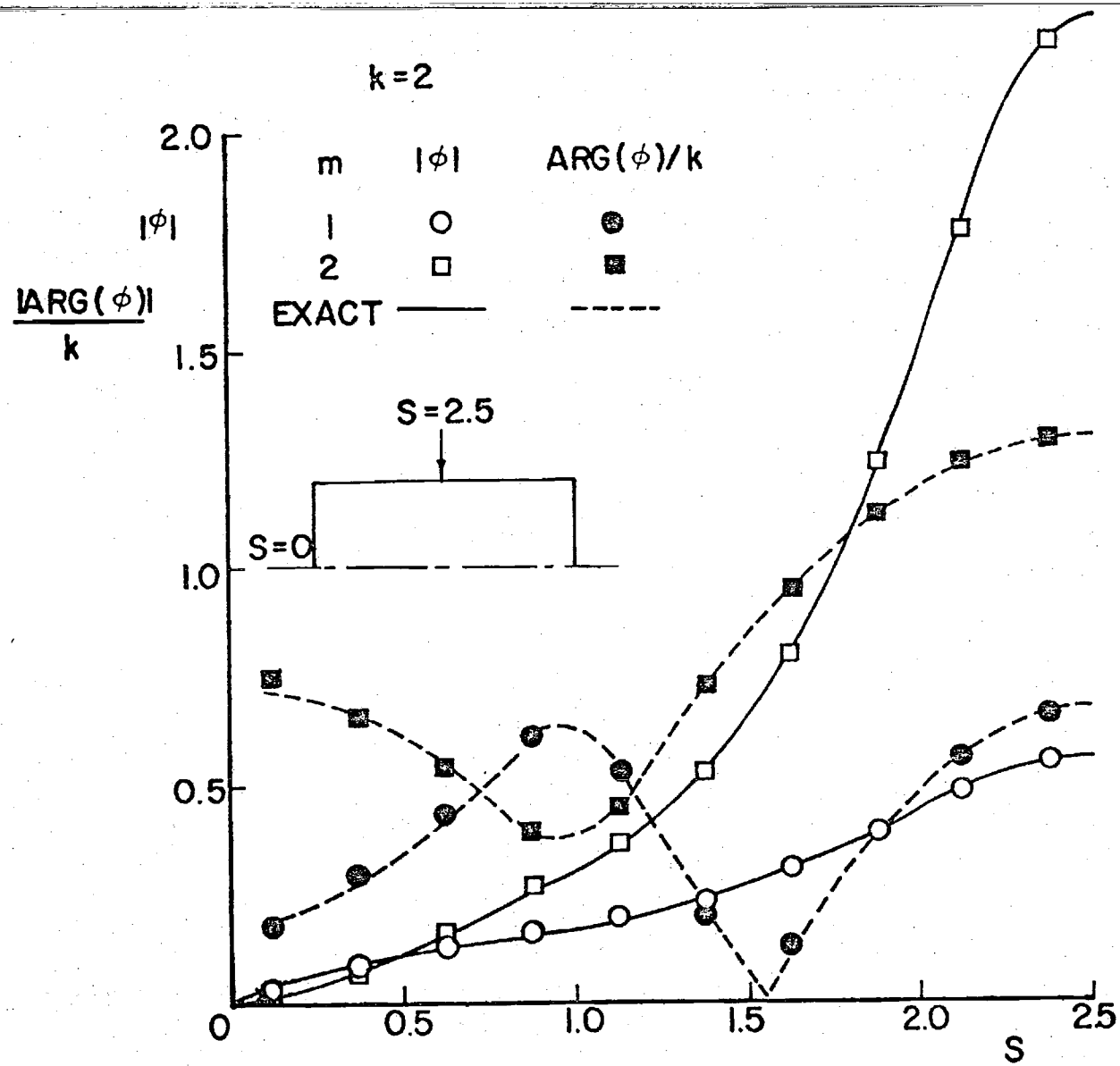
Figure 6. Computed Surface Potential for a Cylinder at the First and Second Tangential Modes for ka = 2.
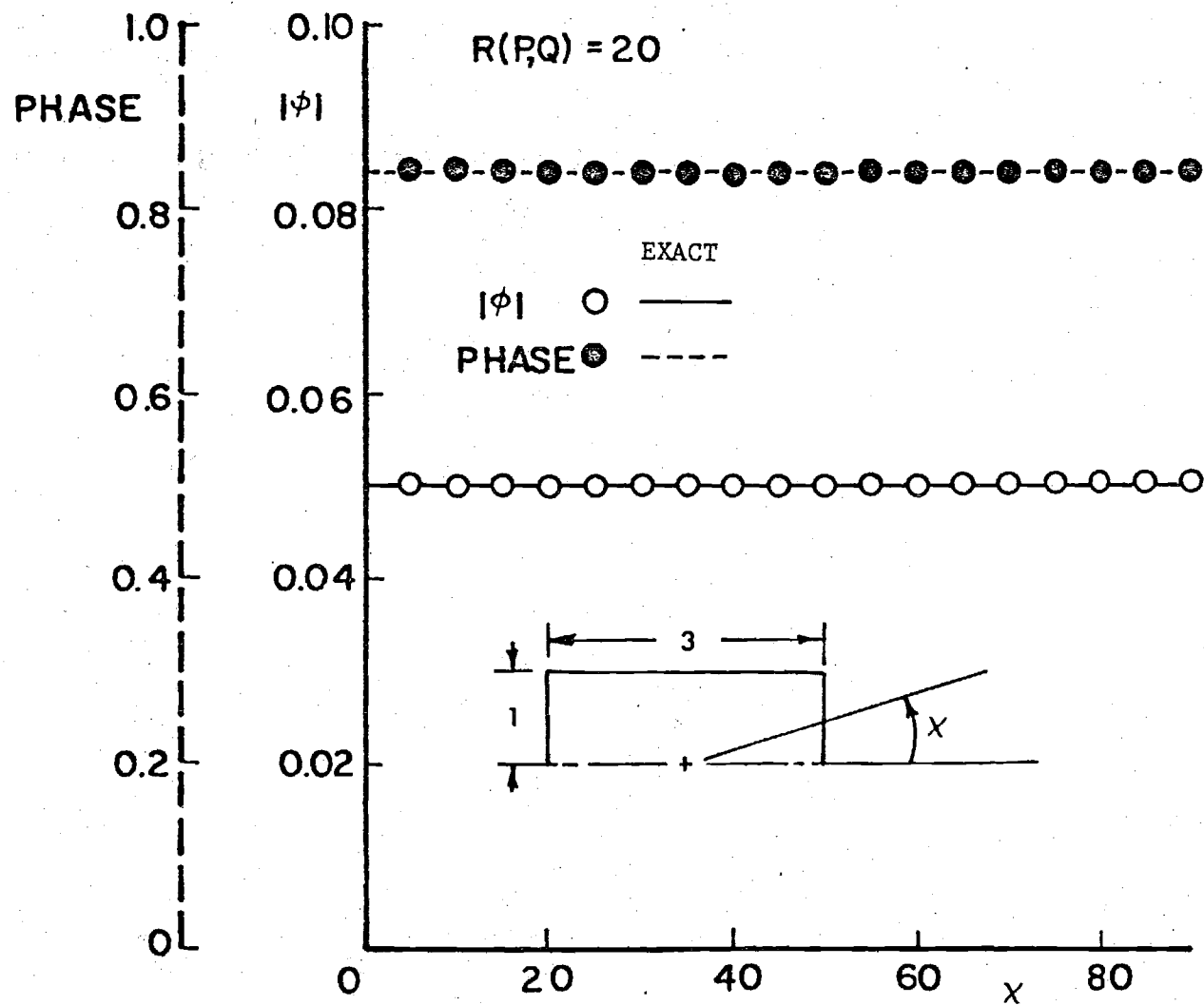
Figure 7. Computed Far Field Potential Distribution for a Cylinder at k = 2, m = 0, and 20 Radii from the Center.
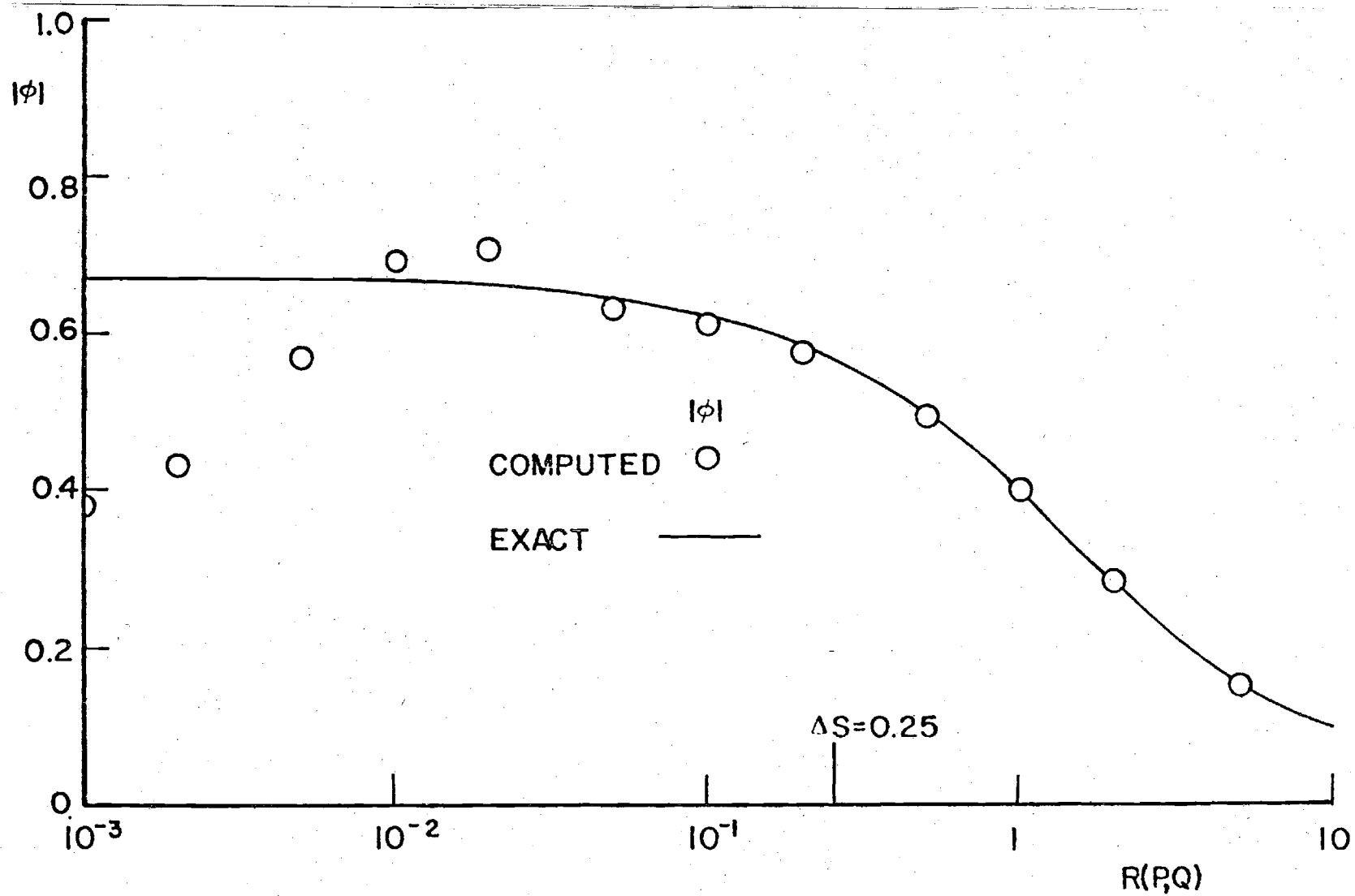
Figure 8. Dependence of the Accuracy of the Computed Far Field Solution of a Cylinder upon the Distance from the Surface for k = 2 and m = 0.

EXTERIOR CONTOUR

SPHERE

INTERIOR CONTOUR

ENTRANCE
TO FAN
SECTION

CENTER
BODY
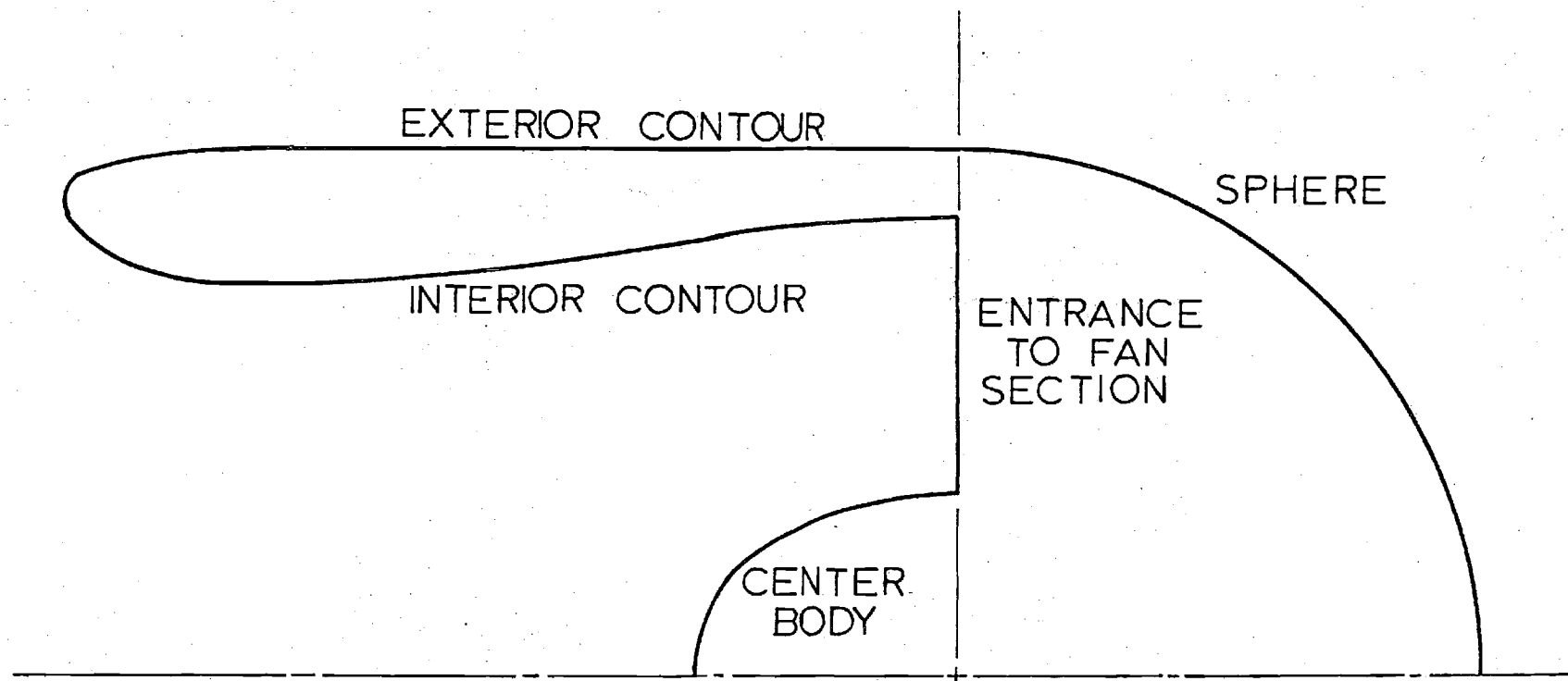
Figure 9. Inlet Geometry.
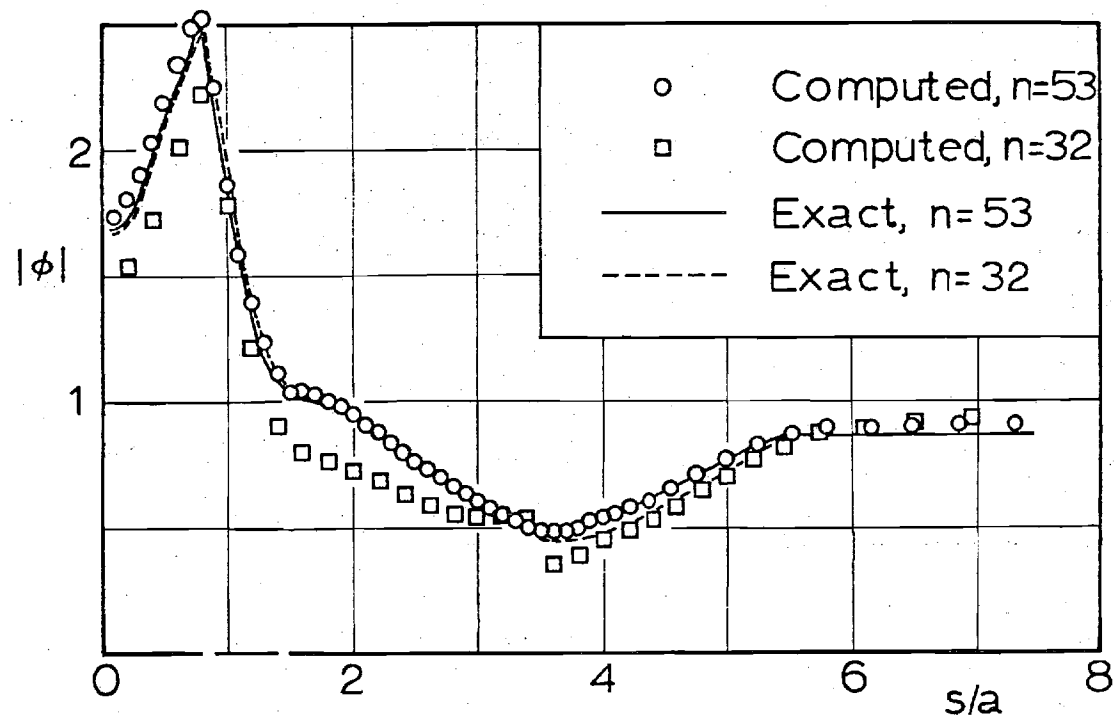
Figure 10. Effect of Increasing the Number of Subintervals
in Computing the Surface Potential for the Inlet
Configuration at ka = 1, m = 0.
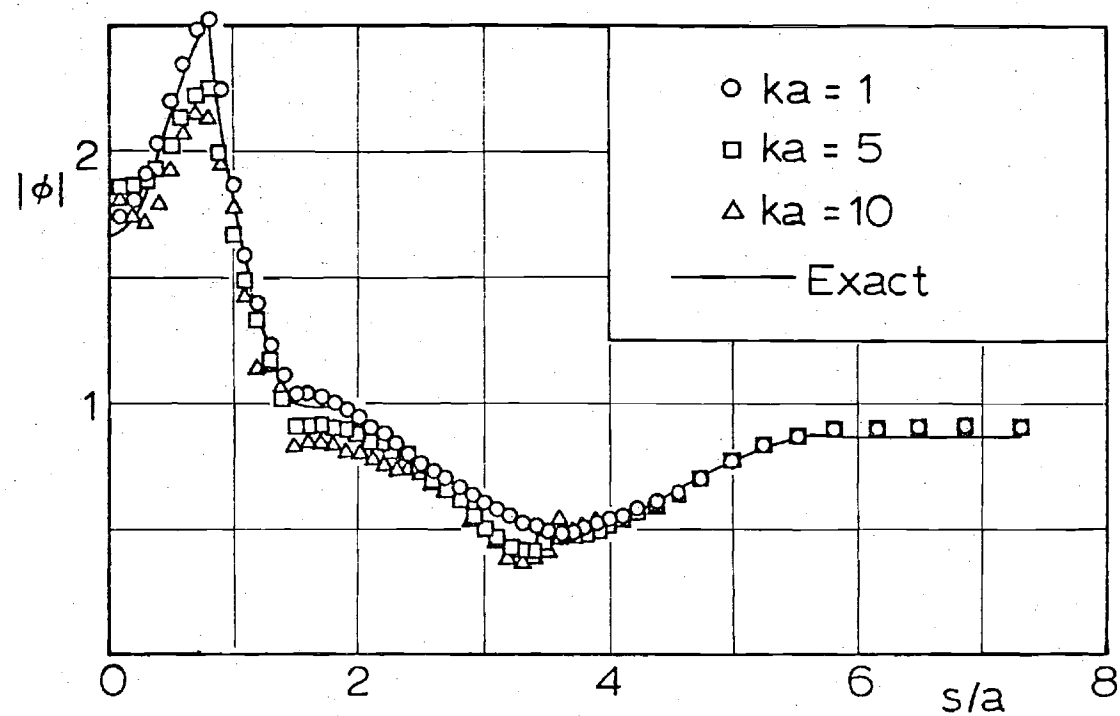
Figure 11. Effect of Increasing Frequency for the Inlet Configuration at m = 0, n = 53 on the Computed Surface Potential.
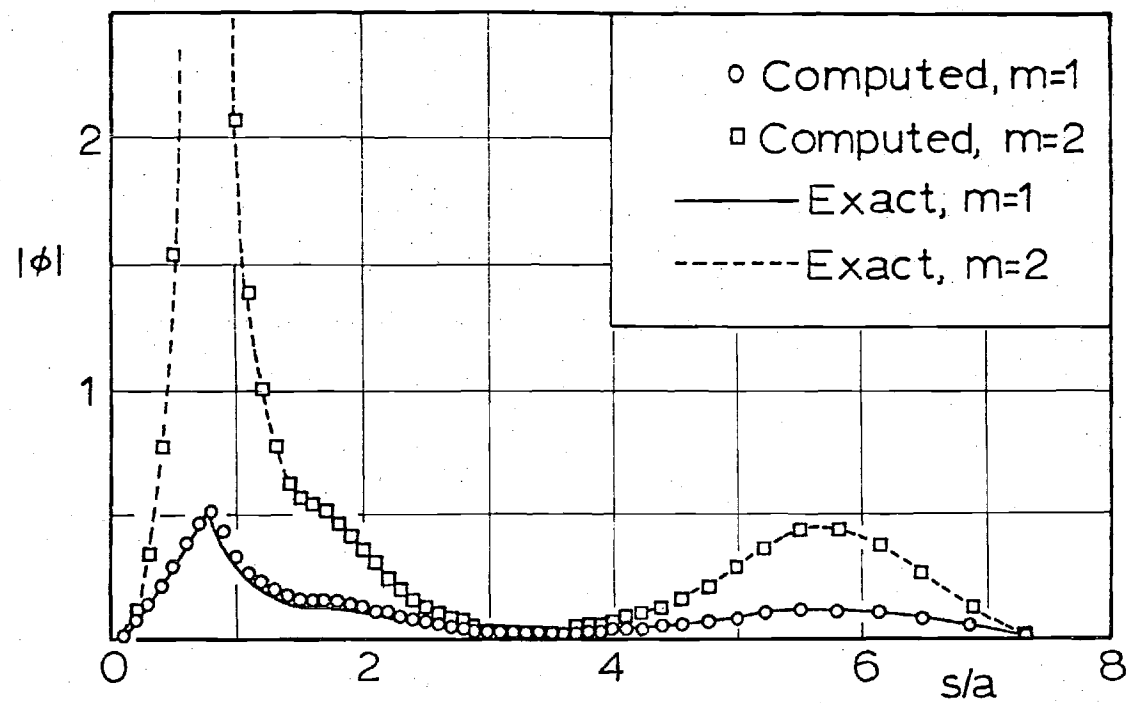
Figure 12. Effect of Mode Number m on the Computed Surface
Potential of the Inlet Configuration for ka = 2
and n = 53.

Appendix C

Paper presented at the AIAA 5th Aeroacoustics Conference in Seattle, Washington, March 12-14, 1979, AIAA Paper No. 79-0675

"Sound Radiation From Finite Length Axisymmetric Ducts and Engine Inlets"
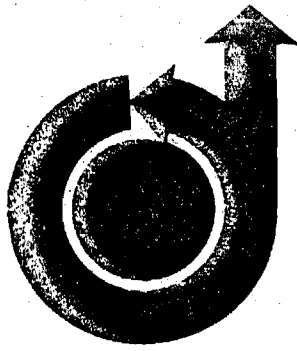
79-0675
Sound Radiation from Finite
Length Axisymmetric Ducts and
Engine Inlets
W.L. Meyer, W.A. Bell and B.T.
Zinn, Georgia Institute of
Technology, Atlanta, Ga.

AIAA 5th AEROACOUSTICS
CONFERENCE
Seattle, Washington—March 12-14, 1979

SOUND RADIATION FROM FINITE LENGTH AXISYMMETRIC DUCTS AND ENGINE INLETS[*]

W. L. Meyer[**], W. A. Bell[†], and B. T. Zinn[‡]

School of Aerospace Engineering
Georgia Institute of Technology
Atlanta, Georgia 30332

Abstract

Results are obtained by numerical integration of a cylindrically symmetric integral representation of the exterior solutions of the Helmholtz equation which is valid (yields unique solutions) at all wavenumbers. The admittance values across the entrance plane of hard walled ducts of various lengths and geometries are computed and compared with certain "classical" (e.g., Weiner-Hopf) values. The internal wave structure is also investigated for straight hard walled ducts and compared with results obtained from other theories. The radiated sound fields from ducts of different geometries are then compared for both unlined and lined configurations. It is found that changes in the duct geometry result in significant changes in the radiated sound field. Thus, it is concluded that the sound suppression by liners predicted from the study of straight ducts may not be applicable to more complicated geometries such as inlet configurations.

Introduction

The development of an analytical method for predicting the sound field radiated from axisymmetric, finite length ducts is of much practical interest in the area of aeroacoustics, especially for the determination of the sound radiated from a turbofan inlet, as having such a capability can eliminate most of the costly full scale testing presently required. In a majority of past investigations of the sound radiated from ducts, either the radiation problem has been completely ignored[1,2,3] or the duct acoustics and the radiation problem have been treated separately.[4,5,6] In these studies, the behavior of the waves inside the duct was determined by specifying some heuristic boundary condition (e.g., a reflection coefficient) at the duct entrance. In the latter references this solution was then used to determine the sound distribution at the entrance plane of the duct and this was used to predict the properties of the radiated sound field. In reality the sound fields inside and outside the duct are not separate entities (i.e., they are coupled) and, therefore, they cannot be properly treated separately. These "separate" treatments of the interior and exterior sound fields in the duct radiation problem undoubtedly introduce errors whose determination requires comparison with available exact solutions.

In this paper the duct sound radiation problem is investigated by utilizing an integral solution[7,8] that considers the combination of the interior and exterior sound fields to be a single entity, thus eliminating the errors associated with many of the previously used approaches. Comparison of the solutions obtained using this method with exact solutions[9] and with those of related investigations should shed some light upon the applicability of the analytical approaches utilized in these other investigations.

The solution approach utilized in this study consists of the numerical solution of a special integral representation of the solutions of the Helmholtz equation for an exterior (i.e., to a given body) domain. The applicability and accuracy of this solution approach have been demonstrated for two dimensional[10,11], three dimensional[8,12], and axisymmetric[9,13] geometries in earlier investigations conducted under this program where it has been shown that the developed approach yields unique solutions at all wavenumbers.

Solution Procedure

The basis of this method is set forth in great detail in Ref. 14 and therefore will not be repeated here. In related studies conducted under this AFOSR program the applicability of this approach to the solution of acoustics problems involving two dimensional, three dimensional, and axisymmetric geometries has been demonstrated. Since the analytical developments and results of these studies have been published elsewhere[7,8,9], they also will not be repeated here. Instead, some of the advantages of this solution approach will be presented. First, as stated earlier, this method treats the duct radiation problem consisting of the sound generation, sound propagation and reflection, and the sound radiation to the outside as a whole without separating it into its component parts as has been done in related investigations. Second, the method can readily handle the infinite domains encountered in radiation problems. This is accomplished by employing a fundamental solution $G(P,Q)$ which satisfies the Sommerfield radiation conditions in the integral equation. In the present study the free space Green's function has been used:

$$G(P,Q) = \frac{e^{ikr(P,Q)}}{r(P,Q)} \qquad (1)$$

where, as shown in Fig. 1, Q is a point on the surface of the body S, P is a point in the exterior domain, r(P,Q) is the distance between these points, and k is the wavenumber. The third advantage is that the computer program developed in a related investigation[9,13] is quite general and is applicable to a variety of acoustic radiation problems involving arbitrary geometries and variable boundary conditions. This computer program can be applied to different problems by merely changing the input data.
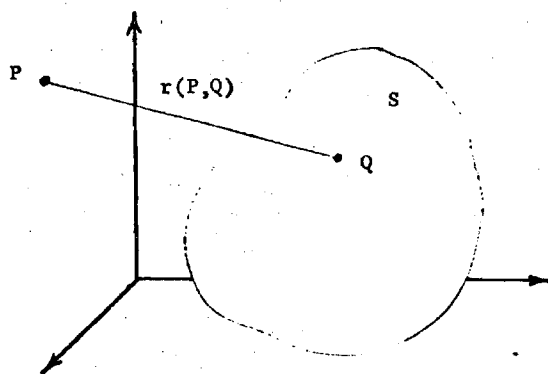
1

Fig. 1. General Geometry of the
Radiation Problem.

It has been shown in Ref. 8 that unique solutions of the external acoustic radiation problem can be obtained at all wavenumbers by solving the following integral equation:

$$\int\int_S (\varphi(Q)\,\frac{\partial G(P,Q)}{\partial n_q} - G(P,Q)\,\frac{\partial \varphi(Q)}{\partial n_q})\,dS_q$$

$$+ \alpha \int\int_S (\varphi(Q) - \varphi(P))\,\frac{\partial^2 G(P,Q)}{\partial n_p \partial n_q}\,dS_q$$

$$(2)$$

$$- \alpha\,\varphi(P)\int\int_S (\vec{n}_p\cdot\vec{n}_q)(ik)^2\,G(P,Q)\,dS_q$$

$$- \alpha\int\int_S \frac{\partial \varphi(Q)}{\partial n_q}\,\frac{\partial G(P,Q)}{\partial n_p}\,dS_q = 2\pi(\varphi(P)+\alpha\frac{\partial\varphi(P)}{\partial n_p})$$

where, as shown in Fig. 2, the point P has been moved to the surface of the body S, $\vec{n}$ represents an external normal from the body, $\frac{\partial}{\partial n}$ represents a normal derivative $(\vec{\nabla}\cdot\vec{n})$, and α is a complex coupling constant.
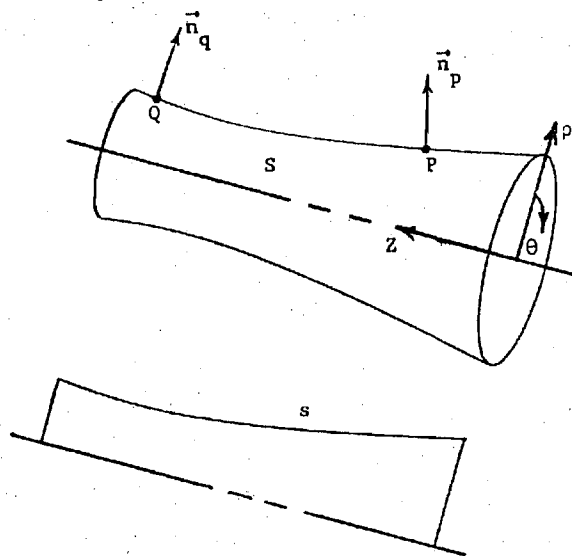
Fig. 2. General Axisymmetric Geometry
and 2-D Projection.

It is shown in Ref. 9 that maximum accuracy is obtained when $\alpha = i/k$. In its present form, Eq. (2) contains no non-integrable singularities, a fact which considerably simplifies its numerical solution. Thus the solution of the entire duct radiation problem has been reduced, with the present formulation, to that of the solution of a surface integral over the body S.

The problem is further simplified in the present study by limiting attention to axisymmetric configurations. In this case Eq. (2) is further reduced to[9]

$$\int_0^\ell \Phi(Q)\,\{K_1(P,Q) + K_2(P,Q)\}\,ds_q$$

$$- \Phi(P)\int_0^\ell \{F_1(P,Q) + F_2(P,Q)\}ds_q$$

$$(3)$$

$$- \int_0^\ell V(Q)\,\{I_1(P,Q) + I_2(P,Q)\}\,ds_q$$

$$= 2\pi\{\Phi(P) + \alpha\,V(P)\}$$

where s is the distance along the 2-D projection of the body in the ρ-z plane (i.e., See Fig. 2), and the influence functions I_1 and I_2 are given by

$$I_1(P,Q) = 2\int_0^\pi G(P,Q)(\cos m\,\theta_q)\,d\theta_q$$

$$(4)$$

$$I_2(P,Q) = 2\alpha\int_0^\pi \frac{\partial G(P,Q)}{\partial n_p}(\cos m\,\theta_q)\,d\theta_q$$

the kernel functions K_1 and K_2 are

$$K_1(P,Q) = 2\int_0^\pi \frac{\partial G(P,Q)}{\partial n_q}(\cos m\,\theta_q)\,d\theta_q$$

$$(5)$$

$$K_2(P,Q) = 2\alpha\int_{0+}^\pi \frac{\partial^2 G(P,Q)}{\partial n_p \partial n_q}(\cos m\,\theta_q)d\theta_q \quad \theta_q \neq \theta_p$$

the forcing functions F_1 and F_2 are

$$F_1(P,Q) = 2\alpha\int_0^\pi G(P,Q)(ik)^2(\vec{n}_p\cdot\vec{n}_q)d\theta_q$$

$$(6)$$

$$F_2(P,Q) = 2\alpha\int_0^\pi \frac{\partial^2 G(P,Q)}{\partial n_p \partial n_q}\,d\theta_q \quad \theta_q \neq \theta_p$$

and

$$\frac{\partial\varphi}{\partial n} = V\cos m\,\theta$$

$$(7)$$

$$\Phi = \frac{\varphi}{\cos m\,\theta}$$

following the notation of Ref. 15. In the above notation m is the tangential mode and θ_p has been taken as zero (i.e., $\cos m\,\theta_p = 1$).

Introducing axisymmetry further simplifies the solution of Eq. (2) to the evaluation of line integrals on the 2-D projections of the body S in the ρ-Z plane as shown in Fig. 2. Also, the formulation is valid for all tangential modes; however, each mode must be solved for separately.

The required solution is obtained by solving Eq. (3) for the surface distribution of the acoustic potential ϕ or the normal acoustic velocity V, whichever is unknown. Also, solutions can be obtained for ϕ by using an effective admittance, defined as $Y = V/\phi = \partial \phi / \partial n / \phi$, as a boundary condition over any part of the surface of the body (e.g., replace V by ϕY in Eq. (3) at the points where Y is known on the body.).

Once the surface distributions of the acoustic potential and the normal acoustic velocity are known on the surface of the body, the radiated sound field can be determined using the following integral representations[14] for φ and $\frac{\partial \varphi}{\partial n}$ in the field:

$$\int \int_S (\varphi(Q) \frac{\partial G(P,Q)}{\partial n_q} - G(P,Q) \frac{\partial \varphi(Q)}{\partial n_q}) dS_q = 4\pi \varphi(P) \tag{8}$$

and

$$\int \int_S (\varphi(Q) \frac{\partial^2 G(P,Q)}{\partial n_p \partial n_q} - \frac{\partial G(P,Q)}{\partial n_p} \frac{\partial \varphi(Q)}{\partial n_q}) dS_q = 4\pi \frac{\partial \varphi(P)}{\partial n_p} \tag{9}$$

where the point P is now located in the space surrounding the body (i.e., See Fig. 1) so that the kernel functions are no longer singular. For axisymmetric bodies, Eqs. (8) and (9) reduce to:

$$\int_0^{\ell} (\phi(Q) K_1(P,Q) - I_1(P,Q) V(Q)) ds_q = 4\pi \phi(P) \tag{10}$$

and

$$\int_0^{\ell} (\phi(Q) K_2(P,Q) - I_2(P,Q) V(Q)) ds_q = 4\pi V(P) \tag{11}$$

Results

In the present investigation, the integral solution technique has been utilized to study the dependence of the radiated sound field and the acoustic characteristics of the duct upon the duct geometry and the acoustic properties of the duct wall. This investigation has been carried out with the objective of evaluating the dependence of the sound field from a jet engine inlet on the inlet characteristics, and to evaluate the validity of the analytical approaches and assumptions utilized in related investigations. First, the effect of the length of the duct on the admittance values at the entrance plane of the duct was investigated. The purpose of this study was not only to show the effect of changing the L/a (i.e., length/radius) of the duct but also to show that the admittance is not a constant across the entrance plane. This is significant as many investigations of similar and related problems assume the existence of a constant "reflection coefficient" at this plane. Therefore, the effect of the radiated sound field on the duct acoustics cannot be properly accounted for. Second, the effect of the internal geometry of the duct on the radiated sound field was investigated. This was done to show that changes in the internal geometry of the duct result in large changes in the admittance values at the duct entrance and, therefore, in

large changes in the radiated sound field; a fact which is often ignored in related studies. Third, the internal wave structure in the duct was investigated to show that this integral solution technique can predict both the internal and external sound fields. In this connection it should be pointed out again that this solution technique automatically accounts for the coupling effects between the internal and external sound fields. Fourth, the radiated sound fields for two, dimensionally similar, acoustically lined duct configurations (i.e., a straight duct and an engine inlet) are compared to show that optimum admittance values for liners, determined from the study of their effectiveness in a straight duct, do not necessarily carry over to the more complicated inlet configurations.

In this study, the surface distributions of the unknowns of the problem (i.e., the acoustic potential and/or the normal acoustic velocity) are obtained from the numerical solution of Eq. (3). Since the unknown functions $\phi(Q)$ or $V(Q)$ appear in the integrands, it is necessary to solve a square matrix; thus, the required computing time increases roughly as the square of the number of points taken on the surface of the body S. In a typical run on the Georgia Tech CDC Cyber 70/74 computer, 140 seconds of computing time were required to solve for the surface values of either ϕ or V at 53 points on the body.

To obtain values for ϕ and V in the far field, Eqs. (10) and (11) are solved by simple numerical integration. The time required for this computation is roughly proportional to the number of points in the field and the number of points on the body. In a typical run, 70 seconds of computing time was required to calculate both ϕ and V at 57 points in the field with 53 points on the body.

To determine the dependence of the admittance at the duct entrance plane on the duct length, these admittance values were computed for hard walled straight ducts having different L/a values, as shown in Fig. 3.
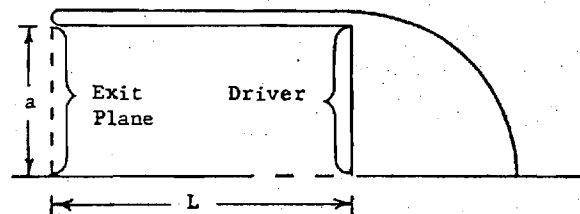
Fig. 3. Geometry Used for Straight Duct Computations.

In this case, driving consisted of a unit acoustic velocity (V = 1) across the driver face. The computed admittance values at the duct entrance plane are plotted for two non-dimensional wavenumbers (i.e., ka = 1 and 3) in Figure 4. Also noted for comparison are the "classical" values for flanged[16] and unflanged[17] pipes. These results indicate that even for plane wave sound excitation the admittance at the duct entrance plane varies with the trans-

verse dimension but it does not depend upon the ducts length-to-radius ratio, at least for the investigated range of L/a and ka values.
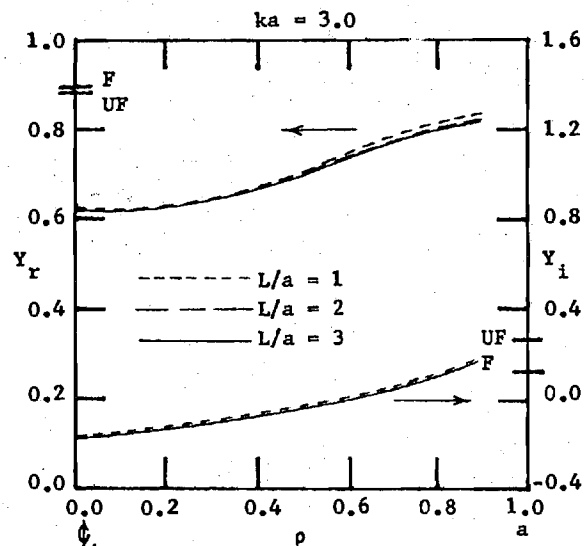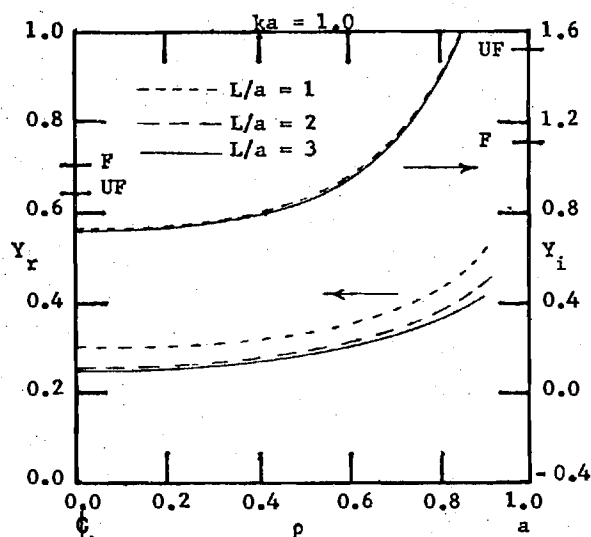

Fig. 4. Admittance at the Exit Plane of a Straight Duct with the Classical Values for Flanged and Unflanged Pipes.

Fig. 5. Inlet Geometry (L/a = 2)

To determine geometrical effects, the admittance at the entrance plane of a hard walled inlet configuration[18] (i.e., See Fig. 5.), with L/a = 2 was also calculated assuming the same type of source excitation for comparison. These results are plotted in Figure 6. When compared with the corresponding results for a straight duct of the same basic dimensions (See Fig. 4.) it is seen that the admittance values change significantly. This is but one indication of the importance of the need to properly account for the internal geometry of the duct when investigating duct radiation problems.

The internal wave structure was also investigated for two hard walled, straight ducts to determine its dependence upon the characteristics of
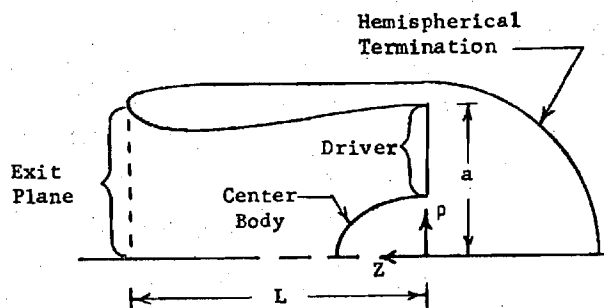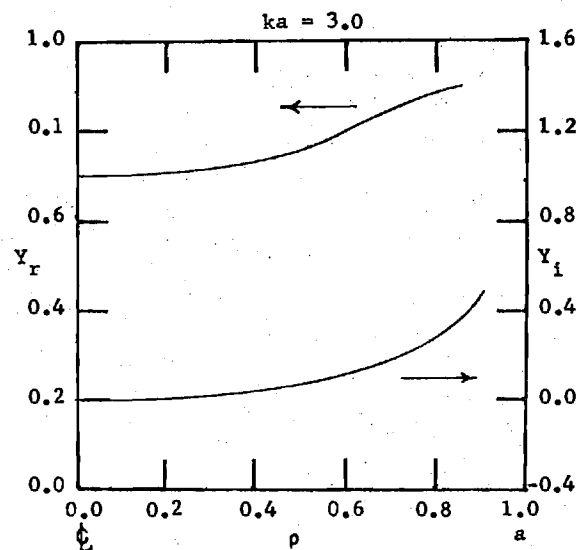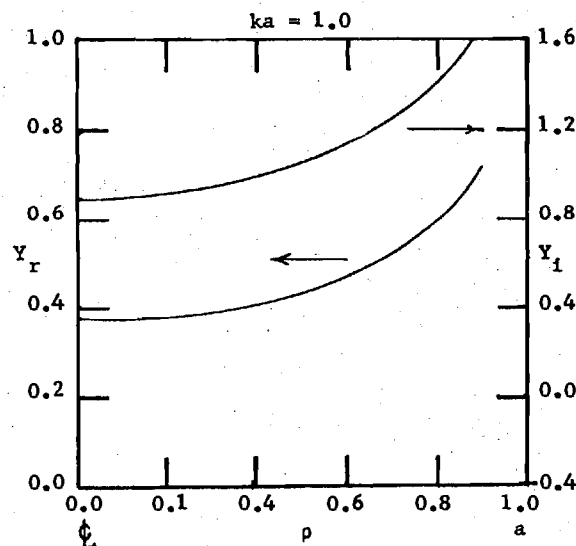

Fig. 6. Admittance at the Exit Plane of the Inlet (L/a = 2)

4

the sound source. The results are presented in
Fig. for two different drivers, one having a
constant unit normal acoustic velocity (i.e., V=1)
and the other a cosine distribution (i.e., V=cos
($\pi\rho$) where $0 \leq \rho \leq 1$), at the sound source plane,
for the case where ka = 1and m (the tangential mode
number) equals zero. These results show that the
difference between the sound sources quickly dis-
appear with increasing distance from the source
plane, as expected for low values of the non-dimen-
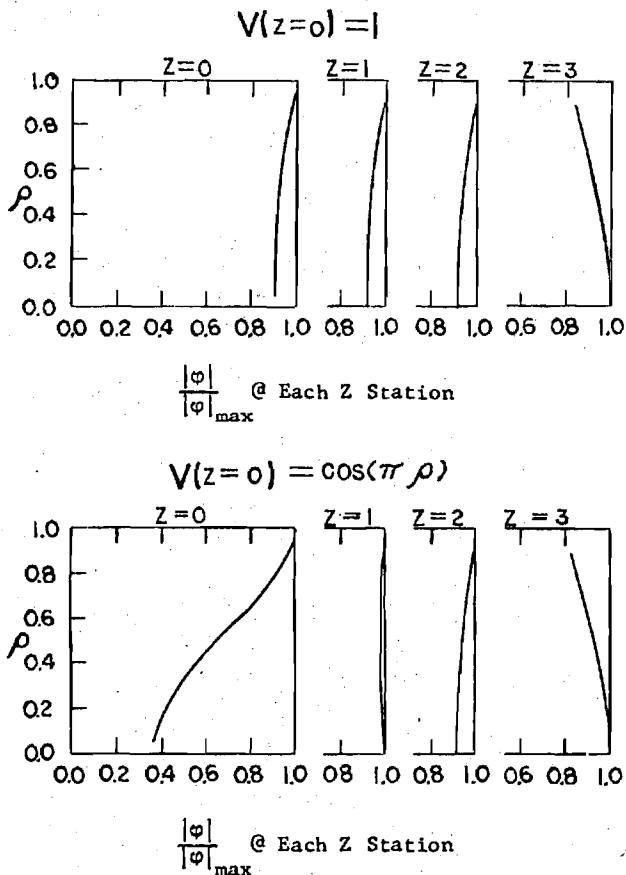sional wavenumber ka. The results for two additional cases are also presented;

$$V(z=0)=1$$

$$\frac{|\varphi|}{|\varphi|_{max}} \text{ @ Each Z Station}$$

$$V(z=0)=\cos(\pi\rho)$$

$$\frac{|\varphi|}{|\varphi|_{max}} \text{ @ Each Z Station}$$

Fig. 7. Radial Distributions of the Acoustic
Potential in a Hard Walled Straight
Duct (L/a = 3, ka = 1, m = 0)

$$V(z=0)=1$$

$$\frac{|\varphi|}{|\varphi|_{max}} \text{ @ Each Z Station}$$

$$V(z=0)=\cos(\pi\rho)$$

$$\frac{|\varphi|}{|\varphi|_{max}} \text{ @ Each Z Station}$$

Fig. 8. Radial Distribution of the Acoustic
Potential in a Hard Walled Straight
Duct (L/a = 3, ka = 3, m = 0)

in Fig. 8 the same two sound sound sources are used
for the higher wavenumber of ka = 2 while in Fig. 9
a sound source with a normal acoustic velocity dis-
tribution of V = sin ($\rho\pi$) and a tangential mode
number m = 1 is used. All of these results indicate,
in agreement with basic acoustics, that the finer
details of the sound source are "washed out" within
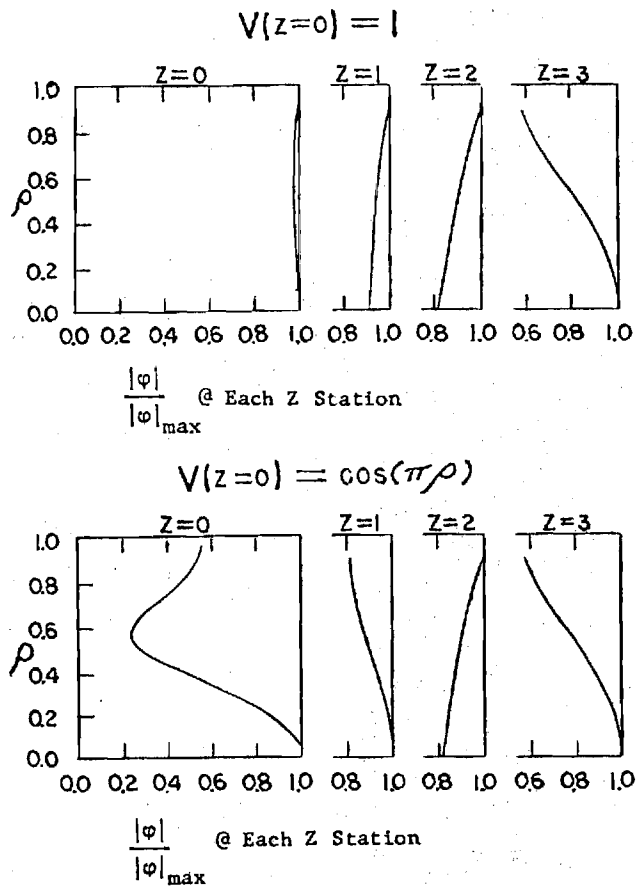a length on the order of ka from the sound source
plane.

Finally, the radiated sound fields from both a
straight duct and an inlet configuration were com-
puted and compared for both lined and unlined walls.
The values used for the wall admittances and the
wavenumbers were chosen to be the same as those
used by Zorumski in Ref. 19 so that comparisons
could be made. Two different liners were run; a
constant admittance liner and a segmented liner.
In the case of the straight duct the results do not
show the same difference in the radiated sound pres-
sure level between the segmented and constant ad-
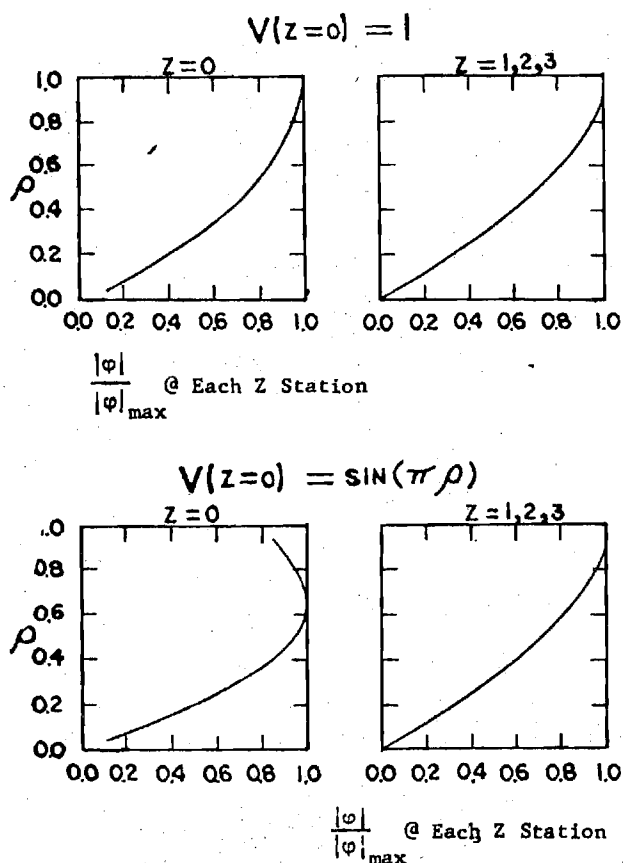mittance liners (See Fig. 10.) as did Zorumski (See
Fig. 11.).

5

$$V(z=0) = 1$$

$$\frac{|\varphi|}{|\varphi|_{max}} \text{ @ Each Z Station}$$

$$V(z=0) = \sin(\pi \rho)$$

$$\frac{|\varphi|}{|\varphi|_{max}} \text{ @ Each Z Station}$$

Fig. 9. Radial Distribution of the Acoustic Potential in a Hard Walled Straight Duct (L/a = 3, ka = 1, m = 1)

———————— Hard Wall
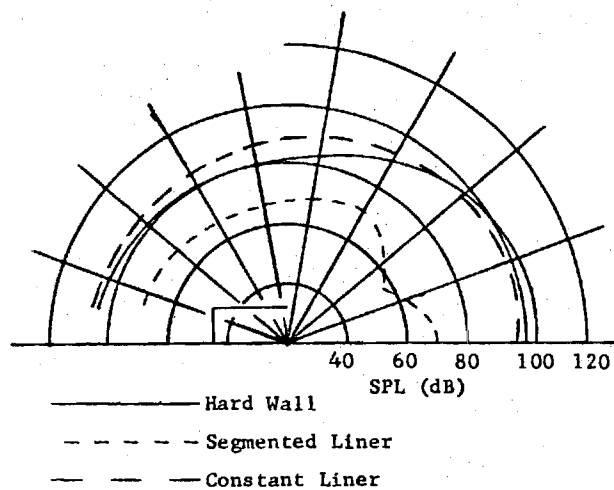
– – – – – Segmented Liner

— — — Constant Liner

Fig. 11. Far Field Radiation From A Straight Duct as Per Ref. 19 (L/a = 2).

To investigate the effect of geometry, the inlet configuration shown in Fig. 5 was run with the same two liners at the same non-dimensional wavenumbers. The opposite trends to those predicted by Zorumski were noted (See Fig. 12.); that is, that the segmented liner is superior to the constant admittance liner in reducing the radiated sound pressure levels. Thus, it is concluded that geometrical details can significantly affect the characteristics of the sound power radiated from dimensionally similar ducts (i.e., ducts having the same L/a ratios.).
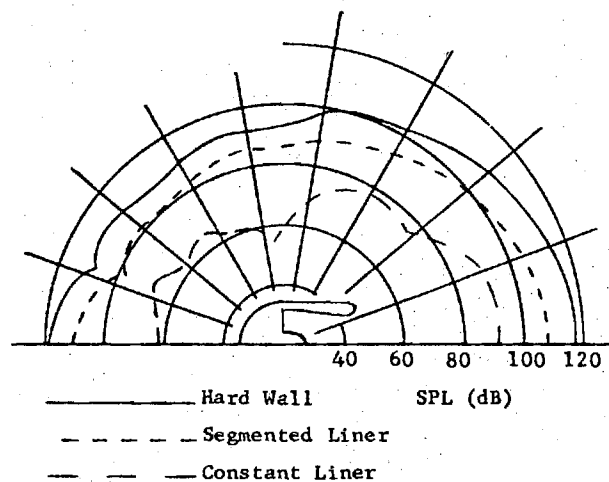

———————— Hard Wall

– – – – – Segmented Liner

— — — Constant Liner

Fig. 10. Far Field (50a) Radiation From A Straight Duct (L/a = 2).

———————— Hard Wall   SPL (dB)

– – – – – Segmented Liner

— — — Constant Liner

Fig. 12. Far Field (50a) Radiation From An Inlet (L/a = 2).

6

References

1.) Nayfeh, A. H., Kaiser, J. E., and Telinois, D. P., "Acoustics of Aircraft Engine-Duct Systems," AIAA Journal, Vol. 13, No. 2, pp. 130-153, February 1975.

2.) Tyler, J. M. and Sofrin, T. G., "Axial Flow Compressor Noise Studies," SAE Transactions, Vol. 70, pp. 309-332, 1962.

3.) Baumeister, K. J., "Finite-Difference Theory for Sound Propagation in a Lined Duct with Uniform Flow Using the Wave Envelope Concept," NASA Technical Paper 1001, Lewis Research Center, Cleveland, Ohio, August 1977.

4.) Plumblee, H. E., Dean, P. D., Wynne, G. A., and Burrin, R. H., "Sound Propagation in and Radiation from Acoustically Lined Flow Ducts: A Comparison of Experiment and Theory," NASA Contractor Report, NASA CR-2306, October 1973.

5.) Lansing, D. L. and Zorumski, W. E., "Effects of Wall Admittance Changes on Duct Transmission and Radiation of Sound," Journal of Sound and Vibration, Vol. 27, No. 1, pp. 85-100, 1973.

6.) Laan, J. N., "Sound Transmission in and Radiation from Hard-Walled Annular Ducts Related to Fan Engine Inlets," National Aerospace Laboratory NLR The Netherlands, NLR TR 75144 U, November 1975.

7.) Meyer, W. L., Bell, W. A. and Zinn, B. T., "Predicting the Acoustics of Arbitrarily Shaped Bodies Using an Integral Approach," AIAA Journal, Vol. 15, No. 6, pp. 813-820, June 1977.

8.) Meyer, W. L., Bell, W. A., Stallybrass, M. P., and Zinn, B. T., "Boundary Integral Solutions of Three Dimensional Acoustic Radiation Problems", Journal of Sound and Vibration, Vol. 59, No. 2, pp. 245-262, 1978.

9.) Meyer, W. L., Bell, W. A., Stallybrass, M. P., and Zinn, B. T., "Prediction of the Sound Field Radiated From Axisymmetric Surfaces," Accepted for publication in The Journal of the Acoustical Society of America.

10.) Bell, W. A., Meyer, W. L., and Zinn, B. T., "Prediction of the Acoustics of Solid Propellant Rocket Combustors by Integral Techniques," Proceedings of the 12th JANNAF Combustion Meeting, Newport, Rhode Island, August 11, 1975, CPIA Publication 273, Vol. II, pp. 19-34, December 1975.

11.) Bell, W. A., Meyer, W. L., and Zinn, B. T., "An Integral Approach for Determining the Resonant Frequencies and Natural Modes of Arbitrarily Shaped Ducts," Proceedings of the 3rd Interagency Symposium on University Research in Transportation Noise, Salt Lake City, Utah, November 12-14, 1975.

12.) Meyer, W. L., Bell, W. A. and Zinn, B. T., "Integral Solution of Three Dimensional Acoustic Radiation Problems," presented at the International Symposium on Innovative Numerical Analysis in Applied Engineering Science, Versailles, France, May 23-27, 1977.

13.) Meyer, W.L., Bell, W.A., and Zinn, B.T., "Prediction of the Sound Field Radiated from Axisymmetric Surfaces," AIAA Paper No. 78-195, presented at the AIAA 16th Aerospace Sciences Meeting, Huntsville, Alabama, January 16-18, 1978.

14.) Burton, A. J., "The Solution of Helmholtz' Equation in Exterior Domains using Integral Equations", NPL Report NAC 30, National Physical Laboratory, Teddington, Middlesex, January 1973.

15.) Chertock, G., "Sound Radiation from Vibrating Surfaces," Journal of the Acoustical Society of America, Vol. 36, No. 7, pp. 1305-1313, July 1964.

16.) Morse, P. M., and Ingard, K. U., Theoretical Acoustics, McGraw-Hill, New York, 1969, Chapter 9.

17.) Levine, H. and Schwinger, J., "On the Radiation of Sound from an Unflanged Circular Pipe", Physics Review, Vol. 73, No. 4, pp. 383-406, February 1948.

18.) Miller, B. A., Dastoli, B. J., and Wesoky, H. L., "Effect of Entry-Lip Design on Aerodynamics and Acoustics of High-Throat-Mach-Number Inlets for the Quiet, Clean, Short-Haul Experimental Engine", NASA TM X-3222, Lewis Research Center, Cleveland, Ohio, May 1975.

19.) Zorumski, W. E., "Acoustic Theory of Axisymmetric Multisectioned Ducts", NASA TR R-419, Langley Research Center, Hampton, Virginia, May 1974.

Appendix D

Determination of the Admittance of the Liner

Nomenclature

A	orifice area
c	speed of sound
d	orifice diameter
f	frequency
f_o	resonant frequency of the resonator
k	wave number
L	backing depth
ℓ_{EFF}	effective orifice length
n	normal
p	acoustic pressure
t	orifice length
V	cavity volume
v	acoustic velocity
Y	specific admittance of liner
y	effective admittance of liner
Z	specific impedance of liner
α	absorption coefficient
σ	open area ratio of the liner
$\bar{\sigma}$	open area ratio of a resonator
$\bar{\rho}$	density
$\bar{\mu}$	coefficient of viscosity
π	3.1415926
φ	acoustic potential
θ	specific resistance ratio
χ	specific reactance ratio

The liner, which was employed in the preliminary testing for this AFOSR contract, was originally developed for another program. Since it consists of a matix of Helmholtz resonators it is highly tuned; that is, it has a rather sharp absorption peak. As discussed in Section II, the liner was designed for use above the 1T cut-off frequency and thus shows little absorption below this frequency where most of the runs for this program will be made. Thus the liner must be retuned so that it becomes effective in the frequency range where most of the testing will be done. In this appendix basic liner theory is reviewed and a relatively simple redesign of the liner is proposed to make it more effective in the frequency range of interest in this research program.

For input into the computer program certain values must be known. First, the sound pressure level at the "driver plane" must be known. Experimentally this corresponds to the nozzle-liner plane and can be directly measured. The other value which must be known is the effective admittance of the liner defined as

$$y = \frac{\partial \varphi}{\partial n} \Big/ \varphi \tag{D-1}$$

where φ is the acoustic potential and $\frac{\partial \varphi}{\partial n}$ is the normal acoustic velocity defined with an outward facing normal.

In Reference 1 equations are given to calculate the specific acoustic impedance of an array of helmholtz resonators, that is

$$Z = \theta - i \chi \tag{D-2}$$

where the specific resistance ratio θ and the specific reactance ratio χ are defined as

$$\theta = \frac{4}{\sigma \bar{\rho} \bar{c}} (\pi \bar{\mu} \bar{\rho} f)^{1/2} (1 + {}^{t}/d)$$

(D-3)

$$\chi = \frac{2 \pi f_o \ell_{EFF}}{\bar{c}\sigma} (\frac{f}{f_o} - \frac{f_o}{f})$$

For the definitions of the variables used here see Figure D-1. It will be noted here that these definitions assume an inward facing normal. The resonant frequency of the resonator is defined as

$$f_o = \frac{\bar{c}}{2\pi} \sqrt{\frac{A}{V\ell_{EFF}}} = \frac{\bar{c}}{2\pi} \sqrt{\frac{\sigma}{L\sigma_{EFF}}}$$

(D-4)

and the effective orifice length is found to be

$$\ell_{EFF} = t + 0.85 \, d \, (1 - 0.7 \sqrt{\sigma})$$

(D-5)

The specific acoustic admittance is defined as

$$Y = \frac{1}{Z} = {}^{v}/p$$

(D-6)

and since the acoustic potential and the acoustic pressue are related by

$$p = i \, \bar{\rho} \, \bar{c} \, k \, \varphi$$
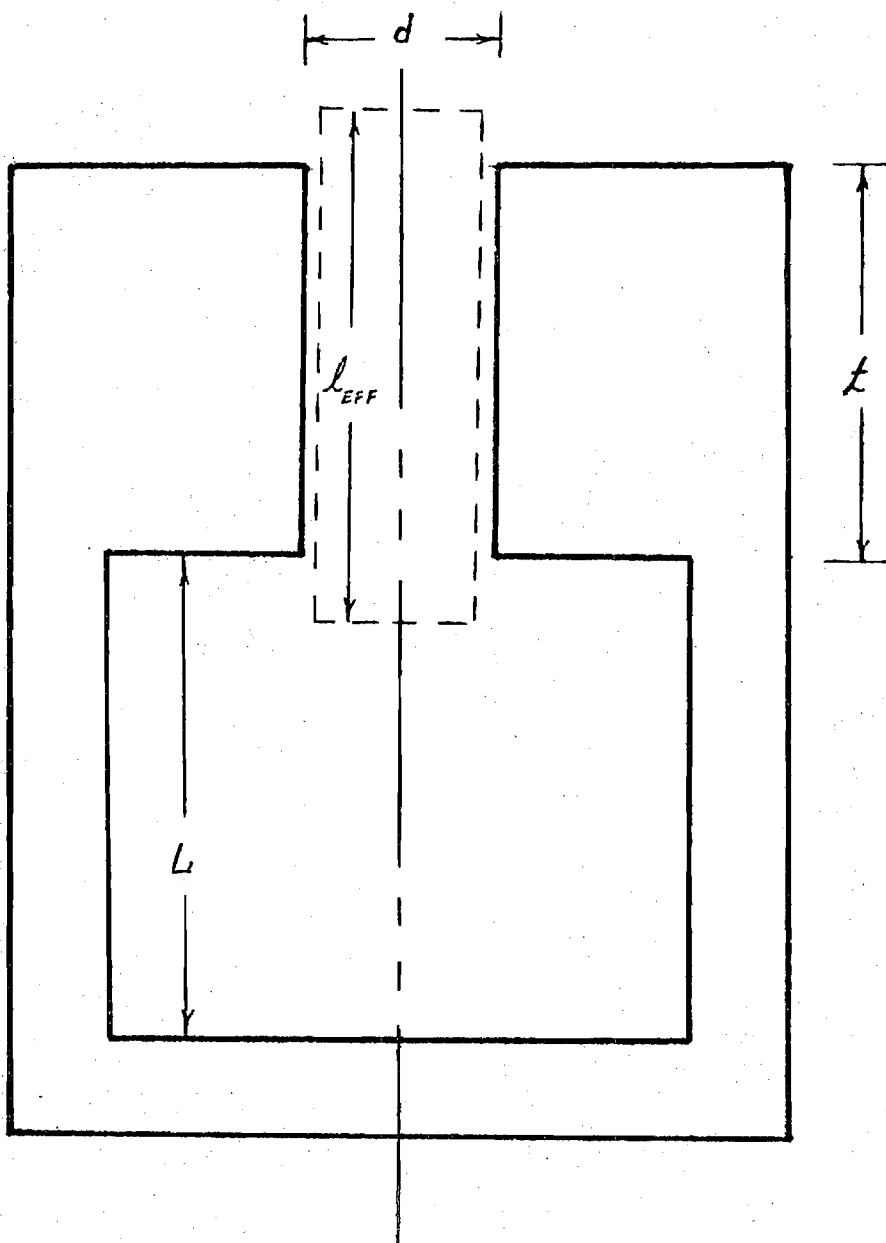
(D-7)

Figure D-1. Helmholtz Resonator

the effective admittance is found to be

$$y = -i\bar{\rho}\bar{c}\, k\, Y = -i\bar{\rho}\bar{c}\, k\, \frac{\theta + i\chi}{(\theta^2 + \chi^2)} \qquad (D\text{-}8)$$

where the minus sign is due to the switch from inward to outward facing normal for the acoustic velocity.

The liner is most effective in damping acoustic waves at its resonant frequency which for our case is ~ 740 Hz. This is above the 1T mode of the duct which is ~ 695 Hz and thus the full effectiveness of this liner is never achieved. A plot of the absorption coefficient of the liner, α, vs. frequency is presented for the present liner configuration in Figure D-2. Here the absorption coefficient is defined as

$$\alpha = \frac{4\theta}{(\theta + 1)^2 + \chi^2} \qquad (D\text{-}9)$$

There are two paths that may be taken to obtain test results at maximum liner efficiency. The first method is to purposely drive a 1T wave by using two drivers driving 180° out of phase. This will create a transverse acoustic wave structure in the tube and the results can then be compared by using a mode number of 1 (instead of zero) in the computer programs. The other alternative is to redesign the liner such that its resonant frequency is reduced below the 1T mode cut-off frequency. This can be accomplished by increasing the backing distance, L. By increasing L from 0.5" to 0.775" the resonant frequency of the liner drops to ~ 685 Hz, below the 1T mode. If the diameter of the backing cavity is also increased from 1.0" to 1.25" the
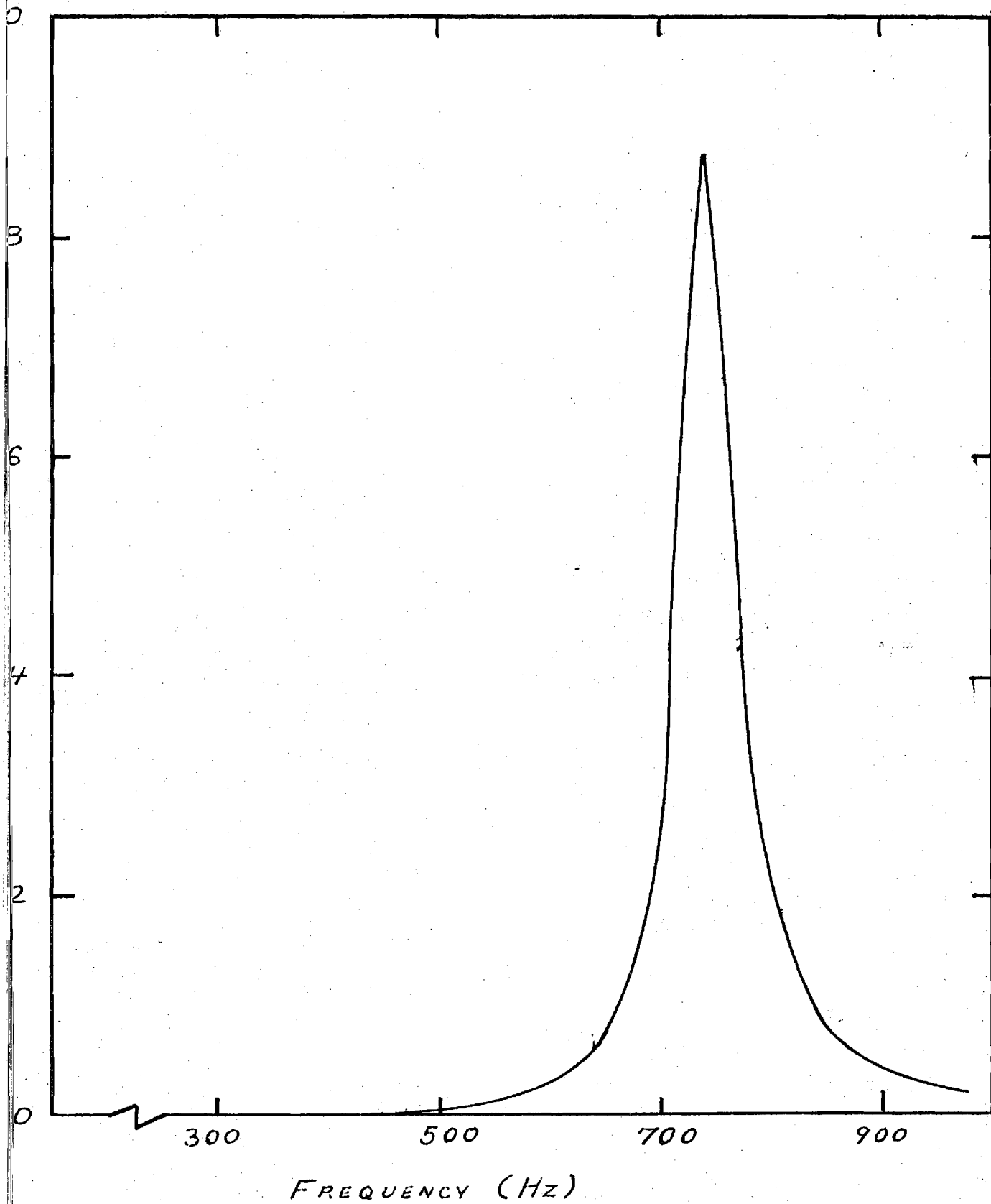
Figure D-2. Absorption Coefficient vs. Frequency
For the Present Liner Configuration.

45

resonant frequency of the liner can be further reduced to ~550 Hz. Thus, by simply drilling out the backing cavity the tuning frequency of the liner can be altered enough so that its absorption peak is well below the 1T cut-off frequency; that is, in the range of frequencies that will normally be used for testing in this research program (i.e., 300-650 Hz).

References

1. Garrison, G. D., "A Study of the Suppression of Combustion Oscillations with Mechanical Damping Devices," Phase II Summary Report, Pratt & Whitney Aircraft Co., PWA FR-1922, July 15, 1966.

Appendix E

Technical Note to be submitted for publication to the AIAA Journal (Draft copy)

"Sound Radiation from Ducts: A Comparison of Admittance Values"

Technical Note

Sound Radiation From Ducts: A Comparison of Admittance Values[*]

W. L. Meyer[**]   Assistant Research Engineer

W. A. Bell[†]   Research Engineer

B. T. Zinn[‡]   Regents' Professor

School of Aerospace Engineering

Georgia Institute of Technology

Atlanta, Ga. 30032

When considering the radiation from an open duct it is found that some of the energy is radiated and some reflected (with a phase shift) back down the duct. It is common to associate an effective admittance (impedance or reflection coefficient) at the exit plane with this phenomonon. In this note three methods for obtaining an effective admittance are compared.

The first method follows the analyses of Helmholtz and Rayleigh in which the end of the duct is approximated by a piston radiating into a half space from an infinite baffle. In this analysis the classical integral representation of the solutions of the Helmholtz equation is solved with certain approximations. Results for this configuration (commonly known as a flanged pipe) using this method are presented in Reference 1.

The second method consists of the solution of a Weiner-Hopf type integral equation. In this analysis the duct is assumed to be semi-infinite in length and infinitely thin. Results for this type of analysis are presented in Reference 2. This configuration is commonly known as the unflanged pipe.

It is interesting to note that these two configurations represent the logical limits of this type of problem in that the first can be viewed as an infinitely thick duct while the second is infinitely thin. Neither of these configurations can account for the case of a duct of finite length, however.

The third method employs a special cylindrically symmetric integral representation of the exterior solutions of the Helmholtz equation.[3,4,5] Using this method it is possible to calculate the acoustic pressure and velocity anywhere in the external field - including the inside of the duct itself. From these values inside the duct an effective admittance can be calculated using a simple standing wave analysis like that used in an

50

impedance tube. All that is required for this method is knowledge of two complex acoustic quantities (i.e., amplitude and phase) at two points in the duct.

The geometric restrictions on the integral technique are that the duct (or any radiating body) must be a finite (i.e. no infinitely thin walls) closed body. A sketch of the duct used in this analysis is presented in Figure 1.

To determine if the length of the duct makes a significant difference in the admittance values at the duct entrance computer analyses of ducts of varying lengths were run (i.e. $L/a = 1,2,3$) at two different non-dimensional wave numbers (i.e. $ka = 1$ and 3). Since the method is capable of calculating the actual radially varying admittance across the exit plane of the duct, these are presented in Figure 2. The driver consisted of specifying a unit normal acoustic velocity while on the rest of the body the admittance was specified as zero. As can be seen the length of the duct L has little effect on the admittance, defined as the ratio of the component of the acoustic velocity normal to the surface to the acoustic pressure. Also noted for the sake of comparison are the values for the flanged and unflanged pipe at the appropriate values of ka.

Computer analyses of a duct with $L/a = 3$ were then done with the same boundary conditions specified as above for various values of ka. For each case the acoustic potential and velocity were calculated at 11 equally spaced points along the centerline of the duct from $Z = 1$ to $Z = 2$. A standing wave analysis was then done employing a Least-Square method to solve the overdetermined system of equations. The results of these analyses are presented in Figure 3 along with the values for a flanged and an
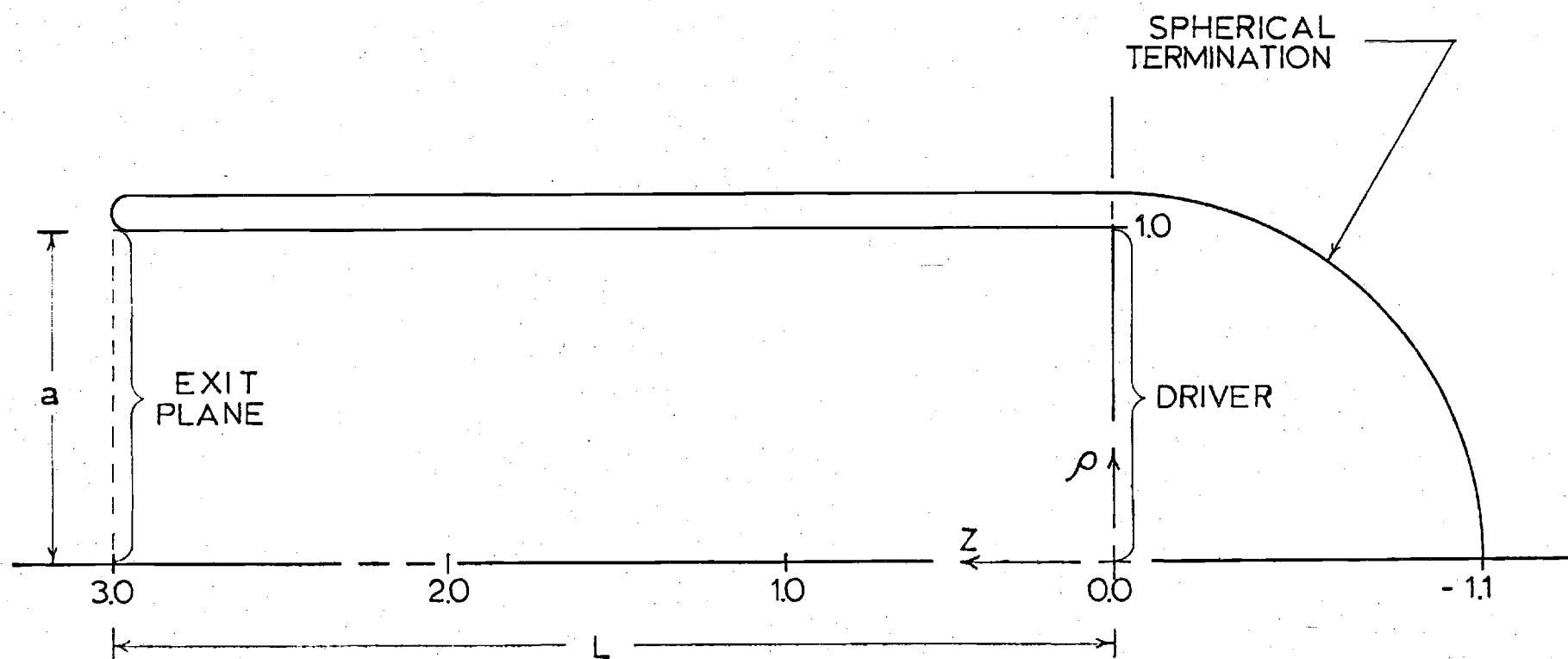
51

Figure 1. Straight Duct Geometry.
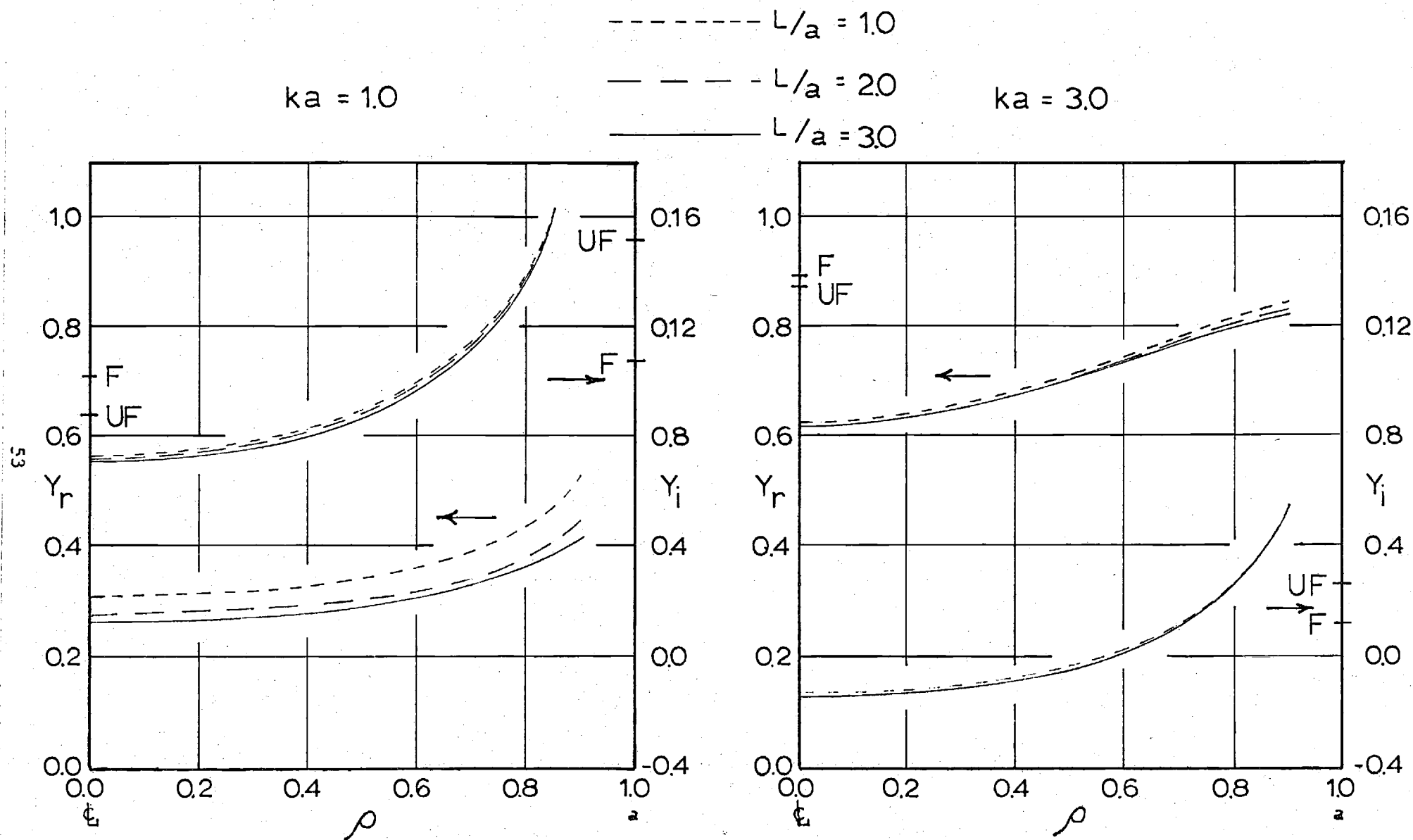
Figure 2. Admittance at the Exit Plane of Straight Ducts.
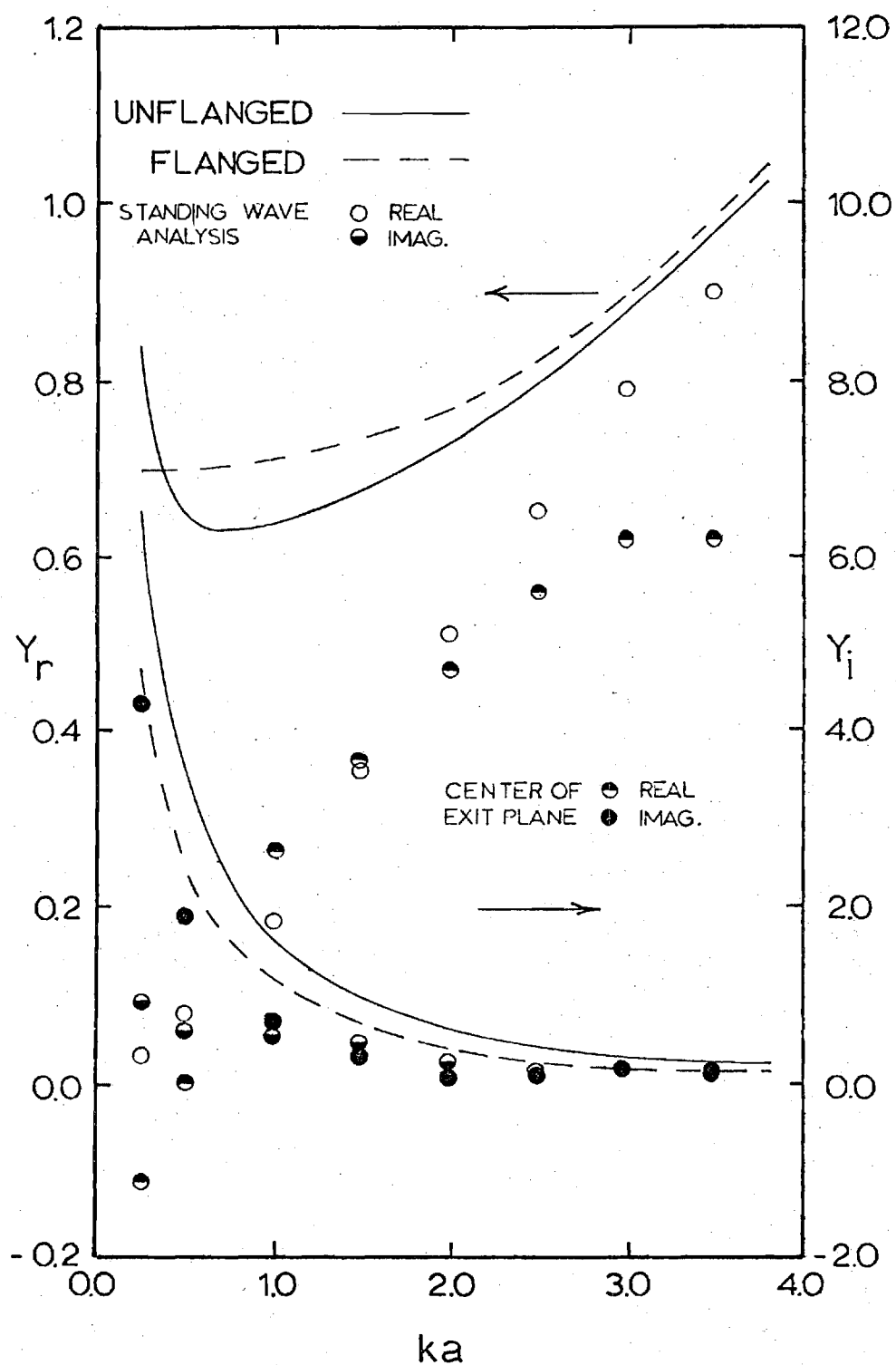
53

Figure 3. Admittance at the Open End
of a Straight Duct.

unflanged pipe. Similar analyses were done off the centerline of the duct; however, no significant differences in the computed values for the admittance at the entrance plane of the duct were found. Also noted for comparison in Figure 3 are the values of the admittance calculated on the centerline of the duct at the exit plane.

References

1.) Theoretical Acoustics, P. M. Morse and K.U. Ingard, McGraw-Hill, New York, 1969, Chapter 9.

2.) "On the Radiation of Sound from an Unflanged Circular Pipe," H. Levine and J. Schwinger, Physics Review, Vol. 73, No. 4, pp. 383-406, February 1948.

3.) "Boundary Integral Solutions of Three Dimensional Acoustic Radiation Problems," Meyer, W. L., Bell, W. A., Stallybrass, M. P. and Zinn, B. T., Journal of Sound and Vibration, Vol. 59, No. 2, pp. 245-262, 1978.

4.) "Prediction of the Sound Field Radiated From Axisymmetric Surfaces," Meyer, W. L., Bell, W. A., Stallybrass, M. P., and Zinn, B. T.,Journal of the Acoustical Society of America, March 1979.

5.) "Sound Radiation from Finite Length Axisymmetric Ducts and Engine Inlets," Meyer, W. L., Bell, W. A., and Zinn,B. T., AIAA Paper No. 79-0675, presented at the AIAA 5th Aeroacoustics Conference, Seattle, Washington, March 12-14, 1979.

Appendix F

Presentations

A. "Predicting the Acoustic Properties of Arbitrarily Shaped Bodies by Use of an Integral Approach," Presented at the 3rd AIAA Aeroacoustics Conference at Palo Alto, California, July 20-23, 1976. (Zinn)

B. "Integral Solutions of Three Dimensional Acoustic Radiation Problems," Presented at the International Symposium on Innovative Numerical Analysis in Applied Engineering Science at Versailles, France, May 23-27, 1977 (Zinn)

C. "Prediction of the Sound Field Radiated from Axisymmetric Surfaces," Presented at the AIAA 16th Aerospace Sciences Meeting at Huntsville, Alabama, January 16-18, 1978. (Bell)

D. "Sound Radiation from Finite Length Axisymmetric Ducts and Engine Inlets," Presented at the 5th AIAA Aeroacoustics Conference at Seattle, Washington, March 12-14, 1979. (Zinn)

AFOSR Final Technical Report

AFOSR-TR-

NOISE SUPPRESSION IN JET INLETS

Prepared for

Air Force Office of Scientific Research
Director of Aerospace Sciences

Bolling AFB, D.C.

by

Ben T. Zinn

William L. Meyer

Brady R. Daniel

School of Aerospace Engineering
Georgia Institute of Technology
Atlanta, Georgia 30332

Approved for public release; distribution unlimited

AFOSR Contract No. F49620-77-C-0066   February 1980

Conditions of Reproduction

REPORT DOCUMENTATION PAGE	READ INSTRUCTIONS BEFORE COMPLETING FORM

1. REPORT NUMBER AFOSR-TR-	2. GOVT ACCESSION NO.	3. RECIPIENT'S CATALOG NUMBER

4. TITLE *(and Subtitle)* Noise Suppression in Jet Inlets	5. TYPE OF REPORT & PERIOD COVERED Final Feb. 1, 1979 - Jan. 31, 1980
	6. PERFORMING ORG. REPORT NUMBER

7. AUTHOR(s) Ben T. Zinn William L. Meyer Brady R. Daniel	8. CONTRACT OR GRANT NUMBER(s) AFOSR-F49620-77-C-0066

9. PERFORMING ORGANIZATION NAME AND ADDRESS School of Aerospace Engineering Georgia Institute of Technology Atlanta, Ga. 30332	10. PROGRAM ELEMENT, PROJECT, TASK AREA & WORK UNIT NUMBERS

11. CONTROLLING OFFICE NAME AND ADDRESS Air Force Office of Scientific Research Director of Aerospace Studies Bolling AFB, DC	12. REPORT DATE February 1980
	13. NUMBER OF PAGES

14. MONITORING AGENCY NAME & ADDRESS(If different from Controlling Office)	15. SECURITY CLASS. *(of this report)*
	15a. DECLASSIFICATION/DOWNGRADING SCHEDULE Unclassified

16. DISTRIBUTION STATEMENT *(of this Report)*

Approved for Public Release; Distribution
Unlimited

17. DISTRIBUTION STATEMENT *(of the abstract entered in Block 20, if different from Report)*

18. SUPPLEMENTARY NOTES

19. KEY WORDS *(Continue on reverse side if necessary and identify by block number)*
Acoustic Radiation
Duct Acoustics
Jet Propulsion Noise
Aircraft Noise

20. ABSTRACT *(Continue on reverse side if necessary and identify by block number)*

  This report summarizes the work performed in the third and last
year of an AFOSR sponsored research program (AFOSR Contract No. F49620-
77-C-0066). This research program was concerned with the development
of an analytical technique, based on an integral representation of the external
solutions of the Helmholtz equation, for the prediction of the sound radiated
from complicated, acoustically lined, axisymmetric bodies having complex
sound sources. The purpose of this research program was to generate

DD FORM 1 JAN 73 **1473**

efficient computer codes for the prediction of the sound radiated from acoustically lined jet engine inlets. During the first two years of work under this contract the above goals were accomplished and are documented in the previous two AFOSR ANNUAL TECHNICAL REPORTS numbered AFOSR-TR-78-0696 and AFOSR-TR-79-0614.

This report is concerned with the progress made during the third year of this contract when experimental tests were run on various configurations for comparison with and verification of the results obtained from the axisymmetric computer codes which model the integral technique. In the experimental tests two geometrical configurations were studied, a straight duct and a jet engine inlet. Both of these configurations were tested with hard walls and the straight duct was tested with an acoustic liner consisting of a matrix of Helmholtz resonators. It was found that very good agreement was obtained for the hard walled configurations while there were some discrepancies with the lined wall case. It is conjectured that this discrepancy in some of the lined wall results is mainly due to the particular liner theory used to calculate the effective admittance of the liner.

Abstract

This report summarizes the work performed in the third and last year of an AFOSR sponsored research program (AFOSR Contract No. F49620-77-C-0066). This research program was concerned with the development of an analytical technique, based on an integral representation of the external solutions of the Helmholtz equation, for the prediction of the sound radiated from complicated, acoustically lined, axisymmetric bodies having complex sound sources. The purpose of this research program was to generate efficient computer codes for the prediction of the sound radiated from acoustically lined jet engine inlets. During the first two years of work under this contract the above goals were accomplished and are documented in the previous two AFOSR ANNUAL TECHNICAL REPORTS numbered AFOSR-TR-78-0696 and AFOSR-TR-79-0614.

This report is concerned with the progress made during the third year of this contract when experimental tests were run on various configurations for comparison with and verification of the results obtained from the axisymmetric computer codes which model the integral technique. In the experimental tests two geometrical configurations were studied, a straight duct and a jet engine inlet. Both of these configurations were tested with hard walls and the straight duct was tested with an acoustic liner consisting of a matrix of Helmholtz resonators. It was found that very good agreement was obtained for the hard walled configurations while there were some discrepancies with the lined wall case. It is conjectured that this discrepancy in some of the lined wall results is mainly due to the particular liner theory used to calculate the effective admittance of the liner.

Introduction

This report summarizes the results obtained during the third year of support under AFOSR contract number F49620-77-C-0066. This contract was initiated February 1, 1977 and the results obtained during the first two years of support are contained in AFOSR technical reports AFOSR-TR-78-0696 and AFOSR-TR-79-0614.

The main objective of the research program conducted under this contract was to develop an analytical technique, both the theory and associated computer codes, for predicting the sound field radiated from axisymmetric jet engine inlet configurations with lined walls and to compare some analytical predictions with the results of experimental tests. The development of the theory, which is based on a special integral representation of the external solutions of the Helmholtz equation, was motivated by the need for an analytical approach that could be used to predict the effects of sound source modifications and acoustic liners on the sound field radiated from an inlet without having to resort to costly, full scale experimental testing. During the first two years of this contract the axisymmetric formulation of the integral solution technique[1,3] was developed along with two efficient, general computer programs; one to solve for the surface distributions of the acoustic quantities of interest and the other to solve for the distributions of the acoustic quantities in the field surrounding the body.

During the third contract year sound radiation experiments were performed with two geometrically different configurations, a straight duct and the QCSEE jet engine inlet of Ref. (4), for comparison with analytical

results for the same bodies. The straight duct configuration was tested with both a hard and a soft wall while the inlet configuration was only tested with a hard wall. Tasks performed during the third contract year included:

A.) Calibration of the anechoic chamber

This was necessary to find out how well the anechoic chamber approximated the results that would be gotten if true free field measurements could be made. These calibrations were done with all of the support apparatus for the test bodies and the microphones in place so as to get an idea of the magnitude of the errors involved.

B.) Set-up of the electronic equipment

This task was not as straight forward as it might seem as it was found that in order to get relatively stable amplitude and phase measurements it was necessary to pre-condition the signals coming from the microphones through the use of both high and low pass filters. Since all of the signals were passed through the same filters, including the reference signal from the reference microphone, any phase or amplitude shift caused by the filters could be subtracted out.

C.) Conduct of the experiments

Each of the experimental tests were run at least twice on two different days and the results of these separate tests were compared. This was necessary to get an estimate of the repeatability of the experimental data. It was also used as a check on the validity of the data as the data was read directly from meters and transcribed by hand as no on line data acquisition system was available for use on this project.

D.) Prediction of the tested liner admittance

A liner was designed and fabricated for the lined straight duct tests. To do this design the theory of Garrison[5] was employed. The liner thus designed was a matrix of Helmholtz resonators which had its absorption peak below the 1T mode of the duct as this was where all of the testing was done.

E.) Data Reduction and comparison with theoretical predictions

The experimental data was both taken and reduced by hand. The data reduction was not a very time consuming process as all that had to be done was subtract the reference microphones values of the amplitude and phase from the values measured at the driver plane and the radiation measurements in the field. This was done so as to negate any shift in the measured amplitude or phase by the signal filters.

The computer programs were then run for the same conditions (i.e., driver power and frequency) as the experimental tests. These results were then compared with the experimental results and a brief error analysis was done.

F.) Determination of the "effective" liner admittance

The results of the experimental tests and the theory were found to be in very good agreement except near the calculated absorption peak of the liner. It was determined that the Garrison theory[5] used to calculate the theoretical liner admittances was probably at fault. Systematic computer runs were then performed parametrically varying the admittance until good agreement was obtained between the theoretical and experimental results.

Included in this report is a list of all the publications generated by this research effort. This is included as Appendix A. Also, Appendix B contains a list of all the conference presentations pertaining to the work performed under this contract and, finally, a copy of the most recent publication that was a direct result of the research performed in the past year on this contract is included as Appendix C.

A. Calibration of the Anechoic Chamber

The anechoic chamber is 10' by 13' by 6 1/2' in height. It has approximately 2' of sound absorbing fiberglass insulation in the floor, walls, and ceiling. A plan view of the anechoic chamber is presented in Fig. 8 of Appendix C.

It was necessary to calibrate the anechoic chamber with all of the microphone stands and the mounting stand for the test apparatus in place so that an estimate of the experimental errors in the free field measurements caused by this apparatus could be made. A University acoustic driver was mounted vertically on the support pedistal for the test apparatus, 37.5" off the floor, so that it would radiate sound equally in all directions, thus approximating a simple source. A ½" diameter Brüel and Kjaer microphone was placed 42.5" from the driver in the field and was used as a reference microphone for the amplitude readings.

A ¼" diameter B & K microphone was then moved in the direction that the test ducts would face, to be henceforth known as direction 1, (See Fig. 8, Appendix C and Fig. 1.) and measurements were taken every 5" out to 45". This procedure was repeated in the direction of the door of the chamber (90° to the original direction of travel) and again measurements were taken every 5" up to 45" from the driver. This will be referred to as direction 2. At each microphone position measurements were made of the amplitude and phase, relative to the driver input signal, at frequencies from 300 to 750 Hz at 50 Hz increments as the tests were all to be run in this range. It should be noted here that the lower limit was imposed by the University driver and that the upper limit was imposed by the requirement that all of the tests be
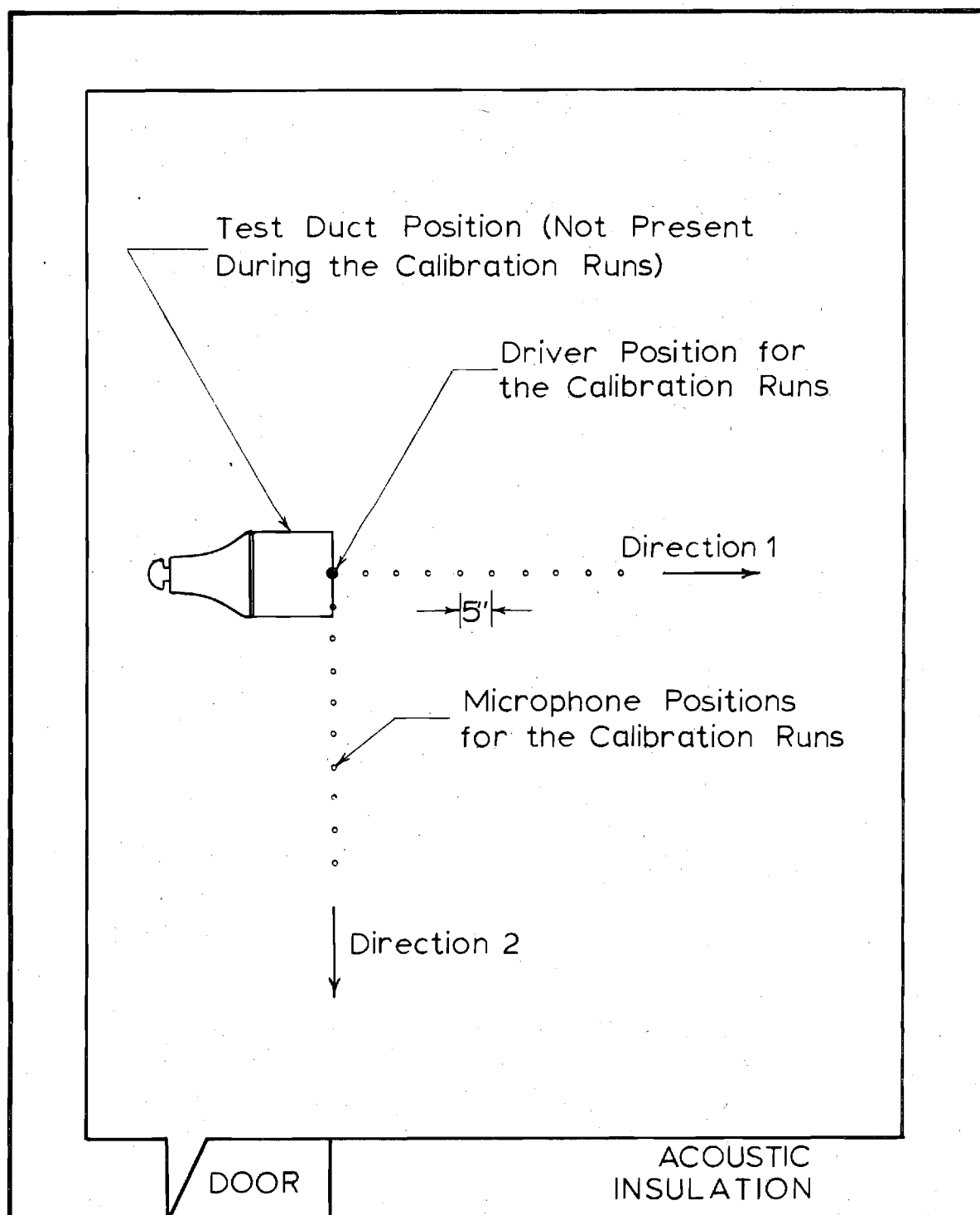
Fig. 1. Plan View of Anechoic Chamber with Driver and Microphone Positions for the Calibration Runs.

run below the 1T mode of the inlet and the straight duct. The latter requirement was to facilitate the data reduction and comparison with the theoretical model and the fact that we had no simple method of driving higher modes in the test ducts.

Results of the amplitude calibration in direction 1 are presented in Fig. 2. The solid lines are the theoretical curves for the Sound Pressure Level in decibels for a simple source in a free field. The equation for these curves is

$$SPL(dB) = - 20 \, Log \, r$$

<div align="right">(1)</div>

where r is the distance from the source. In this plot the amplitude is referenced to the 5" position. The worst point in this direction is at 30" and 350 Hz where the measured reading is 3.5 dB below the theoretical exact curve. All of the test runs were made with the microphones at 40" where the error was always less than 3 dB at all frequencies.

The results of the amplitude calibration in direction 2 are presented in Fig. 3. The worst point in this direction occurs at 30" and 400 Hz where the measured sound pressure level is 9.5 dB below the free field prediction. Again, all of the test runs were made with the microphones at 40" where the error was always less than 3 dB.

In Figs. 4 and 5 the phase comparisons are presented. The X's in these plots denote points where no stable phase reading could be obtained. This was later found to be caused by widely different signal strengths (i.e., voltages) being fed into the phase meter. This was corrected in subsequent tests by using another microphone signal as the reference input rather than
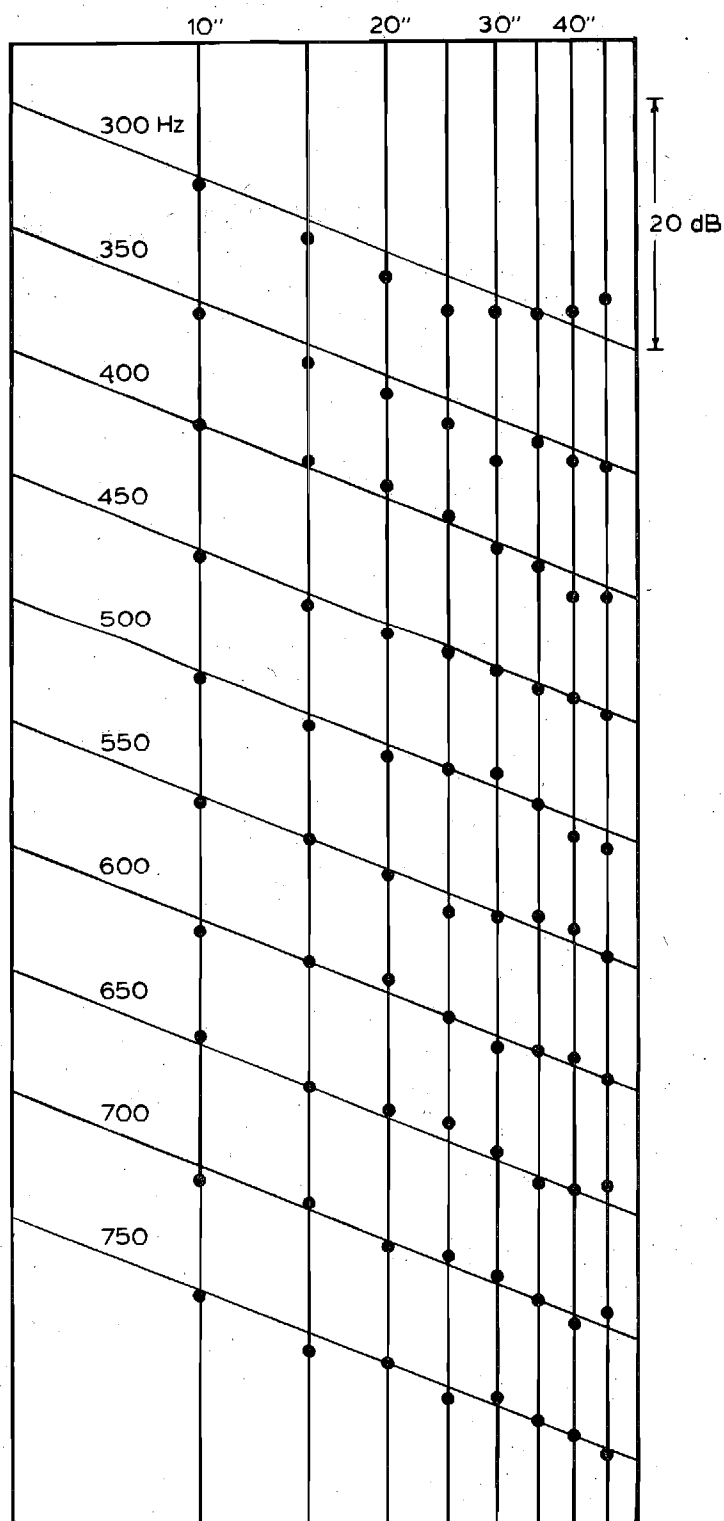
Fig. 2. Anechoic Chamber Acoustic Amplitude Calibration
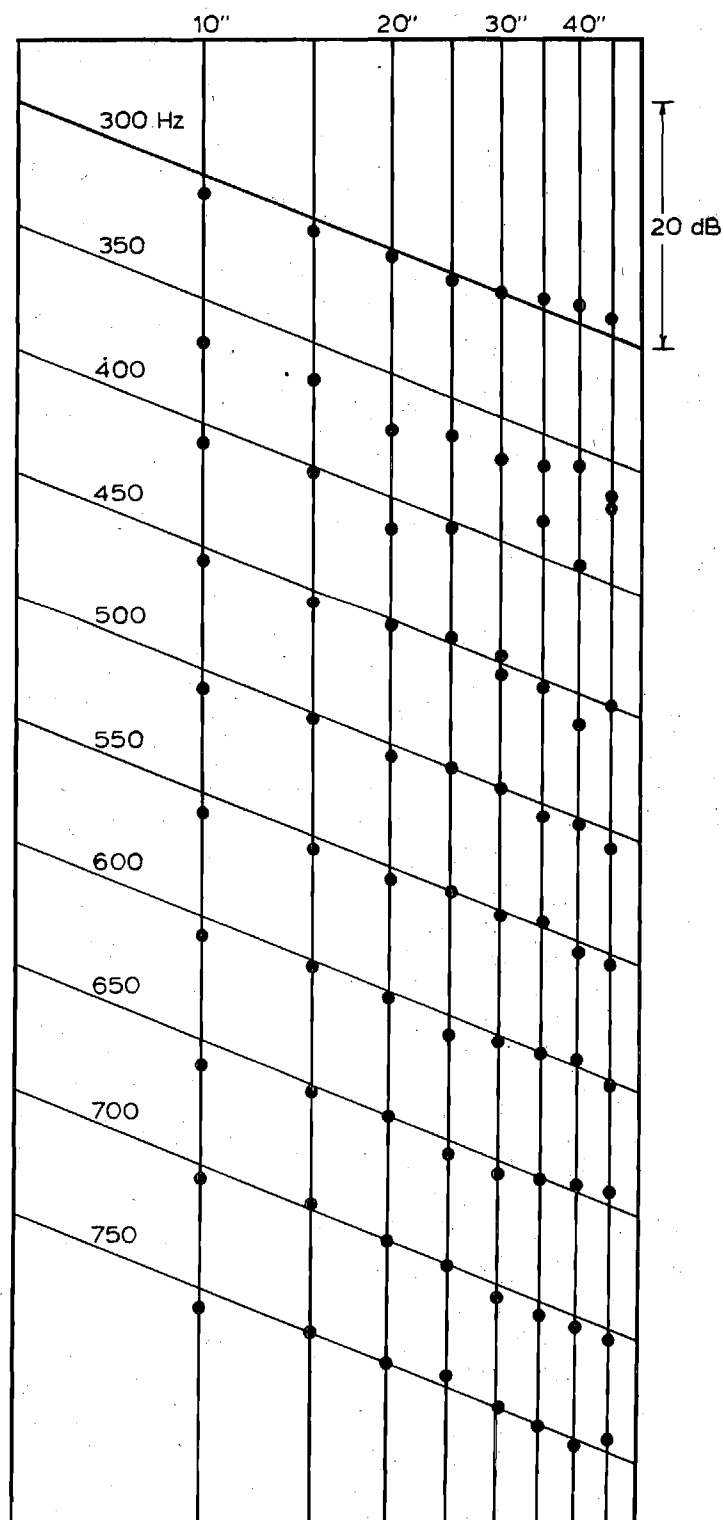   Direction 1.

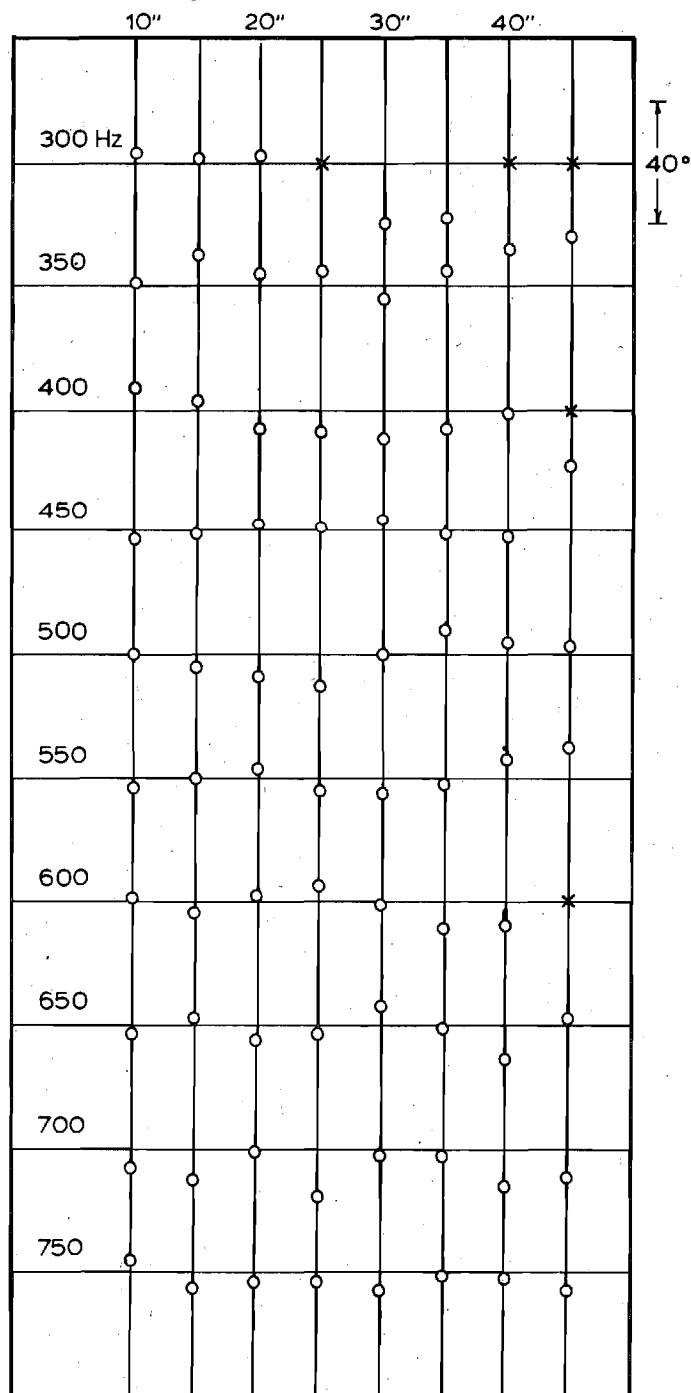Fig. 3. Anechoic Chamber Acoustic Amplitude Calibration
Direction 2.

Fig. 4.   Anechoic   Chamber   Acoustic   Phase   Calibration
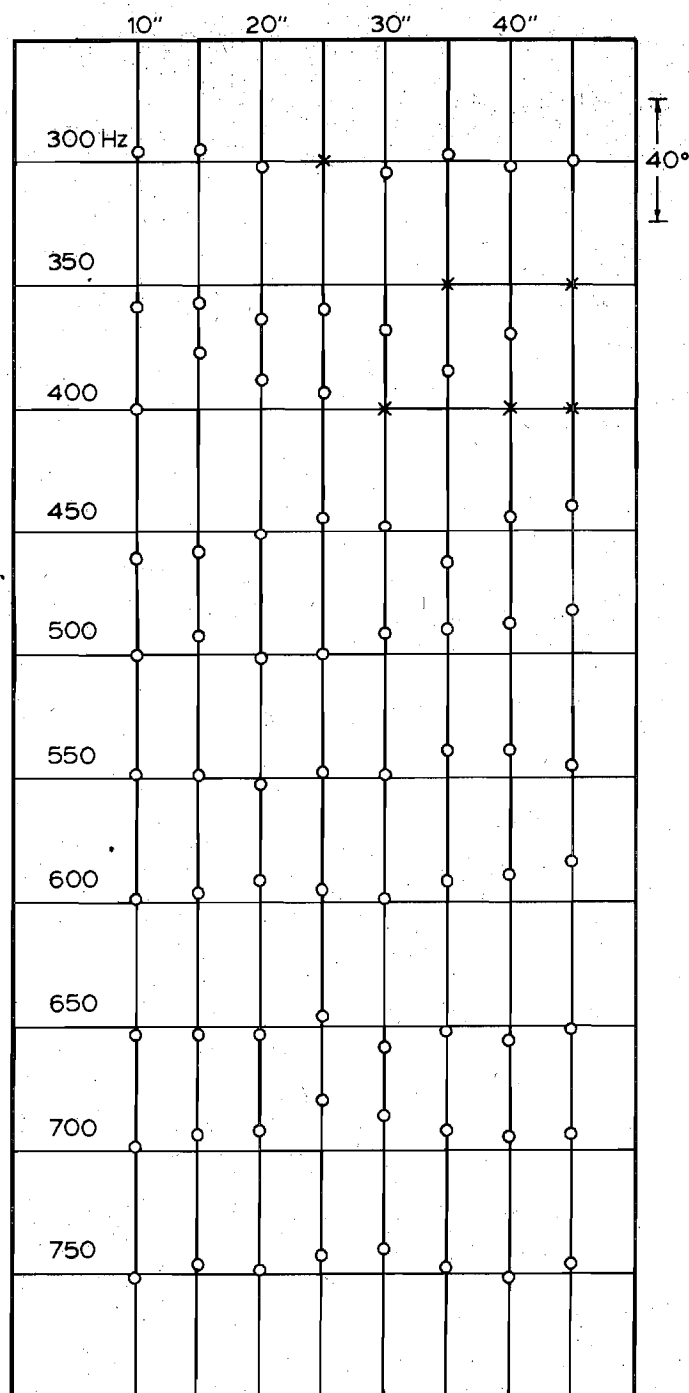Direction 1.

Fig. 5. Anechoic Chamber Acoustic Phase Calibration
Direction 2.

the output from the oscillator that drove the acoustic driver. As can be seen most of the results are within 10° of the values that were calculated using the simple source in a free field assumption. Some values are in error by as much as 20° (See Fig. 4, direction 1 at 30" and 35" from the driver for 300 Hz.); however, these "bad" results are suspect as the phase meter could not be stabilized at adjacent points. The test results in these plots are referenced to the 5" position as it was closest to the driver and therefore subject to the least interference. This is a source of error that could potentially bias the results at a given frequency since if the phase reading at the 5" position was high the rest of the values at all other distances would be low by that amount and vice versa. It is conjectured that this is what happened at a couple of frequencies such as 600 and 700 Hz in Fig. 5.

From the calibration runs that were performed in the anechoic chamber with all of the support equipment for the model and the microphones in place it was concluded that the results obtained from tests in the chamber would be accurate to at least 3 dB in amplitude and 10° in phase. As a matter of fact, the results obtained from tests in the chamber were in general found to be in better agreement with the theoretically calculated "exact" results than the calibration runs would lead one to expect.

B. Set-up of the Electronic Equipment

The equipment set-up can be basically broken down into two separate entities; the sound generating equipment and the sound measuring equipment. During the calibration of the anechoic chamber (See previous section.) these two systems were linked in that the oscillator that produced the driver signal was also used as a phase reference for the sound readings. This arrangement was changed in all subsequent tests as it was found that due to the large voltage difference in the signal strengths between a microphone and the oscillator the phase meter would not stabilize if the signals were close to 180° out of phase. This being the case, another microphone was used as the reference in subsequent tests.

In all of the tests, a 75 watt University Sound heavy-duty driver was employed. The University driver was powered by a Krohn-Hite, Model DCA-50R, wide-band 50 watt amplifier which is capable of amplifying signals from D.C. to 500 KHz. A Model MT-56 Krohn-Hite matching transformer was used to match the impedances of the amplifier and the driver to get maximum power out of the driver. The amplifier was triggered by a Hewlett-Packard Model 202C low frequency oscillator which can produce signals from 1 Hz to 100,000 Hz. The frequency output of the oscillator was constantly monitored by two time base counters; one with fast response for ease of setting the desired frequency and one with slow response for checking the accuracy of the set frequency. The first was a Hewlett-Packard Model 5302 A 50 MHz universal counter and the second was a Monsanto Model 104 A preset/variable time-base counter. In all of the

conducted tests the frequency was always set to within $\pm$ 0.2 Hz of the desired frequency before any measurements were made.

For the actual sound measurements two sizes of Brüel & Kjaer microphones were used; ½ inch microphones were used outside the test duct for the field measurements and ¼ inch microphones were used inside the duct for reference and driver power measurements (See Figs. 4 and 7 of Appendix C.). Also, two different types of pre-amplifiers were used on these microphones; tube type which require a heating element voltage input and transistor type which do not.

The ¼ inch microphones were used with the tube type pre-amplifiers and the signals from these microphones were fed into a B & K two channel microphone selector, Type 4408, and from there into a B & K microphone amplifier, Type 2604. The ½ inch microphones were used with the transistor type pre-amplifiers. In each of the tests two ¼ inch microphones were used and five ½ inch microphones were used. To multiplex the five ½ inch microphone signals an in house fabricated five channel microphone selector was used and these were fed into a B & K Type 2606 measuring amplifier. Both of the B & K amplifiers gave direct decibel readings for the microphones to 0.1 dB, although the readings were certainly not reliable to this accuracy due to amplifier and pre-amplifier drift (this will be discussed in detail in the following section). The two microphone multiplexers were necessary as each of the measuring amplifiers could only handle one microphone at a time.

Although the signals were good enough to give reliable decibel readings they had to be pre-conditioned before good, steady phase

14

measurements could be made. To achieve this, two Krohn-Hite Model 3202 R filters were used. Both of the microphone signals, one being used as the reference signal, were passed through both a high and a low pass filter. These filters were set for all of the tests at 250 Hz for the high pass and 800 Hz for the low pass as all of the tests were run between 300 and 750 Hz. The phase was measured by a Wavetek Model 740 phase meter and was displayed in degrees (-180° to 180°) on a Fluke 8000 A digital multimeter.

Finally, all of the signals were run through an H-P 180 A dual beam oscilloscope. This was used to keep a check on the equipment by constantly checking the signal quality. Also, this was used to check if any of the equipment was being over driven or saturated at any given set of test conditions.

C. Conduct of the Experiments

As stated before, each of the tests was performed twice on separate days for verification of the data as it was read directly from meters and transcribed by hand. The results that are shown for the experimental tests are in fact an average of the two tests run for each experimental configuration. Also, the ambient temperature was monitored during each test so that corrections could be made for the varying speed of sound and the ambient pressure was measured before and after each run so that the characteristic impedance of the medium (i.e., the air in the anechoic chamber) could be calculated. The latter measurement was only important when a lined configuration was being tested.

Since nine measurements were made in the field for each test frequency and since only five ½ inch microphones and stands were available, four of the microphones had to be moved during each test. The fifth microphone, on the centerline of the test duct, was never moved and was used as a reference to check that the test conditions (i.e., the driver power output) were the same with the other microphones in both positions. A second reference microphone, a ¼ inch one, was placed in the nozzle section of the test set-up (See Figs. 4 and 7 of Appendix C.) just in front of the University driver so that a second independent check of the driver power output could be made for each test condition.

The sequence of events for each test was the same so, for the sake of simplicity, the straight duct will be used as the example here. The only difference lies in the fact that the straight duct was run with both hard and soft walls while the inlet configuration was only run with a hard wall.

First, the test duct was set-up in its soft walled configuration (i.e., with its liner exposed). The microphones were then set-up at 40 inches from the center of the entrance plane of the duct at 22.5^O increments from the centerline of the duct (See Fig. 8 Appendix C.). This was accomplished by triangulation and the ½ inch microphones were placed within at least one half inch of their ideal location. The microphones were then calibrated using a B & K pistonphone acoustic calibrator and the barometric pressure was noted. Then, the temperature in the chamber was read and the chamber was closed. Next, the oscillator was set to the desired frequency and the driver power was set by making the microphone at the imaginary driver plane read some pre-selected dB level. All of the other microphones phases and amplitudes were then read and recorded. The chamber was then opened and the temperature was rechecked. The chamber was closed and the test was repeated at a new frequency. The inlet was run at frequencies from 300 to 750 Hz at 50 Hz increments while the straight duct was tested over a frequency range up to 700 Hz. This was due to the different characteristic lengths of the two test bodies.

Once the desired frequency range had been tested, the liner in the duct was taped over so that it was no longer exposed, the microphones were recalibrated, and the whole test procedure was repeated. Having done this the four microphones in the field were moved to their intermediate positions, recalibrated, and another run was made of all the frequencies. Finally, the tape was removed from the liner, the microphones recalibrated again and the final set of measurements were made. Having done all this, the microphones were calibrated one last time and the barometric pressure

was re-read.

Each one of these tests took an entire day and required only one person most of the time. Two people were required when the microphones were calibrated, one in the chamber with the pistonphone and the other outside recording the dB levels.

D. Prediction of the Tested Liner Admittance[*]

For the lined walled tests, a liner was designed using the theory of Garrison.[5] The liner consisted of a matrix of 180 Helmholtz resonators (See Fig. 5 Appendix C.), 9 axial rows by 20 radial rows. It was designed so that its maximum effectiveness (i.e., resonance peak) occurred within the range of frequencies used in testing; that is, between 300 and 700 Hz, below the 1T mode of the duct and above the driving floor of the University driver. The tests were also all run in the liners linear regime as calculated by the theory.[5]

In the Garrison theory the linear regieme is defined as where the maximum acoustic velocity at the orifice of the Helmholtz resonator is below 60 ft./sec.. Using this criterion it is found that the linear regime is below the decibel levels in Table I for a sea level standard atmosphere and the respective driving frequencies. Since in all of the runs the decibel level was always less than 135 dB the linear liner theory was used.

Using the linear theory, the specific acoustic impedance of the liner is given by

$$Z = \theta - iX$$

(2)

where the specific acoustic resistance is given by

$$\theta = \frac{4}{\sigma \rho c} (\pi \overline{\mu \rho} f)^{\frac{1}{2}} (1 + t/d)$$

(3)

---

[*]   See Nomenclature at the end of this section.

Table I

Maximum SPL(dB) where a Helmholtz resonator exhibits linear behavior

Frequency (Hz)	SPL (dB)
300	163
350	160
400	157
450	153
500	148
550	143
600	148
650	152
700	155

and the specific acoustic reactance by

$$X = \frac{2\pi f_o l_{eff}}{\bar{c}\ \sigma} \left(\frac{f}{f_o} - \frac{f_o}{f} \right) \tag{4}$$

In these equations the effective orifice length is given by

$$l_{eff} = t + 0.85\,d\,(\,1 - 0.7\sqrt{\sigma}\,\,) \tag{5}$$

and the resonant frequency of a Helmholtz resonator by

$$f_o = \sqrt{\frac{\sigma}{Ll_{eff}}} \tag{6}$$

For the test conditions these are found to be given as

$$\theta = 0.01398\ \sqrt{f}$$

$$X = 10.186 \left(\frac{f}{f_o} - \frac{f_o}{f} \right) \tag{7}$$

where the resonance peak of the liner f_o is found to be at 558 Hz. These values are related to the acoustic admittance of Appendix C defined as $y = V/\Phi$ by

$$y = -i\,k\,\left(\frac{1}{Z} \right) \tag{8}$$

where Z is defined with an inward facing normal and y is defined with an outward facing normal; thus the minus sign.

Using the definition of the absorption coefficient α; that is,

$$\alpha = \frac{4\theta}{(1+\theta)^2 + x^2}$$

(9)

it is found that the liner absorption curve is very "peaky" (See Fig. 6.). This being the case normal machining errors of 0.0005" were introduced into the admittance calculation and the resonance frequency was found to change by 1.5 Hz. It was found that this change in the resonance frequency could change the results at 550 Hz (i.e. the test frequency closest to the resonant frequency) by 3 dB and 5 degrees.

This will be discussed further in the ensuing sections as good agreement was obtained between the theory and experiment except at 550 Hz for the soft walled duct. It is felt that this disagreement is more the fault of the liner design approach at frequencies close to resonance rather than inaccuracies in the integral equation formulation.

Fig. 6. Absorption Coefficient vs. Frequency for Liner at Test Conditions.
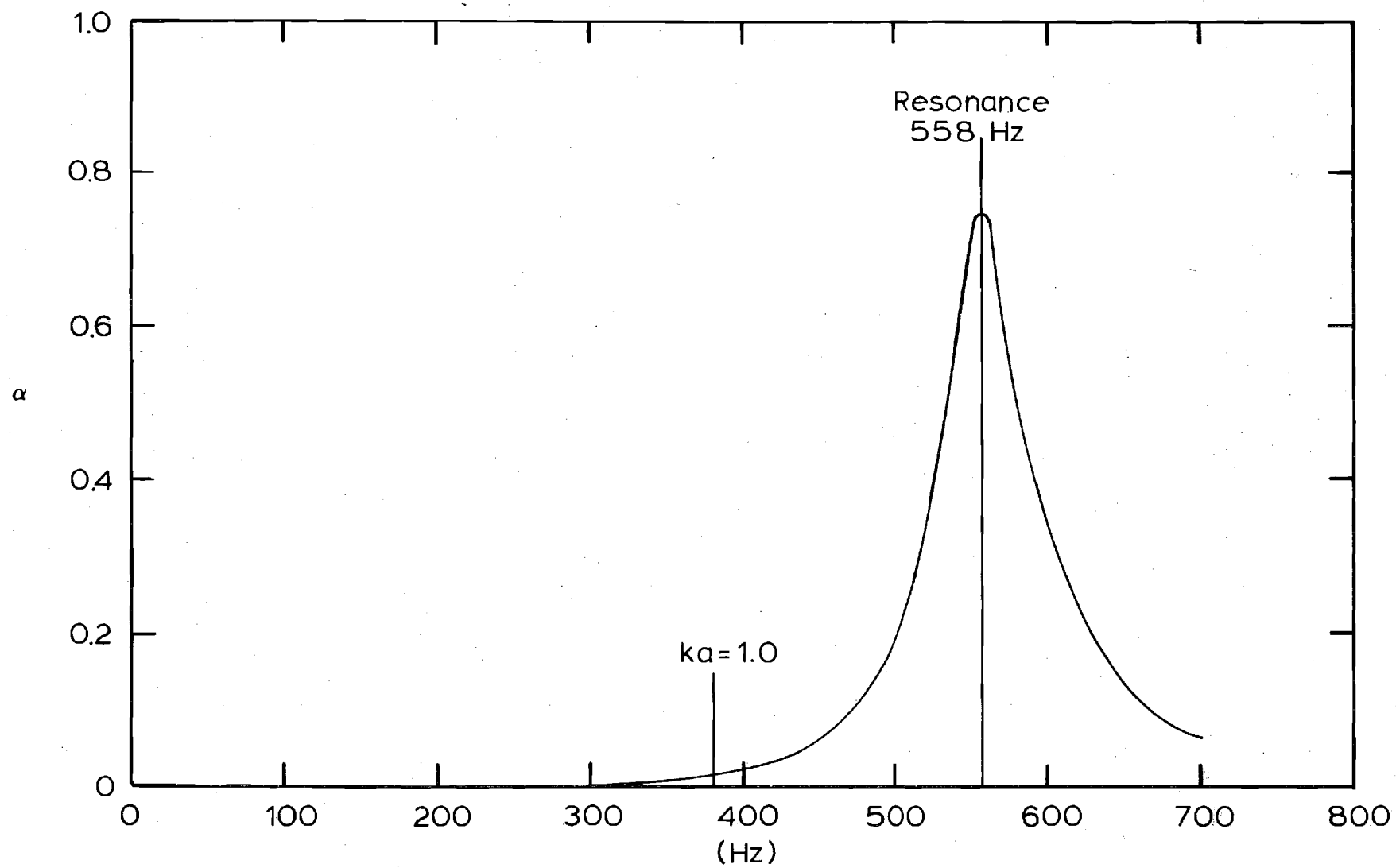
Nomenclature

a	characteristic length of the body
$\bar{c}$	speed of sound
d	Helmholtz resonator orifice diameter
f	frequency
f_o	resonant frequency of a Helmholtz resonator
i	$\sqrt{-1}$
k	wave number
L	backing depth of a Helmholtz resonator
l_{eff}	effective orifice length of a Helmholtz resonator
t	orifice length of a Helmholtz resonator
V	cylindrically symmetric normal acoustic velocity
y	acoustic admittance
Z	specific acoustic impedance of the liner
α	absorption coefficient of the liner
σ	open area ratio of the liner
$\bar{\sigma}$	open area ratio of a Helmholtz resonator
$\bar{\rho}$	density of the medium
$\bar{\mu}$	coefficient of viscosity of the medium
Φ	cylindrically symmetric acoustic potential
θ	specific acoustic resistance
X	specific acoustic reactance

E.) Data Reduction and Comparison with Theoretical Predictions

In the data reduction the speed of sound, the density, and the coefficient of viscosity were corrected for atmospheric conditions. The speed of sound determines the wave number from the frequency and is therefore extremely important in the data reduction for all cases while the density and coefficient of viscosity are only important in the theoretical admittance calculation (See Eq. (3).).

It should be pointed out that the theoretical and experimental models used in this study were not identical (See Figs. 3 and 4 for the straight duct configurations employed and Figs. 6 and 7 for the inlet configurations used in Appendix C.). The theoretical bodies were given hemispherical rear terminations in the interest of conserving computing time and space. It has been found, however, through theoretical studies using the integral equation formulation of the problem, that the exact form of the rear termination of a body has little effect on the sound field radiated to the forward half plane. Since the forward half plane is where all of the experimental measurements were made this is not considered to be a source of major errors.

In both experimental models the University driver was placed at the throat of a nozzle section (See Figs. 4 and 7 Appendix C.) so that the sound waves are plane at the driver plane. This was checked experimentally and the sound waves at the driver plane were found to be plane within 1 dB in amplitude and 5° in phase. The amplitude was measured at this plane and was used as the input for the computer programs. The phase was not measured directly here as all of the other phase measurements were referenced to this microphone.

The straight duct was tested in both a hard walled configuration and in a lined configuration. For the hard walled tests the orifices of the Helmholtz resonators of the liner were simply covered with tape. The inlet tested had an L/a (length/radius) ratio of 2.0. The exact mathematical forms of the curves that make up the inlet contours can be found in Ref. (4). It should be noted here that in the experimental inlet model the centerbody was held in place by four small wing sectional struts set at 90° from each other. Measurements of the driver amplitude were taken between two of these struts.

A comparison between the predicted and measured amplitudes for the hard walled inlet are presented in tabular form in Table II. It should be recalled that the presented experimental data is actually the average of results obtained in two completely separate tests. The average absolute errors between the experimental and theoretical results are included at each frequency. The results are presented on a quarter circle with a radius of 40" centered at the duct entrance plane (See Fig. 8 Appendix C.). The experimentally measured amplitude at the driver plane is also included. The phase results are presented in Table III. The driver phase is taken to be zero as it is the reference phase. The results for the inlet are plotted for 600 Hz in Fig. 11 of Appendix C.

As can be seen from Tables II and III the average absolute error between the theoretical and experimental results for the inlet configuration is always less than 3 dB in amplitude and 10° in phase. At this juncture it seems appropriate to discuss some of the sources of error and their estimated magnitude so as to put the difference between the experimental

26

Table II.

Averaged Experimental/Theoretical Amplitudes for the Inlet 40" from Entrance Plane (SPL in dB)

Degrees Off ℄ \ Freq. (Hz)	300	350	400	450	500	550	600	650	700	750
0	96.6 93.8	96.6 96.2	98.9 99.1	104.2 103.1	108.1 108.4	113.6 113.1	110.3 110.8	107.9 108.1	109.0 106.6	109.5 106.0
11.25	95.9 93.8	96.1 96.1	99.5 99.1	103.5 103.0	108.6 108.3	113.0 112.9	110.0 110.7	108.4 107.9	107.9 106.4	108.5 105.8
22.5	95.3 93.6	96.3 95.9	99.1 98.8	102.4 102.7	109.1 108.0	111.0 112.5	110.6 110.2	107.5 107.5	107.3 105.9	107.2 105.3
33.75	94.7 93.3	97.0 95.6	98.1 98.5	103.5 102.3	107.8 107.4	110.7 111.9	110.2 109.5	107.4 106.7	106.3 105.1	105.6 104.4
45	93.9 93.0	96.9 95.2	97.9 98.0	103.4 101.7	105.8 106.7	111.4 111.1	108.5 108.6	105.9 105.7	104.6 104.1	105.2 103.3
56.25	92.7 92.5	95.8 94.7	97.8 97.5	101.0 101.1	104.7 106.0	110.1 110.1	107.0 107.5	103.8 104.5	104.3 102.8	102.6 101.9
67.5	91.1 92.0	95.0 94.2	98.7 96.9	100.1 100.4	105.0 105.2	109.0 109.1	105.1 106.3	103.0 103.1	101.4 101.3	101.2 100.4
78.75	91.6 91.3	93.7 93.5	97.2 96.2	101.1 99.7	104.4 104.5	107.0 108.3	105.4 105.2	102.0 101.9	100.3 99.8	101.9 98.8
90	91.0 90.7	92.3 92.8	95.9 95.5	101.5 99.0	104.1 103.8	107.2 107.6	103.5 104.5	100.7 100.9	99.4 98.7	99.9 97.4
Driver	127.0	127.0	127.0	127.0	127.0	127.0	127.0	127.0	127.0	127.0
Average Absolute Error	1.18	0.72	0.54	1.01	0.54	0.60	0.59	0.30	1.09	2.03

Table III

Averaged Experimental/Theoretical Phases for the Inlet 40" from the Entrance Plane (Degrees Relative to the Driver)

Degrees Off ₵ \ Freq. (Hz)	300	350	400	450	500	550	600	650	700	750
0	-61	-12	35	98	170	-104	7	72	130	-158
	-66	-13	41	98	167	-92	8	79	141	-160
11.25	-61	-20	41	80	165	-102	5	72	134	-163
	-66	-13	41	99	167	-92	8	79	141	-160
22.5	-62	-15	46	80	170	-87	3	75	137	-162
	-66	-13	41	99	168	-92	8	79	140	-160
33.75	-68	-14	41	76	174	-91	-1	77	139	-166
	-65	-12	42	100	168	-91	8	78	140	-161
45	-68	-12	39	93	177	-93	8	74	138	-167
	-65	-12	43	101	170	-90	8	78	140	-161
56.25	-65	-16	44	107	169	-91	16	73	139	-153
	-63	-10	45	103	172	-88	10	79	140	-161
67.5	-63	-23	48	109	179	-93	14	83	146	-162
	-61	-8	47	106	175	-85	13	82	142	-160
78.75	-61	-20	48	103	-173	-78	11	93	143	-154
	-59	-6	49	109	179	-80	18	87	147	-156
90	-56	-10	43	107	-169	-64	27	94	147	-148
	-54	-2	53	113	-177	-75	25	94	154	-149
Driver	0	0	0	0	0	0	0	0	0	0
Average Absolute Error	3.1	6.1	3.2	9.9	4.3	6.0	3.8	4.0	4.4	3.4

and theoretical results in prospective. First, there are the obvious experimental errors caused by microphone amplifier drift, temperature changes in the anechoic chamber of and the microphone placement in the chamber. Comparing test results and calibrations these errors are estimated to account for up to 0.5 dB in amplitude and 5 degrees in phase. Another source of error is the anechoic chamber which, as stated before, can account for errors up to 3 dB and 10 degrees. A more subtle source of experimental error is due to scale switching on the microphone amplifiers which can account for as much as 0.5 dB (i.e. 100 dB on the 90 to 110 dB scale reads as 100.5 dB on the 100 to 120 dB scale).

The theoretical errors are estimated by comparison with exact solutions for similar geometries. It is found that the computer programs introduce about 1% error, insignificant in dB but accounting for as much as 5 degrees in phase. Another source of error is the assumption of a plane wave at the driver plane; unfortunately the effect of this assumption can not be easily estimated. As none of the above mentioned errors are specifically geometry dependent, these error estimates apply to the straight duct configurations too.

The results of the experimental tests and of the computer runs for the hard walled straight duct configurations are presented in Tables IV and V. The amplitude results are tabulated in decibels in Table IV while the phase results in degrees appear in Table V. Again, the experimental results presented are actually the average of two separate runs.

It can be seen that all of the amplitude results are very good as the experimental and theoretical values at each test frequency have average

Table IV

Averaged Experimental/Theoretical Amplitudes for the Hard Walled Straight Duct 40"
from the Entrance Plane (SPL in dB)

Freq. (Hz) Degrees Off ℄	300	350	400	450	500	550	600	650	700
0	102.3 99.8	104.6 104.2	110.8 110.5	114.1 113.9	110.1 110.4	108.4 108.2	105.8 107.3	108.2 107.3	108.6 108.1
11.25	101.6 99.7	104.9 104.1	111.4 110.4	112.9 113.8	110.9 110.3	107.0 108.0	106.4 107.1	108.3 107.1	107.7 107.8
22.5	100.5 99.5	104.8 103.8	110.3 110.0	113.1 113.4	110.4 109.8	105.9 107.5	107.0 106.5	106.8 106.5	106.1 107.1
33.75	100.2 99.2	105.3 103.4	110.0 109.5	113.1 112.7	108.1 109.1	106.8 106.7	106.2 105.7	105.1 105.5	105.3 106.0
45	99.1 98.8	104.4 102.9	109.7 108.8	112.7 111.8	106.2 108.1	107.2 105.6	104.0 104.5	104.0 104.2	105.3 104.5
56.25	97.9 98.3	103.5 102.3	108.7 108.0	109.5 110.8	106.3 106.9	104.3 104.3	101.9 103.1	103.6 102.7	102.1 102.9
67.5	96.9 97.7	102.3 101.6	108.3 107.2	109.1 109.8	105.1 105.6	102.0 102.8	102.6 101.5	101.4 101.0	99.3 101.1
78.75	96.7 97.0	101.5 100.9	107.0 106.4	110.2 108.9	103.9 104.4	100.3 101.4	101.5 99.8	99.9 99.3	100.5 99.3
90	96.7 96.3	99.7 100.2	105.2 105.8	108.4 108.1	103.9 103.5	100.7 100.2	98.9 98.4	98.8 97.6	95.5 97.6
Driver	126.9	126.9	126.9	126.9	126.9	126.9	126.9	126.9	126.9
Average Absolute Error	0.96	0.96	0.67	0.70	0.71	0.77	0.91	0.68	1.00

Table V

Averaged Experimental/Theoretical Phases for the Hard Walled Straight Duct 40"
from the Entrance Plane (Degrees Relative to the Driver)

Freq. (Hz) / Degrees Off $\mathcal{C}_L$	300	350	400	450	500	550	600	650	700
0	-62 / -65	-8 / -8	69 / 65	-177 / 180	-82 / -90	-17 / -24	37 / 37	96 / 96	164 / 156
11.25	-63 / -65	-12 / -8	74 / 65	179 / 180	-82 / -90	-5 / -24	34 / 37	99 / 96	169 / 156
22.5	-67 / -65	-9 / -7	72 / 66	172 / 180	-78 / -90	-7 / -24	33 / 36	107 / 95	163 / 155
33.75	-73 / -64	-7 / -6	68 / 66	-175 / -180	-81 / -90	-10 / -24	39 / 36	106 / 95	156 / 154
45	-72 / -63	-10 / -5	68 / 68	-174 / -179	-89 / -90	-16 / -25	46 / 35	93 / 94	161 / 154
56.25	-64 / -61	-13 / -3	78 / 70	-167 / -176	-87 / -88	-4 / -24	39 / 36	102 / 94	170 / 153
67.5	-61 / -59	-15 / 0	80 / 74	179 / -173	-77 / -85	-11 / -21	32 / 37	116 / 95	158 / 154
78.75	-58 / -56	-7 / 3	75 / 78	-169 / -167	-68 / -79	-4 / -16	33 / 42	107 / 99	167 / 157
90	-53 / -52	9 / 8	67 / 83	-161 / -161	-78 / -72	10 / -8	52 / 50	114 / 106	164 / 164
Driver	0	0	0	0	0	0	0	0	0
Average Absolute Error	3.7	5.3	6.0	4.6	7.1	14.0	4.3	8.0	7.7

31

absolute errors of one decibel or less. The phase results also compare very well except at 550 Hz where the average absolute error is about twice that at the other frequencies. The probable reason for this is that this frequency is very close to the tuning frequency of the liner, which is about 558 Hz (See Fig. 6.), and that the liner orifices were closed off with tape for the hard walled tests which may not have been 100 percent effective in keeping the liner from influencing the phase results. It should be noted, however, that this method of closing off the liner was effective as far as the amplitude results are concerned (See Table IV.). The amplitude and phase results at 550 Hz are plotted in Fig. 9 of Appendix C for this case.

The experimental and test results for the case of the soft, lined walled straight duct configuration are tabulated in Tables VI and VII for the amplitude and phase, respectively. The results for the amplitude and phase at 500 Hz are plotted in Fig. 10 of Appendix C. The errors in the amplitude are in general less than 3 dB and the errors in the phase less than 10 degrees except at 550 Hz where the errors for both the amplitude and the phase are very large. These differences between the theoretical and experimental results are probably due to the liner theory used for calculating the admittance of the liner and machining errors in the manufacture of the liner.

Table VI

Averaged Experimental/Theoretical Amplitudes for the Soft Walled Straight Duct 40" from the Entrance Plane (SPL in dB)

Degrees Off ℄ \ Freq. (Hz)	300	350	400	450	500	550	600	650	700
0	103.8 101.7	110.1 108.3	112.9 113.9	108.0 107.6	104.7 104.9	88.2 70.9	101.2 104.2	109.1 108.9	108.1 108.0
11.25	103.0 101.6	110.3 108.2	113.6 113.7	106.9 107.5	105.6 104.7	87.0 70.4	102.0 104.0	109.3 108.7	107.1 107.7
22.5	102.9 101.4	110.4 107.9	112.5 113.4	106.5 107.0	104.9 104.2	85.8 69.1	102.4 103.5	107.8 108.1	105.3 107.0
33.75	102.3 101.1	110.6 107.5	112.1 112.8	107.2 106.4	102.5 103.5	86.3 67.1	101.8 102.6	106.4 107.1	104.7 105.9
45	101.4 100.6	109.9 107.0	111.7 112.1	105.8 105.5	101.6 102.5	86.5 65.4	99.6 101.5	105.1 105.9	104.7 104.5
56.25	99.4 100.1	108.8 106.3	110.9 111.3	103.5 104.5	101.1 101.2	83.9 65.8	97.7 100.2	104.7 104.4	101.5 102.9
67.5	98.8 99.6	107.6 105.7	109.5 110.5	102.6 103.4	100.1 100.0	80.1 67.2	98.2 98.7	102.5 102.7	99.3 101.1
78.75	99.0 98.9	106.0 105.0	109.0 109.8	103.3 102.5	99.8 99.8	76.6 68.1	96.6 97.1	101.0 101.0	99.8 99.3
90	99.1 98.2	104.1 104.3	107.4 109.1	101.3 101.8	99.6 97.9	79.2 68.0	93.6 95.6	99.9 99.3	94.5 97.5
Driver	126.9	126.9	126.9	126.9	126.9	126.9	126.9	126.9	126.9
Average Absolute Error	1.06	2.00	0.78	0.63	0.62	15.73	1.59	0.41	1.17

33

Table VII

Averaged Experimental/Theoretical Phases for the Soft Walled Straight Duct 40" from the Entrance Plane (Degrees Relative to the Driver)

Freq. (Hz) / Degrees Off ₵	300	350	400	450	500	550	600	650	700
0	-61 / -63	9 / 4	143 / 134	-125 / -129	-49 / -59	11 / 79	-57 / -65	65 / 69	151 / 144
11.25	-63 / -63	6 / 4	147 / 134	-130 / -129	-48 / -59	15 / 80	-65 / -65	68 / 69	155 / 143
22.5	-67 / -62	9 / 4	146 / 134	-131 / -129	-45 / -59	16 / 82	-66 / -65	76 / 68	148 / 143
33.75	-71 / -61	12 / 5	142 / 135	-125 / -128	-47 / -59	9 / 89	-57 / -66	75 / 68	143 / 142
45	-69 / -60	7 / 7	143 / 137	-118 / -127	-55 / -59	7 / 106	-45 / -66	62 / 67	147 / 141
56.25	-64 / -59	3 / 9	152 / 139	-116 / -125	-52 / -58	10 / 123	-57 / -65	72 / 67	156 / 141
67.5	-61 / -56	2 / 11	155 / 142	-123 / -122	-43 / -54	6 / 129	-68 / -64	85 / 69	143 / 142
78.75	-57 / -53	12 / 15	148 / 147	-120 / -116	-36 / -49	19 / 126	-48 / -60	69 / 72	156 / 145
90	-50 / -50	25 / 19	142 / 152	-109 / -110	-47 / -41	43 / 120	-42 / -52	86 / 80	152 / 152
Driver	0	0	0	0	0	0	0	0	0
Average Absolute Error	4.4	4.8	9.3	3.8	9.7	88.7	8.1	6.1	6.4

F. Determination of the "Effective" Liner Admittance

As stated in the previous sections normal machining errors can change the resonant frequency of the liner by as much as 1.5 Hz which can change the sound field by as much as 3 dB and 5 degrees due to the liners "peaky" absorption curve (See Fig. 6.). Even this can't, however, account for the large differences between the experimental and theoretical results at 550 Hz for the lined straight duct. Noteing that the calculated results were consistently lower than those measured, it was assumed that the liner theory[5] predicted the admittance (i.e. the effectiveness) of the liner to be higher than it actually was. To check this hypothesis a parametric set of computer runs was conducted in which the admittance was systematically varied to see if the true "effective" admittance of the liner at 550 Hz could be determined by comparison with the experimental results. From this set of computer runs it was found that the true "effective" admittance of the liner was approximately

$$y = -0.13 - i0.28 \qquad @ \ 550 \ Hz$$

(10)

which is the real part of the admittance calculated from Eqs. (2-4) and (8) multiplied by 0.35 and the imaginary part multiplied by 0.65. The experimental and theoretical results, calculated using the admittance in Eq. (10), are tabulated in Table VIII. As can be seen these results are more in line with what was found at the other frequencies (See Tables VI and VII.), so it is concluded that the Garrison theory of Ref. (5) does not give the proper admittance for this type of liner near resonance (i.e. it predicts the

Table VIII

Averaged Experimental/Theoretical Acoustic Radiation 40" from the Entrance Plane of the Soft Walled Straight Duct at 550 Hz with $y = -0.13 - i\,0.28$

Degrees Off ₵	Amplitude SPL (dB)	Phase (degrees)
0	88.2 89.7	11 15
11.25	87.0 89.5	15 14
22.5	85.8 88.9	16 13
33.75	86.3 88.0	9 12
45	86.5 86.8	7 12
56.25	83.9 85.3	10 13
67.5	80.1 83.7	6 17
78.75	76.6 82.4	19 24
90	79.2 81.7	43 34
Average Absolute Error	2.49	4.9

admittance to be too high). This exercise also points out that the integral equation technique can be used to determine a liners true "effective" admittance from experimental measurements in the field.

References

1.) Meyer, W. L. , Bell, W. A., and Zinn, B. T., "Prediction of the Sound Field Radiated from Axisymmetric Surfaces," *AIAA Paper* No. 78-195, presented at the AIAA 16th Aerospace Sciences Meeting, Huntsville, Alabama, January 16-18, 1978.

2.) Meyer, W. L., Bell, W. A., Stallybrass, M. P., and Zinn, B. T., "Prediction of the Sound Field Radiated from Axisymmetric Surfaces," *Journal of the Acoustical Society of America*, Vol. 63, No. 2, pp. 631-638, March 1979.

3.) Meyer, W. L., Bell, W. A., and Zinn, B. T., "Sound Radiation from Finite Length Axisymmetric Ducts and Engine Inlets," *AIAA Paper No. 79-0675*, presented at the AIAA 5th Aeroacoustics Conference, Seattle, Washington, March 12-14, 1979.

4.) Miller, B. A., Dastoli, B. J., and Wesoky, H. L., "Effect of Entry-Lip Design on Aerodynamics and Acoustics of High-Throat-Mach-Number Inlets for the Quiet, Clean, Short-Haul Experimental Engine," *NASA TM X-3222*, Lewis Research Center, Cleveland, Ohio, May 1975.

5.) Garrison, G. D., "A Study of the Suppression of Combustion Oscillations with Mechanical Damping Devices," Phase II Summary Report, Pratt & Whitney Aircraft Co., PWA FR-1922, July 15, 1966.

## Appendix A

Publications Generated by this Research Effort

A.) "Integral Solution of Three Dimensional Acoustic Radiation Problems," W. L. Meyer, W. A. Bell and B. T. Zinn, <u>Proceedings of the International Symposium on Innovative Numerical Analysis in Applied Engineering Science</u>, Versailles, France, May 23-27, 1977.

B.) "Predicting the Acoustics of Arbitrarily Shaped Bodies Using an Integral Approach," W. A. Bell, W. L. Meyer and B. T. Zinn, <u>AIAA Journal</u>, Vol. 15, No. 6, pp. 813-820, June 1977.

C.) "Prediction of the Sound Field Radiated from Axisymmetric Surfaces," W. L. Meyer, W. A. Bell and B. T. Zinn, <u>AIAA Paper No. 78-195</u>, presented at the AIAA 16th Aerospace Sciences Meeting, Huntsville, Alabama, January 16-18, 1978.

D.) "Boundary Integral Solutions of Three Dimensional Acoustic Radiation Problems," W. L. Meyer, W. A. Bell, M. P. Stallybrass and B. T. Zinn, <u>Journal of Sound and Vibration</u>, Vol. 59, No. 2, pp. 245-262, July 1978.

E.) "Prediction of the Sound Field Radiated from Axisymmetric Surfaces," W. L. Meyer, W. A. Bell, M. P. Stallybrass and B. T. Zinn, <u>Journal of the Acoustical Society of America</u>, Vol. 63, No. 2, pp. 631-638, March 1979.

F.)   "Sound Radiation from Finite Length Axisymmetric Ducts and Engine Inlets," W. L. Meyer, W. A. Bell and B. T. Zinn, <u>AIAA Paper No. 79-0675</u>, presented at the AIAA 5th Aeroacoustics Conference, Seattle, Washington, March 12-14, 1979.

G.)   "Acoustic Radiation from Axisymmetric Ducts: A Comparison of Theory and Experiment," W. L. Meyer, B. R. Daniel and B. T. Zinn, <u>AIAA Paper No. 80-0097</u>, presented at the AIAA 18th Aerospace Sciences Meeting, Pasadena, California, January 14-16, 1980.

Appendix B

Presentations Generated by this Research Effort

A. "Integral Solutions of Three Dimensional Acoustic Radiation Problems," Presented at the International Symposium on Innovative Numerical Analysis in Applied Engineering Science at Versailles, France, May 23-27, 1977. (Zinn)

B. "Prediction of the Sound Field Radiated from Axisymmetric Surfaces," Presented at the AIAA 16th Aerospace Sciences Meeting at Huntsville, Alabama, January 16-18, 1978. (Bell)

C. "Sound Radiation from Finite Length Axisymmetric Ducts and Engine Inlets," Presented at the 5th AIAA Aeroacoustics Conference at Seattle, Washington, March 12-14, 1979. (Zinn)

D. "Acoustic Radiation from Axisymmetric Ducts: A Comparison of Theory and Experiment," Presented at the AIAA 18th Aerospace Sciences Meeting, Pasadena, California, January 14-16, 1980. (Meyer)

Appendix C

AIAA Paper Number 80-0097 Presented at the AIAA 18th Aerospace Sciences Meeting, Pasadena, Calif., Jan. 14-16, 1980.
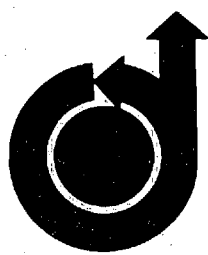
AIAA-80-0097
Acoustic Radiation from Axisymmetric Ducts: A Comparison of Theory and Experiment

W. L. Meyer, B. R. Daniel and B. T. Zinn, Georgia Institute of Technology, Atlanta, Ga.

AIAA 18th
AEROSPACE SCIENCES MEETING

January 14-16, 1980/Pasadena, California

ACOUSTIC RADIATION FROM AXISYMMETRIC DUCTS: A COMPARISON OF THEORY AND EXPERIMENT[t]

W. L. Meyer[*], B. R. Daniel[‡] and B. T. Zinn[**]
School of Aerospace Engineering
Georgia Institute of Technology
Atlanta, Ga. 30332

Abstract

A special integral representation of the exterior solutions of the Helmholtz equation is used to calculate the free field acoustic radiation patterns around two finite axisymmetric bodies; a straight pipe and a jet engine inlet. The radiation patterns around these bodies are then measured experimentally, with the free field being approximated through the use of an anechoic chamber. The inlet tested has a hard wall while the straight pipe is tested with both a hard and a lined wall. The computed theoretical and the measured experimental acoustic radiation patterns are found to be in good agreement. A discussion of possible sources of error, both theoretical and experimental, is included.

Introduction

One of the major problems facing the aircraft industry today is to reduce the noise radiated to the ground from aircraft engines without sacrificing any of the overall efficiency of the aircraft. A major source of engine noise is the compressor or the fan noise which is radiated out of the jet engine through its inlet section. Research efforts directed toward reducing these noise sources have included, among other things, the reduction of the sound level in the jet engine inlet section, by adding sound absorbing materials (i.e., acoustic liners) to the inside of the engine inlet. Weight and volume of these acoustic liners are of prime concern to the aircraft industry as these are directly related to the overall efficiency of the aircraft; thus, efficient acoustic liner designs are sought. In the past, optimum liner designs have been found by extensive full scale testing of engines with various liner configurations which is a very costly and time consuming process. Most of this testing could be eliminated by the development and use of efficient, accurate analytical procedures for the prediction of the sound field radiated from lined jet engine inlets. The development of such a method, based upon a special integral representation of the radiation solutions of the Helmholtz equation, has been discussed at length by the authors of this paper in earlier publications[1-4]. In the present study the applicability of this integral solution technique is investigated by comparing its predictions with the results obtained from an experimental study.

Background

In this paper a special axisymmetric integral representation of the exterior solutions of the Helmholtz equation [3,4] is employed to theoretically calculate the free field acoustic radiation patterns surrounding two finite axisymmetric bodies; namely, a straight duct and a jet engine inlet configuration. The inlet used in these studies is the so called QCSEE inlet (i.e., the quiet, clean, short-haul experimental engine inlet of Reference 5). In previous studies by this group the sound fields radiated from complicated geometries with complex (mixed) boundary conditions were calculated using a solution procedure based on the aforementioned integral representation. The solutions generated were found to be in excellent agreement with "exact" solutions calculated by employing the method of Separation of Variables. A detailed development of the integral equations and solution procedures used along with many comparisons with exact solutions for various bodies, both 3-D and axisymmetric, can be found in Refs. (1-4 and 6). In this connection it should be pointed out that this theoretical technique and solution procedure have been found to be both accurate and computationally efficient when compared to other methods.

Theoretical Method

In this study a so called "integral technique" is employed to calculate the sound radiated from various axisymmetric configurations. The particular method is unique in that it is applicable at all nondimensional wave numbers ka (where k is the wave number and a is an appropriate body dimension), it contains no tangential derivatives on the surface of the body S (See Fig. 1.) and it contains no singular kernels which cannot be handled numerically by straight forward means.
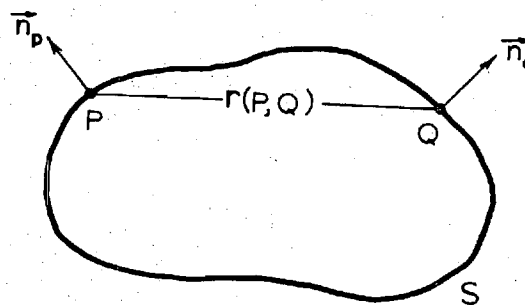

Figure 1.   Definition of Elements on the Body.

The details of the derivation of the particular integral equations used are presented in Refs. (1, 2 and 6) and therefore will not be repeated here. The basic integral equation employed on the surface of the body is written in terms of the acoustic potential φ and it contains surface integrals over the surface of the body S. If we now define $\frac{\partial}{\partial n}$ as the outward normal derivative from the surface, P and Q as points on the surface with their unit outward normals defined as $\vec{n}_p$ and $\vec{n}_q$ respectively, and $\frac{\partial^2 \varphi}{\partial n}$ as the normal acoustic velocity this integral equation takes the following general form

$$\iint_S \left[\varphi(Q) \frac{\partial G(P,Q)}{\partial n_Q} - G(P,Q) \frac{\partial \varphi(Q)}{\partial n_Q} \right] dS_Q$$
$$+ \frac{i}{k} \iint_S \left\{ \left[\varphi(Q) - \varphi(P) \right] \frac{\partial^2 G(P,Q)}{\partial n_P \partial n_Q} \right.$$
$$\left. - \frac{\partial G(P,Q)}{\partial n_P} \frac{\partial \varphi(Q)}{\partial n_Q} \right\} dS_Q \qquad (1)$$
$$- \left(\frac{i}{k} \right) \varphi(P) \iint_S (\bar{n}_P \cdot \bar{n}_Q)(ik)^2 G(P,Q) dS_Q$$
$$= 2\pi \left(\varphi(P) + \frac{i}{k} \frac{\partial \varphi(P)}{\partial n_P} \right)$$

In this equation G(P,Q) can be any fundamental solution of the Helmholtz equation. In this study it has been chosen to be the free space Green's Function of the Helmholtz equation; that is

$$G(P,Q) = \frac{e^{ikr(P,Q)}}{r(P,Q)} \qquad (2)$$

Figure 2.   General Axisymmetric Geometry and 2-D Projection.

where r(P,Q) is the distance between the points P and Q on the surface of the body.

Once the acoustic potential is calculated on the surface of the body using Eqn. (1), the following integral representation for φ may be used to calculate the acoustic potential anywhere in the field surrounding the body. In this case the point P is no longer on the body S but in the field surrounding it.

$$\iint_S \left[\varphi(Q) \frac{\partial G(P,Q)}{\partial n_Q} - G(P,Q) \frac{\partial \varphi(Q)}{\partial n_Q} \right] dS_Q$$
$$= 4\pi \varphi(P) \qquad (3)$$

If the body of interest is axisymmetric, as most jet engine inlets are, certain simplifications may be made[3,4]. Let us now define a new cylindrically symmetric acoustic potential and normal acoustic velocity as

$$\bar{\phi} = \frac{\varphi}{\cos m\theta}$$
$$V = \frac{\frac{\partial \varphi}{\partial n}}{\cos m\theta} \qquad (4)$$

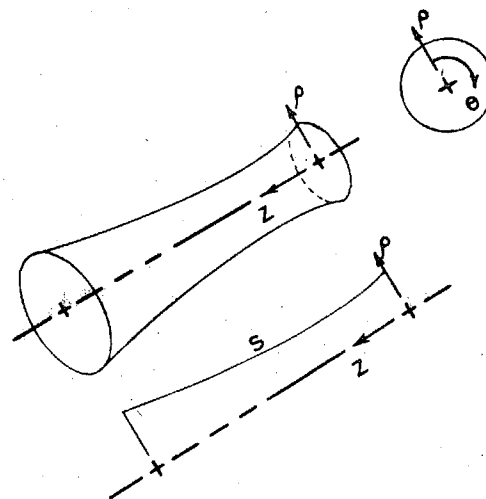where m is the tangential mode number and θ is defined as in Figure 2

and s is the distance along the body in the ρ-z plane (e.g. $0 \leq s \leq \ell$). In doing this we have effectively separated out all the tangential modes; thus, the formulation that will be presented for axisymmetric bodies will be cylindrically symmetric in that all the tangential modes (i.e., m = 0,1,2...) may be solved for separately. Having these definitions, Eqn. (1) can be rewritten as

$$\int_0^\ell \bar{\phi}(Q) \left\{ K_1(P,Q) + K_2(P,Q) \right\} ds_Q$$
$$- \bar{\phi}(P) \int_0^\ell \left\{ F_1(P,Q) + F_2(P,Q) \right\} ds_Q \qquad (5)$$
$$- \int_0^\ell V(Q) \left\{ I_1(P,Q) + I_2(P,Q) \right\} ds_Q$$
$$= 2\pi \left\{ \bar{\phi}(P) + \frac{i}{k} V(P) \right\}$$

where s is the distance along the 2-D projection of the body in the ρ-z plane (See Fig. 2.). The kernel functions K_1 and K_2 are defined as

$$K_1(P,Q) = 2 \int_0^\pi \frac{\partial G(P,Q)}{\partial n_Q} (\cos m\theta_Q) d\theta_Q$$

$$(6)$$

$$K_2(P,Q) = 2 \frac{i}{k} \int_{0^+}^\pi \frac{\partial^2 G(P,Q)}{\partial n_P \partial n_Q} (\cos m\theta_Q) d\theta_Q$$

The forcing functions are given by

$$F_1(P,Q) = 2 \frac{i}{k} \int_0^\pi G(P,Q)(ik)^2 (\vec{n}_P \cdot \vec{n}_\xi) \, d\Theta_\xi$$

$$(7)$$

$$F_2(P,Q) = 2 \frac{i}{k} \int_{0^+}^\pi \frac{\partial^2 G(P,Q)}{\partial n_P \partial n_\xi} \, d\Theta_\xi$$

and the influence functions are defined as

$$I_1(P,Q) = 2 \int_c^\pi G(P,Q)(\cos m \Theta_\xi) \, d\Theta_\xi$$

$$(8)$$

$$I_2(P,Q) = 2 \frac{i}{k} \int_0^\pi \frac{\partial G(P,Q)}{\partial n_P} (\cos m \Theta_\xi) \, d\Theta_\xi$$

One should note that Θ_P has been chosen to be zero (i.e. $\cos m \Theta_P = 1$) in the above equation which can be done without any loss of generality.

Equation (3) may also be rewritten in the form

$$\int_0^l \left\{ \Phi(Q) K_1(P,Q) - I_1(P,Q) V(Q) \right\} ds_\xi$$

$$= 4\pi \Phi(P) \qquad (9)$$

As can be seen, this formulation of the problem reduces the solutions of Eqns. (1) and (3) to the evaluation of line integrals on the 2-D projections of the body (See Fig. 2.). Also, this formulation can account for tangential modes; which must, however, be solved for separately.

The theoretical method described above was checked for accuracy by employing several axisymmetric geometries including a straight duct and a jet engine inlet. The calculated radiation patterns generated by this method were compared with various "exact" solutions. These exact solutions were found by assuming that some simple sources (e.g. monopoles, dipoles, and quadrupoles) were located within the body and then calculating the normal acoustic velocity V and/or the admittance, defined as $y \equiv V/\Phi$, at points on the surface of the body. These values were then used as the boundary conditions on the surface of the body and the acoustic potential was calculated at various points

in the field surrounding the body. These were then compared with the acoustic potential that the simple source would generate at each point in the field. Very good agreement was found; for 53 integration points on the body along s (See Fig. 2.) the error was always below 10% in the real and imaginary parts of Φ for nondimensional wave numbers up to ka = 10. It was also found that increasing the number of integration points generally decreased the error proportionally (e.g. using 102 points the maximum error in the acoustic potential at a field point was about 5% for the inlet at a nondimensional wave number of ka = 10.). The results and details of many such tests are presented in Ref.(3).

The Test Bodies

The integral formulation has been used in the present study to calculate the sound fields radiated from two axisymmetric bodies, a straight duct and a jet engine inlet. The theoretical and experimental configurations do not compare exactly as an accurate description of the "back side" of the experimental bodies would entail the use of too many theoretical points on the bodies. Therefore, different external terminations were given to the theoretical models in the interest of conserving computing time and computer storage space. In this connection it has been found through theoretical studies, that the exact form of the rear termination of the body has little effect on the sound field radiated in the forward half plane. Since we are only really interested in the sound field in the forward half plane, this approximation is not considered to be a major source of error in this study.

The first axisymmetric body tested was a straight duct. Below is a sketch of the theoretical model employed.
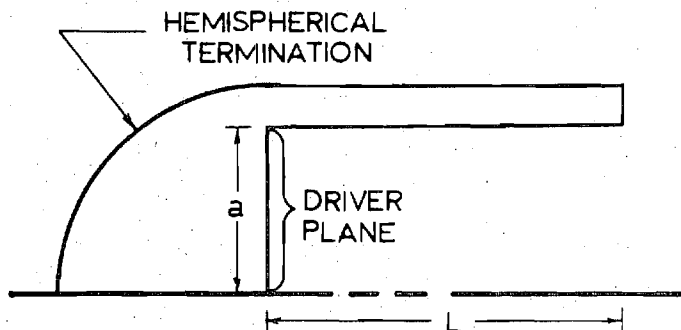

Figure 3.   Theoretical Straight Duct Model.

Its L/a equals 2.110, the same as the experimental model. It will be noted that the theoretical model has a hemispherical termination which differs from the rear termination of the experimental model shown below.
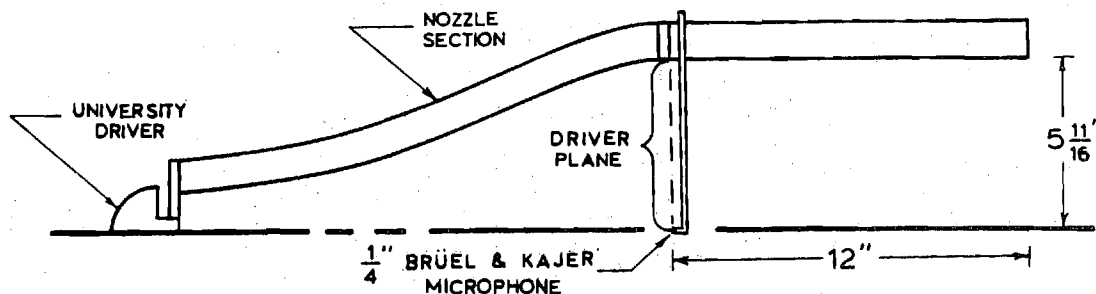
Figure 4.   Experimental Straight Duct Test
             Configuration.

In the experimental model the driver is placed at the throat of a nozzle section, which assures that the sound waves are plane at the driver plane where a 1/4" condensor microphone is located to provide a reference pressure level in decibels. All of the tests were conducted at nondimensional wave numbers ka below the 1T mode of the duct (i.e. $k \leq 1.84$) and thus we were assured of a plane wave at the driver plane. This has been checked out experimentally by sweeping the reference microphone radially across the duct and it has been found to be true within 1 dB in amplitude and 5° in phase (i.e. there is less than 1 dB and 5° variation between the wall and the center of the duct). In the theoretical model the existence of plane wave excitation at the driver plane is assumed.

The straight duct was tested in two configurations; that is, hard wall and lined wall configurations. The lined wall configuration consisted of 180 Helmholtz resonators (9 axial rows by 20 radial rows). A sketch of one of the resonators is shown below.
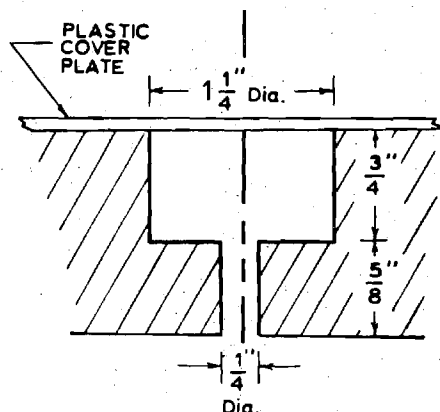

Figure 5.   Helmholtz Resonator.

For the hard walled tests the small holes inside the duct were simply covered with tape.

The second axisymmetric body tested was a model of an actual engine inlet[5]. It has an L/a of 2.0. The theoretical model has a hemispherical termination similar to the one used for the straight duct. A sketch of the theoretical inlet model is presented below.
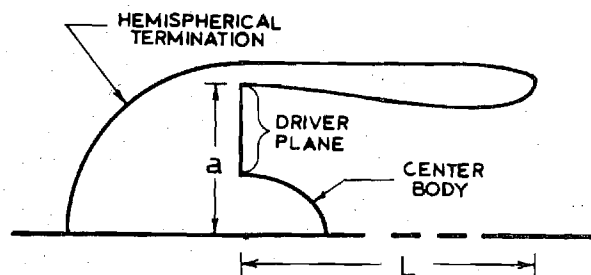

Figure 6.   Theoretical Inlet Model.

In the experimental model the centerbody was held in place by 4 small wing cross-sectional struts set at 90° angles. The microphone measurement for the amplitude and phase at the driver plane was made half way between 2 of these struts. Again, the small condensor microphone was swept across the driver plane radially to check for the presence of plane wave excitation which was found to exist within the same limits as for the straight duct (i.e., less than a 1 dB change in amplitude and 5° in phase across the driver plane). A sketch of the experimental inlet model is presented below.
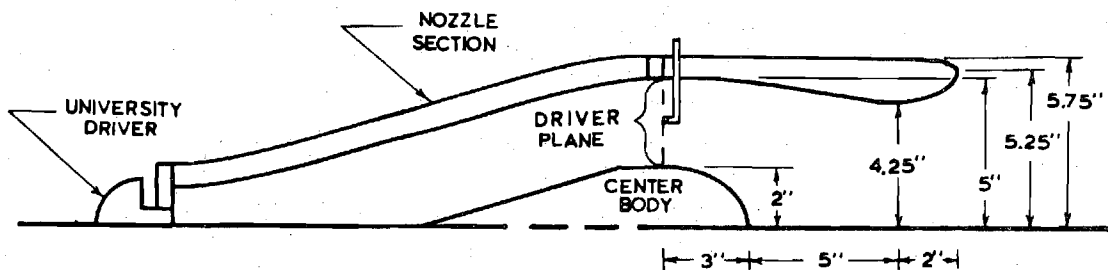
4

Figure 7.   Experimental Inlet Test Configuration.

Again, the exact mathematical form of the curves that make up the inlet contours can be found in Reference 5.

Results

In the anechoic chamber tests conducted under this program, the field measurements were taken 40" from the center of the duct exit plane on a circular arc at $11 \frac{1}{4}°$ increments from the centerline of the duct. One-half inch B & K microphones were used in these tests for the field measurements. The anechoic chamber used in the experiments has interior dimensions of 10' x 13' x 6 1/2' high. The acoustic insulation used in the chamber is fiberglass which is approximately 2' thick. The ducts tested (i.e., the straight duct and the inlet) and the microphones used for the field measurements were 3' off the floor. A plan view of the anechoic chamber with a typical test set-up is presented below.
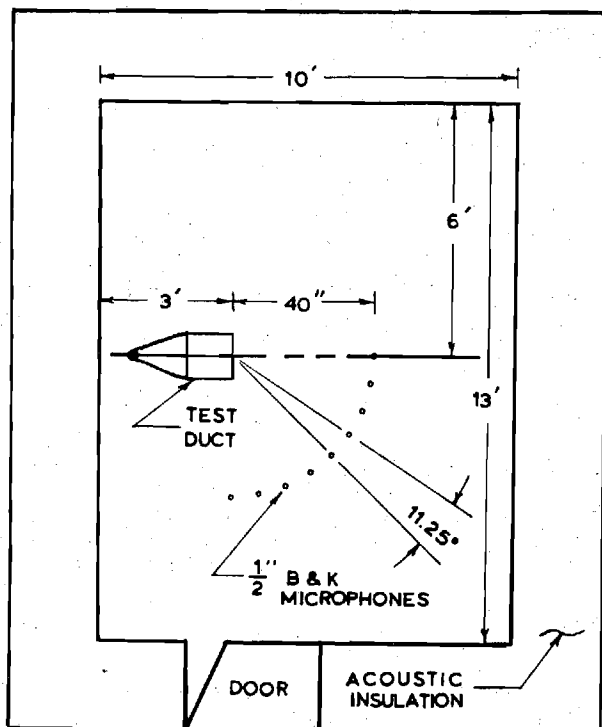

Free field measurements were made in the chamber to check its "anechoicness". For the distances of interest in the chamber (i.e. up to 40" from a source) free field conditions were generally approximated to within 3 dB in amplitude and $10°$ in phase.

The procedure for the tests was to take the measured SPL in dB from the 1/4" B & K microphone at the driver plane and input the data into the theoretical model assuming plane wave excitation at the driver plane. Again, this was checked experimentally for each configuration and found to be generally true within 1 dB in amplitude and 5 degrees in phase. Since a plane wave was assumed, the phase was not measured at the driver plane and zero phase was assumed for this location in the theoretical model. This can be done without any loss of generality as the phase differences between the field microphones and the driver plane microphone are the quantities of interest which were measured in this program. Once the driver plane acoustic pressure was input into the theoretical model, the far field sound distribution was calculated and compared with the measured experimental data.

The computer used for these analyses was the Georgia Tech Cyber 70/74. Typical run times to calculate the distribution of the acoustic potential φ (i.e., See Eqn. (5).) with 100 points on the theoretical body are about 6 minutes and to calculate the acoustic potential in the far field at 20 points (i.e., See Eqn. (9).) are about 1 minute. In the theoretical calculations of the surface potential on the straight duct 102 points were used while in the calculations for the inlet (See Fig. 5.) 97 points were used.

In the numerical integration of Eqns. (5) and (9) a 2 point integration formula was used in the s direction (See Fig. 2.). It should be noted, however, that an even integration formula must be used here as an odd formula would place a point in the center of the integration region which would cause the various kernel functions (i.e., See Eqns. (6)-(8).) to go to infinity when r(P,Q) goes to zero as the points P and Q coincide. In all the investigated cases a 96 point Gaussian integration formula was used in the θ direction.

Tests with the straight duct configuration with both hard and soft walls were conducted in the frequency range of 300 to 700 Hz at 50 Hz increments. Over this frequency range a reasonably plane wave could be excited at the driver plane[*]. Comparisons of calculated and measured data for the hard walled straight duct configuration are

Figure 8.   Anechoic Chamber (Plan View) with Test Set-Up.

presented in Fig. 9 for 550 Hz. The SPL results at this frequency are representative of those at all other frequencies while the phase results are the worst at this frequency. The probable reason for this is that 550 Hz is very close to the tuning frequency of the liner, which was calculated to be around 558 Hz under these test conditions and the tape used to close off the liner holes for the hard walled tests was not 100 percent effective. The average absolute errors for the amplitude in dB and for the phase in degrees are presented in Table I for all of the tests run.
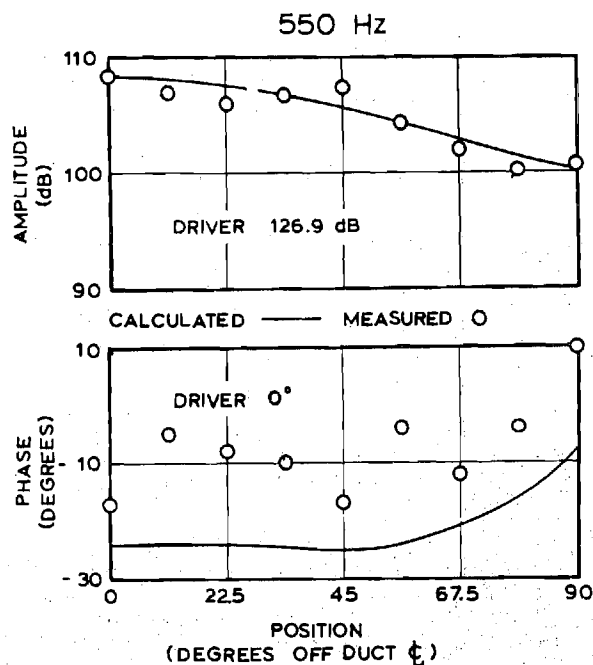
Comparisons of experimental and calculated far field pressures for the lined, straight wall duct are presented in Fig. 10 at a frequency of 500 Hz. These results are typical of those obtained at all but one of the other frequencies tested. At 550 Hz, which is very close to the calculated resonant frequency of the liner, the results show significantly more error (See Table I.). Since the calculated results were lower than those measured it was assumed that the liner theory results predicted the effectiveness of the liner to be higher than it actually was in practice. To see if this was actually the case a set of systematic computer runs were made in which the effectiveness of the liner (i.e., its admittance) was reduced.
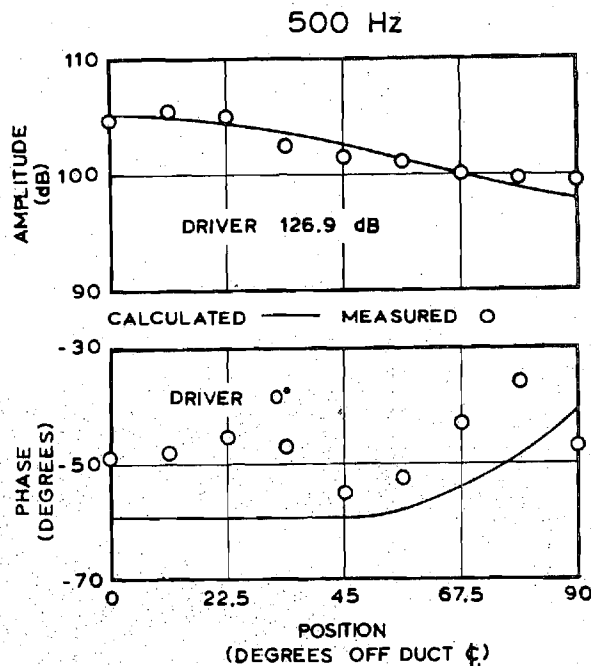

Figure 9.   Acoustic Radiation 40" from the Hard Walled Straight Duct.

Figure 10.   Acoustic Radiation 40" from the Soft Walled Straight Duct.

To predict the sound field radiated by the lined, straight wall duct the admittance at the wall is required. In this case available liner theory[7] was used to predict the admittance of the Helmholtz resonator array. For the particular resonators used (See Fig. 5.) in this study the resonant frequency of the array, f_o , was calculated to be around 558 Hz and the specific impedance of the liner $Z = \Theta - i X$ was found to be given by:

$$\Theta = 0.01398 \sqrt{f}$$

$$X = 10.186 \left(\frac{f}{f_c} - \frac{f_c}{f} \right) \qquad (10)$$

It was found that if the predicted real part of the admittance was taken to be 35 percent effective and the imaginary part of the admittance was taken to be 65 percent effective (i.e. y = - 0.13 - i 0.28 at 550 Hz) than the results from the theoretical calculations were significantly closer to the experimentally measured data. The average absolute errors for the amplitude in dB and for the phase in degrees are now 2.51 dB and 5.00 degrees respectively as compared to the much larger errors incurred using the admittance values predicted by the liner theory (See Table I.).

Tests for the inlet configuration were also conducted over the frequency range 300 - 700 Hz at 50 Hz increments. Since the reference lengths, a, are slightly different (See Figs. 3,4,6 and 7.) the nondimensional wave numbers ka are different. Comparisons of theoretical and experimental data are presented in Fig. 11 for the inlet configuration at 600 Hz. These results are representative of those at other frequencies.
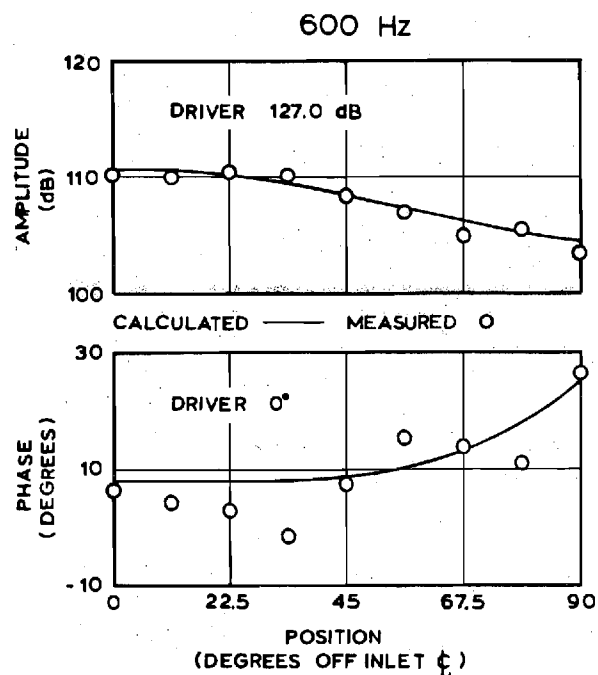
600 Hz

Figure 11.   Acoustic Radiation 40" from the Inlet.

The causes for the errors appearing in the comparisons of the last section will be briefly discussed herein. First, there are the obvious experimental errors caused by microphone amplifier drift, temperature changes in the anechoic chamber and microphone placement in the chamber. These errors can be estimated as identical tests were run on different days, the microphones were calibrated three times during the course of each test, and the microphones were moved and reset during each test as there are 9 positions in the field and only 5 microphones were used in each test. Comparing test results and calibrations, these errors are estimated as being of the order of 0.5 dB in amplitude and 5 degrees in phase. Another source of experimental error is the anechoic chamber itself which, as stated before, can account for up to 3 dB errors in amplitude and 10° errors in phase. A more subtle source of error in the lined duct tests is the liner itself. It was found that by changing the dimensions of the Helmholtz resonators by as little as 0.0005 inches (i.e. common machining errors) the resonant frequency calculated for the liner changed by as much as 1.5 Hz which is significant for this type of liner near resonance due to its highly peaked absorption curve. A sample calculation was run at 550 Hz with this change and the calculated results changed by about 3 dB in amplitude and 5 degrees in phase. Another source of possible error for this particular case is obviously the imperfection of the liner theory itself; the determination of the errors caused by its shortcomings are, however, beyond our current capabilities.

The computer programs also introduce some errors which are estimated to be about 1 percent by comparing these computer results with exact solutions for similar geometries and wave numbers. Although these errors are insignificant when evaluated in dB, they can be as high as 5 degrees in phase. Another source of error is the assumption of a plane wave at the driver plane; the effect of this error or the results in the far field cannot, however, be easily estimated. Other sources of error include the differences between the experimental and theoretical geometries which include not only the different terminations on the back side of the bodies but also the stand required to hold up the experimental set-up in the anechoic chamber. The errors caused by these differences are hopefully small.

Freq. Hz		300	350	400	450	500	550	600	650	700
Hard Walled Straight Duct	dB	0.96	0.95	0.66	0.70	0.71	0.78	0.92	0.67	1.02
	Deg.	3.83	5.56	5.89	4.61	7.44	13.78	4.33	7.72	7.83
Soft Walled Straight Duct	dB	1.06	1.96	0.82	0.63	0.74	15.71	1.61	0.42	1.19
	Deg.	4.67	4.78	9.28	3.67	9.33	88.89	8.11	5.89	6.61
Inlet	dB	1.18	0.72	0.61	1.08	0.69	0.63	0.61	0.38	1.07
	Deg.	3.17	6.39	3.83	10.22	5.00	6.22	4.00	4.50	5.00

Table I. Average Absolute Errors.

Conclusions

Acoustic measurements were made of the sound field radiated from a straight duct with both acoustically hard and soft walls and a jet engine inlet. These measurements were then compared with the results of an integral representation of the solutions of the Helmholtz equation and good agreement between the theoretical and experimental results was observed. This indicates that the integral equations used and the techniques employed for solving them are good approximations to the actual acoustic behavior of arbitrarily shaped axisymmetric ducts radiating into a free space. This is significant in that most theories can not adequately model the coupling between the acoustic fields inside and outside a duct. Thus, this technique can be used with confidence to efficiently predict the sound field radiated from complex axisymmetric geometries.

References

1. Bell, W. A., Meyer, W. L., and Zinn, B. T., "Predicting the Acoustics of Arbitrarily Shaped Bodies Using an Integral Approach," _AIAA Journal_ Vol. 15, No. 6, June 1977, pp. 813-820.

2. Meyer, W. L., Bell, W. A., Stallybrass, M. P. and Zinn, B. T., "Boundary Integral Solutions of Three Dimensional Acoustic Radiation Problems," _Journal of Sound and Vibration_, Vol. 59, No. 2, pp. 245-262, July 1978.

3. Meyer, W. L., Bell, W. A., Stallybrass, M. P., and Zinn, B. T., "Prediction of the Sound Field Radiated From Axisymmetric Surfaces," _Journal of the Acoustical Society of America_, Vol. 65, No. 3, pp. 631-638, March 1979.

4. Meyer, W. L., Bell, W. A., and Zinn, B. T., "Sound Radiation from Finite Length Axisymmetric Ducts and Engine Inlets," AIAA Paper No. 79-0675, presented at the AIAA 5th Aeroacoustics Conference, Seattle, Washington, March 12-14, 1979.

5. Miller, B. A., Dastoli, B. J., and Wesoky, H. L., "Effect of Entry-Lip Design on Aerodynamics and Acoustics of High-Throat-Mach-Number Inlets for the Quiet, Clean, Short-Haul Experimental Engine," NASA TM X-3222, May 1975.

6. Burton, A. J., "The Solution of Helmholtz' Equation in Exterior Domains Using Integral Equations," NPL Report NAC 30, National Physical Laboratory, Teddington, Middlesex, January 1973.

7. Garrison, G. D., "A Study of the Suppression of Combustion Oscillations with Mechanical Damping Devices," Phase II Summary Report, Pratt & Whitney Aircraft Co., PWA FR-1922, July 15, 1966.